FTD-MT-24-123-71

FOREIGN TECHNOLOGY DIVISION

ELECTRICAL BREAKDOWN AND DISCHARGE IN A VACUUM

by

I. N. Slivkov, V. I. Mikhaylov, et al.

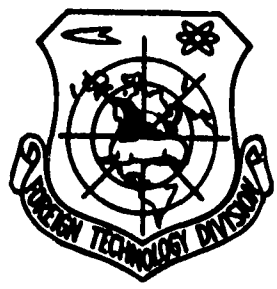

EDITED MACHINE TRANSLATION

FTD-MT-24-123-71

ELECTRICAL BREAKDOWN AND DISCHARGE IN A VACUUM

By: I. N. Slivkov, V. I. Mikhaylov, et al.

English pages: 337

Source: Elektricheskiy Proboy i Razryad Vacuume, Atomizdat, Moscow, 1966, pp. 1-298.

Requester: AFWL

This document is a SYSTRAN machine aided translation, post edited for technical accuracy by: Dean F. W. Koolbeck.

Approved for public release; Distribution unlimited.

UR/0000-66-000-000

PREPARED BY:

TRANSLATION DIVISION
FOREIGN TECHNOLOGY DIVISION
WP-AFB, OHIO.

UNCLASSIFIED

Security Classification

DOCUMENT CONTROL DATA - R & D

(Security classification of title, body of abstract and indexing annotation must be entered when the overall report is classified)

1 ORIGINATING ACTIVITY (Corporate author) Foreign Technology Division Air Force Systems Command U. S. Air Force	2a. REPORT SECURITY CLASSIFICATION UNCLASSIFIED 2b. GROUP

3 REPORT TITLE

ELECTRICAL BREAKDOWN AND DISCHARGE IN A VACUUM

4. DESCRIPTIVE NOTES (Type of report and inclusive dates)
Translation

5 AUTHOR(S) (First name, middle initial, last name)

Slivkov, I. N. ; Mikhaylov, V. I. ; Sidorov, N. I. ; Nastyukha, A. I.

6. REPORT DATE	7a. TOTAL NO. OF PAGES	7b. NO. OF REFS
1966	337	300

8a. CONTRACT OR GRANT NO. b. PROJECT NO. 1256 c. d.	9a. ORIGINATOR'S REPORT NUMBER(S) FTD-MT-24-123-71 9b. OTHER REPORT NO(S) (Any other numbers that may be assigned this report)

10 DISTRIBUTION STATEMENT

Approved for public release; distribution unlimited.

11 SUPPLEMENTARY NOTES	12. SPONSORING MILITARY ACTIVITY Foreign Technology Division Wright-Patterson AFB, Ohio

13 ABSTRACT

Vacuum insulation is widely used in various instruments and installations. However, the mechanisms of the processes which occur in the vacuum gap both in the prebreakdown region and during breakdown cannot be considered sufficiently clear, although these questions have been the subject of numerous studies. This book is a systematized presentation of experimental data and a certain generalization of information on vacuum electrical insulation and self-maintained discharge in a vacuum. The book is intended for engineers and scientific workers occupied with electron and experimental physics; in addition it can serve as a useful supplement for courses in Institutions of Higher Learning on electron physics or electrical phenomena in gases and in vacuum, in which the volume of information presented on vacuum electrical insulation clearly does not meet the requirements of contemporary science and technology.

DD FORM 1 NOV 1473

UNCLASSIFIED

14 KEY WORDS	LINK A		LINK B		LINK C	
	ROLE	WT	ROLE	WT	ROLE	WT
Vacuum Rarefied Gas Ion-Emission Electrical Break-down Vacuum Insulation						

TABLE OF CONTENTS

U. S. BOARD ON GEOGRAPHIC NAMES TRANSLITERATION SYSTEM

Block	Italic	Transliteration	Block	Italic	Transliteration
А а	*А а*	A, a	Р р	*Р р*	R, r
Б б	*Б б*	B, b	С с	*С с*	S, s
В в	*В в*	V, v	Т т	*Т т*	T, t
Г г	*Г г*	G, g	У у	*У у*	U, u
Д д	*Д д*	D, d	Ф ф	*Ф ф*	F, f
Е е	*Е е*	Ye, ye; E, e*	Х х	*Х х*	Kh, kh
Ж ж	*Ж ж*	Zh, zh	Ц ц	*Ц ц*	Ts, ts
З з	*З з*	Z, z	Ч ч	*Ч ч*	Ch, ch
И и	*И и*	I, i	Ш ш	*Ш ш*	Sh, sh
Й й	*Й й*	Y, y	Щ щ	*Щ щ*	Shch, shch
К к	*К к*	K, k	Ъ ъ	*Ъ ъ*	"
Л л	*Л л*	L, l	Ы ы	*Ы ы*	Y, y
М м	*М м*	M, m	Ь ь	*Ь ь*	'
Н н	*Н н*	N, n	Э э	*Э э*	E, e
О о	*О о*	O, o	Ю ю	*Ю ю*	Yu, yu
П п	*П п*	P, p	Я я	*Я я*	Ya, ya

* ye initially, after vowels, and after ъ, ь; e elsewhere. When written as ё in Russian, transliterate as yё or ё. The use of diacritical marks is preferred, but such marks may be omitted when expediency dictates.

FOLLOWING ARE THE CORRESPONDING RUSSIAN AND ENGLISH

DESIGNATIONS OF THE TRIGONOMETRIC FUNCTIONS

Russian	English
sin	sin
cos	cos
tg	tan
ctg	cot
sec	sec
cosec	csc
sh	sinh
ch	cosh
th	tanh
cth	coth
sch	sech
csch	csch
arc sin	$\sin^{-1}$
arc cos	$\cos^{-1}$
arc tg	$\tan^{-1}$
arc ctg	$\cot^{-1}$
arc sec	$\sec^{-1}$
arc cosec	$\csc^{-1}$
arc sh	$\sinh^{-1}$
arc ch	$\cosh^{-1}$
arc th	$\tanh^{-1}$
arc cth	$\coth^{-1}$
arc sch	sech^{-1}
arc csch	csch^{-1}
rot	curl
lg	log

Book Title: Electrical Breakdown and Discharge in a Vacuum

Edited by: B. M. Gokhberg, Dr. of Physics and Mathematics

Authors: I. N. Slivkov, V. I. Mikhaylov, N. I. Sidorov and A. I. Nastyukha

Vacuum insulation is widely used in various instruments and installations. However, the mechanisms of the processes which occur in the vacuum gap both in the prebreakdown region and during breakdown cannot be considered sufficiently clear, although these questions have been the subject of numerous studies.

This book is a systematized presentation of experimental data and a certain generalization of information on vacuum electrical insulation and self-maintained discharge in a vacuum.

The book is intended for engineers and scientific workers occupied with electron and experimental physics; in addition it can serve as a useful supplement for courses in Institutions of Higher Learning on electron physics or electrical phenomena in gases and in vacuum, in which the volume of information presented on vacuum electrical insulation clearly does not meet the requirements of contemporary science and technology.

FOREWORD

Recently problems of vacuum electrical insulation and breakdown in vacuum have taken on ever greater practical significance. In spite of this no monographs on these questions can be found in either Soviet or foreign literature. The few surveys available in journal articles or individual chapters in a few books (mainly on charged-particle accelerators) clearly do not embrace the material accumulated up to the present on the considered questions, and in fact are outdated. In addition, the need for such a monograph is emphasized by the fact the results of numerous investigations in this field are frequently contradictory, which strongly hampers practical utilization of available experimental data.

The authors of this monograph have attempted to systematize and generalize information on vacuum electrical insulation and self-maintaining discharge in a vacuum. They considered it necessary to outline as completely as possible the experimental material, paying great attention to examination of the physical processes which determine the electrical insulating properties of vacuum.

Chapter 1 describes the most general properties and the fields of application of vacuum insulation.

Chapter 2 surveys some of the elementary processes occurring on the surface of the electrodes and, apparently, mainly determining the behavior of vacuum insulation. During the description of various forms of emission from the surface, considerable attention was devoted to the influence of imperfections and contaminants on the surface – i.e., the influence of those factors which in the majority of cases lead to the development of processes representing a "danger" to vacuum insulation. The same chapter contains information on the microrelief of the surface and on changes in its state in vacuum and under the action of an electrical field. It should be noted that this brief survey does not pretend to be exhaustive, as it contains only that minimum amount of information which will be useful to the reader as he deals with the subsequent chapters.

The next few chapters (Ch. 3-6) outline experimental data which characterize vacuum insulation with direct, pulse, and high-frequency voltage. Attention should be called not only to the large divergence in experimental results but, as was pointed out above, out to a certain contradiction among the individual data; it would be improper to conceal these contradictions by rejecting, for one or another reason, the apparently "unreliable" data. At the same time, in order to assist the reader in making out the probable true picture, the authors have attempted to reflect as completely as possible the experimental material, drawing attention to the conditions under which an experiment was carried out. In a number of cases additional explanations were given; these indicate possible reasons why certain data or conclusions of the authors might be inaccurate or even erroneous.

Chapter 7 contains a description of discharge in a strongly rarefied gas. A short examination of such discharge along with discharges in vacuum is necessary because even in a comparatively high vacuum in a number of cases conditions can arise in which the processes occurring in a gas may become essential. One example

of such conditions can be the liberation of gas absorbed onto the surface of the electrode into the surrounding space. In certain cases, with certain configurations of the magnetic and electrical fields, there is a sharp elongation of the path of electrons and gas discharge can be observed even at a pressure of 10^{-9} mm Hg, i.e., at pressures which are unquestionably within the domain of vacuum insulation.

Chapter 8 gives a comparative analysis of different processes which may be responsible for the appearance of breakdown. Despite the large number of studies of vacuum breakdown, the mechanism and cause of the appearance of this phenomenon cannot be considered sufficiently clear in all cases; some presentations are to a considerable extent speculative. It was therefore advisable to place into a separate chapter the description of a number of processes and to carry out a comparative analysis of the effectiveness of different processes which may lead to the appearance of breakdown (in the specific conditions of vacuum insulation operation). One of the main conclusions of the analysis of processes leading to breakdown is that the insulating properties of vacuum are determined mainly by imperfections on the surfaces of the electrodes - e.g., by the presence of dust or individual microscopic aggregates (weakly bound to the main mass of the electrode), the presence on the surface of sharp projections, other defects, etc. This conclusion allows us to hope that there is a real possibility for significant increase in the quality and contemporary level of vacuum insulation.

Chapters 1, 3-6 and 8 were written by I. N. Slivkov, Sections 1 and 4-6 of Chapter 2, by V. I. Mikhaylov; Sections 2 and 3 of Chapter 2, by N. I. Sidorov, and Chapter 7 by A. I. Nastyukha.

As the first attemp at a systematized presentation and analysis of very complex and diverse physical phenomena, this book obviously is not without deficiencies and gaps; therefore the group of authors will be grateful for all remarks and suggestions from the readers.

B. M. Gokhberg

DESIGNATIONS

All formulas and empirical expressions in the book are given in the nonrationalized International System for its basic units (if there is no stipulation [to the contrary]); at the same time multiple units are used in the text, tables, and figures for convenience.

Below is a list of conditional designations of the quantities most frequently encountered in the text and in the formulas.

c - specific heat;
C - electrical capacity;
d - interelectrode gap;
D_s - coefficient of surface diffusion;
e - charge of electron
E - electrical field intensity;
$\bar{E}$ - field intensity for ideally flat electrodes.

With real electrodes $\bar{E}=\frac{1}{l}\int_0^l E dl$, near a protuberance, where l characterizes the size of the area in which field is distorted by the presence of a protuberance; outside this area $\bar{E}$ = E.

h - height (of irregularities on the surface of electrodes, etc.);
I - electrical current;
j - density of electrical current;
k - Boltzmann's constant;
K_{ee} - coefficient of secondary electronic emission;
K_{ie} - ion-electron emission coefficient;
K_{ii} - the ion-ion emission coefficient;
l - distance;
m - mass;
p - pressure;
q - charge;

q_s - charge per unit area;
Q - the activation energy;
r - radius;
R - electrical resistance;
s - area;
t - time;
T - absolute temperature;
U - electrical voltage;
v - velocity;
W_k - kinetic energy;
W_p - potential energy;
α_s - coefficient of surface tension;
δ - density of a substance;
ε - dielectric constant [inductivity] of a substance;
ε_0 - dielectric constant of a vacuum;
λ - coefficient of thermal conductivity;
μ - gain factor of an electrical field;
p - resistivity;
σ_i - ionization cross section;
τ - time constant;
Φ - electron work function for a metal.

CHAPTER 1

AREA OF APPLICATION OF VACUUM INSULATION AND ITS PROPERTIES

The properties of vacuum insulation and of discharges in a vacuum have already been studied for about fifty years. During this time a great many studies have been made; the results of these studies are reflected, to one or another degree, in the number of surveys published in the form of journal articles or individual chapters in monographs on charged-particle accelerators (see, for example, [1-5]). The interest in vacuum insulation and in discharges in a vacuum is explained by their ever-increasing practical significance. This is facilitated to no small degree by the continuous penetration of electrical vacuum instruments and equipment into many fields of human activity; a major role is also played by the vigorous growth of comparatively new branches of science and technology, such as nuclear physics and space and plasma research, where electrical processes in vacuum or in a strongly rarefied gas are either the direct object of research or represent a method for accomplishing it.

We can single out three basic areas of application of vacuum electrical insulation and discharge in vacuum.

The first field is characterized by the utilization of certain advantages of vacuum as an insulator as compared with other insulating media. First of all, it permits obtaining very

intense electrical fields and, consequently, substantial voltage between closely spaced electrodes, high densities of the surface electric charge, and significant electrostatic forces. In this case the use of vacuum insulation is determined by its "competitive capability" as compared with other types of insulation (gas and liquid). From this point of view it is useful to compare vacuum and gas insulation; Fig. 1 shows breakdown voltages for vacuum and gas insulation. It is clear that vacuum has the greatest advantage at voltages up to 20-30 kV. The scattering of the values of breakdown voltages in vacuum which is shown on Fig. 1 reflects the great influence of operating conditions on the quality of vacuum insulation; this will be discussed below.

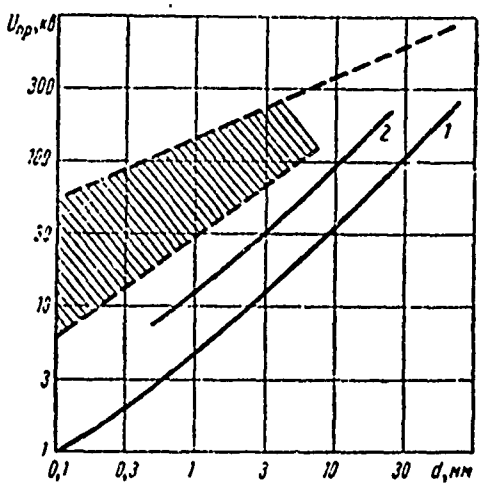

Fig. 1. Dependence of breakdown voltage on interelectrode distance for gas and for vacuum insulation: 1 - air, 1 atm(abs.); 2 - elegas [term not found in available references - Translator's note] 1 atm(abs.). The shaded area relates to vacuum insulation.

Designation: кВ = kV.

[$U_{пр} = U_{br}$]

The further development of vacuum technology and the study of the properties of vacuum insulation should undoubtedly lead to improvements in the latter, with its advantage over the gas type becoming still more substantial. As an example of improvement in vacuum insulation, discovered comparatively recently, we can point to the coating of the cathode with a thin insulating film or the use of semiconductors with ion conductivity as the cathode (Section 8, Ch. 4); this reduces

by several orders of magnitude the currents flowing between the electrodes at voltage below breakdown and also causes the breakdown voltage itself to become noticeably higher than the values of U_{br} shown on Fig. 1 for purely metallic electrodes.

Owing to the relative complexity of obtaining either a vacuum or good surface degassing of parts, in the considered case the application of vacuum electrical insulation is still comparatively small; however, the development of technology and particularly the vigorous growth of space research (with its "cost-free vacuum") will inevitably lead to expansion of the use of vacuum insulation. In certain cases the high quality of vacuum insulation is supplemented by other advantages of vacuum - e.g., absence of losses to friction over gas or fluid when there are moving parts, so that vacuum insulation may turn out to be a very "profitable" during design of electrostatic power generators [6, 7]. One interesting example of the use of the advantages of vacuum and vacuum insulation is the effort to use electrostatic forces for "suspending" in a vacuum the rotor of a gyroscope, rotating at high speed; the reduction of friction in the supports and of fan losses to a minimum is extremely important for operation of this unit [8].

The second of the most important and broadest regions for application of vacuum insulation at present is in those cases when vacuum is the natural medium and basic processes in one or another instrument or piece of equipment cannot be accomplished outside it. This includes the various types of charged-particle accelerators, including electric reaction engines, electron microscopes and the overwhelming majority of the various electro-vacuum instruments. In contrast to the first field, where certain problems can be solved by the application of other types of insulation, in this case there is no choice except to create reliable vacuum electric insulation for those voltages, intensities, and configurations of electrodes which are required for fulfillment of the basic functions. Therefore the ranges of voltages and

other parameters in such an application of vacuum insulation are very wide and very frequently it is a complex problem to guarantee the reliability of the insulation; the solution of this problem frequently limits the design possibilities for one or another instrument or piece of equipment.

The magnitude of the difficulties which can arise due to disturbance of vacuum electric insulation is indicated by the history of development of the strong-current linear ion accelerator MTA, Mark I (Livermore, USA) [9]. This accelerator had truly enormous dimensions. The principal section of the accelerator was a high-frequency resonant cavity over 18 m long and about 17 m in diameter; the ions were accelerated inside it. It was placed in a vacuum tank 18 m in diameter and about 26 m long, evacuated by 44 high-power diffusion pumps. Although it would seem that in the design stage the magnitude of the accelerating field was chosen with a large reserve, at least on the basis of experience with accelerators of smaller sizes, a basic and, in the end, insuperable difficulty was caused by breakdowns during adjustment of the accelerator. The huge dimensions of the resonator meant that a huge quantity of electromagnetic energy would be stored in it. This, together with the negative influence of the magnetic field, which was apparently not foreseen during design, led to a situation in which the electrodes were seriously damaged during breakdowns, which in turn reduced the breakdown voltage. Over the course of a year and a half efforts to obtain stable, breakdown-free operation of the accelerator were unsuccessful; it was disassembled into its constituent parts and further development of strong-current accelerators was carried out on the basis of other electrical and structural parameters.

The third field of application is the direct use of discharge in a vacuum or in a strongly rarefied gas. The possibility of very fast transition without the use of moving parts from high-quality insulation [holding] tens of kilovolts to a high level

of conductivity, with a voltage drop comprising less than 100 V under currents of several kiloamperes, is used in vacuum arresters and in spark vacuum relays. Vacuum arresters have found fairly wide application in laboratory practice for commutation of very high pulse currents [10]. Arresters exist which are capable of switching currents up to 2000 kA at voltages up to 30 kV with a current rise time of $2 \cdot 10^{12}$ A/s [11] and able to switch currents up to 1000 kA at voltages up to 75 kV [12]. Interference-free operation is an advantage of vacuum arresters as compared with those operating on air. In certain cases the fact that the energy required for transfer of the relay or the arrester from the insulating to the conducting state can be very small may be of significance. Thus, an energy of 5 μJ is sufficient to "connect" spark relays on 20 kV and a pulse current of several kiloamperes. These relays have good time characteristics; the instability of activation time is less than ±8.5 ns, while the current rise rate reaches 10^{11} A/s [13].

Spark discharge in a vacuum is used to obtain very powerful pulses of X-radiation and pinches of highly ionized plasma. Sources of powerful X-ray bursts were developed; these made it possible to obtain an X-ray picture of a steel pig 70 mm thick in the course of a single impulse with a duration of 0.2 μs. A group of 4-8 such sources, operating in strict time sequence, provided photographs of massive parts moving at a speed up to 5 km/s [14]. The rapid restoration of the electrical strength of the vacuum gap after termination of discharge (for example, during transition through zero with variable voltage) makes it possible to create high-speed high-voltage switches [15, 300]. We should also note the ever expanding application of special types of discharge and strongly rarefied gases for measuring and producing vacuum, especially in the area of very low pressures. Although the characteristics of the instruments utilizing discharge in a vacuum - e.g., vacuum arresters, relays, and pulse X-ray tubes - are in a certain sense record-setting, these instruments

are as yet used mainly in laboratory practice; their broader application is, in certain cases, impeded by limited service life (longevity) if they are made as nondemountable and mechanically nonadjustable instruments.

As is known, the appearance of self-maintaining discharge between electrodes located in a gas in a very wide range of pressures is determined by processes in the gas itself, although at pressures substantially above atmospheric and those below several millimeters of mercury processes on the surface of the electrodes begin to play a significant role. The gas nature of the appearance of discharges, as a rule, is determined by the dependence of voltage of discharge appearance on the product of gas pressure p and interelectrode distance d; on the low-pressure side it has been traced down to a value pd = 0.02-0.04 (mm Hg)·cm. At low pd there is a region of vacuum insulation in which the appearance of discharge is determined by processes on the electrode, with the pressure and composition of the residual gas with vacuum insulation playing a role only to the degree to which the state of the electrode surfaces depends on them. The transition from a gas nature of discharge appearance to the vacuum nature is manifested outwardly primarily by a change in the dependence of the voltage of appearance of breakdown on pressure; to be exact, this means that there is a reduction in growth of U_{br} with a reduction in p, which is observed during gas discharge in the left branch of the Paschen curve - i.e., when pd < 0.1-1 (mm Hg)·cm. The pressure at which such a transition occurs depends on many factors, in particular on the gap size d and the state of the electrode surfaces: the larger d and the cleaner the electrodes, the smaller the pressure. The experimentally determined boundary of gas discharge pd = 0.02-0.04 (mm Hg)·cm indicated above corresponds to an interelectrode distance of more than 100 mm, while U_{br} is measured in this

case in tens and hundreds of kilovolts [16]. At small gaps the voltage of appearance of vacuum breakdown, i.e., breakdown caused only by processes of the electrodes, may be smaller and therefore the transition from the gas nature of breakdown to the vacuum type occurs at large values of pd.

As a rule, visual observations also allow distinguishing between gas and vacuum discharges: at low pressures, in the domain determined by the left branch of the Paschen curve, the gas discharge develops over the maximum distance between electrodes, where pd is great, while vacuum breakdown arises at the point where the electrical field intensity is close to maximum - i.e., with the smallest distances between the electrodes. However, this "separation" of gas and vacuum discharges is not always manifested in pure form. For example, desorption of gas during various processes of the electrodes can lead to a situation in which vacuum breakdown between the electrodes at the point of maximum field intensity is accompanied in a number of cases by a gas burst encompassing the entire volume. Such gas bursts due to desorption of gas frequently arise in the initial stages of adjustment of electrodes under voltage even with a very low average pressure value.

The nature of breakdown of vacuum insulation depends on the magnitude and form of the applied voltage and the conditions on the electrodes. With direct voltage, in the general case we can observe three basic forms of breakdown of vacuum insulation: first the manifestation of more or less stable dark or predischarge currents with a density less than 10^{-5}-10^{-4} A/cm^2; second the appearance of periodically repeating self-extinguishing low-power pulses (on the order of 10^{-4}-10^{-3} A) of current - microdischarges not accompanied by any noticeable drop in voltage on the electrodes; third there is a more serious disruption of vacuum insulation - breakdown, i.e., the appearance of spark discharge with a sharp

voltage drop on the electrodes and, when the electric power is sufficiently powerful, with a subsequent transition to arc discharge in vapors of the electrode material. Although the enumerated disruptions of vacuum insulation grow continuously in succession, due to the different dependence of these phenomena on conditions on the electrodes, on voltage, etc., they do not always precede one another. In certain cases, for example, there are no microdischargees; in other cases they precede the appearance of noticeable dark currents, etc.

With high-frequency voltage on the electrodes there can be dark currents and breakdown without microdischarges. However, we may observe a type of discharge which arises and exists only under high-frequency voltage - secondary electron resonance discharge. In this case secondary electron emission on both electrodes is of decisive value; the electrodes successively become cathode and in different segments of the period of the high frequency voltage the electrons can move first in one and then in the other direction.

The passage of dark currents and currents during microdischarges between the electrodes in a vacuum, and in particular the event of breakdown, causes erosion of the electrodes and transfer of material from one electrode to the other. As a result the microrelief and the other properties of the electrode surface are changed, which is reflected in the quality of the vacuum insulation.

Vacuum electrical insulation must meet widely varied requirements. For example, in high-voltage accelerating tubes which operate with electrostatic generators the appearance of microdischarges or dark currents of even small magnitude represents an impermissible disruption of vacuum insulation;

this stems from the fact that the working current in these accelerators normally comprises a few, one, or even a fraction of a milliampere. In certain cases a dark current will not directly disrupt the operation of the apparatus, but the electron component of the dark current creates intensive X-radiation which in turn requires creation of special radiation shielding. In certain instruments, especially those operating on pulse voltage, the requirements imposed on vacuum insulation are not so rigid. Frequently substantial dark currents and even individual breakdowns are tolerated in them. In different studies the term breakdown of vacuum insulation is frequently applied to different phenomena - mainly to those which limit the voltage rise on the electrodes in a given specific case. This fact must be kept in mind during analysis of the results of various studies.

One of the particular features of vacuum insulation which must be dealt with in practice is the exceptionally great divergence in experimental values of the voltages - intensities on the electrodes - at which one or another type of disruption of vacuum insulation will appear. For example, the voltage at which dark current of one or another magnitude appears can differ by 2-3 times for a pair of electrodes which are identical in shape, manufactured from a single piece of metal by an identical process, placed in exactly the same vacuum system and set at an equal interelectrode distance. The divergence in the magnitudes of breakdown voltages is also great. Divergence of 1.5-3 times can be observed during measurements of breakdown voltage with all other conditions remaining unchanged and with the same identical electrodes. A substantial improvement in the quality of vacuum insulation can be obtained by proper selection of the conditions under which currents of microdischarges and successive breakdowns proceed. This fact is widely used and is designated as "training" or "conditioning" of the electrodes.

The described "inconsistency" in the quality of vacuum insulation is explained by the very nature of the processes which arise when it is disrupted and which depend decisively on the state of the electrode surfaces - not the entire surface, but individual segments which "favor" these processes. The dimensions of such segments can be measured as a whole only in microns on electrodes with areas of several square centimeters. In certain cases the quality of vacuum insulation is substantially altered by the presence on the electrodes of oxides, foreign inclusions, and adsorbed vapors of organic compounds. The role of the surface microrelief is significant. Here we should note that the overwhelming majority of methods of monitoring the quality of the surface ensure the preparation of only averaged surface characteristics which, as a rule, do not reflect the presence on the surface of the "weak" points indicated above, which determine the quality of the vacuum insulation. Thus, certain of the processes which substantially disrupt vacuum insulation arise on the sharp mocroscopic protuberances whose number can be measured as several per cm^2 on a carefully polished surface. Owing to their small number, detection of these projections represents a problem which is not practically soluble with ordinary methods of surface checking, including microscopic methods. A change in the dimensions of such protuberances and their appearance and disappearance substantially change the quality of vacuum insulation, but are not reflected in the presently existing criteria of surface smoothness. This is also true for the presence of various contaminants and foreign inclusions, etc., on the surface. For this reason the overwhelming majority of investigations of vacuum electrical insulation are carried out with inadequate knowledge of conditions on the surface of the electrodes, which continuously change both under the action of the currents flowing in the vacuum (dark currents and those during breakdowns and microdischarges), and also because of the action of the electrical field on certain surface processes. However, despite this situation, which appears

at first glance to be so unfortunate, the actual state of affairs with regard to the study of properties of vacuum insulation does not actually give any basis for pessimism. There are a few works in which data were obtained which represent the result of a very great number of measurements (which substantially increases their confidence level) and in which the majority of possible conditions influencing the behavior of vacuum insulation has been refined. In many cases in order to achieve a more or less stable (although inadequately known) state of the surface, special treatment of the electrodes was applied over the entire cycle of measurements. Therefore the totality of most of the studies already carried out not only permits obtaining sufficiently reliable data concerning many of the characteristics of vacuum insulation which are of practical importance, but also it represents a large and valuable mass of material for clarification of the physical processes which determine the behavior and characteristics of vacuum insulation. This in its turn allows us to seek methods for improving vacuum insulation.

The various characteristics of vacuum electrical insulation are described in detail in the following chapters. Here we merely wish to emphasize that the available experimental data already permit significant improvement in the working characteristics of a whole series of instruments and devices. Through successful selection of material and electrode configuration, and also by treating them, it is possible to increase the quality of vacuum insulation very substantially. In this connection it would be desirable to call attention to the dependence of breakdown voltage on the parameters of the electrical circuit. This dependence is quite strong; however, in many cases investigators do not take it into account, even when they are particularly concerned with the study of vacuum breakdown.

While in the majority of specialized works the role of effective resistance in the discharge circuit is somehow taken into account and while the magnitude of this resistance is selected fairly frequently, the works in which the influence of shunting capacity (the capacities of the electrodes themselves and of the elements connected directly to them) can be counted on the fingers of one hand. The magnitude of this capacity determines the reserve energy, while the resistance in the discharge circuit determines the magnitude of current flowing after breakdown. Improper selection of the parameters which influence the erosion of the electrodes (as was clearly indicated on the example of the MTA Mark I accelerator cited above) can lead to very unfortunate results. Certainly, the study of vacuum insulation is far from perfection, and much effort will be required both to obtain characteristics of practical importance and more reliable application of vacuum insulation, and also for a clearer presentation of the manifold physical processes which cause its disruption.

CHAPTER 2

ELEMENTARY PROCESSES AND THE STATE OF THE ELECTRODE SURFACES

1. THERMIONIC AND FIELD-EFFECT EMISSION FROM METALS

Homogeneous surfaces. In obtaining emission equations the usual procedure is to simulate the metal with an electron gas in a potential well (in the ideal case, rectangular), whose depth W_a is determined by the difference in the values of the potential energy of the electron in a vacuum free from the field and inside the metal. Such a model does not permit drawing any conclusions regarding the shape of the potential barrier; therefore it is usually supplemented with an image force acting on the charge at the metal surface and it is usually assumed that the electron work function $\Phi = W_a - W_{f0}$ (where W_{f0} is the Fermi energy limit) is work in opposition to the force. In the given case the potential energy of the electron outside the metal (counting from the value of electron energy at rest in a vacuum at infinity) is described by the expression

$$W_p = -\frac{e^2}{4\varepsilon_0 x} - Eex, \qquad (1)$$

where the second case considers the action of a uniform external electrical field E which can be created at the surface (Fig. 2). Thus, the shape of the barrier in the near zone turns out to be indefinite; however this is not essential in the derivation of

the emission relationships. As follows from expression (1), the accelerating electrical field changes the shape of the barrier and reduces its height to the magnitude $W_m = e\sqrt{eE/\varepsilon_0} =$ $= 6{,}06 \cdot 10^{-24}\sqrt{E}$ J $= 3{,}79 \cdot 10^{-5}\sqrt{E}$ eV (the Schottky effect).

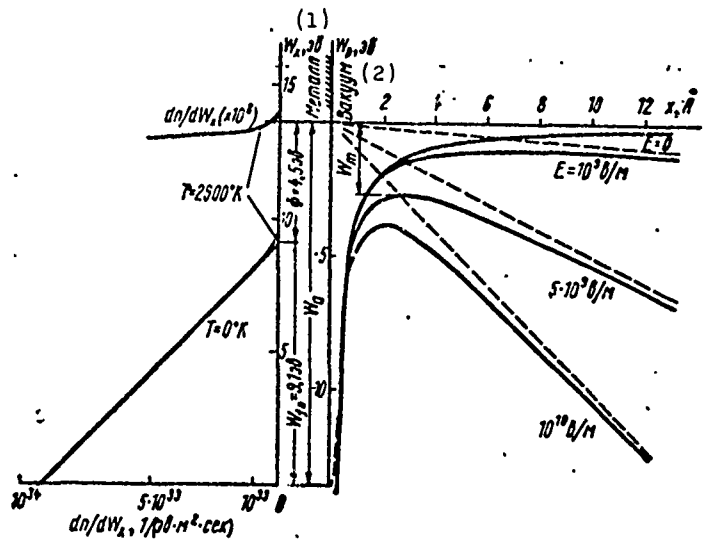

Fig. 2. Energy distribution [see equation (2)] and shape of the potential barrier with different fields for tungsten.

KEY: (1) Metal; (2) Vacuum.

[эВ = eV; В/м = V/m, сек = s].

To calculate the emission current it is necessary to know the quantity of electrons dn arriving from within the metal per unit area of its surface (direction of the normal along the x axis) and having kinetic energy determined by the normal component velocity within the limits from W_x to $W_x + dW_x$. Application of the Fermi-Dirac quantum statistics to the considered model of free electrons leads to the expression

$$\frac{dn}{dW_x} = 8{,}65 \cdot 10^{28}\, T \ln\left(1 + \exp\frac{W_f - W_x}{kT}\right) 1/(\text{eV} \cdot \text{m}^2 \cdot \text{s}). \qquad (2)$$

Here $W_f = W_{f0}\left(1 - \frac{\pi^2}{12}\frac{k^2T^2}{W_{f0}^2}\right)$. At actually achievable temperatures $kT \ll W_{f0}$ (for example, for tungsten when T = 3000°K, $kT \approx 0{,}03\, W_{f0}$), since $W_f \approx W_{f0}$. The shape of the given energy distribution is shown

on Figure 2 for tungsten (W_{f0} = 9.1 eV and Φ = 4.5 eV) when T = 0°K and T = 2900°K. In the region $W_x = W_a$ a portion of the curve is shown with the ordinate increased by 10^8 times.

The framework of wave mechanics provides a very substantial basis for an essential role of the transmission coefficient of the potential barrier $D(E, W_x, \Phi)$, which is considered as the probability of reflection of electrons with energy $W_x > W_a - W_m$ during their passage above the barrier, and also as the probability of passage of electrons with $W_x < W_a - W_m$ through the barrier (tunnel effect).

Thus, the quantity of electrons determined by equation (2) multiplied by the probability of their passage through the barrier and integrated over all values of energy will give the magnitude of the density of the emission current:

$$j = \int_0^\infty D(E, W_x, \Phi) \frac{dn}{dW_x} dW_x \text{ electron/(m}^2 \cdot \text{s)}. \qquad (3)$$

The analytical expression for j can be obtained only in a number of cases by using different approximate expressions for the coefficient of transmission D, depending upon external conditions (T, E).

The entire range of temperatures and fields can be tentatively divided into three regions: thermoionic (high temperatures and weak fields), field-effect (strong fields and comparatively low temperatures), and intermediate.

In the case of high temperatures and E → 0, the use of the classical approximation for the transmission coefficient

$$D = \begin{cases} 1 \text{ when } W_x > W_a, \\ 0 \text{ when } W_x < W_a \end{cases} \qquad (4)$$

after integration of expression (3) leads to the Richardson-Dushman equation [17], determining the density of the thermionic current:

$$j = A_0 T^2 \exp\left(-1{,}16 \cdot 10^4 \frac{\Phi}{T}\right) \text{ A/m}^2, \qquad (5)$$

where $A_0 = 2 \cdot 10^6$ A/(m^2·deg^2), while Φ is measured in electron volts.

With consideration of the Schottky effect the condition similar to (4) takes on the form

$$D = \begin{cases} 1 \text{ when } W_x > W_a - W_m, \\ 0 \text{ when } W_x < W_a - W_m, \end{cases} \qquad (6)$$

where the Richardson-Schottky equation follows from expression (3):

$$j = A_0 T^2 \exp\left[-\frac{1{,}16 \cdot 10^4}{T}(\Phi - 3{,}79 \cdot 10^{-5}\sqrt{E})\right] \text{ A/m}^2. \qquad (7)$$

Table 1 gives the values of emission current density calculated by equation (5) for Φ equaling 4.5 and 3.5 eV at various temperatures, indicating the strong dependence of current density on Φ; this dependence is explained by the form of the distribution (2).[1] The relationship of expressions (7) and (5), equal to $\exp(0{,}44\sqrt{E}/T)$, shows the number of times by which the intensity of emission is increased due to the Schottky effect. These relationships, and also the magnitudes of the reduction in the potential barrier W_m, are given in Table 1 for a number of values of T and E.

[1]Actually, on Fig. 2 the quantity of emitted electrons is proportional to the shaded area of the curve dn/dW_x, lying above the value W_a = 13.6 eV. In view of the extremely steep nature of the curve close to W_a, even an insignificant reduction in the work function leads to an essential increase in the number of emitted electrons.

Table 1. Density of thermionic emission current with E = 0 and coefficient of current gain with different fields.

T°, K	j, а/м²		exp $(0.44\sqrt{E}/T)$		
	Φ=4.5 эв	Φ=3.5 эв	$E=5\cdot10^7$ в/м, $W_m=0.27$ эв	$E=10^8$ в/м, $W_m=0.38$ эв	$E=5\cdot10^8$ в/м, $W_m=0.85$ эв
500	$7\cdot10^{-35}$	$9\cdot10^{-25}$	$5{,}6\cdot10^2$	$6{,}2\cdot10^3$	$3{,}5\cdot10^8$
1000	$1{,}4\cdot10^{-11}$	$1{,}5\cdot10^{-6}$	23	79	$1{,}7\cdot10^8$
1800	0,62	$4\cdot10^2$	5,6	11,5	$2{,}34\cdot10^8$
2500	$3\cdot10^3$	$3{,}3\cdot10^5$	3,5	5,8	50

Designations: эв = eV; в/м = V/m; а/м^2 = A/m^2.

When E grows to such a degree that the width of the potential barrier, at least in the region of its peak, is substantially reduced, so that the tunnel effect becomes noticeable in this region, the transmission factor with $W_x < W_a - W_m$ can no longer be considered equal to zero. In this case we can obtain the following expression for emission current density [18]:

$$j = j_1 + j_2 = j_1 \frac{1}{1-\eta} = j_2 \eta, \qquad (8)$$

valid when $\eta \ll 1$, where $\eta = 1.65\cdot10^{-4}\, E^{3/4}/T$; j_1 is the density of thermionic current determined by equation (7); j_2 is the density of the current caused by the tunnel effect. The tentative boundary between conditions at which either the current due to the tunnel effect or that due to the Schottky effect will predominate can be found by setting $j_1 = j_2$ in expression (8) (in this case $\eta = 0.5$). Such a boundary is determined by the value $E = 4.37\cdot10^4\, T^{4/3}$ (Fig. 3). Below this line $j \approx j_1$ and its magnitude can be evaluated according to equation (8), while above this line the emission current is caused basically by the tunnel effect. Figure 3 also shows the line corresponding to the value $\eta = 0.05$. For the totality of values of E and T which form a region below this line, from equation (7) it follows that the values of emission current density, depressed as

compared with the values calculated by equation (8), will be less than 5%. Thus, the current in the thermionic region is determined by equations (5), (7) and (8).

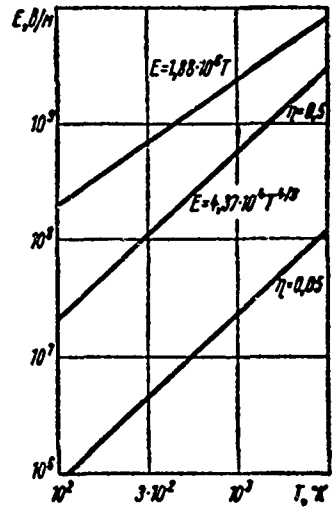

Fig. 3. Areas of application of emission equations (7), (8) and (10).

Designation: В/м = V/m.

When finding the current in the field-effect region, integration of equation (3) is simpliest when the emission above the barrier can be ignored - i.e., when $T \to 0$ [19, 20]. The result of integration under these conditions is the Fowler-Nordheim equation, which defines the density of the field-effect emission current:

$$j = 1{,}54 \cdot 10^{-6} \frac{E^2}{\Phi} \exp\left[-6{,}83 \cdot 10^9 \frac{\Phi^{3/2}}{E} \theta(y)\right] \ \text{A/m}^2. \qquad (9)$$

Here $\theta(y)$ is the Nordheim function, whose variable equals $y = 3.79 \cdot 10^{-5} E^{1/2} \Phi^{-1}$ (Table 2). In equation (9) the work function Φ is measured in electron volts. Table 3 gives values of j calculated according to equation (9). Detailed tables of a similar type, compiled by Golan, can be found in works [19, 21, 22].

Table 2. Nordheim functions $\theta(y)$.

y	0	0,1	0,2	0,3	0,4	0,5	0,6	0,7	0,8	0,9	1
θ	1	0,98	0,94	0,87	0,79	0,69	0,58	0,45	0,31	0,16	0

Table 3. Field-effect emission current density, A/m^2, according to equation (9) at different values of the electric field and work function.

$E \cdot 10^{-9}$ в/м	Φ=2,5 эв	Φ=3,5 эв	Φ=4,5 эв	Φ=5,5 эв
1	$2,9 \cdot 10^{3}$	$2,3 \cdot 10^{-5}$	—	—
2	$3,9 \cdot 10^{9}$	$2,5 \cdot 10^{5}$	4,8	$3,2 \cdot 10^{-5}$
4	$6,3 \cdot 10^{13}$	$3,7 \cdot 10^{10}$	$1,3 \cdot 10^{8}$	$2,8 \cdot 10^{6}$
6	—	$2,4 \cdot 10^{13}$	$4,8 \cdot 10^{10}$	$6,8 \cdot 10^{8}$

Designations: в/м = V/m; эв = eV.

It should be noted that in connection with the deviations from equation (9) which were detected at large densities of the emission current, efforts were made to correct this equation [23] or to create a theory new in principle [24]. Gofman [25] conducted a study of field-effect emission from tungsten in a broad range of current densities; one goal of the work was to carry out a comparison of the results obtained with equation (9) with the indicated calculations. However, an error with a magnitude of 10-15%, unavoidable when calculating E from geometric considerations, prevented him from giving preference to any of these relationships.

The temperature dependence of current in the field-effect emission region is described by the equation obtained by Good and Müller [20]:

$$j(T) = \frac{j(0)\pi\beta}{\sin \pi\beta}, \qquad (10)$$

in which j(0) is determined by equation (9), while $\pi\beta = 2{,}77 \times 10^4 T\sqrt{\Phi}/E$ (Φ in electron volts). The equation is applicable in the range of fields $E > 8{,}83 \cdot 10^5\ T\sqrt{\Phi}$ V/m. The corresponding boundary line for Φ = 4.5 eV, i.e., $E = 1.88 \cdot 10^6$ T, is shown on Fig. 3. For example, when $E = 4 \cdot 10^9$ V/m, Φ = 4.5 eV and $T = 1000°K\pi\beta = 1{,}5$, while from (1) it follows that j(T) = 1.5j(0).

The analytical relationships for the emission current for intermediate values of fields and temperatures were obtained by Murphy and Good [26, 27] and by Guthe and Mullin [28]. The relationships for the thermionic and field-effect emission regions are given in these same works.

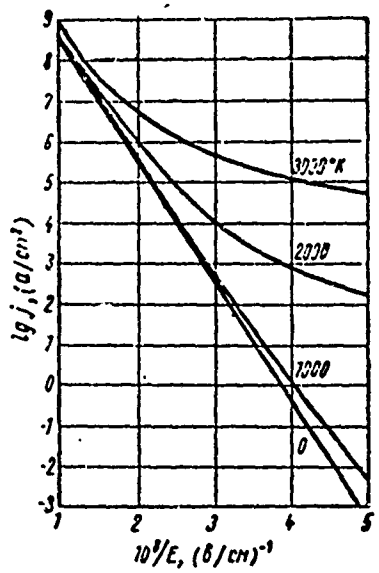

Fig. 4. Calculated dependences of emission current on electric field intensity at different temperatures for ϕ = 4.5 eV [22, 29].

Designations: $a/см^2 = A/cm^2$; $B/см = V/cm$.

Numerical integration of equation (3) for the field interval $2 \cdot 10^9 - 1 \times 10^{10}$ V/m and temperatures from 0 to 3500°K were carried out by Dolan and Dyke [22, 29]. The relationships for Φ = 4.5 eV which they obtained are shown on Fig. 4. The calculation results are confirmed by measurements carried out in the region $E = 2.6 \cdot 10^9$ to $7.0 \cdot 10^9$ V/m with the temperature varied from 300 to 2000°K [30].

Real surfaces. Equation (3) and all of the theories of emission processes whose development is based on it are, strictly speaking, valid for an ideally flat metallic surface with a uniform work function. In the real case the cathode surface may be substantially nonuniform with respect to work function and the magnitude of the electrical field. The presence of nonuniformities can lead to a situation in which the true value of the electrical field E will differ significantly from its average macroscopic value $\overline{E}$. In these conditions the effective emitting area may also depend on the microgeometry and nature of the nonuniformity of the work function. All of these factors are quite complex to take into account even when single-crystal emitters are used; the application of such emitters is characteristic for the majority of specific emission studies [19, 25, 30, 31].[1] Investigation of emission processes in a variety of cases of the technical application of vacuum as an insulating medium leads to a need to examine polycrystalline metal surfaces formed by different various microcrystal facets as emitters. The difference in the work function of crystal facets, and also the presence on the surface of a coating formed by foreign atoms, in combination with microirregularities will lead to a clearly expressed nonuniformity in the distribution of emission current from the surface of a polycrystalline emitter (Fig. 5).[2] Adjustment of the surface can cause a continuous change in the emission picture.

[1] For example, as Gofman showed in [25], the usual procedure for evaluating the emitting surface of a knife-edge emitter [translation not verified - Translator's Note] does not take into account the actual distribution of current density; according to his data, the emission current arrives basically from the region separated from the peak of the spike by an angle of about 30°.

[2] An electrical field determined by the contact potential difference arises between segments with different work functions (spots). The field of spots is relatively weak (on the order of 10^4 V per cm) and can affect emission only when the external fields are small [33].

In view of the fact that it is difficult to obtain quantitative data concerning nonuniformities on the investigated surfaces,[1] under real conditions the essential difficulties arise with respect to identification of the measured emission currents from polycrystalline emitters. The usual experimental procedure is to find the dependence of current I from several sufficiently large segments of the cathode surface (or from the entire cathode) on the average value of the electrical field $\bar{E}$. If the results demonstrate a linear dependence of the type $\ln I \sim \sqrt{\bar{E}}$, the Richardson-Schottky equation (7) is used to obtain data on particular features of the emitting surface; the application of of this equation makes it possible to find the field gain factor $\mu = E/\bar{E}$ and the ratio between the effective emitting area S and the work function Φ. The linear dependence between the quantities $\ln (I/\bar{E}^2)$ and $1/\bar{E}$ is the basis for using the equation of field-effect emission (9). The use of the Fowler-Nordheim relationship, (9), leads to equations which connect S with Φ and Φ with μ in pairs. By selecting a certain value for Φ or μ, it is possible to obtain values of the remaining two parameters.[2]

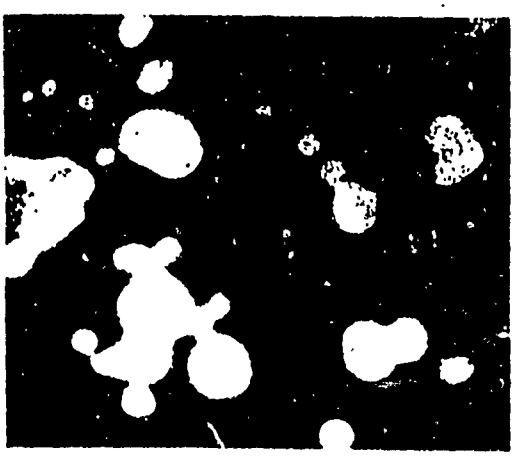

Fig. 5. Picture of field-effect emission from a molybdenum cathode 1 mm in diameter; picture obtained by Tuczek [32].

[1]More briefly, the study of emission relationships is one of the methods of obtaining such data.

[2]Study of this system of equations is usually difficult to accomplish. Charbounnier and Martin [34] proposed a simple method which, in a number of cases, substantially simplifies the procedure for obtaining the final data.

Robertson et al. [35], while interpreting emission currents as currents of field-effect emission, also investigated the temperature dependence of emission in the region of strong fields. They used equation (10) to describe this dependence. This made it possible to find an additional relationship for μ and Φ and, consequently, independent values of S, μ and Φ.

Young and Müller [36] proposed that in addition to studying the temperature dependence of the emission, to obtain an independent determination of μ and Φ measurement of the energy distribution of field-effect electrons should be used; however, this presents an extremely complex experimental problem.

The divergence in experimental values of the relationship $I(\bar{E})$ frequently prevents reliable selection between equations (7) and (10), a fact which introduces an essential indeterminance in the obtained results [37-40]. To clarify the degree of confidence of the obtained data it is possible to use direct electron microscope investigation of the surface [41]; this may be of assistance in assigning preference to one or another emission mechanism.

Unquestionably, during such evaluations it is extremely desirable to have available information on the nature of surface irregularities, values of μ for projections of different geometry, magnitudes of work functions of metals under different conditions, etc. These problems will be examined in the following sections.

2. MICROGEOMETRY OF THE SURFACE

The condition of the surface of metallic electrodes has an essential influence on electrical processes developing in the vacuum gap. Many experimental data such as the dependence of breakdown voltage on electrode material in the prebreakdown stage and in the process of electrical breakdown itself, changes in the characteristics of microbreakdowns during absorption of various gases, and also many other data attest to the definite influence of the state of the electrode surfaces on the properties of vacuum insulation.

The existence of surface microrelief inevitably manifests itself in the fact that the operative external electrical field, E, at each point of the surface of the electrodes will differ to a greater or lesser degree from its average value $\bar{E}$, corresponding to an ideally smooth surface.

For calculation of the field of individual projections it is possible to use the solution of a problem known from electrostatics - the problem of a conducting ellipsoid located in an external field parallel to one of the major axes of the ellipsoid [42]. This is equivalent to a semiellipsoidal projection located on a flat surface. However, the relationships ordinarily applied during calculations of such fields, in which the major semiaxes figure as parameters, do not possess simplicity and clarity. If the radius of curvature of the peak of the projection r is used as one of the parameters the formulas are substantially simplified. On the peak of a semiellipsoidal projection which has the form of a body of revolution, the field gain factor $\mu = E/\bar{E}$ can be presented in the form

$$\mu = \frac{\beta h}{r} + 1, \tag{11}$$

where β is a slowly and smoothly varying function of h/r: when h/r = 5-250, β = 1.0-0.4, i.e., μ is virtually proportional to h/r. The dependence of μ on h/r is shown on Fig. 6.

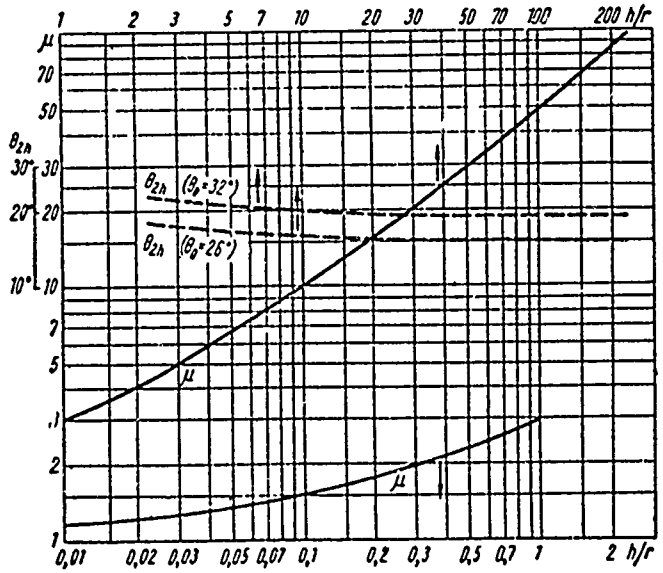

Fig. 6. Dependence of field intensity gain factor μ on the magnitude of the parameter h/r, characterizing the shape of an elliptical peak. (For curves of Θ_{2h} see in Chapter 3).

If the semiellipsoidal projection is not a body of revolution but has an extended form in the top view, the value of μ for its peak is close to the mean geometric quantity calculated for ellipsoids of revolution with radii of curvature equal to the minimum and maximum values of the curvatures of the extended ellipsoid.

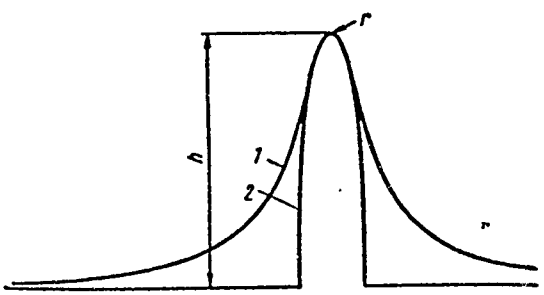

Fig. 7. Various forms of the cusp creating approximately identical intensification of the field at the peak.

By taking intermediate equipotentials of the ellipsoid field as projections we can substantially expand the "assortment" of configurations of projections whose fields may be approximated by relationships connected to ellipsoids. If we characterize the contour of the intermediate equipotential, taken as the contour of the projection, by the same parameters h and r for the axisymmetrical case (the projection is a body of revolution), then expression (11) is valid also for this case, while the quantity μ is close to the corresponding values for ellipsoids. As an illustration Fig. 7 shows the contours of two projections with identical values of h and r; one has the form of a semi-ellipsoid (2), while the other has the form of an intermediate equipotential of a more extended ellipsoid (1). Although their widths differ by 1.62 times even half way up the projections, the value of μ is only 6.5% less for the wider protuberance. The work by Lewis [43] examines the strengthening of the field produced by a system of parallel mounds with the form of an ellipse in cross section. Field strengthening at the peak of such ridges depends very strongly on the distance between them and drops rapidly with distance from the peak of the projections (see page 103).

Numerous measurements of electronic emission from smooth surfaces of metallic electrodes in a vacuum at room temperature in comparatively small electrical fields (on the order of 10^5 V/cm), permit us to speak of significance strengthening ($\mu \approx 20$-70 and more) of the electrical field which occurs on microirregularities of the surface [35, 37, 44]. In the work by Bennette et al. [44], for example, the coefficient of electric field intensification μ, which was evaluated from observations of currents by means of the Fowler-Nordheim equation, fell within the limits 10 to 340.

Experiments of this type, however, do not permit direct judgement of the geometric parameters of the emitting centers.

The use of a procedure which combines observations with a light screen and optical and electron microscopes made it possible to observe single emitting microcusps on the polished surfaces of electrodes. The experimental installation used in the works by Little and Whitney [41] and Little and Smith [45] included a glass anode with transparent conducting and fluorescent layers applied to it. A cathode about 12 mm in diameter (in the form of a Rogovskiy electrode) was installed approximately 0.4 mm from the anode. The cathodes were manufactured from various metals: stainless steel, tungsten, nickel, tantalum, copper, aluminum, and magnesium. The cathode surface was polished either mechanically or electrochemically. Vacuum (on the order of 10^{-7} mm Hg) was created in the system by an ion-sorbtion pump.

Emission currents appearing at a voltage of about 7 V were noted by illumination of the sensitive layer on the anode.

During study of emitting centers with an optical microscope (examining the surface of the cathode through the transparent anode), they observed surface irregularities whose dimensions could not be evaluated due to inadequate magnification (×300). Investigation of emitting segments of the surface by means of a shadow electron microscope permitted detection of single needle-like projections with a height of approximately 2 μm and a diameter-to-height ratio comprising 0.1. Figure 8 shows photographs of cusps on optically polished surfaces of cathodes made from aluminum, nickel, and silver.

As the evaluations show, electrical fields exceeding the average value by several tens of times can be created on such points.

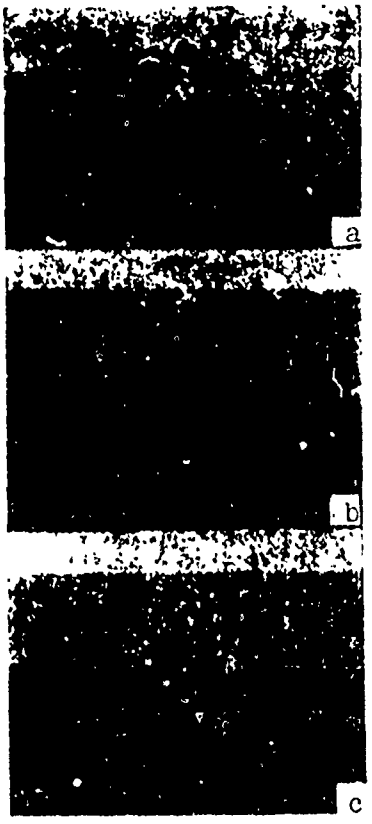

Fig. 8. Micropoints on optically polished surfaces of different metals (×1000): a - aluminum; b - nickel; c - silver.

On the basis of these results we can conclude that the existence of a small number of such projections on the surface of the electrodes is possible; these projections do not correspond to the ordinary characteristics of microirregularities arising, for example, as the result of treatment or of particular features of the crystalline structure of the surface. We will note in this connection that the voltages at which emission currents are initiated under different electrodes [41] manufactured from a single piece of metal and subjected to identical treatment sometimes differ by as much as three times. Kerner [37] remarks that emission properties are sometimes identical on surfaces which are different with respect to treatment (after turning or polishing).

Sing_e microcusps located in electrical fields can experience the action of significant stretching forces; as a result processes leading to a slow elongation and subsequent breakaway of the point become possible. The rate at which these processes occur, dependent on specific conditions existing on the electrode (e.g., on heating of the point by currents flowing over it), can determine the moment of onset of vacuum breakdown. Denholm [46] attempted to establish the correspondence between the time when voltage is applied to the electrodes and the square intensity of the electrical field at which arcing of the gap occurs. For this purpose he used an empirical relationship obtained during investigations on crystalline tungsten wire; according to this relationship, with constant temperature the time of breakaway t under the action of tensile force F_s is determined by the expression

$$t = a \exp\left(-\frac{F_s - b}{c}\right), \qquad (12)$$

where a, b, and c are constants. Denholm used experimental values of E_{br} for steel electrodes at different voltages - pulsed, variable, and slowly-rising direct voltage. Figure 9 shows the dependence of E_{br} on the magnitude of the gap between electrodes for these voltages. As the time interval for action of electric forces he selected the time during which the electric field intensity exceeds 90% of its maximum value. This limitation was made arbitrarily on the basis of the fact that large electrical fields are the most effective. Thus the experimental data covered the approximate time interval from 14 μs to 0.9 s. In this approximation the experimental values of breakdown intensities were connected with the breakdown delay time by a relationship coinciding with expression (12):

$$t = 14{,}2 \exp\left(-\frac{E_{np}^2 - 9700}{8700\, d'}\right) \text{ s.}$$

[np = br]

where E_{br} is the intensity at the moment of breakdown in kV per mm and d' = 0.51-0.88d (d is the gap between the electrodes and millimeters).

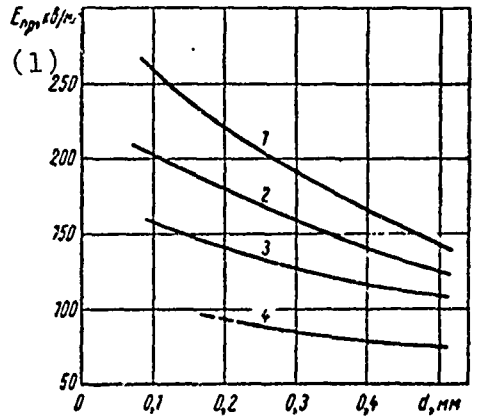

Fig. 9. Maximum values of electric field intensity during breakdown of steel electrodes: 1 - pulse voltage, pulse shape 12/50 μs; 2 - alternating voltage, 50 Hz; 3 - direct voltage with a rise time of 6 kV/s; 4 - insulating strength.

KEY: (1) E_{br}, kV/mm.

As an illustration we will introduce some evaluations of forces arising on a projection and the time of point breakaway.

For an average intensity of approximately 80 kV/mm and with a gain on the point of μ = 12.5 the mechanical stress equals about 41.5 kg/cm^2.[1] With heating to 960°C breakaway of the point from carbon steel occurs in this case after approximately 1 hour.

A certain degree of roughness is inherent to any metal surface. Real surface reliefs are shaped under the influence of conditions and methods of treatment, thermal action, the electrical field, and other factors.

[1] An electric field strengthening of μ = 12.5 is created, for example, by a single point of elliptical form with a ratio of height to base diameter of 1.8.

In accordance with accepted standards surface roughness is determined by one of the following parameters (per [GOST] (ГОСТ) All-Union State Standard 2789-59):

1. Mean arithmetic deviation R_a - the average value of distances (y_1, y_2, ..., y_n) are points of the measured profile to its average length:

$$R_a = \frac{1}{l}\int_0^l |y|\,dx.$$

Surface relief is considered within the limits of a certain base length l which is characteristic for the given type of irregularity.

2. Height of irregularities R_z - average distance between five high points of projections and the low points of depressions located within the limits of the base length (measured from a certain line parallel to the average line of the profile):

$$R_z = \frac{(h_1 + h_3 + \ldots + h_9) - (h_2 + h_4 + \ldots + h_{10})}{5}.$$

Table 4 gives the values of R_a, R_z, and l for various classes of surface finish.

Table 4. Values of R_a and R_z for different classes of surface finish.

(1) Класс чистоты поверхности	R_a, мк (2) не более	R_z, мк (2) не более	l, мм	(1) Класс чистоты поверхности	R_a, мк (2) не более	R_z, мк (2) не более	l, мм
▽1	80	320	8	▽ 8	0,63	3,2	0,8
▽2	40	106	8	▽ 9	0,32	1,6	0,25
▽3	20	80	8	▽10	0,16	0,8	0,25
▽4	10	40	2,5	▽11	0,08	0,4	0,25
▽5	5	20	2,5	▽12	0,04	0,2	0,25
▽6	2,5	10	0,8	▽13	0,02	0,1	0,08
▽7	1,25	6,3	0,8	▽14	0,01	0,05	0,08

KEY: (1) Surface finish class; (2) no more than. [мк = μm]

From Table 4 it is clear that even surfaces with the highest class of finish (up to a mirror shine) are not ideally smooth and have irregularities with heights of approximately 0.05 μm and more. When only average values of surface irregularities are available it is very difficult to judge the field intensity caused by them, since it depends on the mutual arrangement of individual elements of surface relief, the dimensions of these elements, etc. Somewhat more information is yielded by the method proposed for evaluating surface roughness in experiments on secondary electron emission [47]. For this purpose the criterion h_{av}/l is introduced; this is the ratio of the average height of irregularities to the distance between neighboring irregularities, l. For an electrolytically polished nickel surface this ratio was evaluated as 0.06 (h_{av} = 0.6 μm and l = 10 μm). The literature usually contains data relating only to average values of h_{av}.

Surfaces treated on different machine tools are characterized by irregularities whose dimensions lie in a region of several microns; polishing provides a smoother surface, for which the average value of protuberances does not exceed tenths and even hundredths of a micron. With mechanical treatment a high class of surface finish can be obtained only on materials which are physically and chemically homogeneous.

Besides this, mechanical polishing is inevitably connected with the formation of a surface amorphous layer. Besides smashed and strongly deformed grains of metal, this layer consists of residues of abrasive materials and carbides forming under the action of the high temperatures which develop during friction, as well as products of possible chemical reactions and contaminants. Surface deformations impart increased hardness to the surface layers. The normal structure of the metal is located

at a significant depth, depending on the properties of the metal and the nature of treatment: for example, sections of hard steel display a layer of increased hardness to a depth up to 2-5 μm; in copper and aluminum alloys this occurs to depths of 30-80 and 50-150 μm respectively. In a number of cases cracks with dimensions of 1-2 μm have been observed in the subsurface layers [48].

Metal surfaces possess higher microgeometric qualities after electrochemical polishing. Electrolytic polishing is based on preferential dissolution of projecting portions of the surface; it results in a surface which has an insignificant smooth waviness. The best results are also obtained on chemically pure metals. On single-crystal specimens of aluminum the irregularities did not exceed 100-150 Å and might possibly be brought down to atomic dimensions [48]. With electrolytic polishing the metal surfaces are covered with a thin film of oxides arising either during the polishing process or during subsequent treatment and contact with air; the presence of other chemical compounds and contamiants is also possible.

During study of the behavior of copper electrodes in an electrical field in vacuum it was noted that mechanically treated surfaces were the most easily destroyed [49]. Individual depressions reaching 20 μm in size were observed on such surfaces; these depressions arose with an electrical field intensity of approximately $1.3 \cdot 10^5$ V/cm. Separation of a few small particles (about 1.5 μm) on electrolytically polished electrodes occurred at higher fields, that is, at approximately $6.5 \cdot 10^5$ V/cm. In both cases these disruptions were not connected with vacuum breakdown.

Study of electrode surfaces after breakdown in a vacuum shows that crystalline heterogeneities - points of contact of different crystal boundary facets - are the most vulnerable.

After breakdowns craters are frequently located along lines left by polishing [50]. It is possible that a particular role is played in vacuum breakdown by carbon inclusions on the electrode surfaces.

It was noted that after a single breakdown the surfaces of stainless-steel anodes differed in many ways from the surfaces of other metals (copper, aluminum, low-carbon steel, molybdenum, nickel, and tungsten) [51]. In these experiments breakdown was accomplished by pulse voltage with a length of approximately 4.5 μs on a 0.5 mm gap. The anode craters on the surface of the stainless steel have a more individual character; their sizes sizes vary strongly and there is an elevated spot in the center of each crater. Surface etching established the fact that the distribution of craters over the surface coincides with the distribution of carbide grains. Each carbide grain becomes a center on which processes leading to the formation of a crater are concentrated during breakdown. In particular, distortion of the electric field on the carbide grains can lead to focussing of the beam of electrons impinging from the cathode. Since the carbon melting and boiling temperatues are greater than those for steel the carbide grains are destroyed to a lesser degree under the action of electrical bombardment and remain in the form of elevated areas in the centers of the craters.

Heating of the electrodes leads to changes in the initial microrelief of the surface. As a rule the minimum value of surface energy of crystalline bodies does not coincide with the smallest dimensions of their surface. Therefore the effort of the system to reduce its energy is connected with the formation of a certain degree of roughness on the initially smooth surface. The overall increase in the dimensions of the surface is accompanied in this case by a reduction in the total energy due to the emergence of facets with lower surface tension. The natural surface roughness appearing in this way is realized mainly in the form of accumulations of parallel terraces, with the height

and period of the steps varying from grain to grain [52, 53]. For example, in the case of the surface of polycrystalline copper previously polished both mechanically and electrochemically, after annealing in a vacuum at 1000°C the height of projections on the majority of the grains was on the order of 10 μm. The appearance of natural surface roughness is connected with evaporation (and condensation) processes which begin to appear at noticeable rates at temperatures approximately half the melting temperature. Besides this, many other processes influence the formation of relief during heating of metals in a vacuum: surface deformation, recrystallization, phase transformations, differences in anisotropy of expansion coefficients, etc. Figure 10 shows some of the most characteristic forms of relief which occur during heat treatment of metal specimens in a vacuum [54]. Diagrams a-d correspond to reliefs which form on a polished metal surface during heating; those on figures e-h correspond to reliefs forming during cooling of the specimens. The forms of relief in the first group are characterized by the formation of grooves, bands, terraces, and shears. The depth of the grooves during heating of specimens of steel 45 to a temperature of 1100°C and holding for one hour comprised approximately 2-3 μm, while a 5-minute hold led to the appearance of grooves whose depth did not exceed 0.2-0.3 μm.

When heated specimens are cooled reliefs with complex acicular (martensitic) or a striated picture can appear (see Fig. 10f); the formation of these reliefs is connected with rapid cooling. Reliefs of a similar type are observed on specimens of steel and certain other pure metals and alloys. The magnitude of projections with cooling in air reached about 1-4 μm for specimens of steel 45 preheated for 9 hours at 1100°C.

The microrelief of the surface and, in particular, the formation of points can be strongly influenced by processes of surface diffusion of atoms of metals and contaminants present on the surface. At temperatures corresponding to approximately

0.3 T_{melt} [55], the surface atoms of metals take on fairly great mobility and become capable of traveling for considerable distances over the surfaces of metals. The surface migration of Ni, Ag and Mo atoms has been observed at temperatures of 370, 500, and 770°K, respectively, and has also been studied on W, Fe, and other metals in connection with the change in the shape of metallic points in field-emission microscopes [56-62].

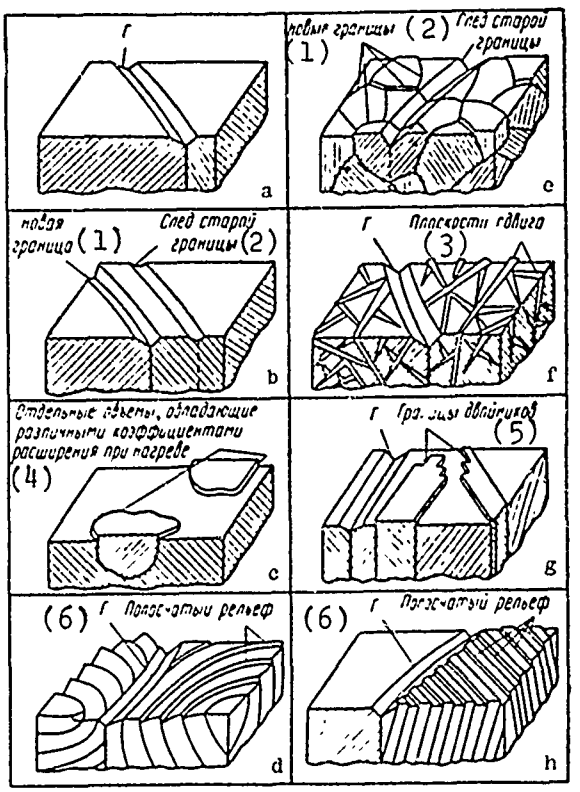

Fig. 10. Diagrams of various types of relief arising on the polished surface of metal specimens subjected to heating and cooling in vacuum. (Г - grain boundary).

KEY: (1) New boundaries; (2) Track of old boundary; (3) Shear plane; (4) Individual volumes possessing different coefficients of expansion during heating; (5) Boundaries of twins; (6) Striated relief.

Displacement of atoms occurs under the action of forces of surface tension, the electric field, and the temperature gradient. According to the theory developed by Herring (see [63]), the flow of atoms over the surface is determined by the expression

$$N = -\frac{D \nabla M_s}{s_0 kT}$$

where N is the flow of atoms, 1/(cm·s); $D = D_0 \exp(-Q/kT)$ is the coefficient of surface diffusion, cm^2/s; s_0 is the area for a single atom, cm^2; Q is process activation energy, J/mole; $M_s = M_0 + V_{at}\left[\alpha_s\left(\frac{1}{r_1}+\frac{1}{r_2}\right)+p_{xx}\right]$ is the chemical potential of the surface; V_{at} is the atomic volume, cm^3; M_0 is the chemical potential of a flat surface; α_s is the coefficient of surface tension N/cm; r_1, r_2 are the radii of surface curvature at a given point, cm; p_{xx} is the external force, N/cm^2 (for an electrical field $p_{xx} = \varepsilon E^2/8\pi$).

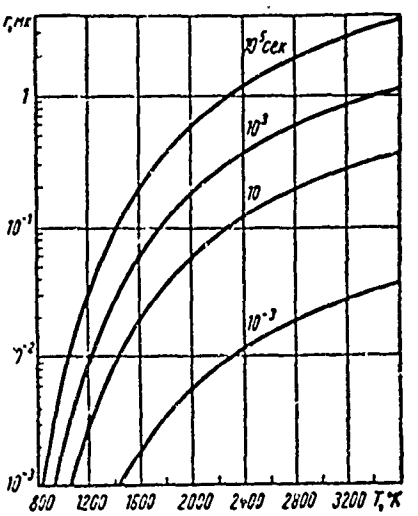

Fig. 11. Values of the radius of the peak of a tungsten point heated to various temperatures. [мк = μm; сек = s]

In the absence of external stresses - for example, when E = 0 - metal atoms migrate under the action of forces of surface tension from the peak to the base of a point; in this case the point is blunted and its height h changes at a rate determined by the expression [59]

$$\frac{dh}{dt} = -\frac{1.25\,a_s V_{sr}^2 D_0}{r^3 s_0 kT} \exp\left(-\frac{Q}{kT}\right).$$

Here r is the radius of the point peak. By integrating this expression we can obtain the relationship between the magnitude of the change in the radius r and the time necessary for this; $r^4 - r_0^4 = at$, where r_0 and r are the initial and final radii of the peak of the point, respectively; a is a constant which depends on temperature, the properties of the metal, and the geometry of the point.

Figure 11 shows values of r obtained from this equation for a tungsten point as a function of temperature with different heating times [45]. From the curves on Fig. 11 it is clear that only very prolonged heating at high temperatures can blunt a point so that its radius is increased to several microns. Heating is most effective for points whose r does not exceed about 1 μm. Figure 12 shows the value of the radius of the peak of a tungsten point as a function of the time of heating at 2800°K. The comparatively rapid blunting which occurs in the initial moments subsequently becomes slower, when the values of r reach about 0.7 μm [58]. When tungsten electrodes having the form of spheres 6.25 mm in diameter and with flat surfaces were heated it was not possible to smooth the projecting portion of the surfaces sufficiently that the field gain factor μ would drop below 10 [45].

For lower-melting metals (Fe, Pt, and Ni) blunting of the points occurs with higher speeds.

In the presence of an electric field the migration of atoms is determined by the combined action of the forces of the electric field and of surface tension. The rate of change in the height of a point is

$$\left(\frac{dh}{dt}\right)_E = \left(\frac{dh}{dt}\right)_0 \left(1 - \frac{r}{a_s}\frac{\varepsilon E^2}{8\pi}\right).$$

The value of field strength E is related here to a spot located on the peak of the point. As is evident from the equations, the action of electrostatic forces can completely compensate surface tension $\varepsilon E^2/8\pi = \alpha_s/r$. In this case the rate of migration equals zero $(dh/dt)_E = 0$, and the geometric form of the heated point is not changed. In particular, this makes it possible to measure the surface tension of the metal at temperatures below the melting point.

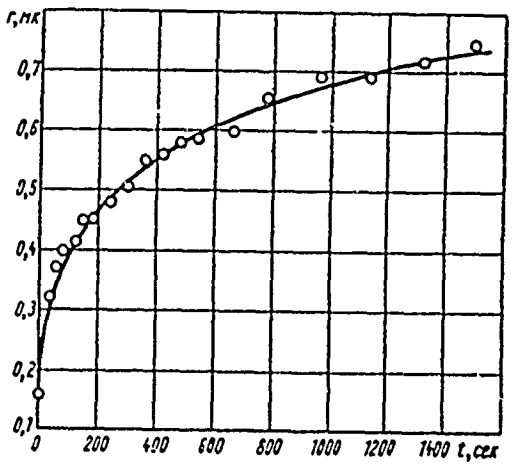

Fig. 12. Radius of the peak of a tungsten point as a function of time of heating at 2800°K.

[мк = μm; сек = sec]

For tungsten at a temperature of 2000°K and with r = 0.55 μm, equilibrium is achieved in fields $E \approx 1.1 \cdot 10^7$ V/cm; this corresponds to values of α_s = 0.029 N/cm (when T = 3380°K, α_s = 0.023 N/cm). Similar evaluations for Mo in the temperature range 1200-1900°K give an α_s value of 0.026 N/cm (the α_s of liquid Mo equals 0.0208 N/cm) [61].

With a further increase in electric field intensity E the atoms of the metal begin to migrate from the base to the peak of the point; this leads to restructuring and to a growth in the point. The time for restructuring a point, as before, depends exponentially on temperature:

$$t \sim T \exp(Q_E/kT).$$

An essential point is the fact that a substantial reduction in surface diffusion activation energy Q_E and a corresponding increase in the rate of migration will occur under the influence of an electrical field. Table 5 gives measured values of surface diffusion activation energy for W and Mo with $E = 0$ and when $E \neq 0$, when restructuring of protuberances was observed.

Table 5. Measured values of surface diffusion activation energy on tungsten and molybdenum.

(1) Энергия, активации, эв/атом	E	(2) Металл	(3) Направление миграции	(4) Область температур, °К	(5) Литература
		(6)	(7)		
3,5 ±0,3	0	Вольфрам	Затупление	1200—1500	[64]
3,2 ±0,2	0	»	»	1200—1600	[60]
3,14±0,08	0	»	»	1800—2700	[59]
2,86±0,15	0	Молибден (8)	»	1200—1900	[61]
2,36±0,2	≠0	Вольфрам (6)	Рост (9)	1200—1600	[65]
2,44±0,05	≠0	»	»	1700—2100	[66]
2,00±0,05	≠0	Молибден (8)	»	1200—1900	[61]

KEY: (1) Activation energy, eV/atom; (2) Metal; (3) Direction of migration; (4) Temperature region, °K; (5) Reference; (6) Tungsten; (7) Blunting; (8) Molybdenum; (9) Growth.

Many authors have observed the change in the shape of an emitting protuberance in an electron projector [61, 65, 66]. The restructuring of the point which occurs in an electrical field is usually connected with conversion of the peak of the protuberance from a rounded to a faceted form. A large number of protuberances with the coefficient $\mu \approx 3$-4 arose in a short time (about 20 minutes) on a smooth tungsten surface serving as an anode and heated to about 1000°K in a field of approximately 100 MV/cm. A reverse-polarity field with a strength of about 43 MV/cm applied to a surface containing a few irregularities caused a growth in these protuberances even at room temperature [45].

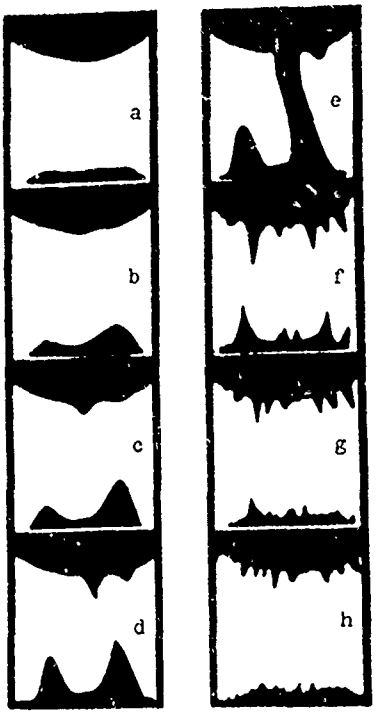

Fig. 13. Growth of oil projections on the surface of electrodes with a change in voltage.

a - 3.2 kV; b - 3.9 kV; c - 4.2 kV; d - 4.8 kV; e - 4.9 kV; f - 8.1 kV; g - 8.8 kV; h - 9.5 kV.

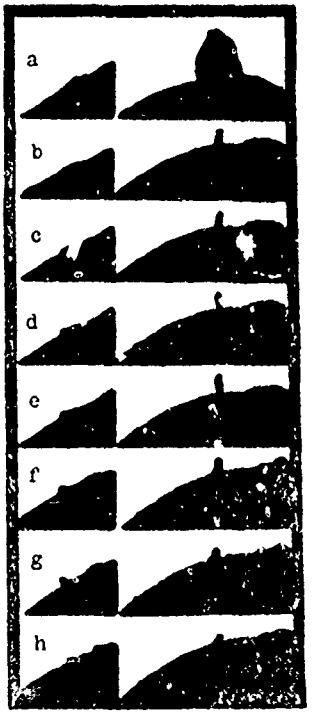

Fig. 14. Displacement of particles and growth of metallic protuberances on the surface of the anode:

a - 20 kV; b - 38 kV; c - 42 kV; d - 50 kV; e - 66 kV; f - 75 kV; g - 79 kV; h - 80 kV.

The changes occurring on the surface of the electrode in an electrical field were observed in the work by Tarasova et al. [67]. They carried out photomicrography of the surfaces of copper electrodes with a pointed shape with a peak radius of about 0.1 mm. The electrodes were located in a vacuum on the order of 10^{-5} mm Hg with a continuous evacuation by an oil-diffusion pump; the oil vapors were not frozen out. In the first series of experiments the electrodes were covered with a substantial film of oil. They were usually in this condition if the system was evacuated with an oil-vapor pump over the course of several days. In the second series of experiments the electrodes were washed with solvents, but once again the oil vapors were not frozen out. The experimenters succeeded in clearly observing a change in the shape of the electrode surfaces, displacement of large particles, and the growth and disappearance of individual protuberances, accompanied by breakdown. Figure 13 shows film strips of the electrode surfaces contaminated with a film of oil. The distance between the electrodes equals 0.1 mm. The upper electrode was the cathode and the lower, the anode. Projections formed by the oil film are elongated with a growth in voltage; the radius of curvature of the peak is reduced. Rough evaluation of the dimensions of the peak radius from the stability conditions $2\alpha_s/r \approx \varepsilon E^2/8\pi$ for various voltages gave a result coinciding with the experimental data.

Figure 14 shows the change in the anode profile in the second series of experiments. The interelectrode distance was approximately 1 mm. The left side shows the segment of the anode reproduced with a magnification of about 2.7 times that of the right-hand series of photographs. The growth of a metallic protuberance and its breakaway (Fig. 14h), caused by gap breakdown, are clearly visible on the left-hand photographs. On the right, on Fig. 14a, we see a round particle (tens of microns) weakly bound to the anode surface. Its breakaway (at

a voltage of 20 kE [sic]) was not accompanied by vacuum-gas breakdown. Frames b-h (right) on Fig. 14 show a protuberance about 20 μm in length which is strongly attached to the electrode. Breakdown, which occurred ahead of the frame 14f, was apparently localized to the right of the thin protuberance and led to a strong change in the profile of the anode peak.

The formation of protuberances in an electrical field on vacuum-deposited metal films was observed by Sudan and Gonzalez-Perez [68]. They studied electron emission from a cold tungsten filament on which copper vapors could be deposited. The copper was atomized during electrical breakdown of an auxiliary vacuum gap formed by the copper electrodes. Evacuation of the system with an ion pump reduced possible contaminants to a minimum. The measurements were conducted in a vacuum on the order of 10^{-9} mm Hg. After breakdown of the copper electrodes, an electron current (observed from illumination of a fluorescent screen) arose at a voltage approximately 2.5 times less than that for the electrode without deposits. Emission proceeded from individual centers of that portion of the surface of the tungsten filament which was turned toward the auxiliary electrodes. In the course of time some of the centers disappeared, which indicated elimination of the protuberances. The picture was repeated during subsequent breakdowns.

The appearance of protuberances on electrode surfaces may be connected also with a growth in acicular crystals - crystalline formations which are characterized by high structural perfection and a very great ratio of length to diameter (approximately 1000) [69].

Spontaneous growth of crystals on metal surfaces was observed with heating up to 200-700°C for such metals as brass, Cu, Au, Fe, Pb, Mg, Mo, Ni, Pd, Pt, Ag, Ta, Ti, W, Zn [70]. Numerous crystals 1-2 μm long could be observed with the electron

microscope after 30-100 hours of heating. Some of the crystals had the form of thin strips with a noticeable surface structure (for example, Fe and Zn).

Spontaneous growth of crystals was also observed on thin metallic layers created by electrocoating or other methods [69]. At ordinary temperatures the crystals grow quite slowly. However, an increase in temperature (and especially the presence of voltage in the substrate or the layer itself) will cause the rate of growth to increase by approximately 10,000 times. Most frequently cylindrical formations with a diameter sometimes less than 0.25 μm will be observed under these conditions.

Very thin crystals (50-150 Å in diameter and up to 10 μm long) grew with deposition of vapors of a metal vaporized by heating in a high vacuum [71, 72]. The technology of the field-emission microscope was used in the experiments. Metals to be evaporated were heated to temperatures corresponding to equilibrium vapor pressures, 10^{-5}-10^{-6} mm Hg. The formation of crystals was observed in terms of their emission image on the screen. The metals Ti, Pt, Ni, Fe, Mo, Cu, Au, Ag, Al, Ba, and others were studied. The time for growth of the crystals comprised about 5-10 minutes. The sizes, shape, and surface condition of the crystals were determined by the method and conditions of their growth. Evaluations carried out on the basis of experimental observations of crystals obtained by deposition of metal vapors showed that the lower boundary of radii of crystals capable of stable growth is approximately 0.01 μm. Under the most favorable conditions smooth crystals of regular form with diameter to 1-20 μm can appear.

3. ADSORPTION AND CONTAMINATION

A common property of solids, including metals, is their ability to hold foreign substances on their surfaces. This property is conditioned by the fact that the atoms on the surfaces are subjected to the action of nonequilibrium forces of attraction, which are saturated in the process of adsorption of foreign atoms or molecules. Thus, as adsorption occurs it is accompanied by a drop in the potential energy of the system. Figure 15 shows a schematic picture of the change in potential energy of the system with approach of a molecule of gas to the surface of a solid. The segment ABC corresponds to physical adsorption connected with the action of relatively weak van der Waals forces. Phenomena of physical adsorption are characteristic for all metals and gases and occur basically at temperatures and pressures which are close to the conditions for condensation of the corresponding gases. In this case the adsorbed gases form several molecular layers on the surface of the metals. Interaction of the gas and metal is not accompanied by substantial changes in the electron structure of the molecules. The molecules of the gas are not dissociated; they are easily moved from place with low potential energy and can be completely removed with heating up to a temperature of approximately $2T_{boil}$ for the appropriate gas. The depth of the minimum at point B does not exceed 1-6 kcal/mole for H_2, N_2, CO, or Ar.

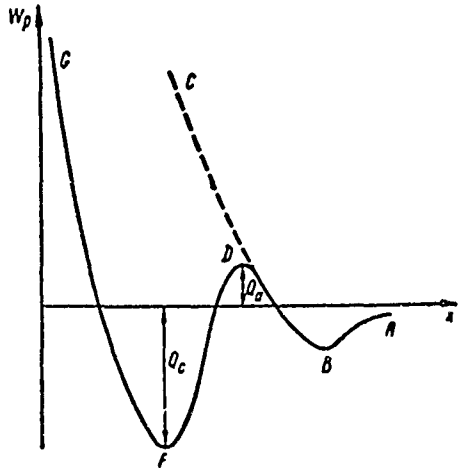

Fig. 15. Change in potential energy of the system with approach of a molecule of gas to the surface of a solid body.

A stronger interaction, virtually corresponding to chemical bonding, arises during chemosorption of gases (segment DFG). As a rule, chemical adsorption is limited to the formation of a single molecular layer. Surface irregularities and defects in the crystalline lattice play a major role. In contrast to physical adsorption, chemosorption can require a certain activation energy Q_a. In this case it will occur at noticeable rates only at elevated temperatures. For example, at room temperature nitrogen is adsorbed by only a few metals (iron, molybdenum and tungsten), while interaction with nickel occurs only at approximately 800°C; this corresponds to an activation energy $Q_a \approx 60$ kcal/mole [63].

Different metals behave differently with respect to one and the same gas. Table 6 gives data on the activity of certain metals with respect to such gases as nitrogen, hydrogen, carbon monoxide, ethylene, acetylene, and oxygen [73]. The plus sign indicates the presence of chemosorption. Absence of chemosorption at 0°C and below is expressed by the minus sign.

Table 6. Activity of certain metals toward gases.

Металлы (1)	(2) Активность газов					
	N_2	H_2	CO	C_2H_4	C_2H_2	O_2
Ba, W, Ta, Mo, Ti, Zr, Fe, Cu	+	+	+	+	+	+
Ni, Pt, Rh, Pd	−	+	+	+	+	+
Cu, Al	−	−	+	+	+	+
K	−	−	−	−	+	+
Zn, Cd, Sn, In, Pb, Ag	−	−	−	−	−	+
Au	−	−	+	+	+	−

KEY: (1) Metals; (2) Activity of gases.

The affinity to chemosorption of different gases can be presented for each metal in the form of a series [74]

$$O_2 > C_2H_2 > C_2H_4 > CO > H_2 > N_2.$$

Except for oxygen, this sequence corresponds to the sequence of changes in ionization potentials of these gases:

Gas	C_2H_2	C_2H_4	CO	H_2	N_2
Ionization potential, eV	11.4	10.5	14.0	15.4	15.6

The strong bonds which arise between phases in contact are characterized by large heats Q_c, which exceed the corresponding values for physical adsorption by 10 times and more. In this connection the removal of adsorbed gases (e.g., O_2) from the surfaces of metals requires heating to very high temperatures (approximately 1500-2000°K). Table 7 gives the magnitudes of heats of chemosorption Q_c for certain metals and gases [75]. The third column of the table indicates the temperatures T_h at which the metal surfaces are freed from adsorbed gases. The temperatures T_h were calculated on the basis of the rough rule establishing a numerical connection between the heat of chemosorption Q_c and the temperature at which complete desorption of the gas occurs [63]:

$$\frac{T_h}{Q_c} \approx 5 \cdot 10^{-3}.$$

For comparison the last column gives the melting temperatures T_{melt} of the metals.

Table 7. The quantities Q_c, T_h, and T_{melt} for certain metals and gases.

Система (1)		Q_c, ×10³ дж/моль (2)	T_h, °K	$T_{пл}$, °K
O_2 на (3)	W	650	3000	3650
	Ni	540	2600	1726
	Fe	314	1500	1808
N_2 на (3)	W	398	2000	3650
	Ta	586	2800	3303
	Fe	167	800	1808
CO на (3)	Ni	147	700	1726
	Fe	134	650	1808
H_2 на (3)	W	188	900	3650
	Ta	188	900	3303
	Ni	130	600	1726

KEY: (1) System; (2) J/mole; (3) on.

If no special precautions are taken the surfaces of the solids will always be contaminated with other materials besides the adsorbed layers. Even a brief (several minutes to several hours) contact with the atmosphere leads to the formation of a thin fatty film which is easily detected from the "condensation figures." Even in a very clean room the air contains extremely fine particles of dust and vapors of organic substances. Organic substances bind themselves so strongly to the surface of solids that they behave as chemical compounds: insoluble in water, difficult to remove with ordinary washing in solvents and even with etching acids or by annealing in vacuum and hydrogen. Detailed information on the cleaning and monitoring of surface cleanliness of parts in electric vacuum instruments is found in work [76].

Many contaminants can arise directly in the vacuum system. Analysis of residual gases in demountable vacuum installations operating with diffusion, oil, and mercury pumps shows that water and hydrocarbons are most strongly represented in them; the hydrocarbons are present even after heating of the system up to a temperature of about 100°C for several hours [77]. Presence of vapors of organic substances in the vacuum leads to the formation of hydrocarbon films on the surface of the metal. Films appear preferentially at sites with large electric-field gradients, along the terraces of crystal fragments, and on the surfaces of scratches [78].

Under the action of electron or ion bombardment polymerization and carbonization of organic molecules occur; this results in the formation of stable chemical compounds. Coatings which appear in this way represent an amorphous mass of brown color which is distinguished by great resistance to various chemical solvents. Electron microscope studies show that the rate of formation of organic films depends on the current density in the electrical beam bombarding the surface of the target [79]. The

dependence of the growth rate of the layer of current density is shown on Fig. 16.

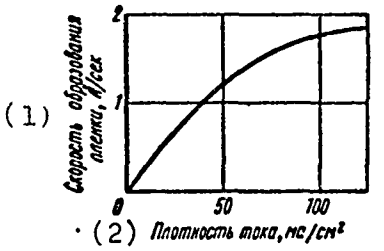

Fig. 16. The rate of growth of an organic film as a function of the current density of the electron beam.

KEY: (1) Rate of film formation, Å/s; (2) Current density, mA/cm^2.

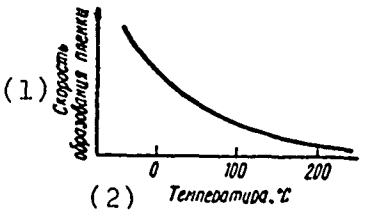

Fig. 17. Rate of formation of an organic film as a function of temperature.

KEY: (1) Rate of film formation; (2) Temperature, °C.

The rate of film formation is also determined by the temperature of the surface. With a change in temperature from 20 to 200°C the film thickness drops (by approximately 10 times), while at a temperature of 250°C film formation is terminated almost completely (Fig. 17). This type of thermal dependence of film growth rate indicates that films arise as the result of condensation of vapors of organic substances existing in the system. Special studies have shown that migration over the surface does not play an essential role.

The major "suppliers" of contaminants are various organic components of the system. The data in Table 8 illustrate the relative characteristics of contaminating capabilities of certain vacuum materials [79]. The quantity of substances placed in the chamber corresponded in these studies to typical experimental conditions existing in demountable vacuum installations. The contaminants which appeared were evaluated with

respect to the thickness of the film formed on the metallic target during bombardment in an electron beam with a current density $j \approx 10$ mA/cm^2 in a period of approximately 100 minutes at a voltage of 2 kV. The table also indicates methods of preventive treatment of the materials.

Table 6. Characteristics of the contaminating capacity of certain vacuum materials.

(1) Материал	(2) Обработка	Толщина пленки, Å (3)
(4) Диффузионное масло . . .	Спецочистке не подвергалось (5)	1700
(6) Силиконовое диффузионное масло	То же (7)	500
(8) Вакуумная замазка . . .	»	1500
(9) Апиезон (типа пицеина) . .	»	50
(10) Резина естественная листовая	Кипячение в водном (11) и спиртовом растворе поташа	1100
(12) Черный неопрен	То же (7)	50
(13) Круглые резиновые прокладки	»	600
(14) Бакелит	Спецочистка (15)	50
(16) Фотопластинки	»	50

KEY: (1) Material; (2) Treatment; (3) Film thickness, Å; (4) Diffusion oil; (5) Not specially cleaned; (6) Silicone diffusion oil; (7) The same; (8) Vacuum putty; (9) Apiezon (picein type); (10) Natural sheet rubber; (11) Boiling in a water and alcohol solution of potash; (12) Black neoprene; (13) Round rubber packings; (14) Bakelite; (15) Specially cleaned; (16) Photographic plates.

The basic contribution comes from vacuum oils, vacuum putties, and the rubbers used for seals. Cleaning rubber by boiling it in potash substantially reduces the contaminants which it releases. The magnitude of the surface of the rubber does not play an essential role: an approximately fivefold increase in its size lead to a growth in film thickness by 1/3 in all. Contamination is sharply increased when the rubber is heated. Silicone oils create substantially less contamination. In a system equipped with two nitrogen traps the rate of growth of such films did not exceed 5 Å/h in a vacuum of $1 \cdot 10^{-9}$ mm Hg [80]. Layers formed

during condensation of silicone oil vapors possess very high insulating properties. Organic contaminants are also brought in by the metallic portions of the installations; effective cleaning of the metallic surfaces is possible only by careful treatment with acids and subsequent prolonged heating.

The glass portions of the installation can be a source of unique contaminants. During heat treatment of glass, in particular after sealing of glass, the internal surface of the vacuum chamber becomes contaminated with oxides of the elements included in the glass composition: SiO_2, Na_2O, K_2O, BaO_3 and others [81, 82]. Contaminant vapors are deposited on the cooler parts in the form of individual particles with dimensions on the order of 10^{-2}-10^{-1} μm (approximately $1 \cdot 10^9$ atoms). These contaminants are very mobile, easily migrating over the surface and from electrode to electrode. The system is cleaned by washing in water or by heating to a temperature above 500°C, at which point decomposition of these compounds begins.

As compared with clean electrodes, the breakdown voltage on electrodes contaminated in this way is reduced by approximately 50%.

4. WORK FUNCTION OF METALS UNDER DIFFERENT CONDITIONS ON THE SURFACE

The work function is a very important characteristic in many processes occurring on metallic surfaces (emission of electrons, surface ionization, etc.). Table 9 (compiled on the basis of data from the Fomenko handbook, [83]) gives the values of the work function for pure metals of polycrystalline structure; these values were obtained by various experimental methods.[1]

[1]For methods of measuring the work function, see the studies [31, 32, 75, 84, 85].

The smoothness and other characteristics of the surfaces of the metals to which these data relate can be established only by detailed analysis of the measurement conditions in each specific case. Therefore we will also introduce the scatter of available values for each metal, since it not only characterizes the principal difference in the data obtained by different methods, but also to a certain degree the influence on the magnitude of the work function of the experimental conditions; this fact can be of definite interest during evaluations carried out with respect to one or another real installation.

Table 9. Work function of pure metals [83].

(1) Металл	(2) Величина работы выхода Ф, эв			(1) Металл	(2) Величина работы выхода Ф, эв		
	(3) рекомендуемая	(4) наименьшая	(5) наибольшая		(3) рекомендуемая	(4) наименьшая	(5) наибольшая
Cs	1,81	1,8	1,96	Au	4,3	4,00	5,1
K	2,22	1,60	2,26	Mo	4,3	4,04	4,59
Na	2,35	1,60	2,47	Fe	4,31	3,91	4,77
Li	2,38	1,40	2,49	Sn	4,38	3,62	4,64
Ba	2,49	1,73	2,55	Cu	4,4	3,85	4,61
Ca	2,80	2,24	2,80	W	4,5	4,25	5,01
Mg	3 64	2,74	3,79	Ni	4,5	2,77-	5,04
Ti	3,38	3,9	4,45	Hg	4,52	4,50	4,53
Pb	4,0	3,92	4,58	Cr	4,58	3,72	4,7
T	4,12	3,.	4,77	Pd	4,8	4,49	4,99
Zn	4,24	3,08	4,65	Re	5,0	4,66	5,1
Al	4,25	2,98	4,36	Pt	5,32	3,87	6,71
Ag	4,3	3,09	4,7				

KEY: (1) Metal; (2) Value of work function Φ, eV; (3) recommended; (4) least; (5) greatest.

A very extensive cause of a change in the work function of metals is the adsorption coating of metallic surfaces. This effect is usually regarded as the consequence of electron exchange occurring between the metals and adatoms at distances below a certain critical value x_{crit}, when the width of the potential barrier between them is substantially reduced [17, 86]. The nature of the influence of the adsorbed layer on the work function depends on the average charge of adatoms on the surface

of the metal, determined by such an exchange. In this case the arrangement of the energy levels of the adatom with respect to the Fermi level of the metal is of essential significance. According to evaluations carried out in work [87] for ionic and covalent binding of the adatom to the metal, the absolute value and the sign of the change of the work function depend on the quantity $(\Sigma - \Phi)$, where $\Sigma = {}^1/_2 (W_i + W_s)$ is the absolute affinity of the adatom for the electron (W_i and W_s are the energies of ionization of levels of the valence and excess electrons of the adatom). For simple gases the quantity Σ, equaling 7-10 eV, exceeds the magnitude of the work function of the metals (2-5 eV), i.e., in this case we can expect an increase in the work function. When $\Sigma < \Phi$ the work function during adsorption should be reduced.[1] Such evaluations agree with measurements of the work function during adsorption of gases on polycry. alline metals (Table 10) and for metals with a small work function (Table 11). The data in the tables relate basically to a monatomic coating, although frequently the authors of the measurements do not report the relative degree of coating of the surface.[2]

---

[1]Electron exchange between an adatom and a metal leads to the formation of strong bonds in this system (ionic or covalent), i.e., to chemosorption. During physical adsorption, caused by forces of intermolecular interaction, the polarization effects in the adsorbed layer can also lead to a change in work function characterized by the quantity $\Phi/W_i - W_s/\Phi$ [75]. As the measurement showed, physical adsorption carried out at low temperatures is accompanied by the reduction in the work function by a quantity varying from several tens of electron volts to 1 eV [75, 85].

[2]The dependence of the work function on the degree of coating of the surface with adatoms is usually nonlinear. In many cases there is an optimum coating (on the order of a monolayer) at which the change in the work function is maximum.

Table 10. Increase in the work function of metals during adsorption of gases on polycrystalline metals [75, 85].

Металл—адсорбированный слой (1)	ΔФ, эв (2)	Металл—адсорбированный слой (1)	ΔФ, эв (2)
Pt—O	1,1—1,2	W—N	0,22—1,38
Pt—H	0,14—0,21	W—CO_2	1,0
Pt—CO	0,24	W—CO	0,86
Cu—H	0—0,35	Ta—H	0,41—0,44
Cu—O	0,27—0,68	Ta—N	0,38
Ag—H	0,34—0,49	Ta—CO	0,67
Ag—O	0,6	Ni—O	0,5—1,6
Au—H	0,18	Ni—H	0,1—0,6
Zr—Cl	0,43	Ni—CO	0,39—1,38
Ti—Cl	0,31	Ni—CO_2	0,96
Pd—O	0,9—1,25	Fe—H	0,19—0,47
W—O	0,6—1,9	Fe—CO	1,15—1,64
W—H	0,48—1,26	Cr—CO	1,15

KEY: (1) Metal - adsorbed layer; (2) eV.

Table 11. Work function of metals during adsorption of electropositive impurities [83].

(1) Металл—адсорбированный слой	Ф, эв (2)	(1) Металл—адсорбированный слой	Ф, эв (2)
Ni—Ba	2,6	W—Ba	1,1—2,07
Cu—Ba	3,35	W—La	2,71
Mo—Cs	1,68	W—Th	2,6—3,2
Mo—Th	2,58	Re—Ba	2,3
W—Li	1,83	Pt—Na	2,1
W—Be	4,50	Pt—K	1,62
W—Na	1,76—2,10	Pt—Ca	3
W—K	1,64	Pt—Rb	1,57
W—Ca	2,40	Pt—Cs	1,38
W—Sr	2,20	Pt—Sr	2,3
W—Zr	3,14	Pt—Ba	1,9
W—Cs	1,36—1,7	Ag—Ba	1,56

KEY: (1) Metal - adsorbed layer; (2) eV.

It is necessary to note that under certain conditions there are deviations in the nature of the change in the work function from that observed in the majority of cases. Thus, during adsorption of hydrogen on nickel and platinum under conditions of incomplete vacuum ($1 \cdot 10^{-5}$ mm Hg) a reduction in work function is detected. This is apparently explained by the preliminary contamination of the metal surface in the atmosphere of residual

gases and by the physical nature of the subsequent adsorption of hydrogen on such a surface. Studies of hydrogen adsorption under purer conditions (vacuum better than 10^{-8} mm Hg) [87] showed an increase in the work function.

Adsorption of carbon monoxide can also lead to a reduction in the work function. Thus, reduction in the work function by 0.3, 0.31, and 0.92 eV corresponds to the systems Cu–CO, Ag–CO, and Au–CO [85].

Table 12 gives the values of the work function with complex adsorbed coatings of various types. As follows from these data, the work function of such surfaces can reach very small values.

Table 12. Work function of metals with complex adsorbed coatings [83].

Система (1)	Ф, эв (2)	Система (1)	Ф, эв (2)
Ag–O–Cs	0,8	W–O–Cs	0,72–1,44
W–H–K	1,8	W–O–Ba	1,34
W–C–Na	1,72	W–Ba–O	1,9–2,5
W–O–K	1,76		

KEY: (1) System; (2) eV.

Weissler and Wilson [88] studied the effect on the work function of spray-coated surfaces of tungsten and silver of ion bombardment in a glow discharge in an atmosphere of various gases. The results are presented on Figs. 18 and 19. Values of 4.67 and 4.2 eV were taken by the authors as the work function of pure tungsten and silver surfaces, respectively. A glow discharge in an atmosphere of oxygen and the freon CCl_2F_2 increased the work function; this is explained by the chemosorption of oxygen and freon decomposition products on the surface of the metals. The reduction in the work function as the result of ion bombardment during discharge in helium, hydrogen, and nitrogen is explained by the formation of physically adsorbed

layers (prior to insertion of the gases a vacuum of $1 \cdot 10^{-6}$ mm Hg was maintained in the system). The results obtained during bombardment of the surface with argon ions confirm the advisability of using this method for degassing and cleaning metal surfaces.

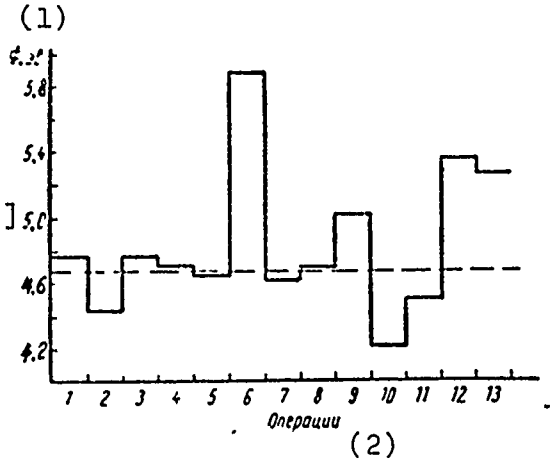

Fig. 18. Change in the work function of a freshly sprayed tungsten surface with the sequence of operations indicated on the graph. 1, 3, 5, 8, 9, 12, 13 - heating to 1100°C; glow discharge; 2 - in nitrogen; 4, 7 - in argon; 6 - in oxygen; 10, 11 - in hydrogen.

KEY: (1) Φ, eV; (2) Operations.

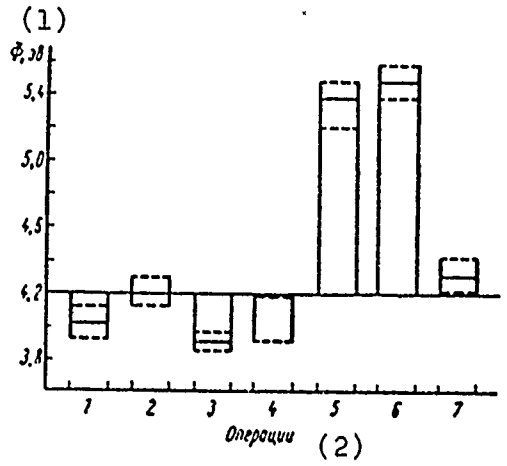

Fig. 19. Change in the work function of a freshly sprayed silver surface after various operations.

Glow discharge: 1 - in helium; 2 - in argon; 3 - in hydrogen; 4 - in nitrogen; 5 - in oxygen; 6 - in freon; 7 - holding in an atmosphere of water vapor. The broken lines show the scatter of measured values.

KEY: (1) Φ, eV; (2) Operations.

The effectiveness of treatment by discharge in inert gases to obtain a pure metallic surface with reproducible work-function values was also demonstrated by the investigations of Chistyakov [89].

Maddison et al. [90] studied the effect of contaminants introduced by different vacuum materials (different pump oils and mercury) on the magnitude of the work function of metals; however, the obtained results do not make it possible to draw definite quantitative evaluations.

Table 13 gives data on the work function of certain chemical compounds of metals: oxides, carbides, nitrides, and silicides.

Table 13. Work function of certain chemical compounds of metals [83].

Соединение (1)	Ф, эв (2)	Соединение (1)	Ф, эв (2)
MgO	3,1—4,4	TiC	2,35—3,35
Al_2O_3	4,7	TaC	3,05—3,17
CaO	1,6—2,37	W_2C	2,6 —4,58
TiO	2,96—3,1	TiN	3,75
FeO	3,85	ZrN	2,92
NiO	5,55	$ReSi_2$	4,0
CuO	4,35—5,34	WSi_2	3,90
MoO_3	4,25	$TaSi_2$	4,31
Cs_2O	0,99—1,17	$MoSi_2$	3,87
BaO	0,99—2,7	$CrSi_2$	3,47
WO_2	4,96		

KEY: (1) Compound; (2) Φ, eV.

5. SURFACE IONIZATION

When there is electronic exchange with a metal, the adatom may be located on its surface in both the ionic and atomic states. The adatom can also be in either of these states to leave the surface. To determine the percentage of ions in a flow of particles from the surface, the conditions under which particles traverse the critical charge-transfer distance x_{crit} are examined; x_{crit} represents the distance at which electron

exchange of the adatom with the metal is terminated. In this case, as also during the formation of a double electrical layer on a surface, the ratio between the work function of the metal and the levels W_i and W_s of the adatom is essential.

Intensive surface ionization with the formation of positive ions is observed in the case when $\Phi > W_i$. For example, this occurs during ionization of alkali elements on metals with a large work function (tungsten and platinum). Under these conditions substantial ion flows from the metal surface are observed only at a certain threshold temperature at which the adsorbed layer of the element being ionized (the element which reduces the work function of the metal) is removed from the metal surface.

An electrical field which exceeds the contact fields of the spots leads either to a reduction in the the threshold temperature without a change in the magnitude of ion current (with intensive surface ionization) or, when the degree of ionization is insignificant, to an increase in the flow of ions; here the nature of the dependence of current on the field is similar to the relationship which is observed during field-effect emission with the Schottky effect. As was already noted, ionization of electropositive elements on metals with a large work function relates to the first case. The second case is satisfied by surface ionization of the majority of elements on all metals. Both cases can be fulfilled simultaneously on different segments of the surface. The dependence of total current from the surface on the field will be determined by the ratio of currents from such segments.

A detailed examination of the phenomenon of surface ionization and surveys of experimental studies can be found in the work by Zandberg and Ionov [91]. We will examine only the

results of a study of surface ionization under "natural" conditions, when the source of the ionizing atoms is made up of metal impurities (from the metal of which the electrode is made), residual gases in the vacuum system, or spray-deposited products of the decomposition of various materials in the vacuum chamber.

Agishev and Belyakov [92] observed ion currents from the surface of nickel beginning with heating up to 400°C; these were caused by impurities of Na, K, Rb and Cs which were contained in the nickel emitter. At 900°C at the beginning of heating the current of K ions grew to 10^{-7} - 10^{-8} A/cm^2; the current of Na ions comprised several percent of these values, while the Rb and Cs ion currents were insignificant and rapidly disappeared. After 30 minutes of conditioning at 900°C the K^+ and Na^+ were reduced by tens of times, but did not disappear completely even after very prolonged heating. In these experiments the field on the nickel surface was less than 10^3 V/cm. The vacuum in the system, $(3\text{-}4)\cdot10^{-7}$ mm Hg, was created by an oil diffusion pump.

Zandberg and Ionov (see [93, 94]) studied the emission of positive molecular ions from tungsten, nickel, iron, and platinum filaments. The system was evacuated to 10^{-7} mm Hg by an oil-diffusion pump with a nitrogen trap. Stable emission of positive ions with mass numbers of 59-202 appeared from the surface of untreated tungsten filaments (with a layer of oxides on the surface) at 400°K; in this emission the line corresponding to a mass of 101 was the most intensive,[1] while there was also emission of atomic ions of alkali metals - impurities in the tungsten. At 1100°K the intensity of all lines grew by 2-3 orders of magnitude. In this case the current density for ions with mass 101 reached 10^{-7}-10^{-8} A/cm^2. Cleaning the fresh filaments with fine emery cloth and subsequent washing with solvents led

[1]Positive ions of this mass were observed also under similar conditions in work [95].

to a sharp reduction in the emission of ions. However, heating at 1100°K in a vacuum of $2 \cdot 10^{-7}$ mm Hg restored emission. Heating of the filament to approximately 1600°K led to an irreversible reduction in the emission of all ions. Emission was restored once again by oxidation of the filament with calcination in the initial vacuum; the spectrum of ions became more saturated after such an operation, while the intensity of many of its lines grew. After prolonged calcination of the filaments at 2600°K the spectrum of ions was significantly impoverished as compared with the spectrum of the oxidized tungsten. Of the alkali-metal ions only the sodium and potassium remained; their emission was unstable. The density of the current of ions of a single mass comprised 10^{-12}-10^{-11} A/cm^2. With an increase in residual pressure from 10^{-7} to 10^{-6} mm Hg the intensity of the majority of lines was increased. Figure 20 [93] shows the curves of the ion currents from oxidized tungsten filament as a function of temperature for several mass lines.[1] For certain lines corresponding to the masses 81, 84, 85, and 86 the graphs are similar to the relationships of surface ionization of atoms with different ratios of W_i and Φ. For the majority of masses the dependences are more complex; as the indicated authors propose, this is connected with the different competing processes occurring on the surface of oxidized tungsten in the temperature interval 400-800°K during catalytic dissociative ionization of organic molecules. These molecules may be supplied by the compounds included in the pump oils or in the products of their decomposition.

[1]This figure also gives the calibration relationship for Cs^+ ions obtained during ionization of a neutral molecular beam of CsCl directed to the filament from a special evaporator.

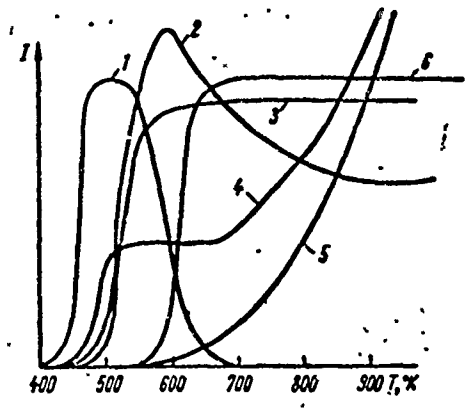

Fig. 20. Nature of the temperature dependences of a current of ions of different masses: 1 - 101 (102, 94, 96); 2 - 59 (97, 83, 109); 3 - 81 (84); 4 - 73 (60); 5 - 85 (86); 6 - Cs^+.

The applicability of the concepts of surface ionization of atoms to the ion emission observed in these experiments was also shown by a study of the influence of the emitter surface electrical field on the observed relationships.

Figure 21 gives the temperature dependences for ions with masses of 59 and 101 at two values of the electrical field: $2.3 \cdot 10^5$ and $2.3 \cdot 10^6$ V/cm. With an increase in the field we observe a reduction in the temperature threshold with virtually no change in the magnitude of the currents; this corresponds to one of the cases of surface ionization examined above.

Stable emission of ions with a mass of 101 was observed from nickel and iron filaments; from filaments of platinum and gold-plated tungsten only emission of alkali-metal impurity ions was observed.

Robertson et al. [35] studied the conductivity arising in a vacuum between an anode in the form of a thin tungsten or platinum filament and a coaxial cathode upon entry into the system (initially evacuated to 10^{-6} mm Hg) of various gases and vapors up to a pressure of about 10^{-3} mm Hg and with interelectrode voltages up to 20 kV. The current grew with increase in voltage,

as is illustrated on Fig. 22 (on this figure $\bar{E}$ is the average electrical field on the surface of the filament, calculated from geometric data). In the majority of cases - excluding input of H_2O and NH_3 - the currents were proportional to the pressure (Fig. 23). For filaments 4-10 μm in diameter and from 2.1 to 7 cm long currents on the order of 10^{-7} A were measured. They were interpreted as the result of surface ionization in the presence of an electrical field occurring on surface irregularities of the filaments, where the field E achieved a value on the order of 10^8 V/cm (the study of field-effect emission from filaments led to a value for the field gain factor $\mu = E/\bar{E} \approx 70$). The temperature dependence of the measured currents was not studied in detail.

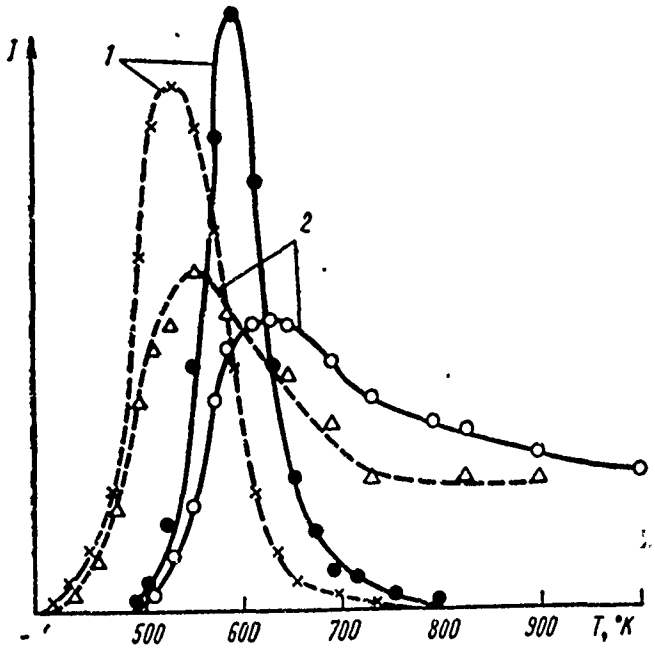

Fig. 21. Ion current as a function of temperature at two values of electric field intensity: solid curves - $E = 2.3 \cdot 10^5$ V/cm; broken curves - $E = 2.3 \cdot 10^6$ V/cm,

1 - ions with mass 101;
2 - ions with mass 59.

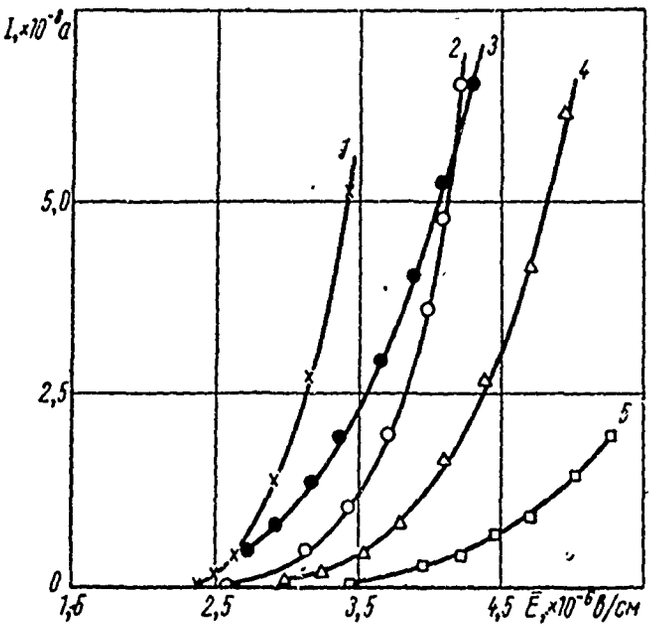

Fig. 22. Total current for various gases as a function of electric field:

Кривая (1)	Газ (2)	Давление (3) ×10⁻⁴ мм рт. ст.	Размеры нити из платины (4)	
			диаметр, мк (5)	длина, см (6)
1	C_2H_4	2,3	10	2,1
2	H_2O	8,4	10	2,1
5	CO	4,6	10	2,1
3	H_2O	5,5	4	7
4	N_2O	45	4	7

KEY: (1) Curve; (2) Gas; (3) Pressure, $\times 10^{-4}$ mm Hg; (4) Dimensions of platinum filament; (5) diameter, μm; (6) length, cm.

[в/см = V/cm]

When ions with an energy of 20 keV impinge on the metal a noticeable electronic emission should be observed. When the coefficient of ion-electron emission is approximately equal to 1.5 electron/ion, from 0.3 to 0.5 of the measured current will be caused by ions formed on the surface of the filament. According to the evaluations by Robertson et al. [35], ionization of the gas by electrons under the experimental conditions is not a significant factor (less than 10^{-4} ions/electron).

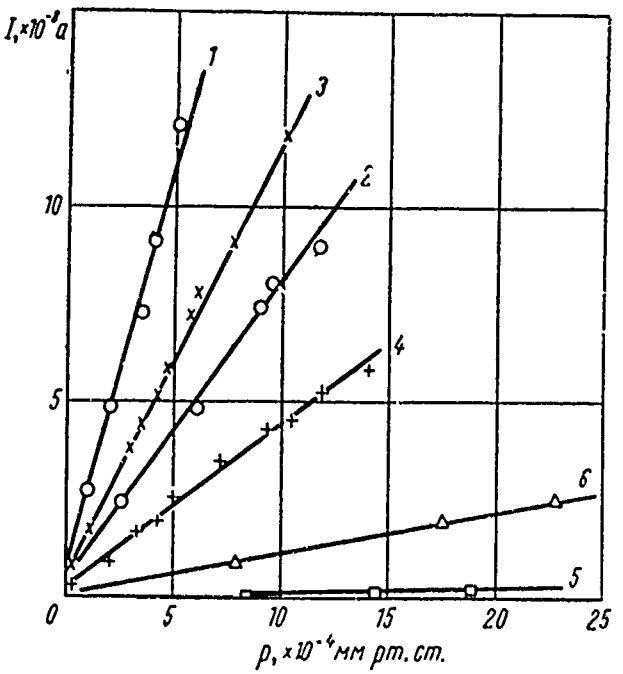

Fig. 23. Total current for various gases as a function of pressure:

Кривая (1)	Газ (2)	$\bar{E}$, ×10⁶ в/см (3)	Размеры нити из платины (4)	
			диаметр, мк (5)	длина, см (6)
1	CO	5,2	10	2,1
2	CO	4,7	10	2,1
3	C_2H_4	3,7	10	2,1
4	C_2H_4	3,2	10	2,1
5	H_2	5,2	10	2,1
6	N_2O	4,8	4	7

KEY: (1) Curve; (2) Gas; (3) $\bar{E}$, $\times 10^6$ V/cm; (4) Dimensions of platinum filament; (5) diameter, μm; (6) length, cm.

[мм рм.см. = mm Hg.]

Bakulina et al. [94] investigated the emission of negative molecular ions from the surface of filaments made of tungsten, molybdenum, and tantalum in a broad interval of temperatures under conditions of a vacuum system evacuated by an oil pump to a pressure of 10^{-7} mm Hg. A current of negative ions with masses of 35 and 37 (Cl^-), 42, 43 and approximately 230 (WO_3^-) appeared from the surface of oxidized tungsten filaments with gradual heating; the appearance began from 1200-1300°K, reached a maximum at 1500°K, and dropped to zero at 1600-1700°K. At 1700-1800°K a current of Cl^- ions appeared once again and new ions with masses of 24, 26, and 27 were detected; the current density for these ions reached 10^{-8} A/cm^2. Other ions with still smaller current density were also detected. After such heating no currents of ions with masses of 42, 43, and 230 were detected again either in the low or high temperature regions.

Emission from molybdenum filaments is similar, except that instead of WO_3^- ions, MoO_3^- ions were observed. The emission of negative ions from tantalum filaments began at a higher temperature (about 1600°K) and a continuous growth was observed with an increase in temperature, except for TaO_2^- ions. The spectrum of emission from tantalum is much richer than the emission spectra from tungsten and molybdenum filaments.

6. SECONDARY EMISSION PROCESSES

Secondary electron emission. Electrons of the metal can obtain the energy necessary for escape from it, in particular, from electrons which impinge from outside and which are capable of penetrating into the depth of the material. Besides such excited electrons of the metal (true secondary electrons) elastic and inelastic scattered primary electrons will occur in the electron beam from the surface. It is usually assumed that all electrons with energies greater than 50 eV are such reflected electrons.

The majority of true secondary electrons have an energy of 5-15 eV, almost independently of the energy of the incident electrons.

The coefficient of secondary electron emission K_{ee}, equal to the ratio of the total electron current from the surface to the current of incident electrons, reaches maximum values for metals equaling 0.5-1.8[1] at primary electron energies ranging from 200 to 800 eV.

It is possible to trace a fairly definite tendency to an increase in $K_{ee\ max}$ with an increase in the work function and density of the metal [98]. This indicates that processes of excitation of electrons of the metal and their movement to the surface are of greater significance as compared with the last stage – transfer through the potential barrier. This is confirmed to a certain degree by the fact that a change in work function

[1]For a normal incident electron flow to the surface of the metal. With an increase in the angle of incidence to 60-80° the quantity $K_{ee\ max}$ grows by 1.5-2 times because of the fact that excited electrons are formed close to the surface and have a pulse direction which is more favorable for escape. The dependence of K_{ee} on the energy of incident electrons for different metals can be found in works [96, 97].

during absorption leads to an insignificant change in K_{ee}. Thus, the absorption of thorium and oxygen on tungsten cause an increase and a decrease, respectively, in $K_{ee\ max}$ by 25% [96, 99].

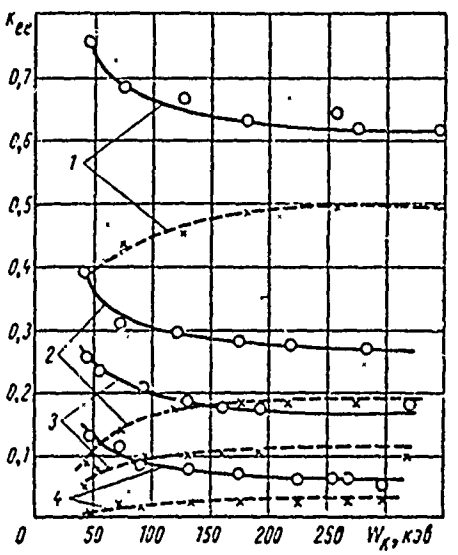

Fig. 24. Emission of secondary electrons with primary electron energies 30-34 keV: o — all secondary electrons; × — secondary electrons with energies greater than 800 eV. 1 — tungsten; 2 — steel; 3 — aluminum; 4 — graphite.
Designation: кэв = keV.

To evaluate the role of secondary electron emission in vacuum breakdown, Trump and Van de Graaf [100, 101] carried out a study of the energy dependence of K_{ee} on the energies of primary electrons from 30 to 340 keV (Fig. 24). It is clear that in this energy interval electron emission includes an essential fraction of reflected electrons. Such electrons with high energy comprise approximately 50% for tungsten at 30 keV, or for W_k = 300 keV the fraction is 80%. At primary electron energies above 200 keV the values of K_{ee} become virtually constant and in all cases are less than unity.

Dependence of secondary emission on the degree of surface roughness has been observed experimentally. A significant influence is noted in those cases when the distance between emitter irregularities is less than or on the same order with their height. For such a surface $K_{ee\ max}$ is reduced by about half as compared with a smooth surface [47]. Usually this is connected with the

fact that electrons emitted in the depressions of irregularities are partially seized by their projecting portions. Rashkovskiy [47] proposes that the reduction in K_{ee} with the indicated ratios of heights and pitch of irregularities is caused by the formation of microspaces which are screened from the field and from which it is difficult for electrons to escape.

Emission of electrons during bombardment of metal surfaces with positive ions. The process of ion-electron emission is a consequence of the transfer of potential or kinetic energy of the ion to electrons of the metal.

In the case of potential emission the Auger neutralization of approaching ions due to the electron transitions which are commencing leads to liberation of ionization energy; owing to this the electrons of the metal become capable of crossing the surface barrier [102]. Potential emission is possible when $W_i > 2\Phi$. The kinetic energy of the ion in this process is not significant. The coefficient of ion-electron emission K_{ie}, which determines the yield of electrons per individual ion, can (depending on conditions) vary from 10^{-4} to several units (maximum values for multiply charged ions).

Kinetic emission, which leads to a substantially greater yield of secondary electrons, is observed at energies on the order of 1 keV and above and is caused by processes occurring during penetration of incident ions into the crystalline lattice of the metal [103, 104]. The major portion of secondary electrons display energies no greater than 20-30 eV, while their average energy lies in the range of a few electron volts. The energy distribution of the knocked-out electrons is virtually unchanged with a change in the energy of the ions.

Trump, Van de Graaf, and their coworkers carried out studies of ion-electron emission in order to clarify the role of positive

ions in vacuum breakdown [100, 105-107]. The experimental conditions set up by Bourne et al. [106] correspond to the actual conditions in a high-voltage vacuum gap. This made it possible to study the effect on the coefficient K_{ie} not only of the type of ions[1] (including certain comparatively heavy ions which may appear in a vacuum gap) and electrode materials, but also of the intensity of the electric field on the cathode. The ratio of the current of secondary electrons, I_2, to the current I_1 of the ions bombarding the cathode with variation in the voltage on the vacuum gap from 10 to 140 kV (this voltage was determined by the energy of the ions) varied from 2 to 20 and was maximum for ions of nitrogen with a steel cathode. Figures 25 and 26 present certain data from Bourne et al. [106]. An increase in the cathode gradient caused a certain increase in the yield of secondary electrons for Al and Mg. For steel, Cu, Pb, and Au the emission of electrons did not depend on the field on the cathode.[2]

Hill et al. [108] measured the coefficient of ion-electron emission for targets of Mo, Cu, Al, and Pb under bombardment by H^+, H_2^+, and He^+ ions with energies ranging from 43 to 426 keV. The dependence of K_{ie} on energy for He^+ ions and for Mo targets developed a smooth maximum in the 200-400 keV region, corresponding to the value $K_{ie\ max} = 14$. At the beginning of this energy interval $K_{ie} = 11$. For H_2^+ ions and the same metal the value $K_{ie\ max} \approx 7$ was achieved at ion energy of 120 keV; at 400 keV the value of K_{ie} dropped to 5. Values of K_{ie} for H^+ ions dropped smoothly from 4 to 2. The relationships were similar for the targets of the other metals.

---

[1]No analysis was conducted of the incident ions in this work, but it was assumed that singly charged ions predominate in the ion current.

[2]In work [105] a change in the field on the cathode from 0 to 200 kV/cm led to an increase in K_{ie} from 4 to 10 for a steel cathode bombarded by molecular ions of hydrogen. The value of K_{ie} was unchanged with atomic hydrogen ions.

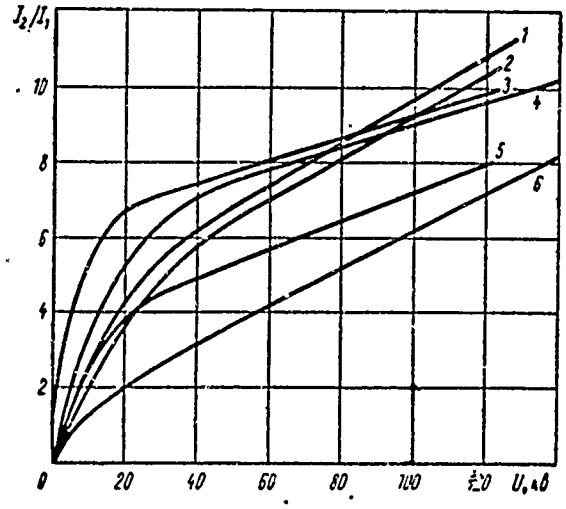

Fig. 25. Emission of electrons during incidence of helium ions with various energies on the surfaces of different metals [106]: 1 – lead; 2 – gold; 3 – aluminum; 4 – magnesium; 5 – steel; 6 – copper.

Designation: кв = kV.

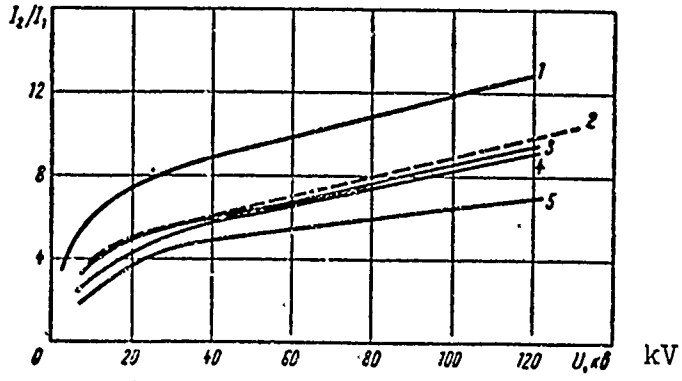

Fig. 26. Emission of electrons during incidence of various ions on the surface of aluminum: 1 – nitrogen; 2 – xenon; 3 – helium; 4 – mercury; 5 – hydrogen.

Aarset et al. [107] studied the curve of the change in K_{ie} with energies of H^+ and H_2^+ ions varying from 0.7 to 2 MeV. The yield of secondary electrons did not depend on the target material (Al, Mg, Fe, Au, and Pb were used) or on the magnitude of the field on its surface (in the interval 0-36 kV/cm) and was reduced

with energy: from 3.8 to 2.3 for H_2^+ ions and from 1.3 to 0.7 for H^+ ions.

The vacuum conditions (10^{-5}-10^{-4} mm Hg) and the methods used for cleaning the targets in the considered works [106-108] (preliminary conditioning under an ion beam until stable values were obtained[1]) provide a basis for assuming the presence of various foreign atoms on the surfaces of the targets.

The experimental data attest to the fact that smaller values of the coefficient of ion-electron emission K_{ie} correspond to purer surfaces; the difference from the values of K_{ie} for contaminated targets is more noticeable in the low-energy region.

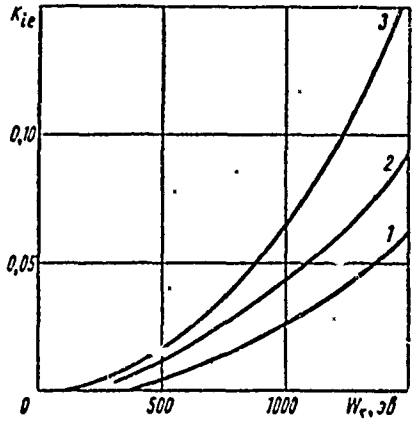

Fig. 27. The coefficient K_{ie} as a function of the energy of Li^+ ions for atomically pure tungsten (1), tungsten with adsorbed layers of oxygen (2) and nitrogen (3). Designation: кв = kV.

Figure 27 shows K_{ie} for atomically pure tungsten and tungsten with adsorbed O_2 and N_2 layers as a function of the energy of incident Li^+ ions [109]. The measurements were carried out in a high vacuum ($2 \cdot 10^{-10}$-$4 \cdot 10^{-10}$ mm Hg) and they show a growth in K_{ie} in the presence of adsorbed layers by an order of magnitude with ion energies less than 350 eV and by 2-3 times with energies above 500 eV.

[1]As a result of such conditioning the yield of electrons was halved as compared with the yield from a fresh target [108].

Measurements of K_{ie} in work [110], made in substantially purer conditions than those in work [108] (vacuum about 10^{-7} mm Hg, heating and ion bombardment of the target) give values of $K_{ie\ max}$ for Mo and H^+ and He^+ ions which equal approximately 1.5 and 2, respectively – i.e., significantly lower than the values of $K_{ie\ max}$ given above for these cases. In addition, measurements carried out immediately after termination of target heating showed that the yield of ion-electron emission was approximately halved as a result of heating and that subsequently, as the initial surface conditions are restored, in the course of a few minutes it grows to the initial value.

Tel'kovskiy [111] measured K_{ie} for pure Mo, Zr, Ni, Ta, Cu surfaces and for H, He, N, Ne, Ar and Mo ions with energies ranging from a few kiloelectron volts up to 120 keV. It was demonstrated that even insignificant contamination of the metal surface (on the order of a monolayer) by foreign atoms leads to dependence of K_{ie} on the magnitude of the current of primary ions. This phenomenon was used to monitor the state of the surface, which was considered to be pure when K_{ie} was constant with a change in ion current amounting to three orders (from 10^{-7} to 10^{-4} A/cm^2). It was possible to obtain such a surface only by sputtering the target metal with argon ions after degassing at temperatures up to 2800°K,[1] while the measurements were carried out at 1300-1500°K in a vacuum of 10^{-8} mm Hg. Figures 28 and 29 show the obtained results. We will note that the value of $K_{ie\ max}$ for H^+ ions and a target of Mo amounts to 1.8 (Fig. 29).

Large [112] measured values of K_{ie} under bombardment with various ions with energies of 20-140 keV on an atomically pure tungsten surface. The greatest values of K_{ie} (approximately 7)

[1]Through chemical and spectral analyses it was established that a single prolonged heating does not lead to complete cleaning of the target because of the formation on its surface of nonvolatile compounds of the carbide, nitride, silicide, etc. type.

were observed in the indicated energy range for O_2^+ and N_2^+ ions. A $K_{ie\ max}$ value of approximately 1.5 was measured for H^+ ions.

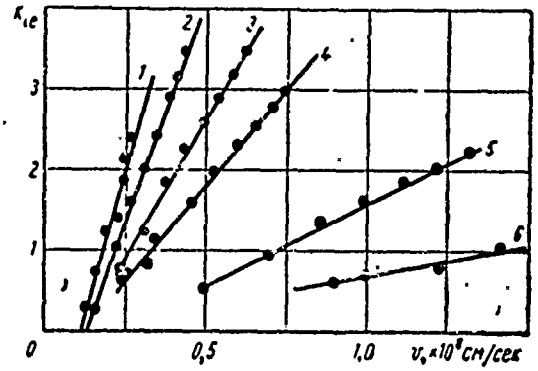

Fig. 28. The coefficient K_{ie} as a function of the velocities of various ions bombarding a molybdenum target: 1 – Mo^+; 2 – Ar^+; 3 – Ne^+; 4 – N^+; 5 – He^+; 6 – H^+.

Designation: см/сек = cm/s.

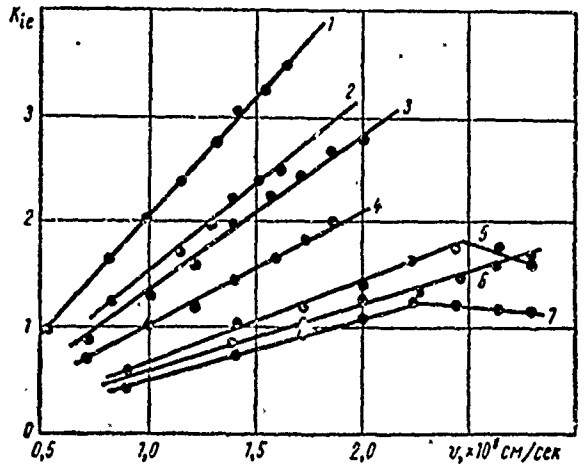

Fig. 29. The coefficient K_{ie} as a function of the velocity of hydrogen ions bombarding targets made of molybdenum, zirconium, and graphite: 1 – $H_3^+ \rightarrow Mo$; 2 – $H_3^+ \rightarrow Zr$; 3 – $H_2^+ \rightarrow Mo$; 4 – $H_2^+ \rightarrow Zr$; 5 – $H^+ \rightarrow Mo$; 6 – $H^+ \rightarrow C$; 7 – $H^+ \rightarrow Zr$.

Designation: см/сек = cm/s.

Thus, under the actual conditions of a high-voltage vacuum gap when ordinary electrode materials are used the yield of electrons from the cathode due to bombardment with positive ions will not exceed a few tens of electrons per ion, even in the presence of various contaminating layers on the surface. Values of K_{ie} a few times smaller[1] correspond to comparatively purer conditions on the surface – conditions achievable by the use of high vacuum and various types of treatment.

Ion-ion emission. Analysis of knocked-out negative (and also positive) ions show that ion emission processes are determined basically by the interaction of the incident ion beam with contaminants of various types present on the surface of the metallic target. In experiments by Fogel', Slabospitskiy, and Karnaukhov involving bombardment of molybdenum with ions of inert gases at energies of 20 keV (see [114]) negative ions caused by the presence of adsorbed gaseous layers on the target surface and also ions caused by the nature of the metal itself (negative ions of Mo oxide and positive Mo^+ ions) existed in the spectrum of ion emission. Cleaning the target by heating it up to ~400°C led (for a hot target) to the disappearance of ions of all types except Mo^+ and C^{2-}. The curves of temperature dependence of ion emission permit assuming that various types of chemical reactions occur on the surface of the targets under the action of the ion beam; the products of these reactions may be the sources of the observed secondary ions.[2] Restoration of the initial emission for various types of ions occurs over the course of a time interval ranging from 1 to 20 minutes after termination of target heating.

---

[1]For measurement conditions which do not disturb the initial state of the surface of a metal located for a prolonged period in a vacuum system evacuated by oil vacuum pumps, Mansfield [113] reports a value of $K_{ie} \approx 11$ for 250 keV H^+ ions and a copper target.

[2]See also [115].

An important role during emission of secondary negative ions is played by the reduction in the work function of the metal with absorption of various electropositive impurities, for example alkali metals [116]; as a result of this there is an increased probability of the formation of negative ions of various gases possessing electron affinity.

As the measurements made by Fogel' et al. showed [117], the total coefficient of secondary emission of negative ions, K_{ii}^{-}, in the energy region 10-40 keV is insignificantly reduced with a growth in the velocity of incident ions[1] and depends substantially on the type of these ions. In the indicated energy range it comprises a value ranging from several thousandths to a few hundredths (Fig. 30). The value of K_{ii}^{-} changes only insignificantly with a change in target material (Fig. 31).

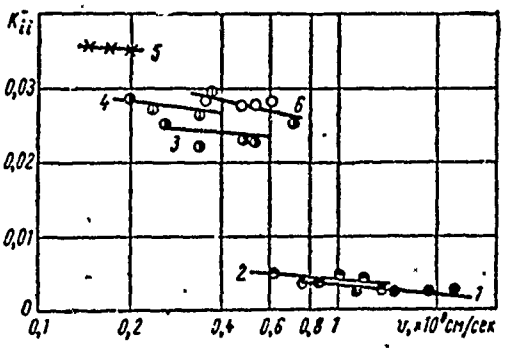

Fig. 30. Emission of negative ions from a molybdenum surface under the action of various ions as a function of their velocity: 1 – H^+; 2 – He^+; 3 – Ne; 4 – Ar^+; 5 – Kr^+; 6 – O^+.

Designation: см/сек = cm/s.

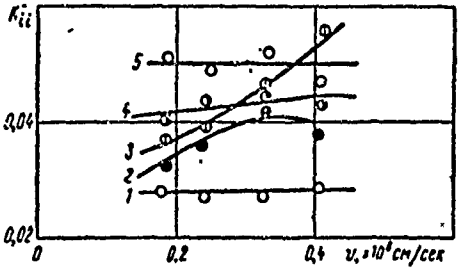

Fig. 31. Emission of negative ions as a function of the velocity of Ar^+ ions bombarding surfaces of various metals: 1 – molybdenum; 2 – iron; 3 – tantalum; 4 – tungsten; 5 – copper.

Designation: см/сек = cm/s.

[1]The energy dependence of the coefficient K_{ii}^{-} for certain definite types of negative ions is more noticeable and passes through a maximum in the region of a few kiloelectron volts.

The dependence of K_{ii}^- on the energy of hydrogen and deuterium ions in the energy region 200-1000 keV obtained by Mitropan and Gumenyuk [118] (Fig. 32) shows that in this case K_{ii}^- is reduced to 10^{-3}-10^{-4}.

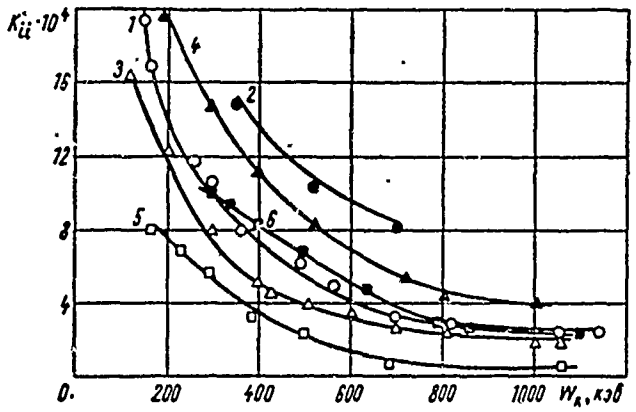

Fig. 32. The yield of negative ions as a function of the energy of H_1^+ and D_1^+ for targets of various materials: 1 – H_1^+ → Al; 2 – D_1^+ → Al; 3 – H_1^+ → → stainless steel; 4 – D_1^+ → stainless steel; 5 – H_1^+ → Cu; 6 – D_1^+ → Cu.

Designation: кэв = keV.

All of the above values for K_{ii}^- were obtained for preheated targets subjected to ion bombardment in a vacuum of 10^{-6}-10^{-7} mm Hg. Measurement of K_{ii}^- immediately after heating of the target in the same experiment showed an essential reduction in the emission of negative ions, which grew up to the initial values after a few tens of minutes.

Mansfield [113] measured the coefficient K_{ii}^- in a pulse regime with bombardment of copper, aluminum, and steel targets with 250-keV H^+ ions. The amplitude of ion current pulses on the target, with a frequency of 1 pulse per minute, was on the order of 10^{-8} A with a pulse length of a few milliseconds. The targets

were not heated and the selected measurement conditions determined the absence of cleaning of the surface as a result of ion bombardment. In this way measurements were carried out of the yield of negative ions from a metallic surface containing various contaminants characteristic for a vacuum system subject to prolonged evacuation by an oil diffusion pump. Under these conditions values were obtained for K_{ii}^{-} which very substantially exceeded the data obtained by Mitropan and Gumenyuk [118]. The values of K_{ii}^{-} comprised 0.43, 0.24, and 0.44 for copper, aluminum, and steel targets, respectively. For the most part the knocked-out ions were comprised of H^{-} ions; it was assumed that their source was a layer of hydrocarbon on the surface of the target.

Mansfield [113] also measured the coefficient K_{ii}^{+} of the yield of positive ions during bombardment of a target by 250 keV H^{-} ions. For each incident H^{-} ion this resulted in 1, 1.1, and 0.54 positive ions being knocked out of copper, aluminum, and steel targets, respectively. These were mainly H^{+} ions.

For comparison we will note that under conditions obtaining during their measurements of the same coefficient K_{ii}^{-}, Fogel' et al. [117] obtained a value of K_{ii}^{+} equal to $4.4 \cdot 10^{-3}$ (bombardment of a molybdenum target with 22 keV H^{-} ions).

Thus, it is possible to establish very essential dependence of the intensity of secondary ion emission on the degree of contamination of the bombarded metallic surface with foreign films.

CHAPTER 3

PHENOMENA IN THE VACUUM GAP AT A VOLTAGE BELOW THE BREAKDOWN VALUE

1. DARK OR PREBREAKDOWN CURRENTS

At voltages below the breakdown level in a number of cases with vacuum electric insulation conductivity which is not accompanied by any visible effects will arise in the insulating vacuum gap. The currents may reach values of 10^{-5}-10^{-3} A with an electrode area of a few square centimeters; they depend strongly on the intensity on the electrodes and vary comparatively slowly in time, although the appearance of substantial jumpwise changes is not unusual. These currents arise under both direct and high-frequency voltages, although below we introduce data obtained only at constant voltage. Some of the first measurements of the general characteristics of dark currents were made by Anderson [119] for steel electrodes several square centimeters in area in a virtually uniform electrical field and a vacuum of 10^{-5} mm Hg. Results of measuring the dependence of currents I on the applied voltage U and on intensity E are shown in Table 14.

From the table it follows that the magnitude of the current depends both on the intensity and on the total applied voltage; however, the dependence on intensity is significantly stronger.

For a tentative determination of the composition of the dark current (its content of negatively and positively charged

Table 14. Dark current I at constant voltage U for steel electrodes [119].

(1) U, кв	Темновой ток I при различных напряженностях (2) $\times 10^{-8}$ а		
	(3) 21,9 кв/мм	(3) 27,4 кв/мм	(3) 30 кв/мм
40	0,5	4	6
80	1	20	33
110	1,5	28	45

KEY: (1) U, kV, (2) Dark current I at various intensitites $\times 10^{-8}$ A, (3) kV/mm.

particles), Anderson measured the rate of heating under bombardment by dark currents for the anode and cathode separately; in the experiments they were well thermally insulated. He found that the rate of heating of the anode is approximately two orders higher than that for the cathode – i.e., the dark current consists of approximately 99% negatively charge particles. Bourne et al. [106], repeating the last measurements, found that at 80-100 kV the current of negatively charge particles exceeds the current of positive ions by 300 times with aluminum electrodes and by more than 1000 times with steel electrodes. Determination of the fraction of electrons in the dark current composition was carried out by Pivovar et al. [120]; for this purpose they applied a transverse magnetic field of such a magnitude that it prevented the electrons from the cathode from arriving at the anode, while positive and negative ions could cross the interelectrode gap without hindrance. Thus, by measuring the dark current with and without the magnetic field it was possible to determine the electron and ion components of the dark current. Table 15 shows the results of these measurements in a vacuum of $1 \cdot 10^{-6}$-$3 \cdot 10^{-6}$ mm Hg, created by oil pumps, for flat electrodes 12 mm in diameter. The total magnitudes of currents under the conditions indicated in the table fell within the limits 10^{-9}-10^{-4} A.

Table 15. Ratio of electron and ion components of a dark current at constant high voltage [120].

(1) Материал		d, мм	(8) U, кв	(4) $\frac{I_{эл}}{I_{ион}}$
(2) катода	(3) анода			
(5) Медь	Свинец (6)	3	70	0
		3	81	2,7
		3	93	72
		5	84	3,5
		5	118	80
(5) Медь	(5) Медь	3	83	5
		3	112	10
		3	128	135
		5	100	1
		5	145	121
(5) Медь	Алюминий (7)	3	98	0
		3	126	21
		3	136	110

KEY: (1) Material, (2) cathode, (3) anode, (4) I_{el}/I_{ion}, (5) Copper, (6) Lead, (7) Aluminum, (8) U, kV.

A growth in the electron component of the dark current with an increase in voltage is clearly visible from the given table. Although we have no data on the individual change of the electron and ion components with intensity, from comparison of Tables 14 and 15 it is possible to conclude that the rapid rise in dark current with an increase in intensity is due mainly to the growth in the electron current, while the increase in the current of ions is substantially less or does not occur at all.

The measurements whose results are given in Tables 14 and 15 were obtained at a voltage on the order of 100 kV and with prolonged holding and conditioning by electrode discharges in a vacuum which was not completely free of organic compound vapors. This must be emphasized, since one of the basic peculiarities of dark currents, strongly hampering their quantitative description and the practical utilization of the obtained results, in the exceptionally strong dependence of the magnitude of the currents and the nature of their change on the experimental conditions,

that is, those conditions which are virtually impossible to control. For example, with two pairs of electrodes which are identical in shape, manufactured from a single piece of metal, and treated with identical procedures, dark currents arising with the application of voltage of identical magnitude can differ by an order of magnitude and more. After a certain amount of conditioning by discharges this difference is usually reduced, but the operating conditions of the electrodes begin to have an effect – that is, the parameters of the electric circuit, the conditions in the inter-electrode gap – conditions which will be difficult to take into account and which are not always borne in mind by various investigators. The numerical data given in this chapter and found by different authors under nonidentical conditions can only provide a range of those magnitudes of currents which are obtained in real cases, while the dependences given for voltage, intensity, electrode material, and so on characterize most often a general tendency and nature of the relationship rather than exact ratios between the current and the given parameters.

In addition to the difficulties listed above, a number of relationships have either been studied inadequately or not at all. In particular, this concerns relationships of current and residual pressure (both its magnitude and the composition of the residual gases). This dependence in the pressure region above 10^{-5} mm Hg can be judged only by indirect data from the work by Linder and Christian [121]. To obtain high voltage they placed a certain quantity of radioactive strontium on a high-voltage electrode located inside an evacuated vessel. With activity of the utilized Sr^{90} source of 250 millicuries the current corresponding to its emission (electrons with 650 keV) comprised 10^{-9} A. In principle the voltage achievable on the electrode cannot exceed a magnitude corresponding to the energy of the emitted electrons – i.e., 650 keV – but in the actual case it was less and reached only a magnitude at which the dark current (plus leaks over the insulator) equaled 10^{-9} A. With a change in the pressure of the residual

gases the highest voltage, namely 370 kV, was obtained with aluminum electrodes and a pressure of 10^{-3} mm Hg. For a pressure of 10^{-2} for 10^{-5} mm Hg the voltage was below 150 kV. In the case of nickel electrodes the highest voltage (240 kV) was obtained at 10^{-5} mm Hg. Considering the strong dependence of dark current on U and E, we can conclude from these data that at a certain pressure current is minimum, with the magnitude of this optimum pressure depending on the electrode material. In the region of lower pressures (10^{-10}-10^{-5} mm Hg), according to the measurements of Pivovar and Gordiyenko [122], a change in pressure has no effect on the dark current. These latter results were obtained on an installation creating a vacuum of 10^{-9}-10^{-10} mm Hg through a reduction in the rate of evacuation and with retention of a high degree of electrode surface purity, corresponding to the value of maximum vacuum indicated above. Therefore the obtained results do not mean that dark current will be identical in vacuum systems designed to obtain a "technical" vacuum of 10^{-5}-10^{-7} mm Hg and in high-vacuum systems where conditions are cleaner.

As was pointed above, the basic characteristic of dark currents is their dependence on the applied voltage and the intensity on the electrodes. In order to obtain more statistical material on this question, Heard [123] photographed on a single frame a large number of curves obtained on an oscillograph screen where the horizontal reflection was proportional to the applied voltage and the vertical reflection was proportional to the magnitude of dark current. Each such photograph was taken with no change in the interelectrode distance and with electrodes of a definite material. Accumulation of a large number of photographs provided a statistical basis for establishing the basic relationships. Owing to the change in dark current in individual breakdowns or in the course of prolonged holding of the electrodes under voltage, a large spectrum of curves was obtained on each photograph; the upper and lower boundaries of this spectrum showed

that range of dark currents which might occur under the given conditions. Measurements were carried out in a vacuum of 10^{-7} mm Hg on an installation where substantial efforts were made to reduce the content of organic compound vapors and with electrodes subject to a very large number of conditioning breakdowns in order to obtain a more or less steady-state value of the dark current during successive breakdowns. It was found that with interelectrode distances of fractions of a millimeter the dark current is determined only by the intensity on the cathode, while the nature of the dependence of current on this intensity is close to the analogous relationship for field-effect emission current (9):

$$I = BE^2 \exp\left(-\frac{b}{E}\right), \qquad (13)$$

where B and b are constants which can be determined empirically for each individual case. On the basis of analysis of the photographs mentioned above, Heard [123] calculated the constant B and b for the upper and lower limits of the values of dark current. Table 16 shows the values of these constants. The experimental data were obtained with a gap of 0.2 mm between hemispherical electrodes 50 mm in diameter. Despite the size of the electrodes and obviously due to the voltage drop from the center to the edge the major portion of the dark current was concentrated on an area of approximately 1 cm^2; therefore the data given in Table 16 can be considered to relate to electrode areas of 1 cm^2. This same table shows the number of conditioning breakdowns and also gives values for dark currents at an intensity of 100 kV/mm which we calculated from the given constants. Heard arranged the materials in Table 16 in the order of rise of the dark currents, and in his opinion it is precisely this arrangement which constitutes the basic value of the table, since specific values of the constants depend too strongly on many conditions and, as will be evident below, differ significantly from the values of similar constants which can be calculated from the experimental results obtained by other investigators. This is

Table 16. The constants B and b (13) and dark currents with E = 100 kV/mm [123].

(1) Материал электродов	Число тренирующих пробоев	(2) b·10⁶ в/м	B·10⁻²¹ а·м²/в²	(2) b·10⁶ в/м	B·10⁻²¹ а·м²/в²	(3) Ток, E=100 кв/мм, а
		(4) при минимальном токе		(5) при максимальном токе		
(6) Закаленная сталь	24 000	44,5	141	5,8	8,7	$0—3\cdot10^{-7}$
(7) Нержавеющая сталь 316	60 000	43,5	32 000	5,2	4,4	$0—3\cdot10^{-7}$
	15 000	34	10 000	4,6	10,5	$10^{-15}—10^{-6}$
(8) Хасталлой В	13 000	30,5	220	3,45	31,5	$10^{-16}—10^{-5}$
(9) 30%-ная никелевая сталь	10 000	28	6 500	16	150	$10^{-14}—2\cdot10^{-10}$
(10) Инвар	26 000	27	135	9,15	67,5	$2\cdot10^{-15}—7\cdot10^{-8}$
(11) Инконель	12 000	18	2 040	3,25	64,5	$3\cdot10^{-10}—4\cdot10^{-5}$
(12) Тантал	15 000	17,5	2 000	1,05	5,9	—
(13) С-15 (анодный графит)	2 500	16	80 000	2,1	71	$10^{-8}—10^{-4}$
(14) Спектрографический графит	10 000	17	25 000	6,4	130	—
(15) Горячекатаная сталь	85 000	14,5	19 000	7	310	—
(16) Марганцевая сталь	27 000	13,5	50	10,5	21	—
(17) Медь, раскисленная фосфором	10 800	13	810 000	12	3 500	10^{-6}
(18) Никель	13 000	12	4 600	1,1	365	—
(19) Медь, переплавленная в вакууме	24 000	9,4	24 000	—	—	$2\cdot10^{-5}$
(20) Алюминий разных марок*	9 000	3,8	2 500	0,31	49	—
	20 000	7,8	4 700	0,59	3 450	
(21) Вольфрам	9 100	—	—	4,04	13 500	$2\cdot10^{-3}$
Молибден (22)	43 000	—	—	2,8	1 400	$6\cdot10^{-4}$
(23) Серебро	25 000	2,94	63 000	0,38	4 200	—

*Certain types of aluminum (numbers of a lower series) gave dark currents greater than those from tungsten and molybdenum.

KEY: (1) Electrode material; (2) Number of conditioning breakdowns; (3) Current, E = 100 kV/mm, A; (4) at minimum current; (5) at maximum current; (6) Hardened steel; (7) Stainless steel 316; (8) Hastalloy B; (9) 30% nickel steel; (10) Invar; (11) Inconel; (12) Tantalum; (13) S-15 (anode graphite); (14) Spectrographic graphite; (15) Hot-rolled steel; (16) Manganese steel; (17) Copper deoxidized by phosphorus; (18) Nickel; (19) Copper remelted in a vacuum; (20) Aluminum of various types*; (21) Tungsten; (22) molybdenum; (23) Silver.

[в/м = V/m; $а\cdot м^2/в^2 = A\cdot m^2/V^2$]

particularly evident from Table 17, which gives analogous constants b and B which we calculated on the basis of experimental data from other investigators.

Table 17. Dark-current density after conditioning of the electrodes with breakdowns and the values of the constants in equation (13) according to experimental data of various authors.

(2) Максимальное напряжение, кв	(3) Вакуум, мм рт. ст.	(4) Размер и материал электродов	Диапазон при измерениях (1): (5) напряженности, кв/мм	(6) плотности темнового тока, а/см²	$b, \times 10^6$ в/м V/m	$B, \times 10^{-21}$ а·м²/в² A·m²/V²	(7) Литература
30	10^{-8}	0,5 см², (8) никель	26—44	$8 \cdot 10^{-9}$—10^{-5}	3,41	$4 \cdot 10^4$	[124]
17	10^{-10}	(9) Диаметр 0,7 мм:					[44]
		(10) а) чистый вольфрам	140—200	$2 \cdot 10^{-7}$—$2 \cdot 10^{-4}$	30,5	$4 \cdot 10^7$	
		(11) б) вольфрам, покрытый цезием	28—47	10^{-8}—$2 \cdot 10^{-4}$	5	$6,4 \cdot 10^6$	
100	10^{-9}—10^{-10}	(12) 1 см², молибден (3 экземпляра)	17—40	$4 \cdot 10^{-10}$—$3 \cdot 10^{-5}$	1,93 3,82 2,85	60 $3 \cdot 10^5$ 700	[122]
27	10^{-5}	(13) Диски диаметром 18 мм, нержавеющая сталь	19—27	$5 \cdot 10^{-5}$—$5 \cdot 10^{-4}$	1,96	$5,5 \cdot 10^5$	[125]

KEY: (1) Range during measurements; (2) Maximum voltage, kV; (3) Vacuum, mm Hg; (4) Size and material of electrodes; (5) field intensity, kV/mm; (6) dark-current density, A/cm^2; (7) Reference; (8) nickel; (9) Diameter; (10) a) pure tungsten; (11) b) tungsten coated with cesium; (12) molybdenum (3 specimens); (13) Disks 18 mm in diameter, stainless steel.

For convenience in comparison with the data in Table 16, the values of the constants and the currents were recalculated for

an electrode area of 1 cm^2. For the same reason only values of currents obtained after conditioning of the electrodes with breakdowns are used for the table.

The measurements by Heard, Brodie, and Bennette, whose experimental data are given in Tables 16 and 17, indicate that with a change in the interelectrode distance or in the shape of the electrode the dark current depends only on the intensity on the cathode E_c, while the total applied voltage and the intensity on the anode do not influence the current. Brodie [124] obtained a virtually identical dark current of approximately 10^{-7} A at values of E_c = 21 kV/mm, for two different configurations of nickel electrodes: in the first case the electrodes were flat and in the second case the cathode was made as a straight filament 0.125 mm in diameter and of such a length that the area of the surface was identical with the area of the electrodes in the first case, while the anode was a cylinder of comparatively large diameter and was concentric with the cathode. In other of Brodie's experiments with flat electrodes and a change in the interelectrode distance within the limits 0.25-2 mm the current depended only on E_c. Analogous results were obtained by Bennette et al. [44] and by Heard [123]. This evident contradiction with the results of measurements given in Tables 14 and 15 is apparently explained by the different experimental conditions. In their experiments Brodie, Bennette, and Heard did not use voltages above a few tens of kilovolts, where the data in the tables cited above relate to higher voltages. At the same time the vacuum conditions in the latter case were substantially less pure. Both of these factors are quite essential and might influence the characteristics of the dark currents. Indirect confirmation of this is found in comparison of the results obtained by Bennette et al. [44] and Brodie [124], on the one hand, and by Pivovar with Gordiyenko [122] and Wijker [125] on the other hand (see Table 17). Clearly, in the measurements carried out by Pivovar and Gordiyenko in very pure conditions but at increased voltages, the dark currents at

comparable intensities were greater than those for clean electrodes in the measurements by Bennette and Brodie. The dark currents were also greater in magnitude in measurements by Wijker, which were made at comparatively small voltages but for which the vacuum conditions were substantially poorer. Yet another distinction should be noted: the measurements of Pivovar with Gordiyenko and by Wijker indicate that the dependence of dark current on voltage (or on the quantity E) diverges substantially from the characteristic corresponding to expression (13). A deviation from the latter with copper and iron electrodes was detected by Hawley [126] in studying dark currents with an interelectrode distance of 0.5-2 mm on alternating voltage in a vacuum of 10^{-5}-10^{-6} mm Hg. He noted that if the relationship $\log (I/E^2) = f(E^{-1})$ which, according to expression (13), should have a form of a sloping line, is depicted on a graph we actually observe broken lines, as shown on Fig. 33. The intensity at the point of break depends mainly on the electrode material (in Hawley's experiments it equals 23-30 kV/mm). From the same figure it is clear that at small intensities (prior to break) the magnitude of dark current depends on the total applied voltage.

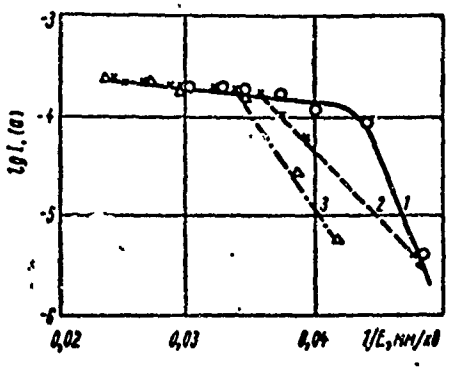

Fig. 33. Dark current with flat copper electrodes [126]: 1 – d = 2 mm; 2 – d = 1 mm; 3 – d = 0.5 mm.

Designations: мм/кв = mm/kV; a = A.

The data from Bennette et al. [44] given in Table 17 give the result of their investigations of the effect of the cathode work function on dark current. These measurements were carried out in a sealed flask of aluminum silicate glass; a reservoir with cesium was located in the lower part of the flask. By varying the

temperature of the reservoir it was possible to control the pressure of cesium vapors in the flask in a range from 10^{-10} to $2 \cdot 10^{-6}$ mm Hg; together with control of the electrode temperatures, this made it possible to monitor the degree of coating of the tungsten by cesium and thus to measure the work function. From the data given in Table 17 it is clear that a reduction in the work function (from 4.5 to 1.6 eV, according to the data of these authors) reduced by approximately 5 times the intensity at which the dark current of a determined magnitude flowed.

Preliminary treatment of the electrodes has a noticeable influence on the magnitude of dark current. Thus according to Brodie [124] with other conditions being equal the dark current will be smaller when the electrode surfaces are hand-finished in addition to machine polishing. The current was less with transition from technically pure (99%) nickel to nickel of increased (99.98%) purity. This divergence in the values of the current was substantially reduced after conditioning of the electrodes by several discharges and even after holding of the electrodes at a high electric field intensity (the remaining divergence was no greater than threefold). With the first supply of a constant-magnitude voltage to the electrodes the dark current grows slowly for several minutes, even in very pure vacuum conditions; this is clear from Fig. 34, taken from Brodie's work [124]. This phenomenon is reversible – i.e., it is observed again when voltage is applied for a second time after a prolonged interval. With prolonged application of the voltage the currents are unstable (they experience smooth changes and jumps, usually with a general tendency toward reduction). Current instability depends on the vacuum: at 10^{-10} mm Hg the current is more stable than at 10^{-8} mm Hg. After intensive heat treatment of a tungsten hemispherical cathode 0.7 mm in diameter, during measurement of dark current in a vacuum better than 10^{-10} mm Hg Bennette et al. [44] found that if the magnitude of the current is less than 1 μA it is stable over the course of

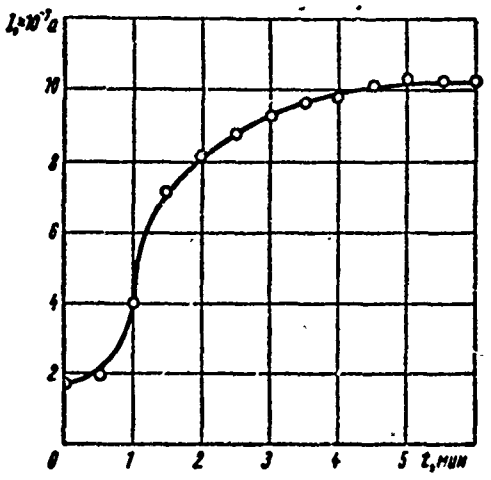

Fig. 34. Change in dark current in the first moments after application of a constant voltage for nickel electrodes with an area of approximately 0.5 cm^2 (E = 22.4 kV/mm, p = = 10^{-10} mm Hg).

Designations: а = A; мин = = min.

many hours; significant fluctuations on both sides are observed with a current which is greater than 10 μA.

Owen and Beyon [127] carried out comparative measurements of dark currents for identical electrodes in a vacuum of 10^{-5} mm Hg created by oil pumps and in a vacuum of better than 10^{-8} mm Hg created by sorption pumps. They found that at 10^{-5} mm Hg on a general background of dark current which is more or less stable in time short-term surges of current appear; at 10^{-8} mm Hg there were no such surges, although the average value of the current was approximately the same. Measurements were made for flat electrodes, carefully polished, in the form of disks 10 mm in diameter made from gold, nickel, and molybdenum. At a voltage of 5-11 kV and an interelectrode gap of 0.3 mm the average value of dark current was 10^{-12}-10^{-8} A.

Strong changes occur in the magnitude of dark current during breakdowns and microdischarges. As a rule, after several breakdowns the dark current is reduced, but further change in the current depends decisively on the parameters of the electrical circuit, which during the post-breakdown discharge determine the magnitude of the current and the nature of its change. Basically two parameters are operative: damping resistance R_d, i.e., the

resistance standing in the discharge circuit, and shunting capacitance C_{sh} – i.e., the capacitance of the electrodes and of structural elements connected directly to them (in certain cases, a special capacitor). If C_{sh} is small and if R_d is measured in megohms, during conditioning with breakdowns dark currents grow to such an extent that they may even limit the increase in voltage on the electrodes (see, for example, the explanation in the text of Fig. 44 in the following chapter). The effect of capacitance C_{sh} on the dark-current characteristic after repeated breakdowns is shown on Fig. 35, which gives data obtained by Heard [123] for electrodes made of Invar with an interelectrode gap of 0.2 mm in a vacuum of 10^{-7} mm Hg. In these experiments R_d = 500 kohm. From the curves it follows that the best results (lowest currents) were obtained at significant magnitudes of shunting capacitance (0.0126-0.025 μF). The obtained relationships satisfy expression (13) at the values of the constants shown in Table 18.

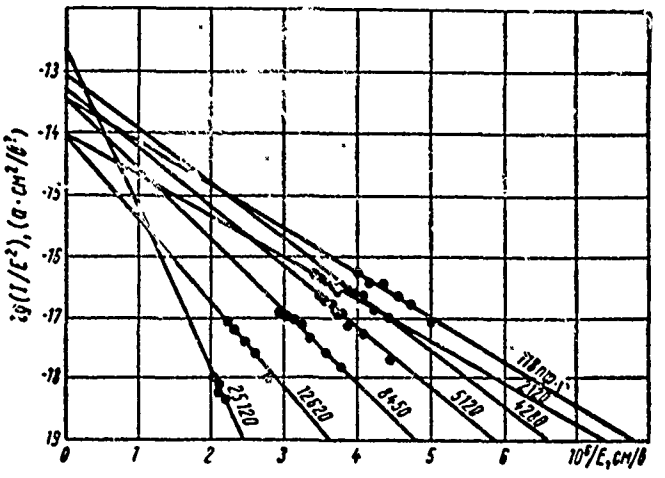

Fig. 35. Dark current for Invar electrodes, shunting capacitances of various magnitudes, after conditioning of the electrodes with repeated discharges. (Numbers on the curves indicate the magnitudes of shunting capacitance).

Designations: а·см^2/в^2 = A·cm^2/V^2; пф = pF; см/в = cm/V.

Table 18. Values of the constants b and B in expression (13), determining the dark current, for Invar electrodes as a function of the magnitude of shunting capacitance.

$C_{ш}$, пФ (1)	b, ×10⁶ в/м	B, ×10⁻²¹ а·м²/в²	$C_{ш}$, пФ (1)	b, ×10⁶ в/м	B, ×10⁻²¹ а·м²/в²
118	1,29	3980	8450	2,08	4170
2120	1,55	1000	12620	3,15	10(~)
4280	1,39	9950	25120	5,11	35000
5120	1,64	6030			

KEY: (1) C_{sh}, pF.

Designations: в/м = V/m; а·м²/в² = = A·m²/V².

As will be evident from the following section, the dark current occurring at comparatively low voltages and in pure vacuum conditions is apparently a field-emission current from sharp projections on the cathode, and the apparent coincidence of the empirical expression (13) with the field-effect emission formula (9) reflects the physical essence of the phenomenon. However, evaluations of the quantities μ and the emitting area S_{em} on this basis utilizing empirical values of B and b may lead to large errors due to emission by several projections with different μ, S_{em}, and work function Φ. At the same time the tendency to a change in μ and S_{em} with a change in the conditions on the electrodes can apparently be determined in this way. Thus, the data in Fig. 35 and Table 18 indicate that an increase in C_{sh} causes a reduction in μ ($\mu \sim b^{-1}$) and, as a rule, an increase in S_{em} ($S_{em} \sim Bb^2$), which is logically explained by the more intensive melting of the emitting projections during discharges, when C_{sh} is large.

The effect of microdischarges and prolonged high-temperature heating of the electrodes on dark current was studied by Pivovar and Gordiyenko [122]. Molybdenum electrodes were conditioned in a vacuum of 10^{-9}-10^{-10} mm Hg by microdischarges until the lowest

dark current was obtained. Then both electrodes were heated separately at 1800-2000°C for several hours, so that evaporation products impinged exclusively from the heated electrode onto the opposite electrode. Voltage was supplied to the electrodes in order to measure the dark current only after complete cooling of the electrode. Figure 36 shows the results of measurements with an interelectrode gap of 4 mm. It is clear that prolonged intensive heating of the cathode led to a strong growth in dark current — to a reduction in the intensity at the appearance of a noticeable dark current by 5-6 times as compared with the case when the electrodes were conditioned by microdischarges. If the surface of the cathode was additionally polished after the described heating, no such large growth in dark current was observed. Prolonged heating of the anode also increased the dark current, but not to the same degree as heating of the cathode. It is noted that the dependence of dark current on voltage (intensity) after anode heating is more reminiscent of the Schottky effect (i.e., $\log I \sim \sqrt{E}$) than of the expression for field-effect emission current similar to equation (13).[1]

The results obtained by Pivovar and Gordiyenko on the effect of cathode heating contradict to a certain degree the smoothing of projections on the emitter surface which is frequently observed during the study of field-effect emission (it leads subsequently to a reduction in the current at the same voltage). Apparently this divergence is explained by the different heating regime, its intensity and duration, or by the different initial materials for manufacturing the cathode — difference in both composition and in lot (in particular, Pivovar and Goridyenko used molybdenum strip, in contrast to the wire or solid cathodes used by other investigators).

[1]The influence of working temperature on dark current is described in the following section.

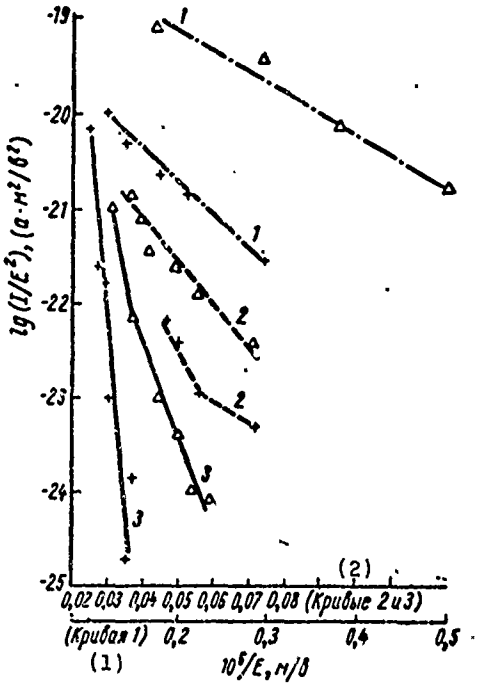

Fig. 36. Dark current for two different molybdenum electrode specimens. Electrode area about 1 cm^2, d = 4 mm, p = $= 10^{-9}$ mm Hg. + and Δ – the two electrode specimens; —— – electrodes conditioned by microdischarges; ---- – after high-temperature heating of the anode; -.-.- – after high-temperature heating of the cathode.

KEY: (1) (Curve 1); (2) (Curves 2 and 3).

Designations: $а \cdot м^2/в^2 = A \cdot m^2/V^2$; $м/в = m/V$.

2. THE NATURE OF DARK CURRENTS

The content of the preceding chapter casts a certain amount of light on the nature of the dark current, although much is still unclear and as yet there is no single view on the nature of the appearance of dark current in a number of practical cases – i.e., under conditions of technical vacuum and with increased voltage. From the preceding section it is clear that in these conditions dark current contains, besides an electron component, a significant current of ions, whose fraction is significant at a rather small intensity. Just precisely what ions "participate" in the dark current and the basic characteristics of the ion component of the dark current are not as yet clear. However, the proposal by Ionov [128] is worthy of attention. He advances the idea that the basic reason for the appearance of an ion current is the surface ionization of substances with low ionization potential (e.g., alkali metals) which exist in the form of impurities in the majority of even the technically pure metals usually used in

electrode material. In support of this explanation Ionov presents results of a work [95] in which emission of ions of alkali metals existing as an impurity in technically pure nickel and tungsten was observed. At a temperature of 470°C and with an electric field intensity E < 0.1 kV/mm the currents equal 10^{-11}-10^{-10} A/cm^2. Besides ions with a mass corresponding to alkali metals, there are ions with a mass on the order of 100; this makes it possible to propose ionization of adsorbed vapors of organic compounds (the measurements were conducted in a vacuum of 10^{-6} mm Hg). If we take into account the reduction in the heat of evaporation of a substance in the form of ions under the action of an electrical field, when E = 100 kV/mm such emission should be observed even at room temperature. Considering the role of surface irregularities in the increase in field intensity on projections and bearing in mind the conclusions drawn in the work by Pivovar and Gordiyenko [122], we can interpret the results given on Fig. 36 in terms of the effect of anode heating on dark current as an increase in irregularities on the anode during heating.[1] In the presence of an ion current the electron component of the dark current may to a significant degree be the result of emission of electrons from the cathode during its bombardment by positive ions.

To refine the electron component characteristics and to clarify its nature, the distribution over the anode surface of the current density of electrons bombarding the anode has been studied in a number of works. For this purpose Tuczek [32] substituted a photoplated, recording the passage of electrons along a foil anode, for the flat anode manufactured of aluminum foil. Pivovar

[1]Another possible explanation is the increase in the concentration of impurities on the anode surface due to their escape from the thickness of the metal to the surface during intensive heating. An increase in the quantity of easily ionized impurities may lead to an increase in the surface ionization current.

and Gordiyenko [122] installed a luminescence screen behind the anode on the axis of a hole drilled through the anode; in other works the anode was made of a luminescent material, similar to the procedure used in electron microscopes (emission microscopes). Hawley [129] and De Geeter [130] observed under the microscope illumination on the anode and tracks arising due to bombardment of the anode with an electron current. As a result of all these measurements it was established that an electron dark current is distributed extremely unevenly over the surface of the electrodes and consists mainly of individual thin beams. The number of such beams, their intensity, and their stability in time depends on many conditions. Thus, after conditioning nickel electrodes with discharges Brodie [124] observed the simultaneous existence of about 20 beams with a cathode area of approximately 0.5 cm^2. The observations of Pivovar and Gordiyenko indicate that after high-temperature cathode heating, leading to an increase in dark current (see Fig. 36), a large number of beams appear, distributed chaotically over the surface of the electrodes. After the electrodes were treated with microdischarges only one-three emission points remained on the cathode; however, they were more intensive. Observations of luminescence on the anode by means of a microscope [130] permitted detection of weakly luminescence spots approximately 0.05 mm in diameter. With flat stainless-steel electrodes several millimeters in diameter, a gap of 0.42 mm, and voltages 60-70 kV there were usually 4-5 spots, although occasionally their number grew sharply up to 20-25.

The work by Little and Whitney [41] on determining the relief of a cathode at points of electron emission led to significant results. The work was carried out at voltages up to 10 kV and with a gap of 0.38 mm between virtually flat electrodes located in an "oil-free" vacuum of 10^{-7} mm Hg. The use in these experiments of a transparent luminescing anode made it possible to find and examine under an optical microscope through the thickness of the anode the points on the cathode at which electrons were being

emitted. In 80% of the cases it was possible to detect projections at the points of emission; however, the dimensions of the projections were so small that it was not possible to determine their shape. Then, using a combination of observations of luminescence on the anode – the luminescence screen – with observation on the optical microscope (as an exact indicator of the position of the emission spot on the cathode), by means of a shadow electron microscope the authors of [41] were able to examine the profile of the emitting projections, which turned out to be similar to those depicted on Fig. 8. Such projections with a height of 1-2 μm and a base diameter 8-10 times less were detected on optically polished surfaces of stainless steel, aluminum, and copper in all cases when a similar procedure was used to trace the point of emission on the cathode. These experiments show quite confidently that the cause of the appearance of dark currents may be field-effect emission from anomalously large and sharp projections which substantially exceed the irregularities usually obtained during mechanical treatment of the surface in size and differ sharply from them in shape. Actually, in the described experiments a current of 10^{-9} A was observed at an average field intensity between the electrodes of 18-19 kV/mm. If the magnification of the field on the peak of the projections is on the order of 100 (evaluation by the authors of work [41]), according to the formula for field-effect emission the indicated current may be emitted by the peak of a single projection similar to that shown on Fig. 9 with a work function Φ = 3.5-4.0 eV. Thus the discussion which has raged for so many years concerning the nature of the electron component of dark current – field-effect emission or thermionic intensified by the Schottky effect - can apparently be considered as decided in favor of field-effect emission. At least this is valid in conditions of superhigh vacuum with pure electrodes and comparatively small voltages for that portion of the electron component of a dark current which is not electronic emission during bombardment of the latter by positive ions.

Bennette et al. [44], proposing that in measurements with tungsten electrodes (sphere 0.7 mm in diameter – plane) with a gap of 0.04-0.25 mm the dark current is caused by field-effect emission from one projection, calculated the magnification of the field on the apex of this projection μ and the radius of the emitting portion of this peak (assuming axial symmetry of the projection). The results of such calculation, presented in Table 19, made it possible to present the change in the emitting projection after conditioning of the electrodes by breakdowns or after short-term intensive heating.

Table 19. Values of μ and of the radius of the emitting portion of the projection peak on tungsten electrodes, calculated by Bennette.

Treatment and shape of electrode (cathode)	μ	Radius μm
Electrodes subjected only to mechanical treatment and degassing in a vacuum.....	Up to 100-300	-
Spherical electrode after breakdown.....	25	0.02
Spherical electrode after heating to 2700°C for 10 s at E = 0.....	11	0.26
Flat electrode after breakdowns.....	20	0.01
Flat electrode after heating to 1100°C for 180 s with E = 0.....	16.5	0.013

It should be noted that such a method of determining μ and the size of the emitting surface can hardly pretend to adequate accuracy for practical conclusions. First of all it is hardly correct to take the value of the work function Φ for the emitting surface comprising a very small portion of the electrode surface as corresponding to a clean surface, even with careful finishing of the electrodes. Doubt in the correctness of such an evaluation of μ at the point of field-effect emission is confirmed

to a certain degree by the results of the considered work. The observed reduction in field intensity at which dark current appears in the case when an "optimal" coating of cesium is applied on tungsten (according to the formulas for field-effect emission) corresponds to a reduction in the work function by 2.8 times – i.e., down to 1.6 eV if we take the initial value of Φ for pure tungsten as equal to 4.5 eV. At the same time the value Φ = 1.2 eV has been obtained in certain measurements for an optimum coating of tungsten with cesium [83]. Secondly the assumption that a single projection does the emitting is inadequately based, even with such a small total electrode surface as used in the described experiments. If emitting is done by several projections which in the general case have different shape and dimensions, it is hardly correct to apply the formulas of field-effect emission for evaluation of the parameters of the projections.[1] This method of evaluation is particularly questionable in the case of electrodes of comparatively large size. It seems to us that such evaluations, which have been made in a number of works, have done more to conceal the physical nature of dark electron currents than to clarify it. Actually, discussion of the nature of the current – whether it is field-effect emission or thermionic with Schottky effect – proceeds basically from evaluations of this type [2, 38, 131]. Figure 37 shows curves of the dependence of one or another current on the average field intensity taken from work [38]; however, they are constructed in the form characteristic for field-effect emission (left curve) and for thermionic emission with the Schottky effect (right curve). It is easy to see that the very shape of the cureves on these graphs (the linearity of the curves) does not yield a preference

[1]At small currents 1-2 projections may actually emit, but the error in determining the current can be very large due to leakages or to currents of a different nature; with large currents the number of emitting projections grows – all of this leads to errors when attempting to conduct an analysis by the field-effect emission formula and can, in particular, lead to an increase in the calculated value of μ and a corresponding decrease in the emitting area.

for one or the other interpretation, while miscalculation of the curves yields the following results:

(1) График на рис. 37 . . .	(2) Левый (автоэлектронная эмиссия)	Правый (термоэлектронная (3) эмиссия)
μ	(4) 10 (принято авторами [38])	18 (Ni); 13 (Au)
Φ, эв	0,16 (Ni); 0,12 (Au)	1,6 (Ni); 1,5 (Au)
(5) $S_{эм}$, см²	$7 \cdot 10^{-20}$ (Ni); 10^{-20} (Au)	0,1

KEY: (1) Curve on Fig. 37, (2) Left (field-effect emission), (3) Right (thermionic emission), (4) 10 (taken by authors of [38]), (5) S_{em}, cm^2.

Designation: эв = eV.

It is clear that according to such an analysis the interpretation of dark currents as currents of thermionic emission gives more realistic values of the work function Φ and the area of the emitting surface, S_{em}. This in fact is the basis and at first glance a convincing argument in favor of such interpretation. However, even more convincing arguments were presented above in favor of the field-effect nature of dark currents. An additional argument is the nature of the dependence of dark current on the cathode temperature. According to measurements by Little and Whitney [41] and also those of Bennette et al. [44], the rise in the dark current during heating of the electrodes up to 1000°K is not very great (as it should be with thermionic emission) and is close to the level to which field-effect emission current should be increased. Measurements by Llewellyn-Jones [132] at temperatures of 197 and 298°K showed that in the second case the current is six times greater, which is also close to the theoretical relationship between field-effect emission current and temperature in this region, when the theory takes into account the temperature "tail" of electron energy distribution per Fermi.

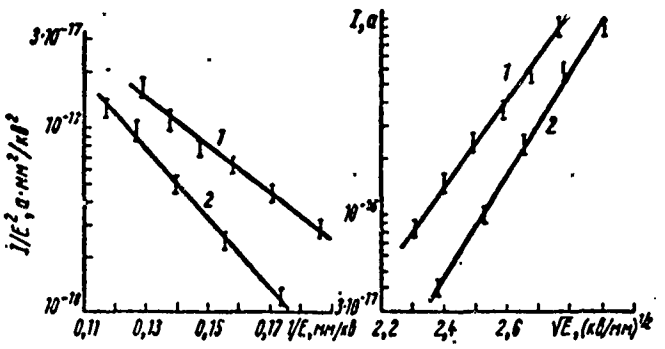

Fig. 37. Interpretation of dark currents as currents of field-effect (left) and thermionic (right) emission: 1 – gold electrodes; 2 – nickel electrodes.

Designations: а = A; мм/кв = mm/kV; кв/мм = kV/mm; $а \cdot мм^2/кв^2 = A \cdot mm^2/kV^2$.

Despite the persuasiveness of the experimental data given above, it seems to us entirely premature to make a final conclusion on the nature of the electron component of dark current as a current of field-effect emission from anomalously large projections in all practical cases of vacuum electric insulation and especially when oxide films, contaminants, etc. are present on the surface of the electrodes. For example, under such conditions the appearance of self-sustaining electron emission, the Molter effect, etc. is completely possible.

Besides this, as was stated above, in a number of cases a growth in dark current with an increase in applied voltage was observed with a change in E_c. Obviously, this represents evidence of a substantial role in the mechanism of the appearance and maintaining of current for processes which depend on the energy which can be obtained by contaminant particles crossing the inter-electrode gap. The emission of electrons from the cathode caused by bombardment with positive ions can serve as an example. In this case the growth in the emission coefficient with an increase in the energy of ions can be the reason for the indicated dependence of dark current on the total applied voltage.

All of the above attests to the fact that there is a whole series of processes which can be "critical" for the existence of dark current. Depending upon specific conditions on the electrodes (their surface condition, microrelief), the electric field intensity, and the total applied voltage, the role of individual emission processes can differ. All the same, in the majority of cases of practical use of vacuum insulation it is clear that the most essential role is played by field-effect emission and surface ionization, accompanied by the emission of electrons from the cathode during its bombardment by ions.

In connection with the fact that field-effect emission from projections on the cathode surface can create an electron current with high local density (which, as will be seen from the material given below, is very "dangerous" to vacuum electrical insulation), it is useful to examine the connection between the configurations of projections and the parameters of the beam of electrons emitted by the peak of the projection. Such parameters include, first of all, the total current from the projection and the shape of the electron beam. The shape of the beam – more exactly, the cross section of the beam close to the anode – governs the intensity of local heating on the anode and, consequently, the intensity of a number of processes accompanying this heating. Such an examination is even more desirable because field-effect emission from a projection due to secondary processes can lead to breakdown.

The current and the configuration of the electron beam are determined primarily by the electrical field close to the peak of the emitting projection. Ordinarily this field is characterized by the coefficient μ. The values of μ on the peaks of projections with different shapes were given in Section 2 of Chapter 2. However, the magnitude of the current and in particular the shape of the beam depend also on the values of μ not only on the surface itself, but close to it, especially along the possible trajectory of the electron beam. Lewis [39] calculated the field in the

presence of periodically arranged projections on a flat surface. The profile of the considered surface and the corresponding designations are given on Fig. 38 (each individual protuberance has a semiellipsoidal profile). The same figure gives averaged values of the field gain coefficient μ with distance from the peak of the projection along the X-axis to the point $x = x_1$:

$$\bar{\mu}(x_1) = \frac{1}{x_1}\int_0^{x_1} \mu(x)\,dx.$$

When $x = 0$ (peak of the protuberance) $\bar{\mu}(0) = \mu$ on the surface of the peak of the protuberance.

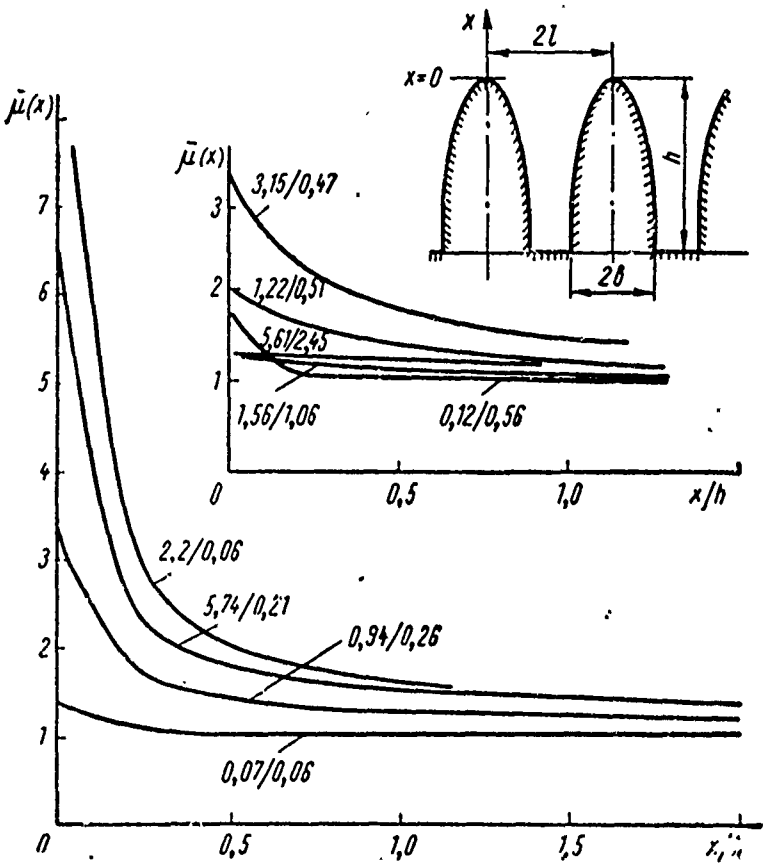

Fig. 38. Multiplicity of the gain in intensity μ close to periodically arranged row-type projections. (The insert shows the profile and mutual arrangement protuberances. Numbers on the curves: numerator – value of the ratio l/h; denominator – b/h).

Besides the direct dependence of $\bar{\mu}(x_1)$ on b, h, and l, from Fig. 38 we can obtain information on the dimensions of the region where the field is distorted by the presence of protuberances. If on the boundary of this region (the boundary remote from the electrode with the protuberances) $x = x_1$, then $\mu(x_1) = 1$ and the difference in potentials belonging to the region of the distorted field $\Delta U = \bar{E}(h + x_1) = \bar{E}\int_0^{x_1}\mu(x)dx = \bar{E}x_1\mu(x_1)$ and, consequently, $\mu(x_1) = 1 + hx_1^{-1}$. These expressions are valid for protuberances of any shape. If the domain of the distorted field is limited by the value $x_1 = h$ or $x_1 = 2h$, then $\bar{\mu}(x_1) = 2$ or $\bar{\mu}(x_1) = 1.5$, respectively. From Fig. 38 it is clear that curves for sharp points and widely separated projections approach these values best of all — i.e., the width of the domain of the distorted field for such protuberances is commensurate with the height of the projections, although μ in this domain has a large value. At the same time for more rounded or more densely arranged projections the quantity μ is essentially smaller and the region of the distorted field itself is substantially wider.

Figure 6 gives values of μ on the peak for individual semi-ellipsoidal projections of height h and with an apex curvature radius r. If $h >> r$, the quantity $\mu(x)$ drops rapidly with distance from the peak along the X-axis. At a distance from the peak equal to r the radius of curvature of the corresponding equipotential is three times greater, i.e., μ drops by 3 times [see formula (11)] and therefore the potential close to the peak of the protuberance can in this case be written in the form

$$U(x_1) = \bar{E}\int_0^{x_1}\mu(0)\frac{r}{2x+r}dx = \frac{\beta}{2}\bar{E}h\ln\frac{2x_1+r}{r}. \qquad (15)$$

considering that on the apex $x_1 = 0$, $U = 0$ also when $x_1 << h$. With distance from the peak equal to the height of the projection ($x_1 = h$), $\mu \approx 1$ — i.e., the potential difference $2h\bar{E}$ occurs on the region of the field distorted by the projection.

In order for field-effect emission to appear not only must there be a high value of electric field intensity directly on the surface, but a fairly high value must be retained with distance from the latter in order that the potential drop corresponding to the work function of an electron for the metal at this distance will not exceed several interatomic distances in the metal. Only in this case is the thickness of the potential barrier on the metal/vacuum boundary reduced — a necessary condition for a field-effect current. This condition can be written in the form

$$cU(x_1) = \Phi$$

where x_1 = (1-3)a, where a is the interatomic distance in the metal.

From this condition and condition (15) it follows that field-effect electrons can be emitted not by any projection, but only by a protuberance whose height is greater than a certain value $h = h_{min}$. Substitution of this value into (15) gives

$$h_{мин} > \frac{4\Phi}{e\bar{E}}, \qquad (16)$$

[мин = min]

since when $h/r \gg 1$, $\beta \approx 0.5$, while r cannot be smaller than several a. According to (16), when $\bar{E}$ = 50 kV/mm, $h_{min} \geq 0.4$ μm.

With an increase in the distance from the peak of an ellipsoidal projection toward the side, μ drops along its surface according to the law (see [42])

$$\mu(\theta) = \mu(0)\cos\theta,$$

where θ is the angle between the vector E (X axis) and the normal to the surface at the given point. As is known, the current density of field-effect emission is reduced by an order of magnitude with a reduction in voltage by 10-15%. If we take as the emitting section that portion of the surface of the protuberance on whose boundary the density of field-effect current is 10 times

less than on the peak, then according to the above for this boundary $\Theta = \Theta_{bdy}$ = arc cos (0.85-0.90). Then the area of the emitting surface equals

$$s_{э.м} \approx 2\pi r^2 (1 - \cos\Theta_{гр}) = (0{,}63 - 0{,}94) r^2, \quad (17)$$

[э.м = e.m; гр = bdy]

and the total current of the projection, according to expressions (9) and (17), comprises

$$I = j s_{э.м} \approx 1{,}5 \cdot 10^{-6} \Phi^{-1} (\beta h \bar{E})^2 \exp\left(-\frac{\text{const}}{\mu \bar{E}}\right). \quad (18)$$

[э.м = e.m]

The angle Θ_{bdy} is also the initial angle of divergence of the electron beam. As shown on Fig. 6, graphoanalytical determination of the divergence angle of this beam after passage of the potential difference 2Eh Θ_{2h}, i.e., the region of the field distorted by the presence of the projection, gave Θ_{2h} = 18-22° when h/r = 200/3 [133]. Subsequent motion of the electrons occurs in a uniform field, where the radial component of electron velocity does not change (the case of flat electrodes is considered), and if h << d at an average value Θ_{bdy} = 20° the radius of the field-effect beam close to the anode will equal

$$r_{э.а} \approx \sqrt{\beta h d}. \quad (19)$$

[э.а = f.e]

The calculation whose results are given above did not consider the influence of the beam charge on the trajectory of the electrons. Evaluation showed that this is valid at a total current emitted by the protuberance of $I \leq 8$-10 mA [133].

Field-effect emission can arise not only on the peaks of protuberances, where μ is great, but also on a comparatively smoother surface at those points where the electron work function Φ is reduced because of surface contaminants or foreign films

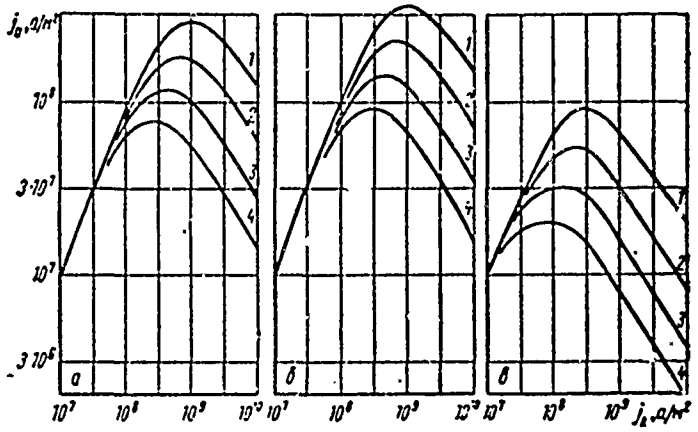

Fig. 39. Current density on the anode as a function of current density on the cathode for an initially parallel electron beam: a — $I = 10^{-4}$ A, E = = 200 kV/mm; b — $I = 10^{-3}$ A, E = 200 kv/mm; c — $I = 10^{-3}$ A, E = 100 kV/mm. Voltage between electrodes: 1 — 12.8 kV; 2 — 25.6 kV; 3 — 51.2 kV; 4 — 102.4 kV.
Designation: $a/м^2 = A/m^2$.

or inclusions. In this case the electrical field may have virtually no radial component over the entire path of the electrons from the cathode to the anode; therefore the widening of the electron beam will be less than during emission from the peak of a projection and arises only because of the action of the space charge and the radial component of the initial velocity. In this case the current density on the anode can substantially exceed that which is observed during field-effect emission from the peak of a projection.

Figure 39 shows calculated values of the density of the electron current on the anode as a function of its density on the cathode in the absence of radial initial velocity and with a uniform field between the electrodes — i.e., when widening of the beam is determined only by the intrinsic space charge. A characteristic feature of these curves is the presence of the maximum

possible density of the electron current on the anode, corresponding to a certain value of current density during emission. Below this density the space charge has little influence on the trajectory of the beam and the beams are virtually parallel; at high emission density the action of the space charge is stronger and the beam becomes more divergent. Figure 40 shows the values of maximum density of the electron current during anode incidence of electrons $j_{f.e.\ max}$, determined from curves similar to those shown on Fig. 39. The broken line on Fig. 40 corresponds to a parabolic beam trajectory and has a different slope with respect to the axes. Such a parabolic trajectory is seen in electrons which are moving in a uniform electric field in the case when beam expansion occurs only because of the radial component of the initial velocity, where the radius of the beam on the anode is substantially greater than that on the cathode.

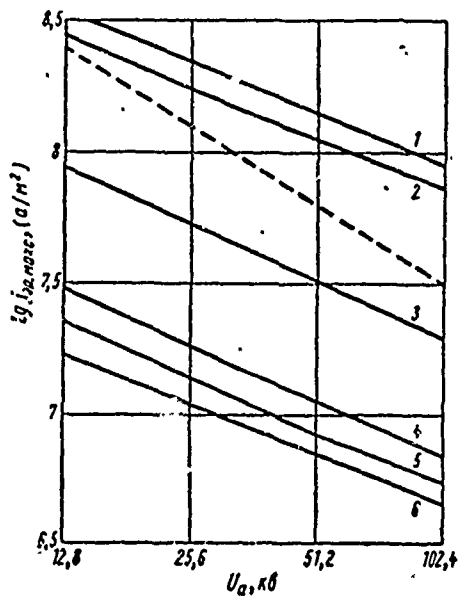

Fig. 40. Maximum possible current density on the anode, $j_{f.e.\ max}$ during escape of electrons from the cathode in a parallel round beam. (The slope of the broken line corresponds to expansion of the beam on a parabola)

KEY: (1) $j_{e.f.\ max}$, (A/m^2).

Designation: кв = kV.

Curve...	1	2	3	4	5	6
E, kV/mm	200	200	100	50	50	50
I, A....	10^{-3}	10^{-4}	10^{-3}	10^{-2}	10^{-3}	10^{-4}

In the range of values of U, E, and I, for which the curves on Fig. 40 are constructed with an accuracy to ±6%

$$j_{э.а.\ макс} = 1{,}09 \cdot 10^{-3}\, I^{0.1}\, U^{1.325}\, d^{-2}. \qquad (20)$$

[э.а. макс = f.e. max]

In this case the density on the cathode should be 3.5-4 times greater than $j_{f.e.\ max}$.

3. MICRODISCHARGES

Microdischarges are self-extinguishing low-powered current pulses with a duration of 10^{-4}-10^{-1} s, repeated periodically with a frequency of 0.1-100 Hz during prolonged application of a constant voltage. Their appearance is accompanied by weak diffusion luminance in the interelectrode gap and by desorption of adsorbed gases from the electrode surfaces (about 10^{16} molecules per current pulse [134]). Microdischarges usually arise earlier than the onset of spark breakdowns if the applied voltage exceeds 15-30 kV and if oxide films and contaminants have not been removed from the electrodes or if the electrodes are in a "technical" vacuum of 10^{-4}-10^{-7} mm Hg which is not free of organic compound vapors. In particular, such conditions can occur in electron microscopes, the vacuum tubes of electrostatic charged-particle accelerators, and other high-voltage electrovacuum devices, especially those operating with constant evacuation. Although the amplitude of currents during microdischarges does not, as a rule exceed 1 mA they can substantially disturb the operation of electrovacuum instruments and equipment with low-power sources of high-voltage supply; this is especially true if high stability of the working voltage is required. This does not exclude the possibility that microdischarges may lead to "annoyances" in electrovacuum systems of higher power by facilitating the appearance of spark breakdowns with transition to vacuum arc.

The first studies of microdischarges were carried out by Bertein [135], Clifford and Fortesque [136], and most completely by Arnal [137-142], as well as a number of other investigators. Microdischarges in accelerating tubes (the so-called electron load) were investigated by McKibben, Blewett, and others (see [143-145]).

The basic parameters which characterize microdischarges are as follows: voltage of their appearance with a smooth rise in voltage U_{md}, the duration τ_{md} and amplitude $I_{md.max}$ of the current pulse and the magnitude of the electric charge transferred in one impulse, q_{md}. The frequency of appearance of microdischarges is also of substantial importance. Some idea of these parameters and the range of the observed values is given by Table 20.

Table 20. Basic characteristics of microdischarges at constant voltage from measurements by different investigators.

(1) Материал и форма электродов	(2) Вакуум, мм рт. ст.	(3) Зазор, мм	(4) $U_{мр}$, кв	(5) $I_{мр.макс}$, мка	(6) $q_{мр}$, к	(7) $\tau_{мр}$, сек	(8) Литература
(9) Медные диски диаметром 20—50 мм	10^{-4}—10^{-5}	3	45	20—50	10^{-8}	10^{-4}—$2\cdot10^{-2}$	[142]
(10) Медные диски диаметром 60 мм	$2\cdot10^{-5}$	5	50	—	10^{-7}—10^{-5}	—	[134]
		36	65				
(11) Медные диски	$2\cdot10^{-5}$	2	20	200	$(1\div4)\times10^{-6}$	$5\cdot10^{-2}$	[146]
		380	120	100	10^{-5}	$5\cdot10^{-3}$	
(12) Медные диски диаметром 12 мм	$(1\div3)\times10^{-6}$	4	67	—	10^{-7}	—	[147]
(13) Медь, катод—плоскость, анод—сфера диаметром 12 мм			100				
(14) Стальные диски диаметром 20 мм	10^{-5}—10^{-6}	1	15—44	10—500	10^{-9}	$5\cdot10^{-5}$—$5\cdot10^{-4}$	[148]
(15) Молибденовые полоски площадью ~1 см²: (16) Хорошо очищенные	10^{-9}	4	135	—	—	—	[122]
Окисленные (17)			40—50				

KEY: (1) Material and shape of electrodes; (2) Vacuum, mm Hg; (3) Gap, mm; (4) U_{md}, kV; (5) $I_{md.max}$, μA; (6) q_{md}, k; (7) τ_{md}, s; (8) Reference; (9) Copper disks 20-50 mm in diameter; (10) Copper disks 60 mm in diameter; (11) Copper disks; (12) Copper disks 12 mm in diameter; (13) Copper. Cathode - flat; anode - sphere 12 mm in diameter; (14) Steel disks 20 mm in diameter; (15) Molybdenum strips ~1 cm² in area; (16) Throughly cleaned; (17) Oxidized.

The data in the table show a broad scatter in measurement results; to a significant degree this is explained by the dependence of the basic parameters of microdischarges on the treatment and conditioning of the electrodes, the pressure and composition of residual gases, and the parameters of the electrical circuit, not to mention such substantial factors as the magnitude of the interelectrode gap and the material of the electrodes.

For freshly prepared electrodes, where the vacuum system and, consequently, the electrodes have a low degree of contamination by organic-compound vapors, the voltage of microdischarge appearance is increased after a few discharges - i.e., the so-called conditioning effect is observed. On the electrodes have been located in the vacuum for a long period and especially when there are voltages on the electrodes which cause continuous microdischarges, the value of U_{md} depends strongly on the quality of the vacuum and mainly on the content of organic vapors. Table 21 gives the results of measurements U_{md} in a vacuum of 10^{-5}-10^{-4} mm Hg in the presence of vapors of the indicated compounds [148].

Table 21. Voltage of appearance of microdischarges as a function of the quality of the vacuum with a 1 mm gap between steel electrodes.

Vacuum conditions	Initial value of U_{md}, kV	U_{md} after $(2\text{-}15)\cdot10^4$ microdischarges over the course of 8 h, kV
Vapors of high-vacuum silicone lubricant	44	33
Vapors of hydrocarbon oil for a diffusion pump	40	28
Vapors of the oil for a pre-evacuation pump...	38	15

Owing to the very prolonged conditioning (up to $2 \cdot 10^5$ microdischarges), in these experiments a tarnish appeared on the electrodes; this was apparently due to cracking of adsorbed organic compounds. There was a certain increase in U_{md}. Clifford and Fortesque [136] found a higher value of U_{md} when the system was evacuated with mercury pumps as compared with evacuation by oil pumps.

The total magnitude of the residual pressure also influences the voltage of microdischarge appearance. The measurements conducted by Mansfield and Fortesque [146] indicate that an increase in pressure from 10^{-5} to 10^{-4} mm Hg increases U_{md} by 12-20%. With a large distance between electrodes (380 mm) they found a very strong change in U_{md} in some experiments: from 125 to 420 kV with an increase in pressure from $2 \cdot 10^{-5}$ to $2 \cdot 10^{-4}$ mm Hg by allowing access of air. With the entry of hydrogen the change in U_{md} is less. Clifford and Fortesque [136] observed a twofold change in U_{md} with a change in pressure within this same range of values.

The influence of the magnitude of residual pressure and of the composition of the residual gases on U_{md} which was described above shows the major role of gases and vapors adsorbed on the surface of the electrodes - especially vapors of organic compounds. As is known, the composition of the adsorbed films is close to the composition of the residual gas only in the initial moments of adsorption (for example, in the first moment after the electrodes are degassed by heating). Then, because of the differences in heats of adsorption and vaporization of the different gases and vapors, an ever growing predominance of hydrocarbons in the adsorbed films begins; these compounds, as it were, overshadow the other gases adsorbed earlier. However, the smaller the percentage content of hydrocarbons in the residual gas and the smaller the absolute value of their partial pressure, the slower and the lesser will be the filling of the adsorbed

film with hydrocarbons. This is apparently explained by the data given above: a reduction in U_{md} with a growth in the partial pressure of hydrocarbon vapors (see Table 21) and an increase in U_{md} with a growth in the total pressure and retention of a constant partial pressure of hydrocarbon vapors (see the data given above from Mansfield, Clifford, and Fortesque). Clearly, the reduction in the content of hydrocarbons in the adsorbed film can explain the increase in the voltage of microdischarge appearance observed in the course of 10-60 minutes after heating of the electrodes up to a temperature somewhat greater than 200°C [146], and also that occurring after the action of a glow discharge in hydrogen or of accelerated argon and hydrogen ions on the electrodes [141].

Table 22. Effect of treatment of a molybdenum anode on the voltage at which microdischarges appear (interelectrode gap 4 mm).

(1) Предварительная обработка анода	(2) Вакуум при измерении, *мм рт. ст.*	$U_{мр}$, *кв*
(3) 1. Свежеприготовленные полированные электроды	10^{-6} — $5 \cdot 10^{-7}$	40—50
(4) 2. Продолжительный прогрев до 1800—2000° С при 10^{-6} *мм рт.ст.*	10^{-6}—$5 \cdot 10^{-7}$	80—90
(5) 3. То же, что и в п. 2, но при 10^{-7} *мм рт. ст.*	10^{-9}—10^{-10}	115
(6) 4. То же, что и в п. 3, плюс кратковременный прогрев до 600° С в атмосфере водорода	10^{-9}—10^{-10}	115
(7) 5. То же, что и в п. 3, плюс кратковременный прогрев в атмосфере кислорода	10^{-9}—10^{-10}	40—50
(8) 6. То же, что и в п. 3, плюс выдержка при атмосферном воздухе в течение 0,5 ч	10^{-9}—10^{-10}	80—90
(9) 7. То же, что и в п. 3, плюс выдержка при атмосферном воздухе в течение 12 ч	10^{-9}—10^{-10}	40—50

KEY: (1) Preliminary treatment of the anode; (2) Vacuum during measurement, mm Hg; (3) 1. Freshly manufactured polished electrodes; (4) 2. Prolonged heating to 1800-2000°C at 10^{-6} mm Hg; (5) 3. Same as 2 above, but at 10^{-7} mm Hg; (6) 4. The same as 3 above, plus short-term heating to 600°C in a hydrogen atmosphere; (7) 5. The same as 3 above plus short-term heating in an oxygen atmosphere; (8) 6. The same as 3 above plus holding in air for 0.5 hours; (9) The same as 3 above plus holding in air for 12 hours.

Designation: кв = kV.

The presence of oxide films and various contaminants on the electrode surfaces has an essential influence of the appearance of microdischarges. Table 22 gives results obtained by Pivovar and Gordiyenko [122], showing the effect of anode surface cleanliness on the voltage at which microdischarges appear.

These experiments show a major role for oxide films which, apparently, are not removed completely with intensive heating in a vacuum which is not sufficiently high or sufficiently pure.

The voltage of microdischarge appearance depends quite weakly on the interelectrode gap. According to measurements by Arnal [138], this relationship has the form

$$U_{мр} = \text{const} \cdot d^{1/3}, \qquad (21)$$

with the value of the constant being determined by the material of the anode, as well as the parameters described above. According to Arnal the material of the cathode has no effect on U_{md}. The effect of the anode material is illustrated by the Arnal measurements through the values of U_{md} with a gap of 3 mm between flat electrodes: 30 kV for a tantalum electrode, 45 kV for copper, 60 kV for manganese, and 65 kV for a beryllium anode. We will add that the measurements by Mansfield and Fortesque indicate that U_{md} is 20% higher for aluminum electrodes than for copper. Expression (21) was confirmed by the measurements of Boersch et al. [148] for freshly manufactured steel electrodes. The results obtained by Mansfield and Fortesque and given in Table 20 also fitted into such a relationship. In their work they also demonstrated a comparatively weak dependence of U_{md} on the intensity at the electrodes, and especially on E_c. Carrying out their experiments in a structure made up of a portion of a multisectional accelerating high-voltage tube closed on the ends by flanges serving as the electrodes in these experiments, by extreme shorting of the

section the investigators were able to reduce field intensity on one electrode or the other by several times. Such a reduction in field intensity at the cathode increased the voltage at which microdischarges appeared by only 10%; a similar reduction of intensity at the anode resulted in a 75% reduction.

With an interelectrode gap of a few millimeters, sparkovers - breakdowns - arise at higher intensities than microdischarges. However, as will be seen from the following chapter, the dependence of breakdown voltage on interelectrode gap is stronger than that corresponding to expression (21). Therefore as the interelectrode distance is narrowed the difference between the breakdown voltage and U_{md} is reduced, so that at gaps smaller than 0.5-1 mm breakdown sets in before the appearance of microdischarges. However, besides this it is clear that there is a minimum value of voltage on the order of 15-20 kV, depending on specific conditions, below which no microdischarges can arise. Such a conclusion can be drawn from existing concepts of the physical nature of microdischarges as mutual ion emission (see below), whose coefficients should be reduced with a reduction in voltage.

The clarification of the nature of current carriers is of great significance in the study of nature of microdischarges. Mass-spectrometry analysis showed that the current of microdischarges contains, besides the basic electron component, positive and negative ions: H^+, H_2^+, CO^+, H^-, C^- and O^-, with the H^+ and H^- predominating among the ions [137]. According to measurements made by Mansfield and Fortesque [146], the currents of electrons, positive ions, and negative ions are found in a ratio of 25:2:1; the measurements by Pivovar and Gordiyenko [147] indicate that the electron current exceeds the current of ions by 3-4 times. This current composition, the strong influence of adsorption of hydrocarbon described above, the effect of oxide films, and the self-extinguishing of a microdischarge after the passage of a

comparatively small charge - i.e., all of the basic features of microdischarges - led to a virtually unamious opinion concerning their physical nature. According to these presentations a microdischarge is a mutual secondary emission of positive and negative ions. Such a mutual emission may be self-sustaining and may even grow when the coefficient of secondary emission of negative ions during bombardment of the cathode by positive ions, K_{ii}^{-}, and the coefficient of secondary emission of positive ions during bombardment of the anode by negative ions, K_{ii}^{+}, are found in the ratio

$$K_{ii}^{-} K_{ii}^{+} > 1. \qquad (22)$$

Although they are the largest component of the current of a microdischarge, electrons apparently do not play a major role in the appearance and maintaining of a microdischarge but represent, as it were, a "byproduct" obtained during bombardment of a cathode by positive ions. The small role of electrons in the mechanism of microdischarges was demonstrated convincingly by Pivovar and Gordiyenko [147], who determined the effect of imposing a transverse magnetic field on microdischarges. The magnetic field prevented electrons arising on the cathode from crossing the gap and bombarding the anode. However, this did not change the voltage required for appearance and flowing of microdischarges, although the discharge carried by a current impulse was reduced by 2-3 times.

The values of K_{ii}^{-} and K_{ii}^{+} are negligibly small for clean electrode surfaces and condition (22) cannot be fulfilled. However, the presence of contaminants of various types, oxide films, adsorbed gases, and especially organic compound vapors on the surface apparently leaves (with a sufficiently high ion energy) to a growth in K_{ii}^{+} and K_{ii}^{-} such that condition (22) is fulfilled and a microdischarge is developed. In the process

of passage of a current pulse the surface of the electrodes is partially cleaned, mainly through removal of adsorbed gases and vapors; the coefficients K_{ii}^{+} and K_{ii}^{-} are reduced and the discharge is terminated until the moment when condition (22) is once again fulfilled because of "replenishment" of the adsorbed layer. Replenishment of the adsorbed layer may occur not only as the result of arrival of molecules of residual gases from the evacuated volume but apparently also through diffusion of impurities and dissolved gases from the body of the electrode material to the surface.

If we make the fairly natural assumption that K_{ii}^{-} and K_{ii}^{+} will grow with an increase in voltage at a constant state of the electrode surfaces and will grow at a constant voltage at an increase in the quantity of adsorbed gases and vapors on the surface, the ideas outlined above concerning the mechanism of microdischarges will not only explain quite comfortably the characteristics of microdischarges described above, but will also clarify such characteristics as the dependence of microdischarge duration and frequency of appearance on the parameters of the electrical circuit, along with the small difference between the voltage of appearance of microdischarges and their arcing voltage.

According to the measurements of some investigators, the reduction in voltage upon appearance of microdischarges comprises no more than 1-2%. A stronger drop in the voltage of the electrodes during passage of the discharge current, caused by high resistance in the electrical circuit, terminates the discharge. However, because of the shortening of discharge duration the surface of the electrode is freed of contaminants in adsorbed gases and vapors to a lesser degree; therefore the following microdischarge arises more rapidly - i.e., the frequency of appearance of microdischarges grows. Measurements carried out

by Arnal with copper electrodes with intrinsic capacitance of 10 pF and discharge circuit resistance R_d = 1 kohm indicates that the duration of microdischarge pulses comprises τ_{md} = $= 10^{-2}$-10^{-1} s, while the frequency of their appearance approximately equals 0.2 Hz. With R_d = 10-40 Mohm the quantity $\tau_{md} = 10^{-4}$ s, while frequency of appearance is greater than 10 Hz. The charge passing per impulse varies in accordance with the magnitude of τ_{md}; however, the integral value of the charge a large time interval is virtually unchanged. Increasing the applied voltage above the threshold of microdischarge appearance leads to an increase in the frequency of appearance and of the amplitude of the current, but without an increase in the integral charge; the voltage of discharge arcing differs insignificantly from the increasing voltage of appearance of microdischarges. Qualitatively this may be explained by the fact that with increased voltage the discharge begins with a small adsorption coating of the electrodes. An increase in electrode capacitance hampers the voltage drop on them during microdischarges, thus favoring an increase in the current pulse duration and in the magnitude of the charge passed. The measurements by Pivovar and Gordiyenko [147] indicate that increasing C_{sh} by 100 times (from 200 to 20,000 pF) increased q_{md} by 2-4 times.

Explaining the basic characteristics of microdischarges on the basis of ion-ion exchange, although quite convincing, does not mean that the nature of microdischarges is completely clear. There are serious reasons for doubting the correctness of such an interpretation. As follows from the materials in the preceding chapter, there are as yet no direct measurements of K_{ii}^{+} and K_{ii}^{-} which would confirm t realizability of condition (22) [113]. The low speed of development of the microdischarge is as yet unclear (current grows to amplitude in 10-20 μs, which leads to a strong growth in the voltage of microdischarge appearance and even to absence of microdischarges during microsecond pulses of voltage). Essentially the factor which limits

the amplitude and density of current of a microdischarge is as yet unknown; this is of great significance, since apparently the possibility of the growth of a microdischarge into spark breakdown of a vacuum gap with transition to arc discharge in electrode material vapors depends on this.

4. TRANSFER OF MATERIAL FROM ONE ELECTRODE TO ANOTHER

Passage of a dark current and microdischarges are accompanied by transfer of material from one electrode to the other. This phenomenon with dark currents was first detected by Anderson [119]: when the cathode was made of steel and the anode of copper, after the electrodes were held for a prolonged period under voltage, even in the absence of breakdowns, a brownish deposit was noted on the cathode - traces of copper transferred from the anode. When the polarity of the electrodes was reversed no transfer of copper was detected. Procedures using tagged atoms permitted more detailed study of the transfer of material from one electrode to the other and, in particular, determination of the ratio of the mass of transferred material m to the quantity of the electrical charge q passing through the interelectrode gap. In the work by Tarasova and Razin [149] the quantity m/q is expressed in "mass/charge" units for a singly-charged ion of the base material of the electrode - i.e., if the entire current and transfer of material were due to the passage of ions of the metal, m/q would equal unity. Measurements with copper electrodes at voltages of 35-100 kV and a vacuum of 10^{-5} mm Hg showed that with a dark current the transfer of material is proportional to the total electrical charge which is passed and m/q = 1/5-8 for transfer of material of the anode to the cathode; transfer of material in the reverse direction is significantly smaller and m/q = 0.045. During microdischarges the transfer of material from the anode to the cathode and in the opposite direction will be approximately equal, and m/q = 1.5-2.6. Virtually the

same values of m/q for dark currents were obtained by Swabe [150], who used a combination of chemical separation of transferred material and its subsequent spectral analysis for the measurements. The electrodes were made of different metals and neither contained the material of the opposite electrode, even as an impurity.

The basic fraction of the charge transferred during dark currents and microdischarges is due to electrons, with the ion current comprising, as a rule, an insignificant quantity. Therefore even when m/q = 1 the basic mass of material is not transferred from one electrode to the other in the form of ions (especially since no metal ions are detected during microdischarges). A number of facts indicate that transfer of material is accomplished, even if partially, in the form of multiatomic electrically charged aggregates, since their breakaway from the electrode occurs in the electrical field. This is supported by the observations of Swabe [150], who detected individual impregnations 3-5 μm in size in the transferred layer, and who found depressions of approximately the same size on the opposite electrode. Besides this, the observations of Tarasova and Razine [149] indicate that the transferred material corresponds in shape to the opposite electrode (to be more exact, this is true of the shape of its activated portion, since transfer is determined by the tagged-atom method). This can be interpreted as the transfer of charged microparticles of materials under the action of the electrical field. The mechanism by which multiatomic aggregates are formed is unclear. It is possible that part of them represent fragments formed during mechanical treatment of the electrode surfaces. For example, Swabe noted that transfer is less with electropolished electrodes than with the electrodes polished mechanically. It is possible that surface diffusion plays a determining role; it apparently leads to the formation of sharp points which are then broken away in the electrical field. Thus Browne [151] covered one electrode with a thin

layer of radioactive polonium; he detected clots of microscopic dimensions on the opposite electrode, in which the density of radioactive material was double the density in the applied layer. This is apparently the result of diffusion of the transferred material on the surface.

The practical significance of material transfer is not limited to the quantitative side of this phenomenon alone, which itself is not great. A more significant fact is that transfer of material leads to a change in the microrelief of the surface, especially at the point on which the transferred material is deposited. As a result of deposition of the material and its subsequent surface diffusion it is possible that new sharp projections will be formed in the presence of an electrical field, which will impair the quality of the vacuum insulation.

CHAPTER 4

EXPERIMENTAL DATA ON BREAKDOWN OF VACUUM INSULATION WITH CONSTANT AND PULSE VOLTAGES

1. EFFECT OF PRELIMINARY TREATMENT AND EXTERNAL CONDITIONS

Like the other properties of vacuum insulation, breakdown voltage depends to a great degree on the physical properties of the electrode material, on microrelief, and on the presence of the surface of foreign inclusions, oxide and dielectric films, adsorbed gases, etc. Usually the preliminary treatment of the electrodes before installation in the vacuum chamber consists in grinding and polishing the working surface and subsequent careful cleaning of the electrodes to remove surface films of fats, oxides, and dust; sometimes preliminary degassing of these parts is included. After such treatment it is forbidden to touch the electrodes with the hands or with tools which have not been degreased. Good results are also obtained with electropolishing [38] in a specially selected regime and by taking measures to prevent subsequent appearance of oxides on the surface. Breakdown voltage is also increased by mechanical strengthening of the surface layer of the working portion of the electrodes. Thus, surface hardening of steel electrodes can increase breakdown voltage by almost 1.8 times [123]. An increase is also observed in breakdown voltage with copper electrodes whose surfaces have been work-hardened.

Major attention should be paid to the struggle against the dust. According to measurements made by Rozanova [152], with nickel electrodes and a gap of 0.4 mm the breakdown voltage was reduced from 65 kV to 7-9 kV with the appearance on the electrodes of freely deposited metallic granules 5-40 μm in size. Similar results were obtained in work [153].

The vacuum chamber itself can be a source of contamination of electrodes by "active" dust particles. Thus, in work [154] a small metallic tube which had not been specially cleaned to remove dust was placed above the electrodes in a common vacuum chamber. When this tube was tapped with a small hammer breakdown appeared between the electrodes, although the voltage on the electrodes was substantially below the usual breakdown level. The lag time of breakdown with respect to a hammer blow corresponded to the time required for free fall of a body in a vacuum from the tube to the electrodes. In their experiments, Donalson and Rabinovitz [81] observed a twofold reduction in breakdown voltage after strong heating of a small segement of a glass tube located close to the electrodes. A check with the electron microscope showed that strong heating of the glass caused liberation from it of alkali-metal vapors, which then condensed on the surrounding parts - in particular, on the working surface of the electrodes - in the form of beads less than 1 μm in diameter. It was this which led to the reduction in the breakdown voltage.

Experience in operating many electrovacuum instruments, charged-particle accelerators, etc. convincingly attests to the damaging influence of organic-compound vapors and active gases on the electrical strength of vacuum insulation. At the same time even comparatively high pressure of inert and low-activity gases (argon, helium, and nitrogen; 10^{-4}-10^{-3} mm Hg) has no

negative influence on the strength of vacuum insulation [155]. Other possible sources of electrode contamination with hydrocarbons are the working fluid of the high-vacuum and forevacuum pumps (the latter is not always taken into account), packings of organic materials, and also insufficiently careful cleaning of the vacuum container. As a rule, a single use of cold traps is not sufficient for complete protection against adsorption of hydrocarbon compound vapors on the surface of the electrodes.

Unfortunately, the literature contains few quantitative data concerning the effect of the quality of the vacuum and especially the influence of residues of hydrocarbons on breakdown at voltages of tens and hundreds of kV. From general considerations we can assume that the negative influence of hydrocarbons is greater during prolonged application of voltage than with pulse voltage, since in the latter case the degree of cracking of the hydrocarbons and the formation of carbon-containing films on the electrodes will be less. The appearance of such a film unavoidably leads to a reduction in the breakdown voltage, despite the fact that the latter is substantially lower with graphite electrodes than for the majority of metals (see below[1]).

Denholm [46] found that the application of traps cooled with liquid nitrogen in the vacuum system with oil pumps increases the voltage which can be withstood for a prolonged period by 8% (steel electrodes, voltage 20-50 kV). Maitland [156] detected a reduction in the probability of breakdown appearance during supply of pulses of voltage (4.5 μs) to copper electrodes when the pressure was increased from $4 \cdot 10^{-6}$ to $6 \cdot 10^{-5}$ mm Hg. However, special measurements carried out by Borovik [157] and by

[1]Carbon contamination of the surface can also occur due to diffusion of carbon from the body of the metal. Successive annealing of parts first in hydrogen and then in vacuum is used to ensure more complete removal of carbon from the surface and from the layer of metal adjacent to it in the electrovacuum industry; sometimes this is cycle is repeated several times.

Donalson and Rabinovitz [81] with constant voltage showed virtually no change with transition from a technical vacuum of 10^{-5}-10^{-6} mm Hg to substantially cleaner conditions and a vacuum of 10^{-9} mm Hg. It is true that in both these works organic compounds were not completely excluded from the high-vacuum region, which somewhat reduces the value of the obtained results. All the same, the values which they obtained for breakdown voltage are substantially lower than the best results of other authors. From the experimental results presented in Section 3 of this chapter (see Table 33 and Fig. 49) it is clear that the highest values of breakdown resistance were obtained in vacuum systems from which sources of organic-compound vapors were completely excluded or when the measurements were carried out with pulse action of the voltage. At the same time, the results cited from the works by Borovik and Donalson show that the transition to a vacuum of 10^{9} mm Hg, quite laborious for vacuum systems, still will not ensure obtaining the best conditions for vacuum insulation.

Significant data on the effect of vacuum conditions on the level of insulation were obtained by Tarasova and Kalinin [158]. These investigators carried out comparative measurements of U_{br} for identical electrodes in three different installations: 1) in a vacuum chamber with a Plexiglas high-voltage input and with evacuation to $3 \cdot 10^{-5}$ mm Hg with an oil diffusion pump without freezing of the oil vapors; in a metal chamber with rubber seals, a glass high-voltage imput, and evacuation to $3 \cdot 10^{-6}$-$5 \cdot 10^{-6}$ mm Hg with an oil-diffusion pump equipped with a cold trap; 3) in a glass installation evacuated to $3 \cdot 10^{9}$ mm Hg by mercury and sorption pumps and in the absence of organic-compound vapors. With repeated measurements of constant and pulse voltages up to 200 kV it was found that the maximum values of U_{br} in all three installations were virtually identical, while the scatter in the values of U_{br} in the best vacuum conditions was substantially less. Thus, the following results were obtained with a 1 mm gap between steel electrodes:

Installation	No. 1	No. 2	No. 3
$U_{br.max}$, kV	96	96	98
$\dot{U}_{br.min}$, kV	20	50	70

This type of influence of vacuum conditions on U_{br} may partially explain the somewhat contradictory data obtained by different investigators on the effect of residual pressure on breakdown, given earlier in this work. Actually, with a small area of electrodes conditioned by breakdowns and with short-term action of voltage $\dot{U}_{br}$ is close to $U_{br.max}$, and the quality of the vacuum should play a significantly smaller role than during the prolonged action of voltage and with large electrode area.

In connection with the problem under consideration we must recall the recommendations made after detailed discussion at the conference in Tomsk (1963) regarding the study of breakdown in a vacuum [159]. In these recommendations it was pointed out that in order to prevent the adsorption of hydrocarbons on the electrodes, besides obtaining a vacuum no less than 10^{-9} mm Hg it is also necessary to completely exclude any organic compounds from the high-vacuum region. In particular, it is therefore not permissible to use oil pumps to create the final vacuum if these pumps are not cut off by a valve with a metallic seal later, during the development of the superhigh vacuum and work with high voltage. Besides this, there should be a cold trap in the high-vacuum region close to the electrodes.

After installation of the electrode system in the working area in a kinetic vacuum system (constantly evacuated), it is usually considered desirable to degrease the electrodes by subjecting them to prolonged heating. For static (sealed) vacuum systems careful degreasing of the electrodes before sealing is mandatory. Slow but prolonged heating of the electrodes up to

several hundred degrees almost always has a favorable influence on vacuum insulation. However, under vacuum conditions which are insufficiently clean heating (especially if it is carried out by electron bombardment or if the heating is rapid) can lead to undesirable consequences due to the formation of carbon-containing or oxide films [46, 79]. Besides this, microirregularities can be increased on the surface as the result of recrystallization and surface diffusion during heating to a high temperature. In this case, as was noted in Chapter 2, the formation of anomalously large and sharp projection is possible; this impairs vacuum insulation. Obviously the effect of such undesirable processes during heating can explain the results given in Table 23 of a study of the effect of electrode heating on breakdown voltage. The measurements were made for steel electrodes with a 1 mm gap and a pressure 10^{-7}-10^{-8} mm Hg [157].

Table 23. Effect of electrode heating on breakdown voltage.

Treatment	U_{br}, kV
1. Heating at 650°C, 1 h	102
2. Additional heating: cathode at 900°C, 3 h; anode at 650°C, 1 h	80
3. After treatment in 2 above, sputtering of a copper layer 10 μm thick on the cathode and subsequent heating of the electrodes at 650°C for 1 h	94
4. After treatment in 2 above, heating of the cathode at 900°C for 1 h and at 1200°C for 3 min; sputtering of a 10 μm layer of copper on the cathode and heating of the electrode at 650°C for 1 h	80

The copper layer was spray-coated in a vacuum of 10^{-6}-10^{-7} mm Hg in order to obtain a surface layer free from dissolved gases, although this method of obtaining pure surfaces is not without faults. However, as is clear from the table, the spray-coating did not lead to an improvement in the vacuum insulation. It is possible that the spray-coated layer was inadequately monolithic; however, at the same time such a result shows that if the negative effect of a dissolved gas on breakdown exists, it is insignificant. The same conclusion is suggested by work [160], where the pulse breakdown voltage remained unchanged, with an accuracy of 5%, with a working temperature of nickel electrodes ranging from room temperature to 800°C. The fact that prolonged degassing is ineffective was also noted by Heard [123]. In all of the cited cases the effect of heating is regarded essentially as the effect of additional or more complete degassing, since it was assumed that the initial electrodes had already undergone a certain amount of temperature treatment and had been degassed to some degree during conditioning by discharges. At the same time in these works breakdown voltage was measured and not the voltage withstood for a prolonged period by the electrodes - as will be seen below, these are far from one and the same thing. Therefore the given data should not be understood to be proof of the ineffectiveness or even harmfulness of heating. Rather they should be regarded as a warning against ill-considered intensive heating of the electrodes and high hopes of an essential increase in breakdown voltage by this method due to complete degassing of the electrodes. However, there is no doubt that a large content of gas in metallic electrodes is undesirable in kinetic vacuum systems and is completely impermissible in sealed instruments.

Table 24 gives data drawn from work [161] concerning the effect on breakdown voltage of preliminary degassing of electrodes made from commercial steel in a vacuum furnace (vacuum during

degassing 10^{-2} mm Hg). After 3 hours of heating the breakdown voltage is increased by more than 5 times. However, it should be noted that the initial value of breakdown voltage is very low - several times lower than that usually observed after a few conditioning breakdowns for electrodes not subjected to preliminary heat treatment.

The greater the area of the electrodes and the more complex their shape, the greater the significance of preliminary treatment of the electrodes before installation in the working area, since the methods described below for treating the electrodes in place (conditioning with breakdowns, cleaning by a glow discharge) can be hampered or can involve large expenditures of time.

Table 24. Effect of temperature and duration of preliminary degassing on breakdown voltage for steel electrodes.

(1)	(2)	(3)		(1)	(2)	(3)	
Температура обезгаживания, °С	Длительность обезгаживания, ч	$U_{пр}$ при различных межэлектродных зазорах, кв		Температура обезгаживания, °С	Длительность обезгаживания, ч	$U_{пр}$ при различных межэлектродных зазорах, кв	
		0,25 мм	0,50 мм			0,25 мм	0,50 мм
20	0	5	7	1000	1	21	31
600	1	10	19	1000	3	28	42
800	1	16,5	27,5	1000	6	28	43

KEY: (1) Degassing temperature, °C;
(2) Duration of degassing, hours;
(3) U_{br} at different interelectrode gaps, kV.

Subsequent treatment of the electrodes in place after degassing by heating is usually carried out either by glow discharge or by repeated conditioning by breakdowns in a vacuum; frequently they are both applied together. From the data given by Anderson [119] and by Denholm [46], the best results are obtained with a glow discharge in hydrogen at 1-10 mm Hg with electropolarity the reverse of the working condition and a current density on the order of 0.25 mA/cm^2. Conditioning under

these conditions for 3 minutes can lead to doubling of the breakdown voltage. However, the comparatively low breakdown voltages obtained by Anderson for copper electrodes may indicate that such conditioning is of low effectiveness or even undesirable in this case, since the incompatibility of copper and hydrogen is well known. It is very probable the treatment of the electrodes by an anomalous glow discharge in inert gases by the procedure developed by Chistyakov [89] to obtain an extremely pure electrode surface in the vacuum system itself may prove more effective.

Conditioning of electrodes by the repeated breakdowns in a vacuum at the approximate working voltage has found wide application, especially in research practice.[1] It is desirable that pulse voltage be used in this case. The number of conditioning breakdowns required to achieve a high steady-state value of breakdown voltage may reach tens of thousands [123] with an electrode area of a few square centimeters, but usually conditioning is limited to hundreds or even tens of breakdowns. Figure 41 shows the typical nature of the change in breakdown voltage in the course of such conditioning. It is clear that the steady-state value of breakdown voltage is double the initial value. The value of breakdown voltage which is achieved in this case will not be retained completely if no voltage is applied to the electrodes over the course of several hours. However, after such an interval 5-10 conditioning breakdowns will be sufficient to completely restore the results of the initial conditioning [125]. Even after short-term access of atmospheric air in a working volume (or better, dry nitrogen), repeated conditioning proceeds significantly faster than for "fresh" electrodes.

[1]The question of increasing breakdown voltage during conditioning of electrodes with breakdowns was considered theoretically by Maitland [162].

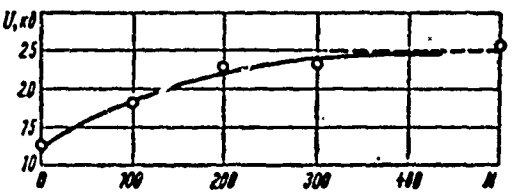

Fig. 41. Growth in breakdown voltage with number of conditioning breakdowns with constant electrode gap and gradually increasing voltage (steel electrodes, d = 1 mm).

[кВ = kV]

Table 25 gives data which characterize the effect of a break in the voltage supply with electrodes made from stainless steel placed in a vacuum system evacuated by oil pumps to 10^{-6} mm Hg (interelectrode gap 0.1 mm, pulse voltage with a duration of 1 ms [125]).

Table 25. Effect of a break in voltage supply on breakdown voltage.

(1) Перерыв в подаче напряжения, ч	(2) Пробивное напряжение, кв: при первом пробое (3)	среднее на пять последующих пробоев (4)	(1) Перерыв в подаче напряжения, ч	(2) Пробивное напряжение, кв: при первом пробое (3)	среднее на пять последующих пробоев (4)
0,1	22,5	26,7±1,0	4	21,5	25,4±1,1
0,5	19,5	25,9±0,9	6	17,5	25,7±1,1
2	22,5	25,8±1,2	7	17	25,3±1,2

KEY: (1) Break in voltage supply, h; (2) Breakdown voltage, kV; (3) at first breakdown; (4) average for five following breakdowns.

Figure 42 shows an example of the change in strength with successive breakdowns. In this case a pulse voltage (1.5/40 μs) of 350 kV is applied to steel electrodes (flat cathode and anode 9.3 mm diameter sphere) at an interval of 20 s through a resistance of 9 kohm [163]. The interelectrode gap, which was initially established with a reserve, was reduced after every 3-4 pulses if no breakdown occurred until three cases of breakdown were observed for every 5 pulses. This distance was fixed as the breakdown distance, the electrodes were separated, and the

procedure was repeated. On Figure 42 breakdowns are noted by vertical lines; the voltage pulses at which there were no breakdowns are marked with points. It is clear that breakdown at large distances between the electrodes (less intensive) usually improves the insulation strength, while breakdowns at the same voltage but with small interelectrode distances impair it (after such breakdowns the following breakdowns set in at significantly larger interelectrode gaps). This reflects the fairly well-known practical rule that after a powerful breakdown in order to restore good insulation it is desirable to conduct additional conditioning of the electrodes by discharges of lower power - for example, at somewhat reduced voltage.

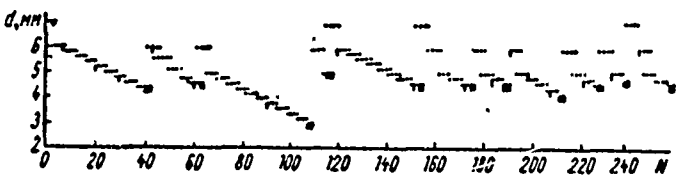

Fig. 42. Change in electrical strength during repeated supply of voltage pulses (1.5/40 μs, 350 kV) and with a change in the interelectrode gap (cathode - flat; anode - 9.3 mm diameter sphere): vertical line - voltage pulse accompanied by breakdown; point - voltage pulse with which breakdown is observed [sic].

In practice it was also established that it is more convenient to condition large-area electrodes at a voltage somewhat below the voltage of appearance of regular breakdowns. Under these conditions the random breakdowns will, as it were, gradually liquidate weak points without damage to the remaining surface of the electrodes, and in this way the level of vacuum insulation is increased. A fairly good indicator of the state of the electrode surfaces during such conditioning is the magnitude of dark current (and apparently the average current of microdischarges and post-breakdown sparks); in practical work in physics laboratories dark current is recorded by X-ray radiation. The voltage

on the electrodes during conditioning is controlled in such a way that the X-radiation is maintained at a certain level with a constant tendency toward reduction. This method is particular useful with high-frequency voltage where the measurement of currents flowing in the gap is extremely difficult. Figure 43 shows the curve of the change in X-radiation in the process of electroconditioning [164]. Reduction of X-radiation with conditioning of the electrode at one and the same voltage is clearly evident. It is also noticeable that the appearance of breakdown is observed, as a rule, at other than the highest magnitude of electron current.

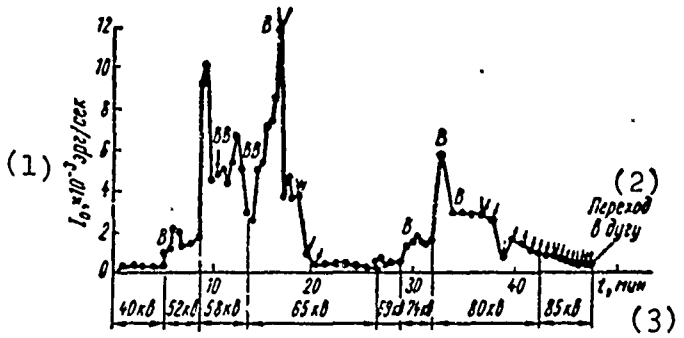

Fig. 43. Intensity of X-radiation with a gradual rise in voltage and with conditioning of the electrodes by breakdowns: arrows indicate breakdowns; B - gas flare in the volume; the highest peak of X-radiation corresponds to an electron current of approximately 2 mA.

KEY: (1) I_0, $\times 10^{-3}$ erg/s; (2) Transition to arc; (3) t, min.

[кВ = kV]

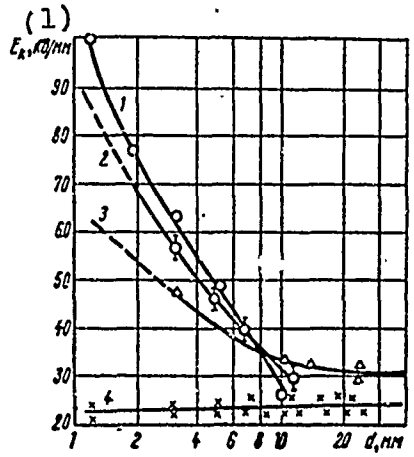

Fig. 44. Change in the nature of dependence of breakdown voltage at the cathode on the interelectrode gap with electroconditioning by low-power discharges.

Hemispherical electrodes; copper cathode 40 mm in diameter, steel anode 10 mm in diameter. Sequence of curves 1, 2, 3, and 4 corresponds to an ever greater number of conditioning discharges.

KEY: (1) E_c, kV/mm.

The change in breakdown voltage with repeated breakdowns depends very strongly (sometimes decisively) on the parameters of the electrical circuit: generator power (capacitance of capacitor with pulse voltage), resistance in the discharge circuit, and the capacitance of the electrodes and of the elements and structures connected directly to them. Sometimes the ratio of these parameters will be so inappropriate that instead of an increase in breakdown voltage in the course of successive breakdowns there will be a reduction in it. Figure 44 shows curves of the dependence of breakdown voltage at the cathode, E_c, on the gap for spherical electrodes (steel anode 10 mm in diameter, copper cathode 40 mm in diameter). Curve 1 was taken for "fresh" electrodes after conditioning by a glow discharge, but without breakdown conditioning; curves 2, 3, and 4 were taken for the same electrodes in succession after an ever larger number of breakdowns [32]. It is clear that with an increase in the number of breakdowns not only is the absolute value of breakdown voltage reduced, but the nature of the relationship between breakdown voltage and the interelectrode gap changes. It is also clear that in this case changes occur in the mechanism of breakdown itself. In the case just given the voltage source was a low-power (150 μA) direct-voltage electrostatic generator.

The current which passes across the vacuum gap during breakdown was so small that apparently it was incapable of melting the microirregularities formed on the cathode during breakdown or in the course of prebreakdown phenomena. Besides this, at such a generator power the voltage might be limited not by the onset of breakdown, but by dark currents, especially in the final stage of the experiment. Curve 4 can be considered confirmation of such a supposition, since in this case E_c is constant.

The effect of electrode capacitance C_{sh} and the resistance R_d in the discharge circuit on breakdown voltage is explained by the fact that this capacitance determines, to a significant degree, the current across the gap in the initial stages of breakdown; the resistance, like the power of the generator or its capacitance, determines the current and its duration in the final stages of breakdown and during the subsequent discharge. The magnitude and duration of the current influence the final change in the surface of the electrode during breakdown. These changes, without question, depend also on the electrode material, vacuum quality, etc. Therefore the optimum values of C_{sh} and R_d can be different under different conditions, and in order to obtain the maximum value of breakdown voltage during repeated breakdowns we must select C_{sh} and R_d specifically in each construction. In many cases of practical application of vacuum electrical insulation, especially in kinetic vacuum systems, even with a large strength reserve individual breakdowns are not excluded; these occur predominantly at the beginning of operation with high voltage. Therefore even in the absence of special conditioning by breakdowns it is possible to use the influence of the parameters of the electric circuit on the level and quality of vacuum insulation as a method for increasing the quality of the latter.

To illustrate the importance of the selection of R_d and C_{sh}, Tables 26 and 27 show the dependence of breakdown voltage on the magnitudes of these electric-circuit parameters. The data in Table 26 relate to hemispherical electrodes 50 mm in diameter made of invar with a gap d = 0.25 mm (constant voltage; R_d = 100 kohm) [123]. Table 27 gives the results of tenfold measurements with virtually flat electrodes 32 mm in diameter and with a gap d = 0.4 mm [46]. The filter capacitance of the direct-voltage low-power generator was 0.01 μF, while C_{sh} = = 500 pF; R_d separated electrodes with intrinsic capacitance of 500 pF from the 0.01 μF capacitance; owing to the low power of the rectifier, the field current of the discharge was very small even at R_d = 0.

Table 26. Effect of the capacitance shunting the discharge gap on breakdown voltage after repeated breakdowns.

(1) $C_ш$, пФ	$U_{пр}$, кв (2)
24	10
$1{,}25 \cdot 10^4$	60
$5 \cdot 10^3$	5

KEY: (1) C_{sh}, pF; (2) U_{br}, kV.

Table 27. Effect of damping resistance R_d on the average and maximum values of breakdown voltage.

(1) $R_д$, ком	Среднее $U_{пр}$, кв (2)	Максимальное $U_{пр}$, кв (3)	Среднее отклонение $U_{пр}$, % (4)
0	48,6	53	4,11
100	38,7	49,5	21,6

KEY: (1) R_d, kohm; (2) Average U_{br}, kV; (3) Maximum U_{br}, kV; (4) Average deviation in U_{br}, %.

Despite its practical importance, the question of the selection of R_d and C_{sh} has been little studied. Judging from the data in Tables 26 and 27 and also from the fragmentary and rather vague data provided in certain other works, it is clear that the most favorable ratio is $R_d \approx 10^5$ ohm, with C_{sh} of such a magnitude that with the working voltage the energy stored in this capacitance will be approximately 10-20 J.. Such parameters of C_{sh} will probably ensure a spark-discharge power sufficient to melt irregularities appearing in the initial stages of breakdown or under dark currents and microdischarges; at the same time with a large value of R_d the current across the gap after discharge of capacitance C_{sh} will be small and will be rapidly cut off; as a result the degree of destruction of electrodes and the accompanying increase in surface irregularities will be insignificant.

The effect of a magnetic field on the properties of vacuum insulation depends on its orientation with respect to the electrical field of the electrodes.

A longitudinal magnetic field has no direct effect on breakdown voltage. However, with a magnetic field of significant magnitude (several hundreds or even thousands of oersteds), it is clear that the same effect on constant voltage should be observed as that with high-frequency voltage: with a magnetic field strength above a certain magnitude, depending on the interelectrode gap, during breakdowns because of better pinching of the discharge there is strong destruction of the electrode surfaces. This leads to an essential reduction in breakdown voltage during subsequent breakdowns. This effect should depend strongly on C_{sh} and it is possible that selection of C_{sh} may give good results.

When the magnetic field is perpendicular to the electric field and its magnitude is sufficient to prevent continuous motion of electrons from the cathode to the anode, the data of Pivovar et al. [120] indicate that vacuum insulation will be improved. Under such conditions these investigators found a more than 20% increase in the maximum achievable voltage on the electrodes (voltage up to 160 kV, gap 3 mm). However, in their experiments a resistance of 40 Mohm was installed in the discharge circuit and voltage might be limited not by breakdowns, but by dark currents or microdischarges. If a magnetic field which is perpendicular to the electric field only changes the point of incidence of electrons of dark current on the anode, then according to the measurements made by Bennette [165] a sudden change in the magnitude of the magnetic field may lead to a current surge if the anode is not free of contaminants.

When the vacuum is insufficiently high a transverse magnetic field may lead to impairment of vacuum insulation because of elongation of the path of electrons prior to incidence on the anode and thus to the appearance of "electron avalanches."

In order to give a clearer presentation of this phenomenon and to demonstrate methods of improving vacuum insulation in specific conditions, we will describe experience in adjusting the fast molecular hydrogen ion injector of the thermonuclear research installation "Ogra" [166]. This injector must create a beam of ions with a current force of several hundred milliamperes and energies up to 200 keV. In the injector an ion source of the arc type is held under high (positive with respect to ground) voltage and ions from the output slit (4 × 40 mm) of the source are attracted and accelerated by the electrical field created by two electrodes: one close to the source, which is negative with respect to ground (10-15 kV), and a grounded output electrode.

Thus, the voltage between the source and the first electrode exceeds the voltage corresponding to the energy of the emerging ion beam by 10-15 kV. This electric field configuration prevents the electrons which are formed from the residual gas outside the interelectrode gap which is accelerating the ions from being accelerated in this gap and bombarding the ion source, which would disrupt its operation. The accelerating electrodes are flat and have an area of 400 cm^2. The face surface of the source, where the ion-escape slit is located (i.e., the anode of the accelerating gap), is also flat and has an area of 80 cm^2. The ion source itself and the accelerating electrodes are located in an external magnetic field of 1-2 kOe, perpendicular to the electrical field in the accelerating gap. The vacuum in the working gap is on the order of 10^{-5} mm Hg. High accelerating voltage with respect to the ground is supplied to the ion source through a resistance of 7.5 kohm from a constant-voltage rectifier.

With copper electrodes and a working ion source, in an accelerating gap of 8 mm it was initially impossible to raise the voltage above 75 kV, owing to unremitting breakdowns. With an increase in the gap breakdowns were observed more rarely (one every few minutes), but in this case electron avalanches occurred; these melted the parts under a positive potential with respect to the ground. Bezbatchenko et al. [166] present the origin of avalanches as follows. Electrons formed as the result of ionization of residual gas in the interelectrode gap do not always reach the anode - the face surface of the ion source - by the direct and shortest route. In a magnetic field which is perpendicular to the electric field the electrons move along a trochoid, and if the interelectrode gap is sufficiently great (greater than the height of the trochoid) the electrons may escape from the accelerating gap. In the end the electrons

nonetheless impinge on the source or on other parts which are under a high positive potential, but the total length of the electron path to their "death" grows sharply. This creates the possibility of an exponential ionization growth ("multiplication") of electrons - i.e., the formation of an electron avalanche. Conditions especially favorable to the formation of a powerful avalanche are created during partial discharges (microdischarges) in the accelerating gap, when in addition to the appearance of a large quantity of electrons in the gap there is an increase in the pressure in the entire vacuum container (owing to desorption of gases from the electrodes). With a change in the geometry of the accelerating system the point of avalanche incidence (the melted area) is, as a rule, one and the same; the metal may be melted over several millimeters despite intensive water cooling.

An effective method for combatting avalanches which may arise (or, more exactly, countering the damaging consequences of these avalanches) is capture - the installation of an auxillary trap-electrode on the avalanche path. When the length of the avalanche path is shortened by approximately 3 times the power of the avalanche is reduced to such an extent that the appearance of an avalanche does not lead to melting of the electrode, even if the trap-electrode is uncooled. The method of applying high negative voltage to the intermediate electrode also has an influence on the power of electron avalanches which appear. If the power of the generator of this voltage is sufficiently great that the common potential of the punctured gap is negative during a breakdown between the source and the intermediate electrode, the harmful action of the avalanche will be very much weakened. The power of the avalanche grows strongly when the internal resistance of the negative-voltage generator is so great that the potential on the intermediate electrode during breakdown between it and the ion source becomes positive.

Although the measures described for combatting avalanches were successful, they nonetheless were insufficient to raise the working voltage to the required level - as before, breakdown caused a disruption in this area. Measures which render a decisive influence on increasing the electric insulating strength include the following: 1) replacing the electrode material first with stainless steel and then with vacuum-smelted molybdenum; 2) preliminary degreasing in an alkaline electrolytic bath with subsequent electropolishing of the working surfaces and sintering to 800°C of individual parts in a vacuum furnace; and 3) preventing accumulation of dust on the electrodes before their installation in the working volume. Together with installation of a trap-electrode on the avalanche path and selection of the power of the high-voltage source, these measures made it possible to raise the voltage on the electrodes and thus to increase the ion energy to 200 keV with a total current in the ion beam on the order of 1 A. In this case the accelerating gap was somewhat increased as contrasted with the initial; this became possible because of the successful supression of electron avalanches of the methods indicated above. With an ion current up to 2 A and ion energy of 200 keV the accelerating gap was 18 mm; at an energy of 120 keV the gap comprised 8 mm. When the current was cut off the electrical strength of the accelerating gap was 15-20% higher.

Fragmentary data from several sources indicate that the passage of electron currents through the gap does not lead to a reduction in breakdown voltage if the surface of the electrodes is not damaged - e.g., due to the formation of dielectric films. According to Heard [123], dark currents sometimes reach such magnitudes that the anode becomes red hot; however, this does not reduce breakdown voltage. The work by Mason (see Section 4) also indicates the absence of a negative effect due to the passage of an electron current. It is clear that a negative

effect of a current of ions may be caused not by the total value of the current but by a high density - i.e., by the possibility of intensive heating of even a very small segment of the anode.

2. EFFECT OF DURATION OF VOLTAGE APPLICATION AND THE PROBABILITY OF APPEARANCE OF BREAKDOWN

On oscillograms the appearance of breakdown is marked by a sharp drop in voltage in a time period of less than 10^{-7} s. With pulse voltage in the form ordinarily used to study breakdown, $U = U_0[\exp(-t/\tau_2) - \exp(-t/\tau_1)]$, where the quantities τ_1 and τ_2 determine the pulse front and its subsequent drop, respectively ($\tau_1 < \tau_2$), breakdown can be observed both on the pulse front and on its falling portion. Thus, Denholm [46] observed breakdown on both the front and the falling portion of a voltage pulse with a 12/50 μs. In work [163] a delay of several microseconds was observed with a pulse voltage (1.5/40 μs) up to 350 kV on a gap of more than 5 mm - i.e., the appearance of breakdown was also noted on the voltage oscillogram on the dropping portion of the voltage curve.

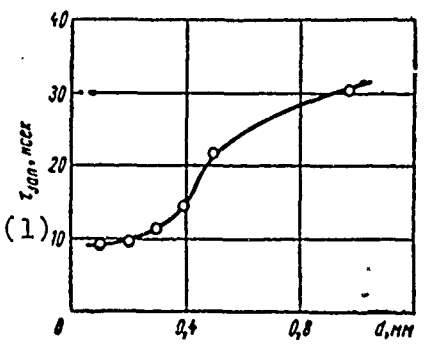

Fig. 45. Delay in the appearance of breakdown of copper electrodes with 10% overvoltage.

KEY: (1) τ_{del}, ms.

Kassirov and Koval'chuk carried out a study [167] of breakdown delay time (drop on the voltage oscillogram) with rectangular pulses of up to 40 kV. The measurements were conducted in a vacuum of $2 \cdot 10^{-5}$ mm Hg for copper electrodes which were conditioned by successive breakdowns until a stable but very low value of breakdown voltage was achieved (23 kV with a gap of 1 mm and pulses 0.2 μs in length). The breakdown delay curve with 10% overvoltage is shown on Fig. 45. For this overvoltage a delay exceeding the average values shown on Fig. 45 was observed in 5-8% of the cases; at the same time, intermediate values were extremely rare. With an increase in overvoltage these anomalous scatterings drop out and the average delay time for different gaps converges and comprises 5-7 ns for 80% overvoltage and gaps of 0.1-1 mm.

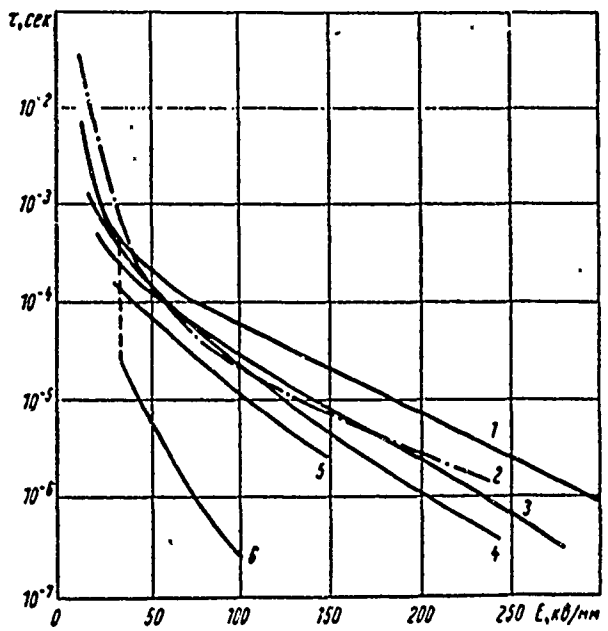

Fig. 46. Delay in appearance of breakdown of electrodes made from liquid metals with a gap of 0.125 or 0.25 mm: 1 and 4 - anode purified of mercury by heating; 2 - calculated curve according to equation (57); 3 - anode completely covered with mercury; 5 - cathode of liquid gallium; 6 - anode contaminated with traces of mercury; 1, 3, 4, and 6 - cathode of liquid mercury, anode of tungsten.

Designations: сек = s; кВ/мм = kV/mm.

Warmolz [168] studied the delay in the onset of breakdown with electrodes made from liquid metals. In his experiments a small cup filled to the edges with mercury or gallium was used as the cathode, while the anode was a rounded surface of tungsten wire 1 mm in diameter or a tungsten wire 2 mm in diameter bent into a semicircle with its plane perpendicular to the cathode. The interelectrode gap was held constant at 0.125 or 0.25 mm. It was found that breakdown delay depends strongly on the state of the anode surface (Fig. 46). If the anode is coated with a solid layer of mercury (for example, if a mercury drop held on a wire by strong adhesive forces is used as the anode) or if all traces of mercury are removed from the anode by heating before each breakdown, the delay characteristics will be very similar to one another. If the anode is not cleaned after the preceding breakdowns and if it is contaminated with traces of mercury, with a macrovoltage on the cathode E_c < 250 kV/cm the delay curve drops steeply; the breakdown voltage is substantially reduced along with this.

There has been very little qualitative study of the dependence of breakdown voltage on duration with small operating times. Almost the only more or less complete measurements of the pulse coefficient K were made by Kalyatskiy and Kassirov [169, 170]. Table 28 gives some results from their work. In these works the pulse front duration was varied in order to obtain different voltage operating times. This was achieved by varying the quantities C_{sh} and R_d. This method of regulation may lead to strong distortion of the real relationship because of the influence of the quantities R_d and C_{sh} on breakdown voltage. Examples of such an influence were given in Tables 26 and 27. The value of the obtained results is also somewhat reduced by the very low absolute values of breakdown voltage which, apparently, are explained by insufficiently clean vacuum conditions (Table 33) and by improper selection of electric-circuit parameters.

Clearly the failure to consider the effect of a change in C_{sh} and R_d on U_{br} can explain the "anomalous" curve of the pulse coefficient obtained by Wijker [125], which shows an increase in K from 1.0 to 1.5 with transition from pulses with a duration on the order of 10^{-4} s to millisecond pulses. In the same work the breakdown voltage of industrial frequency turned out to be lower than that with constant voltage, which contradicts the results obtained by Denholm and given in Table 29; he used disk electrodes 32 mm in diameter made from steel and a rise rate of constant voltage of 6 kV/s in the measurement [46].

Table 28. Pulse coefficient K (factor of the increase in breakdown voltage) with pulse durations of 2.5 and 0.2 μs.

Материал (1)	Зазор, мм (2)	Пробивное напряжение, кв (3)	K при длительности импульсов (4)	
			2,5 мксек	0,2 мксек
(5) Алюминий	1,5	42	1,3	2,0
	1	29	1,4	1,8
	0,25	16	1,0	1,05
(6) Сталь	1	32	1,55	2,2
(7) Медь	1	29	1,4	1,8
(8) Свинец	1	24	1,7	2,6
(9) Графит	1	12	1,7	2,7

KEY: (1) Material; (2) Gap, mm; (3) breakdown voltage, kV; (4) K with pulse duration of;;(5) Aluminum; (6) Steel; (7) Copper; (8) Lead; (9) Graphite.

Designation: мксек = μs.

Table 29. Pulse coefficient with voltages of different types.

Зазор, мм (1)	$U_{пр}$ при постоянном напряжении, кв (2)	(3) Коэффициент импульса	
		при переменном напряжении (50 гц) (4)	при импульсном напряжении (12/50 мксек) (5)
0,1	16	1,28	1,65
0,2	28	1,29	1,57
0,3	38	1,26	1,49
0,4	47	1,20	1,41
0,5	54	1,13	1,29

KEY: (1) Gap, mm; (2) U_{br} at constant voltage of, kV; (3) Pulse coefficient; (4) with alternating voltage (50 Hz); (5) with pulse voltage (12/50 μs).

The probability of breakdown. Practical utilization of vacuum insulation requires more than knowledge of the dependence of breakdown voltage on the various parameters of the electrical circuit, the interelectrode gap, and the material and construction of the electrodes. It is also necessary to know the probability of breakdown, since to a significant degree this determines the strength reserve of vacuum electrical insulation. Closely connected with the probability of breakdown is the dependence of breakdown voltage on the electrode area and on the duration of the applied voltage, where under the latter we understand both the total time of operation under voltage and also the duration of a single pulse when pulse voltage is applied periodically.

Figure 47 [163] presents an example of the curve of breakdown probability at different distances between steel electrodes and with a pulse voltage of 350 kV. It is clear that the maximum and minimum distances differ by approximately 2.5 times.

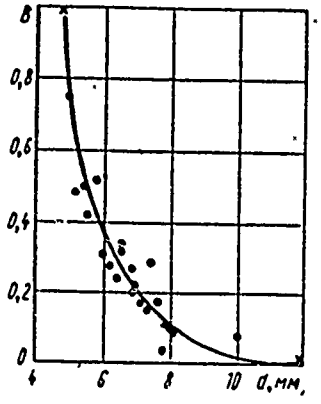

Fig. 47. Breakdown probability B with pulse (1.5/40 μs) voltage of 350 kV for steel electrodes (cathode - flat; anode - 9.3 mm sphere).

As was already stated, the scatter in the values of breakdown voltage is explained to a significant degree by the different conditions of the electrode surfaces. When a probability curve similar to that on Fig. 47 is taken the state of the surfaces depends mainly on the processes occurring during the preceding breakdowns. However, changes occur in the surface

not only during breakdowns and during subsequent discharge. Above (in Table 25) data are given concerning the effect of a break in the supply of voltage on breakdown. The very fact of the existence of such a relationship proves the existence of comparatively slow processes which change the state of the electrode surfaces and also proves the influence of the applied voltage on these processes. In the cited case the presence of voltage on the electrodes weakens the processes which impair vacuum insulation. However, there is a countereffect of voltage: formation of carbon-containing films, the growth of protuberances due to the influence of the electrical field and of dark currents on surface diffusion, and also creep and destruction of the electrode material under the action of electrostatic forces, etc. These processes, which were examined in Chapter 2, are comparatively slow, but, in all probability, they determine the drop in U_{br} with an increase in the duration of action of voltage during times which are several orders of magnitude greater than the time for development of breakdown.

One of the characteristics of dependence of U_{br} on duration with large time intervals is the frequency of appearance of breakdowns with a constant applied voltage. Figure 48 shows such a characteristic obtained by Denholm [46] for steel electrodes.

During prolonged application of voltage breakdown usually arises with a certain frequency and a value of voltage above which the frequency of appearance of breakdowns grows sharply is taken as the breakdown voltage. It is clear that such a determination of breakdown voltage is rather indistinct and, strictly speaking, it is unnecessary to know the frequency of breakdown appearance to which the quantity corresponds, in addition to the magnitude of breakdown voltage. Table 30 gives values of breakdown voltage and voltages sustained by flat electrodes 32 mm in diameter without breakdowns for 1 hour (10^{-6} mm Hg; oil pumps) [46].

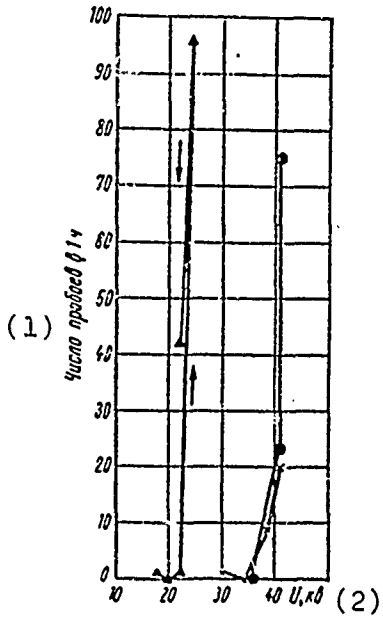

(1) (2)

Fig. 48. Frequency of breakdown appearance during prolonged application of voltage to steel electrodes 32 mm in diameter: × - d = 0.5 mm, conditioned electrodes; ● - d = 0.5 mm, unconditioned electrodes; ▲ - d = 0.25 mm, unconditioned electrodes.

KEY: (1) Number of breakdowns in 1 hour; (2) U, kV.

Table 30. Breakdown voltage and voltage withstood by a gap without breakdown for 1 hour.

Материал (1)	Зазор, мм (2)	$U_{пр}$, кв (3)	$-U_{1\ ч}$, кв (4)
(5) Сталь	0,25	33	20—24
	0,5	54	34,5—35,5
	0,8	—	46—51
(6) Медь	0,5	42	25,2
	1,0	—	51—58
(7) Алюминий	0,5	44	32,4
	1,0	60	41—46

KEY: (1) Material; (2) Gap, mm; (3) U_{br}, kV; (4) U_{1h}, kV (5) Steel, (6) Copper, (7) Aluminum.

Denholm, whose data are given in Table 30, notes that the voltage withstood without breakdown for 1 hour differs little from the voltage which can be withstood for several hours and even days. At least the scatter during repeated measurements within a period of a single hour exceeds this difference.

As a result of many years of research the fact that breakdown is always initiated by processes of some small segment of the electrodes can be considered firmly established. Therefore, other conditions being equal, the probability of breakdown is increased with an increase in electrode area. A curve similar to that given on Fig. 47 is extended to the right and becomes more sloping. In measurements this was fixed as the increase in frequency of appearance of breakdowns or as a reduction in average breakdown voltage with an increase in electrode area. Actually, such a reduction has been noted by a number of investigators [171, 172]. For example, the breakdown voltage of the surface of electrodes was 5% less for spherical electrodes 20 mm in diameter than for electrodes 9.3 mm in diameter (pulse voltage, 150-350 kV) [163]. The effect of electrode area on breakdown voltage is examined in more detail in Section 5.

The effect of the area of the electrodes on the voltage which can be withstood over a prolonged period is even more noticeable than its influence on breakdown voltage. This is clearly visible from comparison of the data in Table 27 with those given in Table 31 and obtained for electrodes of large area.

Table 31. Voltage which can be withstood for 10 min without breakdown with an electrode area of 20 cm^2.

Материал (1)	Зазор, мм (2)	$U_{10\ мин}$, кв (3)	Материал (1)	Зазор, мм (2)	$U_{10\ мин}$, кв (3)
(4) Сталь со следами пыли	0,7	26	(5) Сталь без следов пыли	0,7	30
	1,0	32		1,0	45
	2,0	40		2,0	72
	2,5	42	Инконель и никель (6)	2,3	77
				1	50

KEY: (1) Material; (2) Gap, mm; (3) $U_{10\ min}$, kV; (4) Steel with traces of dust; (5) Steel without dust; (6) Inconel and nickel.

Unfortunantly, the conditions under which these results were obtained were not given in work [173], from which the data in Table 31 were taken.

3. DENPENDENCE OF BREAKDOWN VOLTAGE ON THE INTERELECTRODE GAP

The material outlined in the preceding two sections shows a strong dependence of breakdown voltage on the experimental conditions; in many cases these have not been taken into account by the investigators themselves. It is therefore not suprising that the results of measurements made by different investigators differ significantly. At the same time, as yet no widely accepted procedure for measuring breakdown exists and there is not even a clearly established concept of just what breakdown is. Therefore different phenomena may be classified as breakdown in different works.

In many works where the high-voltage source was a low-power generator or where the object was separated from the voltage source by a resistance of tens of megohms, the maximum voltage which could be obtained on the investigated vacuum gap was ordinarily taken as the breakdown voltage [172]. It is clear that in these conditions the limitation of the achieved voltage might cause dark currents or microdischarges. In other works, mainly with lower limits on the current which could flow across the investigated gap, the breakdown voltage was regarded as that voltage at which discharge appeared with a sharply falling volt-ampere characteristic and subsequent transition (if the generator power permitted) to a low-voltage arc disch[illegible] in vapors of the electrode materials and in liberated gases. In our discussion of breakdown it is precisely this phenomenon which we will use.

A certain distinction in experimental data can be explained also by different methods of counting and different definitions:

breakdown voltage may be considered to be most probable [123], moderate [163], and the maximum achieved [125] voltage during multiple breakdowns; however, the divergence due to this cause is usually smaller than that caused by the difference in experimental conditions or than the difference in the criterion of "breakdown."

To illustrate the magnitude of the scatter in the values of breakdown voltage obtained in different works, Table 32 presents U_{br} for steel electrodes creating an approximately uniform field in a gap of 1 mm.

Such a large scatter is due mainly to the strong influence of experimental conditions; these conditions are far from always adequately described, which hampers analysis and makes it advisable to a significant degree to present here the sum total of all available information on the dependence of breakdown voltage on interelectrode gap. Therefore Fig. 49 shows only those experimental data which describe the upper and lower boundaries of the totality of results of published works - i.e., the maximum and minimum magnitudes of breakdown voltage in one and the same gap. This characterizes the region of scatter between data of different works, but not the scatter during measurements in each specific work. Thus if we take one or the other into account the domain of obtained values of breakdown voltage would be expanded even more. Besides this, Fig. 49 presents results of those works which are unique in the given range of voltages. Information on the experimental conditions under which the results presented in Fig. 49 were obtained is given in Table 33.

Table 32. Breakdown voltage with a gap of 1 mm between steel electrodes.

(1) Литература	$U_{пр}$, кв (2)	Литература (1)	$U_{пр}$, кв (2)
[123]	89—172*	[164]	86
[119]	122	[174]	43
[100]	109	[169]	32
[157]	103—112		

*Depending on the type of steel and the surface treatment.

KEY: (1) Reference; (2) U_{br}, kV.

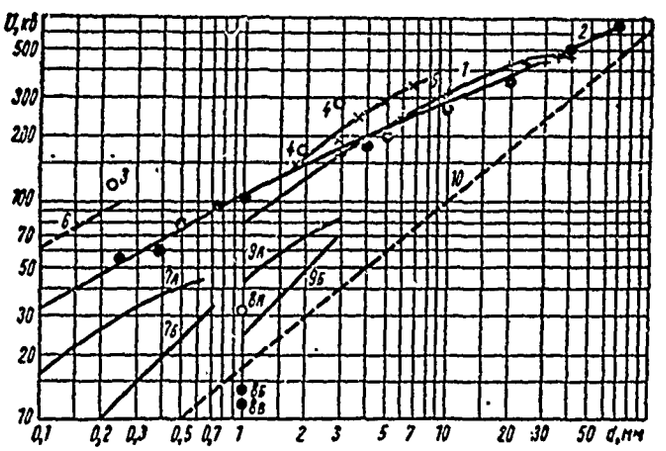

Fig. 49. Breakdown voltage as a function of interelectrode gap for electrodes with small curvature. (The numbers on the curve correspond to the numeration in Table 33).

Designation кв = kV.

Table 33. Experimental conditions during determination of the dependence of U_{br} on gap d for the curves shown in Fig. 49.

Curve	Electrical parameters	Vacuum, mm Hg and type of pump	Electrode characteristics	Treatment of electrodes	Breakdown criterion	Reference
1	Low-power constant voltage	10^{-5}; mercury	Disks, nickel	Low discharge in H_2	Maximum achieved voltage	[119]
2	The same	-	Cathode -disk 51 mm in diameter; anode - sphere 25.4 mm in diameter; steel	The same	The same	[100]
3	-	Sealed glass vessel; carbon cooled with liquid oxygen	Hemispheres 20 mm in diameter; molybdenum	Heating of assembled unit at 1400°C	The same	[175]
4	-	-	Hemispheres 10 mm in diameter; molybdenum	Heating to incandescence	-	[176]
5	Pulses 1.5/40 μs; R_d = 9 kohm; C_{sh} = 100 pF	$(3-7)\cdot10^{-6}$; oil	Cathode -disk 100 mm in diameter; anode sphere 30 mm in diameter; steel	Conditioning with breakdowns before each measurement	3 breakdowns per 5 pulses; average from 10 measurements	[163]
6	Constant voltage; R_d = 40 kohm; special setting of C_{sh} = 12,500 pF	10^{-7}; mercury, metal seals	Hemispheres 50 min in diameter; Invar	Conditioning with breakdowns (10^4 arcs)	Most probable breakdown voltage	[123]

Table 33 Cont'd.

Curve	Electrical parameters	Vacuum, mm Hg and type of pump	Electrode characteristics	Treatment of electrodes	Breakdown criterion	Reference
7	Alternating voltage, 50 H_z; R_d = =100 kohm	10^{-5}; oil	Disks 18-40 mm in diameter; A, copper; B, steel	Preliminary degassing at 700°C. Temper color (contaminants!) on the electrodes after operation	Maximum voltage from 10 breakdowns	[125]
8	10^{-4} s pulses, generator capacitance 100 pF	$2 \cdot 10^{-5}$; oil	Cathode - hemisphere 12 mm in diameter; anode - disk 30 mm in diameter; A - steel; B - lead; C - graphite	Conditioning by breakdowns until stable breakdown voltage is obtained	Average with multiple breakdowns	[169]
9	Constant voltage; R_d = 100 Mohm; C_{sh} = 1000 pF	$5 \cdot 10^{-6}$; oil	Disks 80-120 mm in diameter; A - steel; B - copper	Conditioning by breakdowns	Average voltage of flashes (microdischarges?)	[174]
10	Semiempirical breakdown criteria (see Section 5, Chapter 8).					[297]

From Fig. 49 and Table 33 it is clear that the best results, which is no paradox, were achieved in the 1920's - in the very first works concerned with the study of vacuum electric insulation. Credit must be given to the high experimental technique of these works, whose level with respect to the purity of experimental conditions is comparable with the level of the most modern studies. In fact, in the work by Piersol [175] hemispherical electrodes pressed from sheet molybdenum were soldered on tungsten rods in a vessel made from refractory glass. This vessel was connected with another one containing a sorbent - cocoanut palm charcoal. The electrodes were degassed for 48 hours at a temperature of 1400°C, while the vessel itself was heated to 500°C and the sorbent to 380°C and the entire system was subjected to constant evacuation. At the end of the preliminary temperature treatment both vessels were sealed from the evacuation system, the vessel with the sorbent was immersed in liquid air, and the vessel with the electrodes was subjected to continued heating at 500°C for another two hours. After this procedure the vessel with the electrode was sealed away from the vessel with the sorbent, with this sealing being carried out with precautions against the liberation of undesirable compounds from the glass during its heating. Such careful preliminary preparation of the electrodes and the vacuum vessel made it possible to bring the voltage on a 0.23 mm gap up to 120 kV without breakdowns. In this case the intensity on the cathode equaled 540 kV/mm, and this high electrical insulation strength was retained for a period of 9 months. Unfortunantly we do not have more detailed information, and in particular data on how reliable and reproducible the obtained results were. However, it should be noted that from the position of the present state of the art the successful selection of the electrode material, the methods of treating it (hardening during pressing), and finally the vacuum conditions might ensure a very high insulation strength, and we can only express our regret that such experiments were not repeated.

The curves on Fig. 49 characterize not only absolute values of breakdown voltage, but also the nature of the dependence of the latter on the gap between the electrodes. With an electrical field between the electrodes which is close to uniform, the dependence of breakdown voltage on the gap d usually can be expressed in the form

$$U_{пр} = \text{const} \cdot d^{\alpha}, \qquad (23)$$

[пр = br]

where the value of the coefficient α determines the nature of the dependence of U_{br} on d. If α = 1 - i.e., $U_{br} \sim d$, the intensity during breakdown does not depend on the applied voltage; with a reduction in E with a growth in voltage α < 1. Besides its great practical importance, the quantity α is also very significant for clarification of the mechanism of vacuum breakdown, of which more will be said in Chapter 8.

Table 34 gives the summary results, taken from work [177], of the determination of the quantity α from experimental data accumulated up to 1961.

Table 34. Values of α obtained in various works.

α	(1) Число экспериментальных данных	α	(1) Число экспериментальных данных	α	(1) Число экспериментальных данных	α	(1) Число экспериментальных данных
0.2	9	0,5	22	0,8	13	1,0	5
0,3	12	0,6	28	0,9	8	1,1	2
0,4	18	0,7	46				

KEY: (1) Number of experimental data.

It is clear that the most probable value is $\alpha = 0.6\text{-}0.7$; however, the deviations from this magnitude are very significant. The scatter may be partially explained by the fact that Table 34 summarizes data obtained at various voltages, although the possibility of the existence of a dependence of α on voltage is very evident. Thus, in a number of works (see, for example, [100, 123], and others) note is taken of the more or less well-known fact that up to 30-50 kV breakdown arises at a constant value of intensity on the cathode, while at higher voltages the effect of total voltage appears - i.e., a reduction in breakdown intensity with an increase in voltage ($\alpha < 1$). In actuality, extrapolation of the curve $U_{br} = f(d)$ from the region where $\alpha < 1$ into the region of lower voltages will sooner or later lead to breakdown stresses exceeding the values at which the appearance of intensive field-effect emissions sufficient for the appearance of breakdown is inevitable. However, the magnitude of the voltage at which this occurs obviously depends to a significant degree on the experimental conditions, the surface treatment of the electrodes, the electrode material, etc. In particular, it is clear from the curves on Fig. 49 that the total-voltage effect is detected even at 20-30 kV. At the same time the results obtained by Piersol and Hayden (points 3 and 4 on the same figure) show that even at voltages above 100 kV it is possible to obtain such a high value of breakdown intensity that it is possible to assume that the total-voltage effect is absent in these cases. At the same time, note must be made of the absence in the literature known to us of works reporting a single experiment in which a change in α from $\alpha = 1$ to lower values with transition from voltages of tens of kilovolts to higher voltages has been demonstrated. Since the majority of the data used in Table 34 were obtained for metallic electrodes in technical vacuum conditions with voltages above 20-30 kV, it is obvious that the value $\alpha = 0.6\text{-}0.7$ is the most probable under precisely these conditions.[1]

[1]For graphite electrodes or for metallic electrodes which are coated with insulating films, α can differ from the α for metallic electrodes (see Sections 5 and 8).

The following should be borne in mind in connection with the data in Table 34. In 1952 the work by Cranberg [178] appeared, which presented the first formula based on simple physical considerations which connects breakdown voltage with the gap between the electrodes and which takes into account the effect of total voltage. For a uniform field coinciding with expression (23) and with $\alpha = 0.5$, this formula approximately truly reflects the general nature of the experimental relationship. The work by Cranberg was a significant forward step and had a profound influence on subsequent investigation of vacuum breakdown. However, this influence also had a negative side: in certain subsequent works the agreement of data obtained by the authors with the Cranberg formula is confirmed, although more detailed examination shows a noticeable difference from $\alpha = 0.5$. This circumstance, which is explained by the fact that at the time no other criterion but the Cranberg formula existed for comparison, does not in the least belittle the value of the indicated works and simply must be borne in mind when the original works are read. In particular, according to the Cranberg formula (which will be examined in more detail in Chapter 8) $\alpha = 0.5$ is valid only for a uniform field. Therefore, for example, it is not legitimate to consider the curve of $U_{br} = f(d)$ obtained by Trump and Van de Graaf [100] (Fig. 49) as confirming the Cranberg formula. Although α is close to 0.5 for this curve, the field between the electrodes is essentially nonuniform. Thus, with a gap d = 70 mm and with a spherical anode 25.4 mm in diameter and a flat cathode 53 mm in diameter, the intensity on the electrodes exceeds the average by 2-3.5 times. If this is taken into account and the appropriate recalculation is carried out, we obtain $\alpha = 0.59$.

Breakdown at low voltage. Boyle et al. [179] investigated the characteristics of vacuum insulation with micron gaps between thoroughly degassed tungsten electrodes and with rectangular voltage pulses 1 μs in length. The interelectrode gap was formed

of intersecting wires 0.75 mm in diameter. In addition to breakdown voltage, the prebreakdown currents were also measured. This made it possible to calculate the local intensity of the emitting portion of the cathode and, by comparing it with the macrointensity, to find the field gain factor μ on cathode microprojections. Because the microirregularities of the electrodes are comparable with the gap when the magnitudes of the gap are so small, the coefficient μ depends on the magnitude of the gap. Table 35 gives the results of measurements in a vacuum of 10^{-9} mm Hg and data from the indicated calculations. The magnitudes of the currents and, correspondingly, the values of μ are averaged values for 100 measurements.

Table 35. Properties of vacuum insulation with very small gaps.

Зазор, мк (1)	Максимальный предпробойный ток, ма (2)	Пробивное напряжение, в (3)	Увеличение поля μ (4)	Макронапряженность на катоде, Мв/мм (5)	Локальная напряженность на катоде, Мв/мм (6)
0,5	1,1	390	8	0,78	6,23
2,0	3,9	850	17,5	0,425	7,2
5,2	8,2	1500	26	0,289	7,5
8,0	15,8	2200	28	0,275	7,7

KEY: (1) Gap, μm; (2) Maximum prebreakdown current, mA; (3) Breakdown voltage, V; (4) Field gain μ; (5) Macrointensity on the cathode, MV/mm; (6) Local intensity on the cathode, MV/mm.

During calculation of local intensity with respect to prebreakdown current, considering that this represents field-effect emission from a single protuberance, Φ was taken as equal to 5 eV. The current density corresponding to the maximum values of prebreakdown current was found to equal $6.0 \cdot 10^{10}$-$1.3 \cdot 10^{11}$ A/m^2. Processing of voltage oscillograms showed that the delay time for appearance of breakdown at minimum overvoltages comprised about 0.3 μs, while the voltage fall time was less than 0.01 μs.

4. INFLUENCE OF THE MATERIAL AND TEMPERATURE OF THE ELECTRODES

One consequence of the fact that breakdown in vacuum is determined primarily by processes on the electrodes is the dependence of breakdown voltage on the material from which the electrodes are made. Table 36 gives a summary of the available data. Some additional information can be drawn from Tables 30 and 31.

The Heard data which are given in the table represent the results of recalculation by the Cranberg formula of data obtained at voltages up to 100 kV. Heard [123] confirms that under the conditions of his experiments (Table 33) this formula proves out quite well, although he does not give specific data. In view of the repeatedly mentioned divergence between measurements of the different investigators, it follows that comparison of different material should be made according to results of some one work. Therefore, for example, it would be premature to draw the conclusion which follows from direct comparison of the data in Table 36 concerning the fact that electrodes of Invar withstand higher voltage than those of tungsten or molybdenum. Besides this, when the experimental conditions are different the relationship between the strength of vacuum insulation can vary with different electrode materials. This is clearly evident on the example of copper and aluminum: according to the data in Table 36, breakdown voltage for copper electrodes is higher than for aluminum; in works [81, 120], where microdischarges may have been taken for breakdown, the picture is reversed.

If the cathode and anode are made of different materials, the anode material is the determining factor when the number of conditioning discharges is small and the energy liberated on the electrodes during breakdown is also small. However, during breakdowns transfer of material occurs in both directions, and in the end a mixture of materials of undetermined composition is formed

Table 36. Breakdown voltage for electrodes of various materials.

Material	Breakdown voltage calculated for a 1 mm gap, kV	
	per Heard [123]	from other sources
Tungsten	-	96-102[а]
Molybdenum	-	92[а]
Invar	192	-
Stainless steel	179	122[б], 105[в], 109[г]
Manganese steel	172	-
Hardened steel (Rockwell hardness 65 units)	159	-
Copper covered with chromium (0.025 mm), with annealing at 500°C	143	-
Inconel	134	-
32% nickel steel	134	-
Hastelloy B	126	-
Nickel	89.5	84-86[а], 96[б]
Copper coated with chromium (without annealing)	89.5	-
Hot-rolled steel	89	86[а], 102-112[в], 32[д]
Copper deoxidized with phosphorus (commercial copper)	71	78[а], 37[б], 98[в], 29, 5[д]
Kiralloy	71	-
Tantalum	71	-
Aluminum	45-57	64-70[а], 88[в], 29[д]
Copper remelted in vacuum	54	-
Lead	54	14[д]
Graphite	36	40[а], 12[д]
Silver	27	-

а Rozanova and Granovskiy [164].

б Anderson [119].

в Borovik and Batrakov [157].

г Trump and Van de Graaf [100].

д Kalyatskiy and Kassirov [169].

both on the cathode and on the anode. If the cathode and anode are made from materials with strongly differing properties, the breakdown voltage may turn out to be lower than when both electrodes are made of a material which is lower in rating as regards the voltage it can withstand. The data in Table 37 confirm this.

Table 37. Breakdown voltage with a 1 mm gap between electrodes of different materials.

Материал (1)		$U_{пр}$, кв (4)	Литература (5)
(2) анода	(3) катода		
Алюминий (6)	Алюминий (6)	88	[157]
Сталь (7)	Сталь (7)	102—112	
Сталь (7)	Алюминий (6)	85	
Алюминий (6)	Сталь (7)	83	
Инконель (8)	Инконель (8)	134	[123]
Графит (9)	Графит (9)	52	
Графит (9)	Никель (10)	48	
Инконель (8)	Графит (9)	62	

KEY: (1) Material; (2) anode; (3) cathode; (4) U_{br}, kV; (5) Reference; (6) Aluminum; (7) Steel; (8) Inconel; (9) Graphite; (10) Nickel.

However, it is clear from the table that the anode material is the dominant factor.

A number of regularities in the influence of material transfer with electrodes of different kinds are evident from Fig. 50. This figure gives the results of three series of successive measurements of the breakdown distance at 300 kV for a steel cathode and two interchangeable (in the course of the measurements) anodes: aluminum and steel [163]. The measurements were carried out by the procedure described in Section 1 (see Fig. 42). First the breakdown distance was measured for the steel anode, then for the aluminum anode, and after this for the steel anode once again. The cathode was not changed during these measurements. From Fig. 50 it is clear that after the return to the steel

anode during the first few measurements the breakdown distance remains the same as that with the aluminum anode, and only after a few breakdowns (first and second series) is the strength corresponding to the steel anode restored. The number of measurements was increased from series to series. It is clear that this led to a situation in which the return to the strength corresponding to steel occurred later during the repeated measurements with a steel anode in the second series than in the first, while in the third series their results became, in general, less definite. These measurements show that with a small number of discharges the prevailing influence of the anode material can be explained by its transfer to the cathode - i.e., by the fact that both electrodes are coated with an identical material - the material of the anode (for breakdown with electrodes of liquid metals, see Section 2).

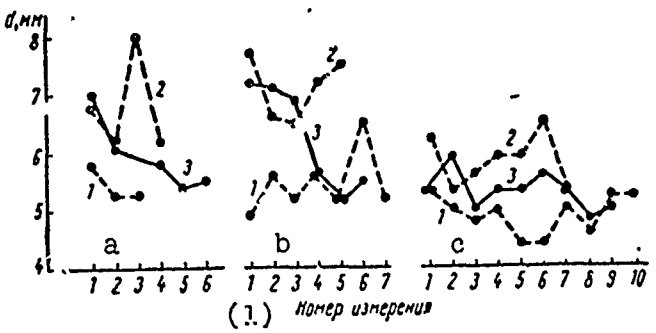

Fig. 50. Change in electrical strength with exchange of a flat anode and with a steel cathode (sphere 20 mm in diameter). Pulse voltage, 300 kV: 1 - steel anode; 2 - aluminum anode; 3 - repeated measurements for the steel anode. a - first series of measurement; b - second; c - third series of measurements.

KEY: (1) Number of measurements.

There has been very little study of the influence of electrode operating temperature on breakdown, although besides the practical value this characteristic can introduce a substantial contribution to the understanding of the physical processes which lead to disruption of vacuum insulation. From earlier works we should note the indirect data obtained by Mason [180] at voltages up to 50 kV. He determined the influence on breakdown of thermionic emission from a cathode consisting of tungsten wire 0.7 mm in diameter bent into a semicircle. The anode (a copper disk 23 mm in diameter) was arranged perpendicularly to the plane of the semicircle (cathode). To obtain thermionic emission the cathode was heated up to 1500-1700°K. The thermoemission current, amplified by the Schottky effect, reached 70 μA; however, instead of the expected reduction in breakdown voltage this led to a certain increase in U_{br}. From the point of view of our interest this experiment indicates that even such intensive heating of a tungsten cathode, if it changes breakdown voltage at all, changes it in the direction of a certain increase. It is clear that there is no such essential reduction in electrical strength during heating of a tungsten anode, or else a high-voltage kenotron, in which during the reverse blocking half-period the incandescent tungsten filament acts as the anode - thermionic emitter - could not possibly operate.

However, in work [181] just the reverse is asserted: under conditions close to those obtaining in a high-voltage kenotron, heating of a tungsten anode or cathode to 2000°C (up to a temperature below the appearance of noticeable thermoemission) it is possible to initiate breakdown. Unfortunately, no experimental data or conditions under which this occurs (for example, preliminary or sudden heating with voltage already applied) are given.

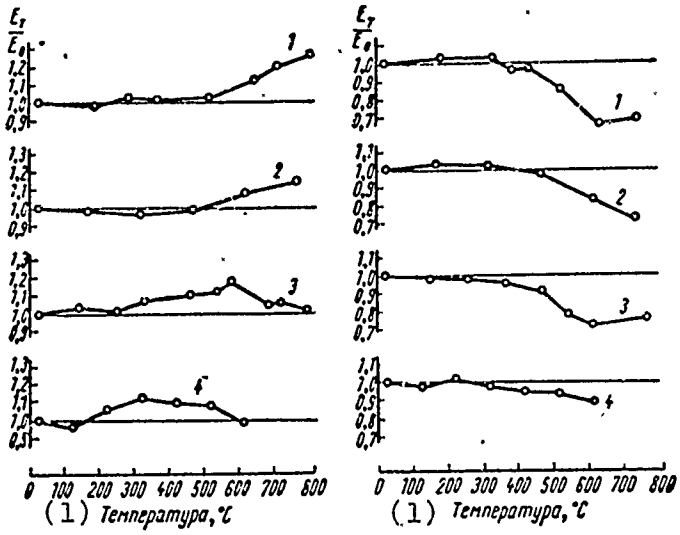

Fig. 51. Effect of electrode working temperature on the electrical strength of the vacuum gap between hemispherical electrodes 32 mm in diameter. Pulse voltage, 300 kV: left - cathode heating; right - anode heating.

1 - nickel electrodes; 2 - steel; 3 - copper; 4 - aluminum.

KEY: (1) Temperature, °C.

The influence of temperature was studied in more detail with a pulse voltage of 250-300 kV [160] and in a vacuum of approximately $3 \cdot 10^{-6}$ mm Hg. In this work the electrodes - whole hemispheres 32 mm in diameter - contained a tungsten spiral heated by current. Figure 51 shows the results of measurements made with heating of the anode or the cathode. The ratio E_T/E_0 is plotted along the ordinate; here E_0 and E_T are the breakdown macrointensities on the surface of the electrodes at room temperature and the temperature plotted along the abscissa, respectively. During these measurements the temperature of the opposite electrode was increased somewhat, equalling 40, 80, or 190°C with heated-electrode temperatures of 200, 500, or 800°C, respectively. The measurements were carried out both with successive (from point to point) increases in temperature

and with a reduction in temperature. The measurement results in both cases coincide within the scatter limits. However, with heating of copper anodes and especially of nickel anodes above the temperature at which the reduction in electrical strength begins, "damage" of the electrodes is observed - i.e., E_{br} drops and is not restored even with a reduction in temperature. Such a phenomenon was observed with rapid heating of the anode (30-50° per minute) and was substantially reduced when the heating rate was slowed by 5-7 times. The possibility that this effect of anode heating may have influenced the results given in Fig. 51 is not excluded, although all measurements were made with slow anode heating.

The same work reports experiments with heating of both electrodes. Measurements carried out with nickel electrodes at 600, 730, and 800°C gave quantities coinciding within ±5% with those obtained at room temperature. Judging from Fig. 51, we can propose that during these measurements the effects of the anode and the cathode mutually compensated one another.

Cooling of the anode below room temperature leads, according to Maitland [182], to a certain increase in the electrical strength in vacuum insulation. The results of measurements with constant voltage of 7-40 kV and flat electrodes made from the same material are given in Table 38.

Table 38. Increase in breakdown voltage with cooling of the anode.

Electrode material	Anode temperature, °C	Increase in U_{br}, %
Copper	−195	20
Molybdenum	− 91	(3)
Tungsten	− 76	6

5. ROLE OF ELECTRODE CURVATURE WITH SMALL NONUNIFORMITY OF THE FIELD

A change in the curvature of the electrodes has an immediate influence on several parameters from which the electrical insulating strength of vacuum depends. First of all this occurs as a difference in the macrointensity on the electrodes from the average in the gap and a change in the area of the "active" surface of the electrodes (under "active surface" we understand that portion of the electrode surface where breakdown may be initiated). Besides this, electrode curvature is a dominant factor in the electron-optical properties of the interelectrode gap - i.e., the trajectory along which ions and electrons travel in the gap. The latter also can play a determining role in the initiation of breakdown.

If both electrodes are identical in shape and size, then with an increase in curvature of both electrodes the active area is reduced, while surface macrointensity is increased with an unchanged gap. These two factors in general operate on breakdown voltage in opposite directions, which hampers analysis of experimental data. If the curvature of only one electrode is altered, an increase in macrointensity on one electrode and a reduction on the other will ensue. And since the intensity on the cathode and that on the anode influence breakdown differently, the picture is clouded still more. It is clear that the different relationship of the indicated factors and their different effects on breakdown explain the apparent contradiction between the results in different works: some speak of an increase in electrical strength with an increase in curvature [81, 172, 183, 184], while others note the reverse [157, 163].

For an approximate evaluation of the dimensions of the active area of electrodes it is logical to assume that the range of values of surface macrointensity within the limits of this area is closely connected or even determined by the scatter of breakdown voltage for the given electrodes with multiple measurements. In other words, to evaluate the active area it is possible to assume that macrointensity in the center of the active area E_0 and that on its boundary E_{bdy} are related to one another as the maximum and minimum values of breakdown voltages with repeated measurements and small electrode areas.

Then

$$\frac{E_0}{E_{гр}} \approx \frac{U_{пр.макс}}{U_{пр.мин}}. \qquad (24)$$

[гр = bdy; пр = br;
макс = max; мин = min]

The following might be another method of determining the active area - a method possibly stricter and more exact: on the basis of the breakdown proability curve as a function of gap for electrodes with a small area, construct the probability curve for the electrode of interest. This can be done if we assume that for each element of the surface of this electrode the breakdown probability is the same as for an equal element of an electrode of smaller area and for a gap equal to the distance between the corresponding elements of the electrodes with which we are dealing. However, such a method requires knowledge of many parameters and therefore is inconvenient for evaluation. Therefore further evaluation is carried out on the basis of expression (24).

For spherical electrodes (solid sphere or segments) of radius r with interelectrode gap $d < r$, one can propose in the first approximation that with removal from the line of centers

the surface intensity is inversely proportional to the distance between the corresponding points of the electrodes. If this distance is d + Δd on the boundary of the active area, then the active area will equal

$$S_{акт} = \pi r \Delta d = \pi r d \frac{U_{пр.макс} - U_{пр.мин}}{U_{пр.мин}}. \qquad (25)$$

[акт = act; пр.макс = br.max;
пр.мин = br.min]

On the other hand, the ratio of macrointensities on the electrode E_0 to the average intensity in the gap $\bar{E}$ depends on d/r. When d/r - 0.1-0.5, $E_0 d/U$ = 1.03-1.18. Therefore if d << r, a change in r leads mainly to a change in S_{act} and has little effect on E_0, while when r < 10d E_0 will also be changed substantially.

After these preliminary remarks we will examine the results given in Table 39 regarding measurements for electrodes in the form of 10 mm diameter disks with a spherical working surface with radius of curvature r under constant voltage [81]; the electrodes have been subjected to few conditioning breakdowns. A vacuum of 10^{-5}-10^{-9} mm Hg was created with oil pumps. The scatter from the average value of U_{br} given in the tabl was ±10%; R_d = 500 kohm. The voltage rise rate was approximately 3 kV/s. The values of U_{br} given in the parentheses were obtained after prolonged conditioning of the electrodes by breakdowns (see below).

Similar measurements with an increase in electrode diameter to 20 mm gave results coinciding with those shown in Table 39.

Table 39. Effect of radius of electrode curvature on breakdown voltage with small d/r.

Материал электродов (1)	Радиус r, мм (2)	$U_{пр}$ при различных d, кв (3)	
		0,07 мм	0,2 мм
(4) Алюминий	101,6	7,3 (9,7)	17 (21)
	12,7	10 (16)	19,5 (30)
(5) Медь	101,6	6,6 (9,1)	16,5 (20)
	12,7	10 (15)	21 (~29)
(6) Нержавеющая сталь	101,6	10 (13)	25 (~29)
	12,7	14 (17,5)	31 (38)

KEY: (1) Electrode material; (2) Radius r, mm; (3) U_{br} with various d, kV; (4) Aluminum; (5) Copper; (6) Stainless steel.

An increase in breakdown voltage with an increase in electrode curvature is clearly visible from the data in this table. In all probability this can be attributed completely to the reduction in the active area of the electrodes. Actually, at the selected values of d and r the field between the electrodes is virtually uniform, while according to (25) the active area varies by 8 times. If for evaluation we take $(U_{br.max} - U_{br.min}) \div U_{br.min} = 0.5$, which substantially exceeds the scatter during measurements given above, the active area will have a diameter of less than 10 mm. Therefore the identical U_{br} which is observed for electrode diameters of 10 mm and 20 mm does not contradict the assumption made above that an increase in breakdown voltage with an increase in electrode curvature occurs because of the reduction in the active area of the electrodes.[1]

[1]The major influence on the measurement results of the procedure for determining U_{br} from flashes in the container and the lighting of a neon lamp installed in parallel with a 100 μA microammeter connected to the discharge circuit is not excluded. Therefore, for example, microdischarges may be taken for breakdown.

In a later work by the same authors [184, 185] similar measurements were given for electrodes of similar shape, but conditioned by breakdowns. The nature of the dependence of U_{br} on curvature (the figures in the parentheses and Table 39) remains, in general, as before. But in this work the change in electrode area influenced U_{br}. Thus, with a reduction in electrode diameter from 18 to 10 mm, U_{br} grew by approximately 11% when d = 0.078 mm and by approximately 8% when d = 0.2 mm (radius of curvature of electrodes 102 mm). Such contradictory data on the influence of electrode area on U_{br}, obtained in two studies by the same authors and with the same electrode dimensions, can be explained by the dependence of the active area of the electrodes on their conditioning by breakdowns. Expression (25) was obtained for the case when the state of the electrode surfaces was approximately identical in the central portion and on the periphery. This can occur, for example, after mechanical, electrochemical, or thermal treatment of the electrodes and after conditioning by a glow discharge encompassing the entire surface of the electrodes. But if the electrodes are conditioned by breakdowns in a vacuum, the greatest number of breakdowns occurs on the central portion of the electrodes, where E is great, and the "state of conditioning" of these portions of the electrodes will be better than that of the peripheral segments. With conditioning and with an increase in breakdown voltage for the central portion of the electrodes, their active area should be increased at the expense of the peripheral regions, where the smaller value of surface intensity is, as it were, compensated by a lower level of conditioning - i.e., a lower value of breakdown intensity. Clearly, this effect causes the difference obtained in the works cited above in the dependence of U_{br} on the change in the diameter of the electrodes from 10 to 18-20 mm for weakly conditioned and well-conditioned electrodes.

The effect of the change in the active area apparently explains the results obtained by Pivovar et al. [172], who also detected an increase in U_{br} with a decrease in the radius of curvature of the electrodes. Although in this case d/r = 0-1 and the change in r should have led to an essential change in the macrointensity on the electrodes, we must bear in mind the fact that the voltage on the investigated gap was supplied through R_d = 25 Mohm, while the maximum achievable voltage served as the criterion of breakdown. Under these conditions limitation of the voltage may possibly have been determined by the dark currents or by microdischarges, whose magnitude depends to a very great degree on the electrode area and might have a value averaged in time of about 1 mA. An additional argument favoring such an interpretation of the results may be the fact that during repeated breakdowns the breakdown voltage was reduced substantially - i.e., a phenomenon was observed similar to that shown on Fig. 44, where the limitation of the achievable voltage by dark currents is more clearly visible.

The effect of electrode curvature has been studied in other works. Table 40 gives the results of measurements with a pulse voltage of 1.5/40 μs for steel electrodes in a vacuum of $5 \cdot 10^{-6}$ mm Hg [163]. The intensity on the cathode and on the anode was calculated from known formulas for fields of two spheres.

Table 40. Effect of electrode curvature on breakdown with d/r > 0.1.

(1) Форма и размеры электродов		d, мм		(4) $E_к$, кв/мм		$E_а$, кв/мм (5)	
(2) катода	(3) анода	$U_{пр}$ = =200 кв	$U_{пр}$ = =350 кв	$U_{пр}$ = =200 кв	$U_{пр}$ = =350 кв	$U_{пр}$ = =200 кв	$U_{пр}$ = =350 кв
(6) Пластина диаметром 100 мм	(7) Сфера диаметром 30 мм	2,9	6,6	64,5	45,5	78,5	69,5
(6) Пластина диаметром 100 мм	Сфера диаметром 9,3 мм (8)	2,6	6,4	63,0	34,5	108	113
(8) Сфера диаметром 9,3 мм	Пластина диаметром 100 мм (6)	3,6	10,0	88	98	42	18,5

KEY: (1) Shape and size of electrode; (2) cathode; (3) anode; (4) E_c, kV/mm; (5) E_a, kV/mm; (6) Plate 100 mm in diameter; (7) Sphere 30 mm in diameter; (8) Sphere 9.3 mm in diameter.

[пр = br; кв = kV]

Analysis of other data from the same work showed that a change in the diameter of spherical electrodes from 9.3 to 20 mm changes the macrointensity on the electrodes during breakdown by less than 5% (the effect of area). Therefore the data in Table 40 reflect the influence of the intensity on the electrodes on breakdown. From the table it is clear that at 350 kV and with different electrode configurations the quantity d varies by more than 1.5 times, E_a by six times, and E_c by almost three times. This shows that the appearance of breakdown depends both on E_c and on E_a, with the intensity on the cathode rendering a dominant influence. However, this dependence is not valid for all electrode materials. For example, similar measurements for graphite electrodes [186] in sphere/sphere (diameter 1 -30 mm) and sphere/plane configurations with pulse voltage of 150-300 kV showed that breakdown arises at a constant 30 kV/mm value of macrointensity on the cathode, although for electrodes of different configurations the value of E_a varied from 3 to 55 kV/mm. With a large value of E_a the macrointensity on the cathode began to drop.

The data in Table 40 once again demonstrate the reduction in the average breakdown intensity with an increase in voltage. At the same time, as is clear from these data, with a strong nonuniformity of the field between the electrodes the macrointensity on one of the electrodes can even grow.

The greater influence rendered by cathode macrointensity on breakdown as compared with the anode value was also shown in work [157]. For sphere/plane steel electrodes with d = 1 mm the breakdown voltage was 103 kV if the sphere was the cathode and 112 kV with reverse polarity. It is clear that the dominating influence of cathode macrointensity can explain the increase in breakdown voltage observed in a number of works [172, 183] with a reduction in the radius of curvature of 1 anode, since in this case E_c is reduced.

6. BREAKDOWN IN SHARPLY NONUNIFORM FIELDS

Investigating the properties of vacuum insulation at 10-20 kV with a cathode in the form of a thin filament located along the axis of a cylindrical anode, Ahearn [187] noted that with achievement on the cathode of a macrointensity value of about 100 kV/mm the current between the electrodes instantaneously grew from 10^{-10} to 10^{-3} A. Ahearn called this phenomenon breakdown of the vacuum. The original volt-ampere characteristic was not restored after breakdown, and the "aftereffect" could be liquidated only by intensive calcination of the cathode. The voltage of breakdown appearance depended on the magnitude of the resistance connected into the discharge circuit, while with a resistance greater than 100 Mohm breakdown did not occur at all. This latter fact showed the significance of the current flowing in the prebreakdown stage for the appearance of breakdown.

During microscopic examination of the cathode surface after breakdown craterlike depressions with sharp projecting edges were observed. All of these data led Ahearn to the conclusion that the current surge - breakdown - occurred in the conditions of his experiment because of destruction of the surface of the cathode and the formation on it of new protuberances. The cause of the destruction was local heating due to bombardment by ions, Joule heating by electrons, or the action of electrostatic forces. The latter reached a magnitude of 4.5 N/mm^2 (45 atm), if a tenfold increase in the field on irregularities of the cathode surface is accepted. The current after breakdown represents a field emission current from the newly forming projections, amplified by secondary processes.

A more detailed study of breakdown with a cathode with a small radius of curvature was carried out by Dyke and coworkers [188-190]. They were the first to use the spherical electron field-effect microscope-projector for such investigations (a

spherical glass vessel coated inside with a luminophore and an aluminum film served as the anode, in the center of which a tungsten point - the cathode - was installed). Rectangular voltage pulses up to 100 kV with a length of 0.5-1 μs could be applied to the cathode. A vacuum of better than 10^{-8} mm Hg was maintained in the vessel with complete absence of organic compound vapors. The application of an electrode system of the electron projector type and the use of the pulse procedure made it possible to obtain, besides oscillograms of current and voltage, additional information on the processes on the cathode by means of high-speed photography of the emission image of the cathode on the screen - i.e., on the spherical anode. It was found that the appearance of breakdown is preceded by a number of clearly expressed phenomena. With a gradual increase in the amplitude of the voltage pulses distortion began in the oscillogram of the field-effect emission current: initially the rectangular current pulses became sharply rising in shape, i.e., there was an arbitrary growth in current in the course of the voltage pulse (Fig. 52, [191]). Simultaneously a bright ring, encircling the former emission image of the cathode, appeared on the projector screen. These phenomena were thoroughly reproducible and appeared at a definite current for the given cathode. However, their appearance indicated that a further increase in voltage by 1-2% (or an increase in current by 30-40%) would, without fail, lead to breakdown - to an approximately 100-fold surge of current in a period of less than 0.1 μs. Breakdown was accompanied by an irreversible change in the cathode point: subsequent photomicrography confirmed that during breakdown there was strong melting of the peak of the point, whose radius was increased from the prebreakdown value of a fraction of a micron up to several microns. Similar phenomena were observed with point cathodes of different dimensions and with correspondingly different amplitudes of the applied voltage, and in every case the onset

of breakdown was connected with achievement of a field-effect current density on the cathode of 10^{11}-10^{12} A/m^2. A number of additional experiments and calculations permitted a fairly clear presentation of the physical essence of the described phenomena. The spontaneous rise in current is logically explained by the strong heating of the cathode peak by Joule heat from the passing field-effect current and by the consequent thermal field-effect emission. The latter causes the appearance of the bright ring around the emission image of the cathode. At field-effect current densities greater than 10^{11} A/m^2 the further growth in current with an increase in voltage is retarded due the influence of the space charge of the electrons. However, if the temperature of the point is raised to the melting temperature, the evaporation which begins and the subsequent ionization of the vapors lead to compensation of the space charge of the electrons, to a growth in current because of this, to an increase in temperature, and finally to a surge of current and to melting of the cathode point. The results of the experimental determination of the current density leading to breakdown and to destruction of the emitting point are given in Table 41. The same table gives calculated values of the current density at which the peak of the emitting projections is heated to 3000°C in the period of action of the high voltage (1 μs). This calculation (see Section 3, Chapter 8) also showed that 1 μs after the beginning of heating the temperature of the projection peak reaches only 25% of its steady-state value. During the evaluation the electrical conductivity and heat capacity of tungsten were taken as constant and independent of temperature; the emitting point was approximated by a cone with a rounded apex, representing the electron emitter.

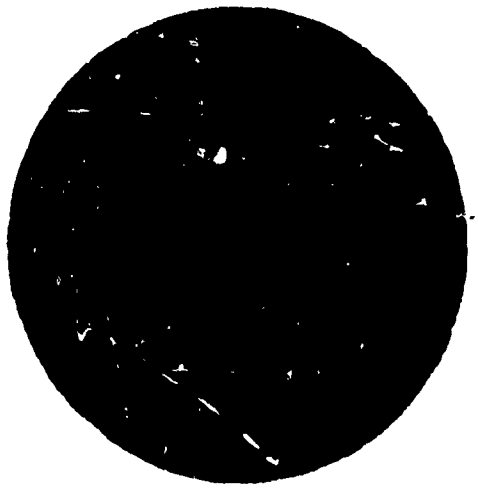

Fig. 52. Oscillogram of the spontaneous rise in current in time with a constant pulse voltage (time mark scale 0.5 μs).

Table 41. Current density j leading to breakdown with a tungsten cathode in the form of a cone with a rounded peak - the emitter (τ = 1 μs).

Радиус эмиттера, мк (1)	Полный угол раствора конуса, град (2)	$j \times 10^{11}$ а/м²		Напряжение, кв (5)
		расчетная (3)	экспериментальная (4)	
0,15	3	7,1	4	4,9
0,25	5	7	6	9,2
0,2	16	27	10	16,1
0,32	6	7,4	7	14,2
0,38	6	5,8	5	13,3
1,5	10	2,5	3	60

KEY: (1) Emitter radius, μm; (2) Total apex angle of cone, deg; (3) calculated; (4) experimental; (5) Voltage kV.

[$a/m^2 = A/m^2$]

A number of subsequent investigations confirmed and refined the outlined results from Dyke et al. Consideration of the temperature change in the electrical resistance of tungsten gave a significantly better coincidence of experimental and calculated magnitudes of the density of current leading to breakdown. The results also showed that a growth in electrical resistance with temperature causes a progressively rising deflection of the curve of temperature growth in time from the ordinary curve with saturation which is characteristic for heating with constant heat liberation: the temperature begins to grow very rapidly and to very high values. Figure 53 presents the results of this calculation, carried out by Gor'kov et al. [191], and also the "critical" values of current density which they measured at various apex angles of cone-shaped emitters. Good correspondence of experimental and calculated values is evident, along with a strong growth in the critical current density with an increase in the cone apex angle above 60°.

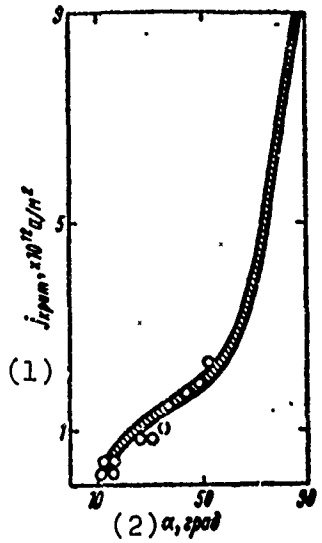

Fig. 53. Critical values of the density of the field-effect emission current from a cone-shaped tungsten point with different apex angles (complete) of the cone: shaded region - calculation; points - experimental data.
KEY: (1) j_{crit}, $\times 10^{12}$ A/m^2; (2) α, deg.

The more rapid growth in temperature due to the variability of electrical resistance can be qualitatively explained to some degree by the sharp transition from comparatively slow current rise to its surge during breakdown, observed on oscillograms.

However, there is no quantitative agreement between the calculated curve of current rise and the corresponding experimental characteristic. Moreover, in certain cases a slowing in the growth of current is actually detected before its surge at the moment of breakdown [192, 193]. The reason for this is apparently the effect of the space charge of electrons, since the slowing of the growth is observed most clearly when the cathode has a reduced work function - i.e., when the intensity on the cathode is low and the effect of the space charge is correspondingly greater. Therefore the hypothesis of Sokol'skaya and Fursey [193] that the process during breakdown in the given geometry of electrodes has much in common with processes during the "electrical explosion" of thin wires appears attractive. The change caused by electrostatic forces in the shape of the emitting portion of the cathode with melting of the apex of the point or at a temperature close to melting temperature should be influential, at least in processes leading to a surge in current. Significant magnitudes of electrostatic forces (10 N/mm^2) with such small dimensions of the emitter can cause a noticeable change in the geometry of the latter within 10^{-8}-10^{-7} s.

Detailed study of the prebreakdown phenomena in an electron projector made it possible also to define more precisely the properties and nature of the bright ring appearing on the screen at a current which is close to the breakdown value. Oscillographing of the ring current confirmed even more convincingly the thermionic origin of this current [193]. It was shown that the source of the ring current is the side portion of the point apex. At this place the configuration of the electrical field is closer to the field of a cylinder than that of a sphere. Therefore instead of a proportional increase in the electron image along all the axes, characteristic for the apex of the point, the increase is retained only in the azimuthal direction, while in the radial direction the gain drops sharply. Hence we have the image in the form of a bright but thin ring [194].

Phenomena leading to breakdown with point cathodes of other materials were also investigated. The picture of the phenomena turned out to be close to that obtained with points of tungsten, but the critical values of current density differed for different materials. Thus, they are less for molybdenum and tantalum emitters than for tungsten, comprising $5 \cdot 10^{10}$-$5 \cdot 10^{11}$ A/m^2 [195].

The experiments carried out by Dyke et al. also showed that processes on the anode and, in particular, the emission of positive ions do not affect the appearance of breakdown. Primarily, with strongly pointed cathodes, when breakdown voltage was small, and in the case of cathodes with a large radius of curvature, when breakdown voltage was an order of magnitude higher and reached 60 kV (see Table 41), no essential differences were detected in the prebreakdown phenomena. At the same time, with small voltages even the lightest (hydrogen) ion was not able to move from the anode to the cathode during the period of voltage application (1 μs). To obtain a more conclusive picture, an additional experiment was conducted; two emitting peaks, placed close together and virtually identical, served as the cathode. The current of one of these exceeded the current of the other by approximately two times, and therefore breakdown proceeded because of heating by the current flowing on this point. Despite the fact that there were many positive ions in the gap and the conditions of their bombardment of both points were virtually identical (especially for ions originating far from the cathode), the second point remained undamaged and retained its [original] volt-ampere characteristic.

The presence of adsorbed gases and various contaminants on the emitting point facilitates the appearance of breakdown and destruction of the point. The reason for this is the reduction of the work function of electrons in certain places and a change in the shape of the point due to the growth of contaminant

crystallites [196]. Besides this, desorption of the gas and its ionization by electrons lead to the formation of positive ions close to the point; these ions bombard the cathode and compensate the space charge of electrons, which favors the growth of field-effect emission. In general, owing to the above-listed phenomena the presence of contaminants and adsorbed gases and vapors (although it does not change the general picture of the breakdown process) will lead to strong instability of emission from the point and more rapid destruction of the emitter [197]. The effect of contaminants on field-effect emission was considered in Chapter 2.

To reduce the influence of imperfect vacuum conditions, studies were made of the work of point-cathodes in conditions of constant heating of the points up to 800-1000°C, when the equilibrium quantity of contaminants and adsorbed gases on the emitter surface is substantially less. The results of measurements of critical values of current density for conical tungsten points according to the data from Yelinson et al. [198] are given in Table 42; the pulse voltage duration was 1-3 μs.

Table 42. Critical values of current density for tungsten points [197] (averaged values).

(1) Полный угол конуса, град	$j, \times 10^{11}$ а/м² (2)	Полный угол конуса, град (1)	$j, \times 10^{11}$ а/м² (2)
10	1,5	40	5,0
20	2,0	50	11,5
30	2,8		

KEY: (1) Total cone apex angle, deg; (2) j, $\times 10^{11}$ A/m^2.

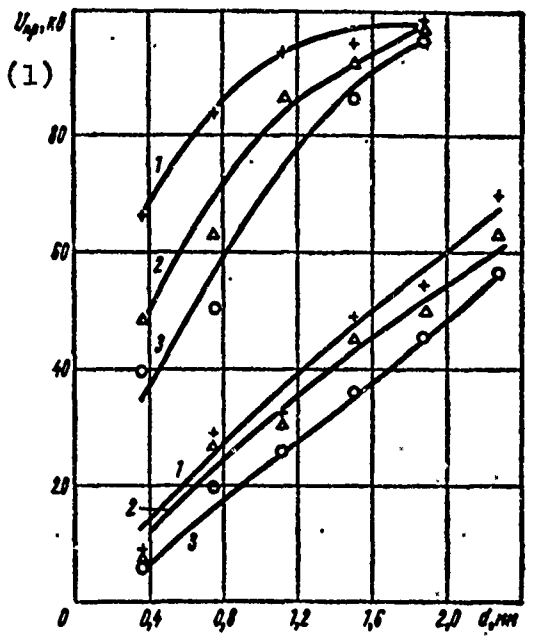

Fig. 54. Breakdown voltage for nickel needle/plane electrodes. Upper group of curves - needle-anode; lower group - needle-cathode. 1 - maximum, 2 - middle, 3 - minimum values.

KEY: (1) U_{br}, kV.

Polarity reversal of electrodes in structures similar to the electron projector - i.e., transition to an electrode geometry where the anode is a point and the cathode is flat or spherical - sharply increases breakdown voltage. Figure 54 shows breakdown voltages obtained by Hashimoto [199] for needle-plane nickel electrodes. It is clear that U_{br} is approximately three times higher when the needle is the anode. Unfortunately, the radius of curvature of the peak of the point is unknown. Similar results were obtained by Rozanova [200] for tungsten electrodes. With such an electrode configuration and with gaps of 0.13-0.52 mm, in Rozanova's experiments the difference between the breakdown voltages during reversal of electrode polarity increased with an increase in field nonuniformity. Up to values of 1000 kV/mm the intensity on the anode had no effect on breakdown voltage, while breakdown set in at a virtually constant magnitude of cathode intensity of 1000 kV/mm, independently of polarity and of electrode curvature, although E_c grows somewhat with an increase in nonuniformity of the field.

7. DISCHARGE IN A VACUUM OVER THE SURFACE OF SOLID INSULATION

With a gradual rise in constant voltage on electrodes between which an insulator is pressed - i.e., in the case when the electrical field is directed along the surface of the insulator - a number of phenomena occur which are intensified as the voltage rises. First of all dark currents appear, slowly varying in time. These currents can differ by several orders of magnitude with different insulator specimens, even if they are made from the same material. An especially great difference in values of dark current is observed when the vacuum conditions are not sufficiently clean; however, the general tendency is a rapid growth in current with an increase in voltage, similar to the growth in the field-effect emission current.

The magnitude of the dark current (10^{-11}-10^{-7} A) can sometimes change suddenly by one or two orders; as a rule this change tends toward the smaller side, and occurs with prolonged application of voltage [174]. Besides these currents, short-term individual surges of current occur, first very small (10^{-6}-10^{-5} A), but growing up to 10^{-3} A and more with the rise in voltage. Like the dark currents, the surges of current are not accompanied by visible effects.

The following stage in the breakdown of electric strength is jumping of a spark along the insulator surface. Finally, uninterrupted surface discharges arise; they convert into an arc if the power of the voltage source permits. Oscillographing showed that arc discharge with a voltage drop of less than 100 V on the arc is observed with currents no lower than 0.7-1.6 A. If the electric circuit cannot provide such a current, the discharge is unstable and the voltage drop on it comprises several kV. Noticeable liberation of gases occurs during discharges and during the arc, especially with insulators of organic materials.

Thus, the picture of the phenomena in the case when there is a solid insulator between the electrodes is qualitatively very similar to that observed in a purely vacuum interelectrode gap. The basic difference is the significantly smaller voltage or intensity at which one or another breakdown of electrical strength occurs. As an example we can introduce the figures obtained for the case when a polished Plexiglas cylinder 20 mm in diameter and 22 mm high was installed between flat electrodes [157]. During the first slow rise of voltage current jumps of 2 μA appeared at 30-40 kV and the first irregular sparks along the surface appeared at 70 kV; however, they were low in power and rapidly terminated. A further rise in voltage to 140-150 kV caused more or less regular surges of current 200 μA in magnitude; when the voltage was reduced to 125 kV, there was no disruption of vacuum insulation except for a dark current of very low magnitude. After a certain delay - conditioning - the voltage on the electrode could be raised to 180 kV, when continuous discharges with an average current value of 20-40 mA appeared over the surface of the insulator. This voltage was fixed as the breakdown voltage. In these experiments a resistance R_d = = 200 kohm was placed in the discharge circuit - i.e., the current of the post-breakdown discharge was strongly limited.

From the given figures it is clear that the first surges of current and the first sparkovers along the insulator set in, respectively, at 20 and 40% of the magnitude of breakdown voltage which was finally obtained. From these same data it is clear that there is a substantial improvement in the vacuum insulation after conditioning by prolonged application of voltage. The findings of Gleichauf [174, 201] indicate that a high steady-state value of surface breakdown voltage is achieved after 100-200 breakdowns if R_d = 10 Mohm. When R_d is several times smaller than the given value the steady state is arrived at more rapidly and the achieved value of U_{br} is higher, although it is

insignificant. The value of U_{br} is favorably affected by preliminary holding of the insulator under vacuum for a day or more. Just as in the case of purely vacuum insulation after a prolonged break in voltage supply, the first breakdowns set in at a smaller voltage than at the end of the preceding conditioning period, but after several breakdowns U_{br} grows rapidly to a still greater value. As a supplement to the above, Table 43 gives the figures which characterize the increase in surface breakdown voltage as the result of conditioning with breakdowns.

Table 43. Effect of conditioning with breakdowns on surface breakdown voltage [5].

Материал изолятора (1)	Высота образца изолятора (зазор между электродами), мм (2)	$U_{пр}$, после тренировки, кВ (3)	Кратность повышения в результате тренировки (4)
(5) Винипласт	2	[illegible]	3
	4	[illegible]	3
(6) Плексиглас	4	50	1,5—2
	7	63	1,5—2
(7) Фарфор глазурованный	10	85	4
(8) Стекло пирекс	5	20	1,5—2

KEY: (1) Insulator material; (2) Height of insulator specimen (gap between electrodes), mm; (3) U_{br}, after conditioning, kV; (4) Factor of increase as a result of conditioning; (5) Polychlorovinyl sheets; (6) Plexiglas; (7) Glazed porcelain; (8) Pyrex glass.

Experiments which Gleichauf set up with various replacement of electrodes or insulator under vacuum showed that the increase in breakdown voltage in the process of conditioning is connected with "improvement" of both the electrodes and the insulator, with the effect of conditioning being approximately equal for the electrodes and the insulator. Here the breakdown voltage did not depend on the electrode material - copper, aluminum, or steel. Systematic measurements of the currents before breakdown in these experiments did not reveal any connection between the magnitude of the currents and the appearance of breakdown.

The surface-breakdown voltage is very sensitive to the configuration and surface quality of the insulator close to the cathode and to the configuration of the cathode at this point. For example, recessing of the insulator into the cathode (which reduces the intensity at the point of insulator-cathode contact) leads to an increase in breakdown voltage of almost 100% [201]. To illustrate the importance of the type of connection of insulator with the cathode, Fig. 55 depicts the model of a base insulator manufactured from pyrex glass. In this case when the electrode with the groove under the insulator was the cathode the breakdown voltage reached 90 kV; with opposite polarity it totaled 28 kV. If both electrodes were manufactured without grooves - i.e., like the upper electrode on Fig. 55 - with the same interelectrode gap U_{br} = 25 kV [202]. Good results are also obtained by rounding the edges of the insulator at the point where it adjoins the cathode. The quality of the lateral surface of the insulator close to the cathode also influences U_{br}. Roughening (with a sand blast, coarse abrasive, etc.) of a small segment of the side surface of the insulator adjacent to the cathode [201] gives a positive effect. On the other hand, crimping of the insulator side surface outside the region adjacent to the cathode does not yield any increase in U_{br} [5], in contradiction to the situation observed when the insulator is in a gaseous medium.

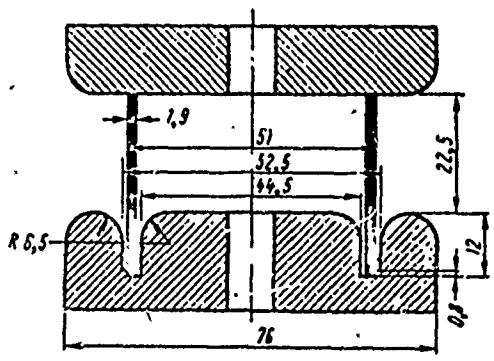

Fig. 55. Insulator with different methods of connecting its faces to the electrodes.

Table 44. Surface breakdown voltage for insulators 22 mm high made of different material.

Material	U_{br}, kV	Material	U_{br}, kV
Polychlorovinyl sheets	150-200	Ebonite	120-140
Plexiglas	170-180	Molybdenum glass	100-130
Unglazed porcelain....	170	Quartz	82
Laminated insulation..	160	Chamotte.....	75
Glass 23	140	Fibra	75
		Textolite	50-70

Table 45. Surface breakdown voltage for cylindrical insulators made from materials with different physical properties.

(1) Материал	$\delta \cdot 10^3$, кг/м³	ρ, ом·м	$\varepsilon/\varepsilon_0$	(2) Размеры изолятора, мм: (3) диаметр	(4) высота	(5) Качество поверхности	(6) $U_{пр}$, кв
(7) Плавленый кварц	2,2	10^{12}—10^{14}	3,7	12	22,5	(8) Оплавленная	65
(9) Стекло пирекс . . .	2,23	10^{11}	4,8	12,5	22,5	То же	45
(11) Стекло пирекс, покрытое силиконовым маслом	2,23	10^{11}	4,8	12,5	22,5	(10) »	56—73
(12) Натриевое стекло . .	2,5	10^{11}	5	12,5	22,5	»	40
(13) Проводящее стекло	2,2	10^{6}	4	13	22	(15) »	6—17
(14) Стеатит	2,6	10^{12}	5,5	13	22,5	Совершенно гладкая	50
(16) Рутил	3,8	10^{12}	80	15	22,5	То же	40
(17) Титанат бария . . .	6,05	$2 \cdot 10^{3}$	3000	15,5	15	(10) »	8
(18) Двуокись циркония	5,73	10^{12}	60	11,1	22,5	»	40
(19) Полистирол	1,05	10^{13}	2,5	12,5	22,5	Гладкая	75
(21) Тефлон	2,22	10^{16}	—	14	22,5	(20) »	50
(22) Сера	2,07	10^{15}	4	45	23	Грубая (23)	45

KEY: (1) Material; (2) Dimensions of insulator, mm; (3) diameter; (4) height; (5) Surface quality; (6) U_{br}, kV; (7) Fused quartz; (8) Fire-polished; (9) Pyrex glass; (10) The same; (11) Pyrex glass coated with silicone oil; (12) Sodium glass; (13) Conducting glass, (14) Steatite; (15) Completely smooth; (16) Rutile; (17) Barium titanate; (18) Zirconium dioxide; (19) Polystyrene; (20) Smooth; (21) Teflon; (22) Sulfur; (23) Rough.

[кг/м^3 = kV/m^3; ом·м = ohm·m]

Table 44 gives values of surface breakdown voltage obtained by Borovik and Batrakov [157] for insulators in the form of well finished cylinders pressed between flat electrodes creating a uniform field along the surface of the insulator; diameter of the insulators is 20 mm, their height is 22 mm, voltage is constant, R_d = 200 kohm, vacuum 10^{-5}-10^{-7} mm Hg.

To clarify the question of precisely which physical properties of the insulator material govern the breakdown voltage, Gleichauf [201] tested materials with strongly differing values of electrical resistivity ρ, permittivity ε, specific density δ, and vapor tension p. The results of these tests are given in Table 45. Samples of insulators in the form of cylinders were wedged tightly against the surface of flat electrodes. The voltage was constant; R_d = 10 Mohm.

From the data in Table 45 it is clear that the smallest U_{br} is obtained for insulators with low resistivity. As an additional check, tests were made of insulators made of pyrex glass and of conducting glass coated with a film of silicone oil, which reduced surface leakages. For the conducting glass this led to an increase in U_{br} by 50%; as is clear from the table, for pyrex glass the increase was no more than 25%. No influence of the remaining physical properties on electrical conductivity was found, although these properties were varied extremely widely. Thus, the vapor pressure of sulfur at room temperature comprises about 10^{-7} mm Hg, i.e., several orders of magnitude greater than that for pyrex glass; however, the breakdown voltages are identical for the two materials. There is also no strong effect rendered by permittivity (see the data for rutile), although with a growth in ε there can be strong increase in the intensity on the cathode at points of loose fitting of the insulator. It is true that U_{br} is very low for barium titanate; however, if ε had any effect, the reduction in U_{br} would be more significant.

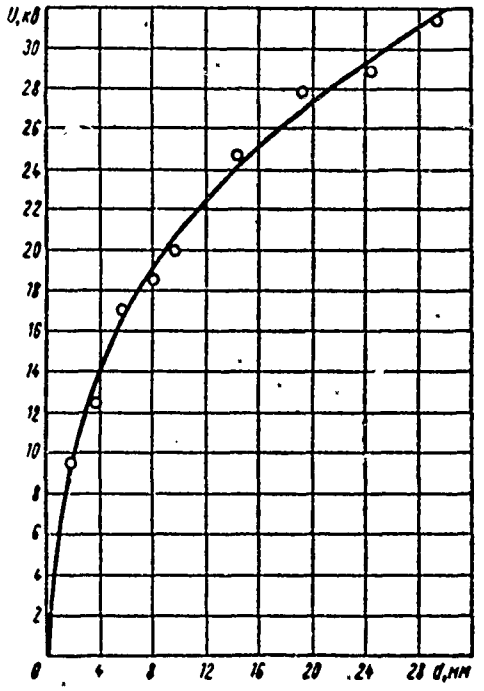

Fig. 56. Dependence of breakdown voltage on the length of a pyrex insulator pressed between flat electrodes.

[кВ = kV]

The coefficient of secondary electron emission usually grows for insulators with an increase in their density. It is precisely this fact which explains the effort to establish the dependence of breakdown voltage on the density of the insulator material. However, it is clear from the table that density does not play a determining role. Thus, a connection was found for breakdown voltage only with the resistivity, while from the experiments with an oil-film coating intended to reduce the surface resistance it is clear that it is precisely the latter which plays the essential role. At the same time it should be noted that the largest U_{br} was obtained, as follows from Tables 44 and 45, for materials combining high values of ρ with small magnitudes of δ and ε.

Just as in the case of purely vacuum insulation, the breakdown voltage grows more slowly than the length of the insulator. This is clearly evident from the data presented on Fig. 56 and in Table 43. A reduction in breakdown intensity with an increase

in insulator length is observed even with very short insulators. Thus, the findings of Brish et al. [13] indicate that during breakdown along the face surface of a mica lining compressed between flat plate electrodes with sharp edges, after repeated breakdowns in pure vacuum conditions the breakdown voltage corresponds to the empirical formula

$$U_{пр}(кв) = (0{,}25 - 0{,}027)\,b \quad \text{when} \quad b = 30 - 100\ мк, \qquad (26)$$

[пр = br; кв = kV; мк = μm]

where b is the thickness of the mica lining (the edge of the mica and the edges of the electrodes coincide). The probability of breakdown or the scatter of the breakdown voltage with repeated breakdowns and b = 60 μm is characterized by the data in Table 46.

Table 46. Probability of breakdown over the face surface of a mica lining 60 μm thick between flat electrodes.

$U_{пр}$, кв (1)	Вероятность (2)	$U_{пр}$, кв (1)	Вероятность (2)
1,5	0,005	2,1	0,19
1,6	0,02	2,2	0,14
1,7	0,05	2,3	0,14
1,8	0,08	2,4	0,03
1,9	0,15	2,5	0,02
2,0	0,17		

KEY: (1) U_{br}, kV; (2) Probability.

The reduction in breakdown intensity with an increase in insulator length is apparently connected to some degree with distortion of the distribution of voltage along the insulator. Therefore high-voltage insulators are made up of several sections, with coercive [positive ?] distribution of the voltage between them. An example of the structure of a partition insulator (high-voltage vacuum input) is shown on Fig. 57. The insulator is comprised of twelve identical rings of pyrex glass with an outer diameter of 200 mm, connected through aluminum rings.

The latter project somewhat beyond the edge of the glass rings. The height of each aluminum ring is 3 mm and that of the glass rings is 2.5 mm. Vinyl acetate was used to ensure vacuum-tightness. A polyurethane cylinder is inserted inside the insulator from the side turned toward the compressed gas (SF_6, 15 atm.abs.). The conductivity of this cylinder is selected so that at the working voltage a current with a strength of 100 μA flows along the cylinder, ensuring uniform distribution of voltage between the sections of the insulator [203].

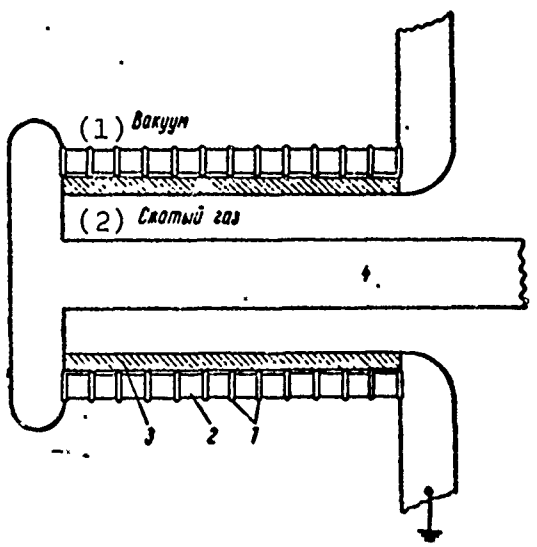

Fig. 57. Sectional high-voltage vacuum input: 1 - metallic rings; 2 - ring of pyrex glass; 3 - compound distributing resistor of polyurethane; 4 - high-voltage input.

KEY: (1) Vacuum; (2) Compressed gas.

However, despite the sectional construction, the voltage withstood by such an insulator is frequently less than the total breakdown voltages of the individual sections [5]. It is possible that this occurs because of insufficiently uniform distribution of voltage between the sections with partial disruption of the vacuum insulation - for example, surges of current and partial discharges along the insulator.

One reason for the nonuniform distortion of distribution of the field along the insulator is found in the peculiarities of the flowing of dark electron current along the insulator or

close to its surface. Because of scattering on residual gases or for other reasons a part of the electrons may impinge on the insulator surface and knock out secondary electrons. When the coefficient of secondary electron emission is greater than unity this segment of the insulator takes on an initially small positive surface charge, which creates a field attracting other electrons. The arrival of the following party of electrons in its turn causes further growth in the positive charge on the surface insulator, for the same reason. However, the growth of the charge is limited, since the appearance of a strong surface charge leads to a situation in which electrons impinge on the insulator without having succeeded in picking up sufficient energy in the field of the electrodes. In this case the coefficient of secondary electron emission is less and the growth of the charge is terminated - i.e., some sort of dynamic equilibrium is established. The current of electrons close to the insulator represents, as it were, a chain of individual electron flows arising and terminating on the surface of the insulator. In this case the maximum energy of the electrons of such a flow is determined not by the total applied voltage, but by the length of one link in the chain described above. An experimental check of the described scheme of electron motion along the insulator - measurement of the electron energies - was undertaken by the authors according to the setup proposed by Boersch et al. [204]; it showed that the maximum energy of the electrons was on the order of 50 eV, although the total applied voltage comprised about 10 kV. The total current of electrons along the insulator in this case was reminiscent of the passage of electrons in a multistage electron multiplier with, however, the essential difference that the total gain factor was close to unity. The magnitude of the surface charge was approximately proportional to the average field intensity between the electrodes and depended on the angle between the direction of the field and the lateral surface of the insulator.

For glass when the indicated angle equals zero and when $E = 0.5$ kV/mm the surface density $q_s = 4 \cdot 10^{-5}$ k/m^2. When the angle equals 30° (insulator is extended toward the anode) $q_s = 0$; with a still larger angle $q_s < 0$. The appearance of a surface charge leading to distortion of the distribution of voltage along the insulator definitely has a negative influence on insulation strength.

Evidently the setup examined above is not the only possibility for the appearance of a charge on the surface of the insulator. For example, Gleichauf [174], while photographing the X-radiation caused by dark electron currents flowing along the insulator, observed a deflection (removal) of the electron current from the insulator surface. This can be explained only by the fact that the surface of the insulator was charged negatively in his experiments, although it was parallel to the field of the electrodes.

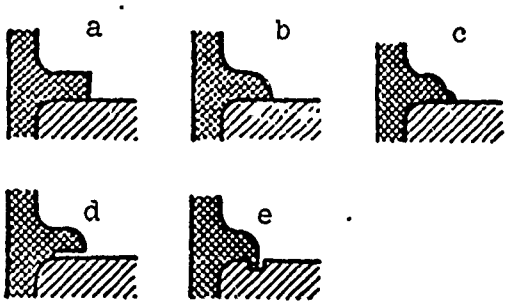

Fig. 58. Effect of the way the insulator is connected with the cathode on the voltage at which a dark electron current U_I and breakdown voltage U_{br} appear:

Graph.....	a	b	c	d	e
U_I, kV	22	28	35	40	40
U_{br}, kV	35	40	48	70	65

Using the example of different constructions of the insulation for a single electrostatic lens in an electron microscope, Holse [205] demonstrated the great influence of the type of cathode-insulator connection on the quality of the insulation. The lens consisted of three electrodes, coaxial with an opening in the center of disks made from stainless steel with an outer diameter of 60 mm. A Plexiglas, lucite, or polystyrene insulator was used to connect the disks along the periphery. The central disk served as the cathode and the two end disks, connected together, were anodes. The distance between the disks at the insulator location (i.e., of the length of the insulator) was 10.4 mm. Figure 58 shows the designs of the points of connection of the insulator with the cathode, while the values of breakdown voltage and the voltage of appearance of luminance on a special luminescent screen, where the luminescence appeared because of the development of an electron dark current at the cathode-insulator connection, are given in the notes below the figure. Holse arrived at the conclusion that the quality of the insulation is improved in those structures where the insulator-cathode connection has, as it were, a trap for electrons - a trap which serves to prevent passage of electrons along the surface of the insulator parallel to E.

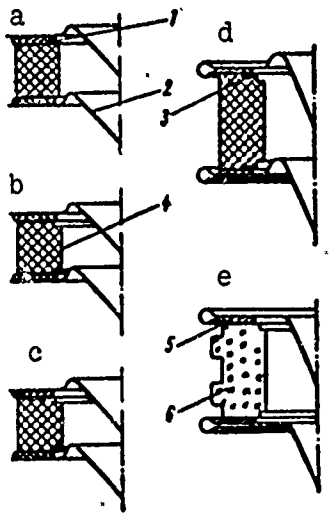

Fig. 59. Examples of various structures of single gaps in an accelerating tube: 1 - Pb wire; 2 - electrode (anode above); 3 - layer of metallization; 4 - porcelain insulator; 5 - layer of BF 4 glue; 6 - glass insulator. Remaining data given in Table 47.

To conclude this section, on Fig. 59 we present examples taken from Tsygikalo [5] showing structures of insulating sections of accelerator tubes, while Table 47 presents additional information and the values of the surface breakdown voltages. The effort to ensure good contact between the electrodes and the insulator (metallization of the insulator ends on Fig. 59) and to remove the electrical field from the point of this connection, especially at the cathode end, by covering it with the insulator projection (see Fig. 59, b-e) or by using electrodes of appropriate form are particularly noticeable.

Table 47. Insulating characteristics of individual sections of accelerating tubes.

(1) Эскиз на рис. 59	(2) Материал	(3) Высота изолятора, мм	$U_{пр}$, кв
а	Фарфор (4)	25	30
б	»	25	38—60
в	»	25	70
г	»	25	75*
д	»	50	130*
е	Стекло (5)	50	100—120
∂	»	50	100—110
ж	Эпоксидная смола с наполнителем (6)	25	80—100

*Breakdown not in vacuum, but over the outer surface of the insulator.

KEY: (1) Drawing on Fig. 59; (2) Material; (3) Height of insulator, mm; (4) Porcelain; (5) Glass; (6) Epoxy resin with a filler.

[пр = br; кв = kV; а = a; б = b; в = c; д = d; ∂ = e]

8. COATING ELECTRODES WITH INSULATING AND SEMICONDUCTING FILMS

The possibility of improving vacuum electrical insulation by applying thin insulating films on the electrode surfaces was studied in work [206]. Measurements were carried out with flat electrodes 150 mm in diameter with the peripheral portion

done per Rogovskiy - i.e., the edges of the electrode were rounded so that the surface intensity at this point did not exceed the intensity in the central portion of the electrodes. A vacuum of 10^{-7}-10^{-6} mm Hg was created with mercury and sorption pumps in a metallic container with seals of separable indium joints. An electrostatic generator with a short-circuit current of 35 μA served as the source of constant high-voltage, up to 400 kV.

The following were used as materials for the insulating films: magnesium fluoride, three types of epoxies, silica, Mylar strip, Formvar, titanium dioxide, and oxides of cerium, iron, and tin. The first three types of materials were most completely studied, since in general they gave the best results. Application of the oxides of cerium, iron and tin lowered the quality of electrical insulation as compared with uncoated electrodes. The electrode base material - the substrate under the insulating films - was carefully polished aluminum. In some experiments (to determine the effect of the substrate properties on total electrical insulation) the surface of the substrate was artifically roughened or a different material - stainless steel - was used.

The basic measurements were carried out with a constant interelectrode gap equalling 5 mm. The voltage withstood without breakdowns for 5 minutes and also the magnitude of dark currents at this voltage were determined. To achieve the best results the voltage on the electrode was raised in stages of 10 kV every 5 minutes; the observed breakdowns had a conditioning effect. However, even at such low power as that of the high-voltage generator used in the work, the insulating film was finally damaged as the result of a greater or lesser quantity of post-breakdown discharges; this damage was the more intensive (the voltage withstood was reduced the more strongly) the thicker the film. When films were applied only to

the cathode the destruction on the anode during discharges was less when the cathode film was thicker; the reverse picture was observed on the cathode. With a 130 μm film no traces of the breakdowns could be detected on the anode even under the microscope at a magnification of 90, while on the cathode the region of damage and even total removal of the film reached a diameter of 0.8 mm.

The results of measurements from [206] are given in Table 48, from which it is clear that the strongest influence of the film coating on the cathode is rendered on the dark currents: they are reduced to 10^{-7} and even to 10^{-9} A, i.e., by 2-4 orders as compared with currents with carefully polished uncoated aluminum electrodes. The maximum increase in the voltage which can be withstood for a long period comprises about 70% and is observed when the aluminum cathode is coated with an epoxy film; however, the strength of such a film under discharges is not high. Good results were obtained when the cathode was coated with silica. The dependence of supportable voltage on interelectrode gap for silica differs from the same characteristic for films of other materials; in the latter case they show virtually no difference from the characteristics for uncoated electrodes. For silica films the supportable [breakdown] voltage varies only within the limits 240 to 290 kV with an increase in the gap from 3 to 8 mm. Application of a film to the anode or to both electrodes at once has a negative influence: the supportable voltage is strongly reduced, although with the films on both electrodes the dark current is very small (approximately 10^{-9} A).

Table 48. Effect of coating the electrode with insulating films on dark currents and on the voltage supported without breakdowns for 5 minutes.

	Материал электродов (1)		(2) Зазор, мм	(3) Максимально выдерживаемое напряжение $U_{макс}$, кв	(4) Число разрядов тренировки		(5) Темновой ток, а
	катода (6)	анода (7)			(8) до $U_{макс}$	(9) до порчи электродов	
(10)	Полированный алюминий	Полированный алюминий (10)	6,3	220	25	320	10^{-5}
	0,2 мк MgF_2 на Al	То же (11)	6,3	250	50	280	10^{-7}—10^{-6}
	10 мк MgF_2 на Al	»	6,3	250	50	280	10^{-7}
(12)	2,5 мк MgF_2 на нержавеющей стали	Нержавеющая сталь (13)	5	190	100	600	10^{-9}
	2,5 мк MgF_2 на Al	Полированный алюминий (10)	5	230	70	200	10^{-10}—10^{-9}
(10)	Полированный алюминий	2,5 мк MgF_2 на Al	5	120	5	25	10^{-9}
	2,5 мк MgF_2 на Al	2,5 мк MgF_2 на Al	5	180	15	200	10^{-9}
(14)	130 мк эпоксидной пленки на травленой поверхности Al	Полированный алюминий (10)	5	330	90	110	10^{-9}
(15)	130 мк эпоксидной пленки на полированном Al	То же (11)	5	300	0	17	10^{-9}
(16)	25 мк эпоксидной пленки на полированном Al	»	5	330	0	12	10^{-8}—10^{-7}
	3 мк SiO на Al	»	5	260	35	270	10^{-9}
(17)	2,5 мк полоски милар на Al	»	5	240	90	125	10^{-9}—10^{-7}
(18)	2,5 мк формвара на Al	»	5	240	330	460	10^{-8}

KEY: (1) Electrode material; (2) Gap, mm; (3) Maximum voltage withstood U_{max}, kV; (4) Number of conditioning discharges; (5) Dark current, A; (6) cathode; (7) anode; (8) to U_{max}; (9) to electrode damage; (10) Polished aluminum; (11) The same; (12) 2.5 mm MgF_2 on stainless steel; (13) Stainless steel; (14) 130 μm epoxy film on etched Al surface; (15) 130 μm epoxy film on polished Al; (16) 25 μm epoxy film on polished Al; (17) 2.5 μm Mylar strip on Al; (18) 2.5 μm Formvar on Al.

[мк = μm; на = on]

As a result of these studies the author of work [206] formulated the following conditions which must be observed for the application of an insulating film on the cathode to improve the quality of electrical vacuum insulation. The material of the film must possess high resistivity (10^{-11} ohm·m), low permittivity ($\varepsilon/\varepsilon_0$ = 1.5-4) and substantial electrical insulating strength (no less than 100 kV/mm). The thickness of the film should be 10-25 μm; the film must be chemically stable and mechanically strong and must possess high resistance to wear and good adhesion to the substrate; before application of the film, the substrate should be carefully polished and all contaminants removed. Gas inclusions in the body of the film are undesirable and at least their size should be significantly smaller than the film thickness. It should be borne in mind that these recommendations, as noted in work [206], cannot be considered as final owing to the inadequate number of experiments carried out. This is particularly true of the requirements for the magnitude of electrical resistance and permittivity of the film material. It is not clear whether the nature of film conductivity (ion or electron conductivity) plays a role. The remaining requirements amount to a significant degree to common sense rather than to direct consequences of the experimental results. At the same time, the improvement obtained in the work under discussion by the application of thin insulating films to the cathode was very substantial and this method may have practical significance in those cases when it is desirable to reduce dark currents or when relatively high values of intensity of static fields on large electrode surfaces are required. A profit is possible only if the energy liberated on the electrodes during breakdown is insignificant; otherwise the film is destroyed very rapidly and the level of vacuum insulation drops below that for uncoated electrodes.

Unquestionably, report [207] is of great interest; it indicates that coating the cathode with a layer of lime-sodium glass made it possible to obtain a voltage of 500 kV with a 10 mm gap on flat electrodes of large area at a temperature of 100°C, when this glass displays ion conductivity ($\rho = 10^2$-10^4 ohm·m). In these experiments the anode was made of stainless steel. Similar electrodes may find application in nuclear physics - for electrostatic high-energy charged-particle analyzers.

CHAPTER 5

VACUUM INSULATION WITH HIGH-FREQUENCY VOLTAGE

1. GENERAL PROPERTIES

The electrical breakdown of a vacuum under high-frequency voltage is distinguished by a number of features from cases when constant or pulse voltage is applied to the electrodes. These differences arise both from peculiarities of the motion of charged particles in a high-frequency electrical field and also from the specific dependence of the operation of high-frequency (hf) oscillators (their resonant loops) on changes in the load parameters – in the given case the appearance of conductivity (appearance of breakdown) in the vacuum gap.

The equation of motion for a charged particle in a uniform hf field has a clear graphic interpretation. If a particle with zero initial velocity leaves an electrode in the ψ phase of sinusoidal hf voltage, its distance from the electrode at any moment of time is directly proportional to the segment between the tangent to the sinusoid at angle ψ and the sinusoid itself (the particle velocity is proportional to the difference between the ordinates of the cosinusoids at ψ and at the given moment) (Fig. 60). If the initial velocity is different from zero, the final velocity is the sum of the initial cosinusoid and that determined along the ordinates, and to determine the distance it

is necessary to draw, instead of the tangent, a straight line intersecting the sinusoid in the same phase ψ at an angle which is proportional to the initial velocity. Clearly, depending on the phase at escape the particle can either return to the electrode or accomplish oscillation with one or another velocity with forward motion. With motion of this type the particle may reach the opposite electrode in any phase of the hf voltage – i.e., at any polarity of this electrode. The presence of secondary emission also allows the existence of those processes of "chain" exchange by charged particles between electrodes which cannot occur with constant application of voltage. One of such processes leading to breakdown of vacuum insulation – secondary electron resonant discharge – is examined below.

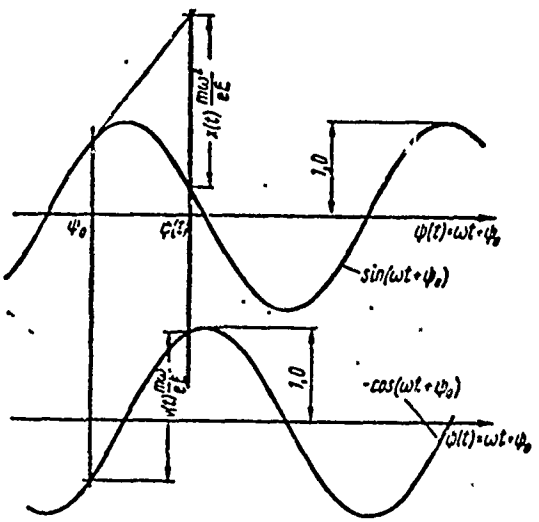

Fig. 60. Graphic determination of velocity v(t) and distance traveled x(t) for charged particles in an hf field. $E(t) = E \sin \omega t$; ψ_0 – initial motion of a charged particle with zero velocity from the electrode.

In certain cases the maximum energy which can be acquired by a charged particle in an hf field between electrodes is significantly less than the energy corresponding to the voltage between them. This will hold true when the time required for the particle to travel between the electrodes is comparable to or greater than the duration of the hf-voltage half-period. In the latter case the energy which can be acquired depends only on the ratio of mass to charge for the particle and on the intensity and frequency of

change of the electrical field, while the total applied voltage does not play a role. Table 49 presents values of the maximum energy which can be acquired by a particle with zero initial velocity in a uniform field; it also gives the magnitudes of the maximum path in the period of hf voltage at frequency f.

Table 49. Path of a proton and an electron and the energy acquired by them in a uniform hf field (within one period at zero initial velocity).

E, кв/мм	f, Мгц	Максимальный пробег, м (1)		Максимальная энергия, кэв (2)	
		электрона (3)	протона (4)	электрона (3)	протона (4)
0,01	12	1,9	10^{-3}	6,25	$3,3 \cdot 10^{-3}$
5	12	970	0,53	$1,57 \cdot 10^{6}$	830
20	200	14	$7,6 \cdot 10^{-3}$	$9 \cdot 10^{5}$	49
20	3000	0,06	$3 \cdot 10^{-5}$	400	0,22

KEY: (1) Maximum length of path, m; (2) Maximum energy, keV; (3) electrons; (4) protons.

Designations: кв/мм = kV/mm; Мгц = MHz.

As is evident from the values in the table, when the frequency is fairly high the energy which can be acquired by a particle in an hf field is not great. From the point of view of the electrical strength of vacuum insulation, this means weakening of those processes which break down the insulation and which are connected with bombardment of the electrodes by charged particles. Therefore not surprising that the first experiments showed vacuum insulation to have high strength under hf voltage. Thus, Halpern et al. [208], using a 50-mm gap and unconditioned copper electrodes at a frequency of 2800 MHz, obtained a voltage of about 1 MV without breakdown of the vacuum insulation. An essential fact, however, is that in this case the voltage was applied in pulses of 2 μs.

With high frequency and large gaps the processes which lead to breakdown and also the postbreakdown arcing cannot be fitted into the duration of a single half-period of the applied voltage.

In this case the conditions for development of breakdown – the formation of plasma in the gap and the consequent conditions for passage of a current between the electrodes – differ from those encountered with constant voltage and even with alternating voltage at low frequency or with a small gap (when the above-mentioned processes can be accomplished in a single half-period). Clearly this explains the difference between the postbreakdown destruction of electrodes at small and large gaps (see below). It is also possible that certain features in the process of spark discharge at hf voltages are explained by the lower inductance of the hf system as compared with direct-current circuits where, as a rule, substantial forces are not taken for the reduction of inductance (characteristic for hf systems).

High-frequency voltage, especially high-amplitude voltage (tens and hundreds of kV), is usually created by means of various resonant systems in which the object itself – the load – is a component part. A typical example is hf charged-particle accelerators, where the actual accelerating system is a cavity resonator on which (thanks to the high Q) a voltage is developed which exceeds by tens and hundreds of times the voltage created by oscillator tubes. Successful operation of such a system requires a precisely determined ratio between the parameters of the hf oscillator itself and those of the connecting elements (feeders) and the parameters of the load (resonator). The appearance of an additional active load in the resonator because of damage to the vacuum insulation not only reduces its Q and leads to a reduction in voltage, but can also lead to interruption of oscillations in the resonator and even (with a large coupling coefficient) to termination of operation of the hf generator. In this case the resonator is, as it were, disconnected from the voltage source. For example, during breakdown in a resonator the discharge is limited to a spark, while the liberation of energy in the discharge does not exceed the energy stored in the resonator itself – i.e., a comparatively small quantity when the size of the resonator

is not particularly great. This leads to rapid extinguishing of the postbreakdown discharge and restoration of the electrical strength of the vacuum gap. Therefore breakdowns in hf resonators have the nature of more or less frequently appearing sparks of comparatively low power, causing a short-term voltage drop. In certain cases, however, the extinction of the postbreakdown discharge does not lead to complete restoration of the voltage on the resonator, due to the appearance of another form of hf discharge (which will be examined in the following section) – secondary electron discharge. The voltage at which such a discharge exists (0.05-10 kV) is substantially lower than the voltage at which arcing appears – i.e., it is lower than the voltage existing on the gap prior to the appearance of arcing. Secondary electron discharge can appear not only in the working gap or in the area where the spark passed, but also in other places (on the feed elements, etc.); at these points with restoration of the voltage certain "resonant" conditions which are necessary for the existence of such a discharge can be created.

When the power stored in the resonator is low and when the so-called destructive arcs (see below) are absent, the consequences of spark discharge (e.g., destruction of electrodes) are less perceptible than is the case with constant voltage. The conditioning action of the sparks is also small and the scatter of the voltage values at which arcing occurs is, correspondingly, very substantial. Besides this the electrodes often have a very large surface, which requires a great number of conditioning sparks. In these conditions (low power of the discharge or a large electrode area) the electrical strength of the vacuum gap depends to a very great degree on the preliminary (mechanical, etc.) treatment. Thus, according to studies by Nikolayev [209], at a frequency of 24 MHz and a voltage amplitude up to 450 kV the breakdown voltage varied by three times from specimen to specimen with identical geometric parameters even after 500 conditioning arcs were applied to electrodes with an area of approximately 1 cm^2. It should be

noted that in these experiments the energy stored in the resonator comprised 3 J, even at maximum voltage; therefore the conditioning action of the sparks was very weak and the traces of the preliminary treatment did not disappear from the surface even after a large number of sparks.

2. SECONDARY ELECTRON RESONANT DISCHARGE

With comparatively small hf voltage between flat electrodes in a vacuum a stable conductivity can arise; there is as yet no firmly established name to designate this phenomenon. In the English literature this form of discharge is called the "multipaction effect"; in the German, "Pendelvervielfachung"; and in the Soviet literature, vtorichnoelektronnyy rezonansnyy razryad [secondary electron resonant discharge], "rezonansnyy vysokochastotnyy razryad" ["resonant high-frequency discharge"], and mul'tipaktsiya [multipaction]. The mechanism of this discharge can be represented as follows. Electrons which, for whatever reason, leave one of the electrodes (for example, No. 1) when this electrode is a cathode can be accelerated by hf voltage and, arriving on the opposite electrode (No. 2), may cause secondary electron emission. If the time of passage of a primary electron is close to the half-period of the hf voltage, the secondary electrons escaping from electrode No. 2 (which at this time becomes the cathode) will also be accelerated and will cause secondary emission from electrode No. 1. When the coefficient of secondary emission is greater than unity such a mutual exchange will lead to the appearance of a noticeable current between the electrodes.

The elementary quantitative theory of this discharge in a uniform field was developed basically by Gill and Von Engel [210] and by Hatch and Williams [211]. Since it is outlined in a number of monographs [212-214] it will not be given here. We will note only that in order to simplify calculations, in this theory the ratio (coefficient K) of the initial velocity of a secondary

electron and the velocity of the primary electron is taken as constant. Although this proposition has no physical basis, the obtained relationships do not depend strongly on K, so that the error introduced is not substantial. The minimum voltage of the discharge corresponds to a certain positive angle of escape of electrons, ψ_{max}, with respect to the sinusoid of the applied voltage. The magnitude of this angle depends on K, and when K = 0 (zero initial velocity), $\psi_{max} = 32.5°$. With an increase in voltage above the minimum the discharge is not terminated, but the exchange of electrons will proceed at smaller angles of escape. The minimum value of the escape angle, ψ_{min}, and consequently the maximum voltage at which a discharge can exist are determined by the following condition: an escaping electron is not returned to the same electrode. Thus, discharge can be observed in a region of hf voltage values which is limited from above and from below. On the other hand, the coefficient of secondary emission can be greater than unity only within a certain range of primary electron energies (0.03-3.0 keV). This also limits the region of discharge existence. Conditions of "resonance" between the time of electron flight and the duration of the hf voltage period can be observed, in addition, with times of electron flight between the electrodes which equal the duration of any odd number of half-periods.

In the general case the amplitude value of the discharge voltage equals

$$U = 4\pi^2 (fd)^2 \frac{m}{e} \left(\pi n \frac{1+K}{1-K} \cos\psi + 2\sin\psi\right)^{-1}, \qquad (27)$$

where n is the number (odd) of half-periods of the applied voltage during which the electron crosses the discharge gap d (n = 1, 3, 5, ...); ψ is the phase (angle) of escape of electrons participating in the discharge ($\psi = \psi_{min} - \psi_{max}$); f is the frequency of the applied voltage.

According to formula (27), the smaller the frequency the lower the voltage at which discharge occurs. However, formula

(27) reflects only the condition that the time of motion of electrons from one electrode to the other is equated to a whole odd number of half-periods of the applied voltage. The other condition – that the energy of impinging electrons must be such that the coefficient of secondary emission will be greater than unity – limits the range of fd values at which discharge can exist. In particular, many authors have found experimentally a value of fd below which discharge is not observed:

$$(fd)_{мин} = 80-90 \text{ MHz}\cdot\text{cm}. \qquad (28)$$

[мин = min]

According to Zaydin and Kushin [215], the quantity $(fd)_{min}$ is influenced by the presence in the gap of electrons from an external source. Thus, when a small thermionic cathode was place in an opening made in one of the electrodes, discharge was triggered (with pulse supply of voltage) even at fd = 60 MHz·cm (the parameters of the research apparatus did not permit obtaining smaller values of fd).

Figures 61 and 62 show domains of existence of secondary electron resonant discharge calculated on the basis of elementary theory.

A check undertaken by several investigators [211, 215, 216] showed coincidence of experimental data with the theoretical relationships to 10-20% for the lower boundary $U = \phi(fd)$ if K is considered equal to 0.25-0.33. Therefore the curves shown on Figs. 61 and 62 can be used to determine the possibility of appearance of secondary electron resonant discharge in specific conditions.

Figure 62 also shows the results of measurements made by Zaydin and Kushin [215] to determine the boundaries of existence of secondary electron discharge: the upper boundary, corresponding

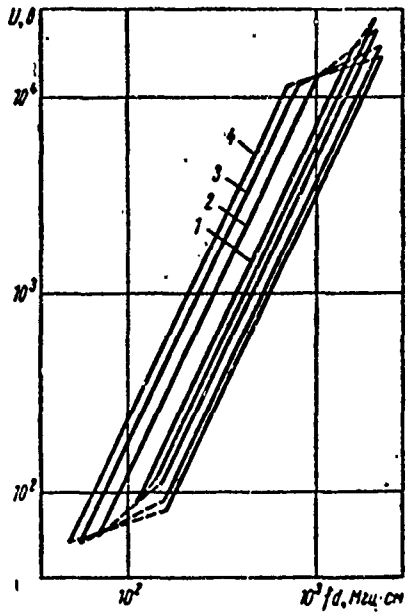

Fig. 61.

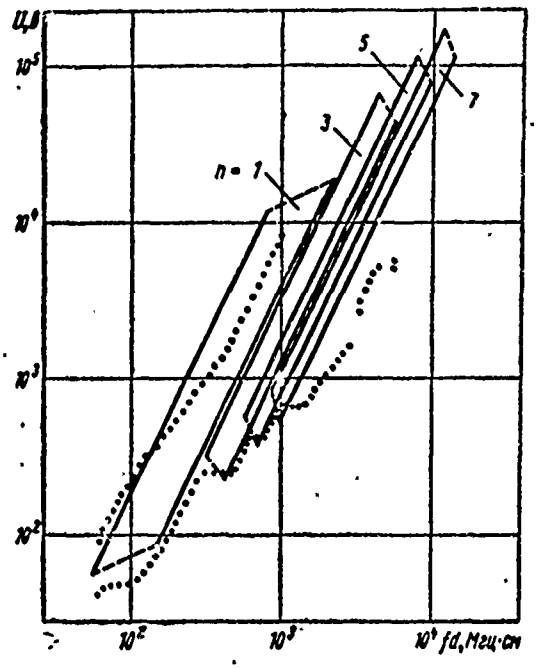

Fig. 62.

Fig. 61. Domains of existence of secondary electron discharge when n = 1 and with various initial velocities: 1 — K = 0, ψ = 0-32°; 2 — K = 0.1, ψ = -38-27.5°; 3 — K = = 0.25, ψ = -56-21°; 4 — K = 0.33, ψ = -64-17.5°.

Fig. 62. Domains of existence of secondary electron discharge at various n and with K = 0.25. Solid curves show the calculation and the dotted curves show measurement results [215].

[в = V; Мгц = MHz]

to voltage of discharge ignition with a reduction in voltage, and a lower boundary corresponding to the voltage at which the discharge burns. The measurements were conducted with pulse excitation of a toroidal resonator at a frequency of 62-143 MHz, with a controllable interelectrode gap, and with an initiating discharge of electron current from an auxiliary thermionic cathode. It is clear that the experimental results and the calculated curves differ by no more than 1.5 times. Characteristic deflections which evidently correspond to the appearance of discharge with different values of n are clearly noticeable on the lower curve.

Under real conditions even with a strictly constant amplitude of the voltage both the initial velocities of the electrons and the phases of their escape are distributed in a more or less wide range, while the discharge current (if it is recorded on an oscillograph) is "grouped" in a certain region of angles.

Subsequent analysis of the equations of motion for electrons in an hf field showed the existence of conditions guaranteeing stability of the discharge. Thus, if for any reason an electron or group of electrons is deflected from synchronous motion — i.e., if these electrons expended an odd number of hf voltage half-periods on motion from one electrode to the other — then because of the change in escape phase of the secondary electron their time of flight to the opposite electrode is also changed; however, this deflection from the synchronous will have the sign opposite to the sign of deflection from synchronism of primary electrons. Thus compensation of the initial deflection occurs and after a few periods synchronism is completely restored.

Such stability of discharge exists only within a certain domain of values of escape angle (and angle of arrival) of the electrons. In the approximation the domain of stability is limited by the angles ψ_{min} and ψ_{max}, mentioned above [217]. The very presence of a domain of stability leads to the possibility of prolonged existence of a discharge with a current which does not change in time. Although the coefficient of secondary emission can substantially exceed unity, the discharge current is always limited.

One of the internal causes for the limitation of discharge current, especially with flat electrodes of large area, is the effect of the space charge of electrons. As is easily understood from all that has been said, electrons move from one electrode to the other in the form of a more or less compact group or cluster. The intrinsic space charge tends to expand this cluster and thus

to accelerate the motion of electrons on the front of the cluster and retard the electrons moving in the tail. As a result of this some electrons may arrive on the opposite electrode with angles lying outside the zone of stability. In these conditions the secondary electrons which they generate will not "participate" in the discharge. The greater the space charge of the cluster the greater the fraction of the electron flow which leaves the stability region. In the absence of other factors leading to loss of electrons, the stationary state can be defined as that dynamic equilibrium when loss of electrons due to the fact that some fall outside the limits of the stability domain and the increase in the number of electrons due to the fact that the coefficient of secondary emission is greater than unity will mutually compensate one another [218].

With infinite flat electrodes, when the bunch of electrons represents, as it were, a layer moving from one electrode to the other, the intensity from the space charge close to the boundary surface of this layer (seam) equals

$$E_q = \frac{4\pi}{\varepsilon_0} q_s, \tag{29}$$

where q_s is the charge of the layer per unit of its surface. This intensity does not equal that created by the external voltage acting on the electrons located on the leading and trailing edges of the layer, where the electrons on the trailing layer are retarded by the action of E_q. For the electrons located on the rear boundary of the layer to participate in the discharge the relationship

$$E_q < \frac{U_M}{d}, \tag{30}$$

must be fulfilled. Here U_M is the amplitude of the field intensity of the electrodes, which is unperturbed by the action of the discharge. The maximum possible current density will obviously be determined from the condition of equality of the right and left sides of relationship (30). This gives

$$j_{\text{макс}} = q_s f = \frac{\varepsilon_0 f U_м}{4\pi d}. \qquad (31)$$

[макс = max]

When there is a discharge with n > 1, a total of n bunches are simultaneously present in the interelectrode gap. The space charge of a bunch acts on the electrons in one direction during the entire time of flight. At the same time the external field is variable in time and its resultant action is essentially equivalent to the action of one half-period. Besides this, with large n the domain of stability of the discharge is substantially narrowed; this is clear, in particular, from Fig. 62. All of this leads to intensification of the action of the space charge as compared to the action of the external field of the electrodes. As a result, with n = 3, 5, 7, ... the maximum possible discharge current equals

$$j_{n\,\text{макс}} = \frac{\varepsilon_0 f U_м}{12\pi n(n+3)}, \qquad (32)$$

[макс = max]

i.e., more than 3n times less than the current in a discharge with n = 1. Thus, although discharges with any large odd n are possible in principle, in this case the currents are so small that discharges with n > 5-7 are virtually never observed.

Formula (31), which like formula (32) was obtained by Callebaut [218], represents the known law of "three halves," which is easily verified by substituting the value of f from expression (27) into this equality. A certain difference in the numerical coefficient is evidently explained by the particularly approximate nature of the obtained equality between the right and left sides of expression (30). At the same time the possibility of partial compensation of electron space charge by the ions forming due to ionization of the residual gas is not taken into account here.

In certain cases – for example, in the resonators of hf charged-particle accelerators – the appearance of secondary

electron resonant discharge is undesirable. At the same time, conditions under which, according to Figs. 61 and 62, secondary electron discharge can arise are observed in these devices. To prevent the appearance of discharge a number of measures are taken, in particular the supplementary supply of constant voltage between the electrodes. In this case the time of electron flight in one direction will differ from the flight time in the other direction; resonance conditions are disrupted and discharge does not arise.

An analytic examination with n = 1 and zero initial velocities (K = 0) carried out by Zager and Tishin [217] showed that supplying constant voltage narrows the stability domain; at a constant voltage equal to 18.5% of the minimum voltage of discharge emission calculated according to formula (27), this domain disappears entirely. However, the simultaneous application of constant and hf voltage to the electrodes makes possible the return of electrons to their own electrode in the hf-voltage period with a velocity sufficient for effective development of secondary electrons. This can lead to a secondary electron discharge developing only at the electrode to which the positive pole of the fixed bias is applied. According to the analysis carried out by these authors, such a discharge can exist only at small values of bias and a bias which prevents secondary-electron discharge encompassing both electrodes does not permit the development of even "single-electrode" discharge.

An experimental check of the conditions for blocking secondary electron discharge by supplying a fixed bias, carried out at 15-23 MHz and in the range fd = 90-300 MHz·cm, showed that complete blocking of the discharge requires a fixed bias which is close in magnitude to the minimum voltage for discharge ignition. We will recall that the latter can be determined approximately by means of relationship (27), by setting K = 0.3.

In cavity resonators the application of a fixed bias between the electrodes requires insulation of one of the electrodes from the entire resonator with respect to the constant voltage while good conductivity is retained with respect to the high frequency. In practice major difficulties are encountered in accomplishing this, so that other methods of suppressing secondary electron discharge are being sought. In certain cases the method proposed by Polyakov et al. [219] is effective. It consists in the introduction of an additional electrode and the supply of a positive ("electron-evacuating") voltage of several kilovolts. This electrode is placed close to but outside the working gap.

The appearance of secondary electron discharge can apparently be prevented by selecting the appropriate electrode shape. Thus, according to Aitkin's observations [220], ignition of discharge is hampered when the electrodes have such a form that the electron "exchange" process (beginning, for example, in the central portion of the electrodes) is gradually displaced toward the periphery of the electrode and then to the edge, where it disappears without developing to a noticeable current. As an example of electrodes of such a form we can cite spherical electrodes and electrodes which are flat but which are sloped toward one another — i.e., when the interelectrode gap has the form of a wedge.

If the region in which secondary electron discharge can exist lies below the voltage at which the given interelectrode gap should operate, the appearance of discharge prevents the voltage from rising to the needed value. However, if the voltage is raised sufficiently rapidly discharge cannot be developed and the "dangerous" region can be bypassed. According to measurements made by Polyakov et al. [219], at a frequency of 100 MHz a rise rate of 5-6 kV/μs is sufficient to accomplish this.

Zaydin and Kushin [215] detected a dependence of ignition of discharge on the prehistory of the electrodes and on the arrival

in the gap of electrons from the external source. With the first (or the first after a prolonged interruption) rise in voltage 60-140 MHz in frequency in the form of 800-μs pulses with an amplitude corresponding to the domain of discharge existence, discharge may not appear for several tens of minutes. However, it is sufficient for discharge to appear in the time of a single pulse for discharge to be triggered regularly during subsequent voltage pulses. At the same time if there is an external source of electrons the discharge appears immediately that the voltage reaches the value at which discharge can exist. In the given work a small thermionic cathode was used as such an electron source. From this we can draw out a practical rule: the rise in voltage connected with passage of the "dangerous" domain of existence of secondary electron discharge should be carried out in the absence in the gap of charged particles capable of initiating discharge. For example, in accelerators the source of accelerated ions or electrons should be switched off during the voltage rise.

Naturally, a radical method of combating this phenomenon is the creation of electrodes with which the coefficient of secondary emission would be smaller than unity. Several methods are known for treating the surface to reduce the coefficient of secondary emission: coating with black palladium, black platinum, or carbon black. However, in the majority of radio engineering vacuum devices (e.g., in charged-particle accelerators) the application of such coatings is impossible in practice due to the impermissible reduction in Q of the resonant system (resonators) and also because of the substantial reduction in the threshold of arcing appearance (which will be discussed in the following section). More or less successful efforts have also been made to coat the working surface of the electrodes with a very thin (about 100 Å) layer of titanium. With a clean surface this metal has a secondary electron emission coefficient less than unity; however, the high sorption capacity of titanium may be reflected unfavorably in the electric strength of the vacuum insulation and therefore such a method requires additional investigation.

The reduction in the coefficient of secondary emission during adsorption of electrically negative gases can apparently explain the fact that Zager and Tishin [217] observed termination of burning of a secondary electron discharge in ten minutes after brief inlets of chlorine into the working volume and its subsequent evacuation. These same authors noted a hampering effect on ignition of secondary electron discharge in the course of a few minutes after passage of a high-power gas discharge betweeen the electrodes. This may also be explained by the reduction in the coefficient of secondary emission owing to cleaning of the surface during the gas discharge. Obviously, in many cases a large value of the secondary emission coefficient is explained by the contamination of the electrode surfaces. Therefore the creation of pure vacuum conditions facilitates suppression of secondary electron discharge in those cases when it is undesirable.

Investigation by Zaydin [221] demonstrated the possibility of prolonged suppression of secondary electron discharge by the application of a thin layer of sulfur on copper electrodes. Such a layer, applied by vacuum evaporation or by precipitation from a very dilute solution, was found to be a fairly stable coating, although the high vapor tension of sulfur, it would seem, should lead to its rapid volatization. Apparently the stability of the sulfur layer is connected with the fact that it enters into chemical combination with the material of the electrodes. Zaydin explains the suppression of discharge through application of a sulfur layer by the liquidation of local sources of electrons on the electrodes (by the "poisoning" of the sites of field-effect emission) and not by the reduction in the coefficient of secondary emission.

Secondary electron discharge, as noted above, is observed in hf charged-particle accelerators – linear ion and electron accelerators and cyclotrons – where suppression of such discharge is connected with known difficulties. In this case discharge can

arise not only directly between the electrodes which are accelerating the particles, but also in very different places where resonance conditions are created: in the supply feeders, between different parts of the cavity resonators, etc. Owing to the large surface area where discharge can develop, the total current of secondary electron discharge is usually so great that it leads to strong loading of the hf supply system. However, during the design of these devices an effort is made to insure that the working level of voltage will fall outside (usually above) the domain of existence of secondary electron discharge. In this case the basic problem in combating the indicated discharge is the "transition" across the domain in which it exists; this is usually achieved by the fastest possible voltage rise or by the other methods described above.

Besides this, in cyclotrons a discharge is observed [222] which represents, to a certain degree, a hybrid of secondary electron resonant discharge and Penning discharge, which is described in Chapter 7. Owing to the dip in the electrical field inside the cyclotron dees and to the presence of the magnetic field, electrons leaving one plate of the dee close to its edge (for precision we will call this plate the upper) may reach the lower plate of the same dee. This can occur only in that portion of the period of hf voltage applied to the dees when the dee under consideration is under a negative potential, since only in this case will the sagging electrical field "pull out" electrons. Besides this, in order for electrons from the upper plate to reach the lower plate it is necessary that during the period of electron flight the reduction in voltage between the dees be maintained constant. Then electrons from the upper plate will bombard the lower plate with energies differing from zero, which creates the possibility of secondary electron generation. When $K_{ee} > 1$, as during secondary electron discharge, the process will develop but only in the course of that quarter period of hf voltage when the considered dee is negative and the voltage on it is reduced.

3. HIGH-FREQUENCY BREAKDOWN (SPARKING)

Among the extremely few works on vacuum insulation under hf voltage we should cite first of all the comprehensive investigations by Chupp, Heard, and other researchers [223-225]. These works were undertaken in connection with the problem of creating large resonance charged-particle accelerators and were concerned mainly with the influence of electrode material, electrode treatment, and soldering methods on electrical strength. The influence of a longitudinal magnetic field on breakdown voltage and on electrode destruction (during breakdowns) was also clarified.

The magnet, vacuum system, and hf oscillator of a high-power cyclotron were used for the experiments. A voltage up to 1.3 MV at a frequency of 13-14 MHz was developed on the closed end of a quarter-wave coaxial resonator. The hf voltage pulse length was 176 ms; repetition frequency was 90 or 180 pulses per minute. The working chamber was evacuated to a vacuum above 10^{-6} mm Hg by oil diffusion pumps equipped with traps cooled by freon and by liquid nitrogen. The electrodes and the internal portion of the vacuum system were cleaned with fine sandpaper and were washed with water and acetone. In addition, before the final washing the electrodes were etched in concentrated hydrochloric acid. In certain experiments with copper electrodes the cleaning process in a galvanic cyanic bath was utilized; however, this additional treatment did not yield any improvements.

The studies were carried out with the following electrode geometry: a cylinder several centimeters in diameter between electrically connected parallel plates. As the voltage was raised dark currents appeared first of all; this led to an increase in the load on the hf oscillator (an increase in the active component of the current). The appearance of dark currents was accompanied by x-radiation whose intensity grew exponentially with an increase in voltage – i.e., the dark currents had the same characteristic

as occurs with constant voltage. A further rise in the voltage led to sparking. There were more intensive but short-term flares of x-radiation, with a glow appearing around the electrode with large curvature (where it is greater than E) and penetrating 2-3 cm into the gap from the electrode surface. From the radio engineering point of view sparking led to a drop in the input impedance of the resonator, which caused an interruption in the hf oscillations and, consequently, a sharp drop in voltage on the investigated gap. This led in turn to suppression of the spark and thus created the possibility of automatic restoration of voltage on the resonator. Therefore, judging from the oscillograms, even during the extent of one pulse of hf voltage it was possible to observe several sparks with subsequent restoration of voltage.

In the described works the frequency of appearance of sparking was used as the breakdown voltage criterion. Breakdown voltage was determined as the voltage for which a small increase led to strong growth in the frequency of sparking – with the frequency not being reduced in time.

With a rise in voltage to a magnitude below the breakdown value the frequency of sparking at first is usually greater than during the subsequent period. After achievement of breakdown voltage the frequency of sparking grows sharply so that in order to obtain the previous frequency it is necessary to reduce the voltage (sometimes by 30% and more). The subsequent breakdown voltage turns out to be lower. Total return to the initial value can occur upon the expiration of a prolonged period and then only under the condition that the destruction of the electrodes during the initial sparkings was not excessively great. Prolonged holding of the electrodes at a voltage below the breakdown value leads to a gradual reduction in the frequency of sparking.

On the whole the curves of the dependence of sparking frequency on the applied voltage are generally similar when different

electrode materials are used. On a semilog scale they have approximately identical and constant slope and differ only in the degree of shift along the voltage axis (Fig. 63).

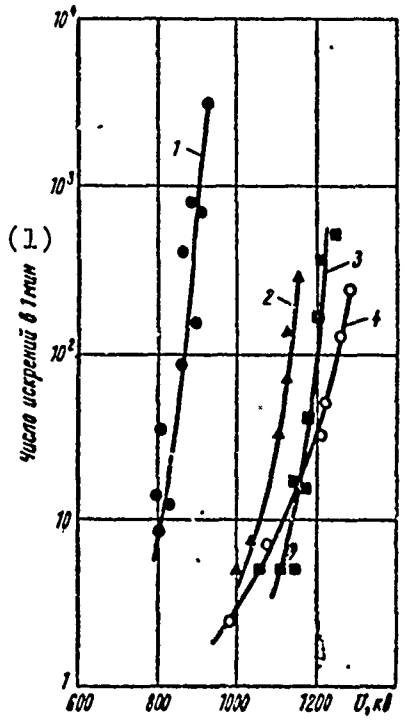

Fig. 63. Frequency of appearance of sparking as a function of hf voltage amplitude (d = = 81 mm, H = 8000 Oe): 1 — copper reduced by phosphorus; 2 — Inconel; 3 — stainless steel; 4 — Incoloy.

KEY: (1) Number of sparkings in 1 min.

Designation: кв = kV.

Results of measurements made during a steady frequency of sparking (after a prolonged application of voltage) and with electrodes of various metals are given in Table 50.

The presence of a longitudinal magnetic field, which reached 15 kOe in the described experiments, had no influence on the voltage at which sparking appeared up to the appearance of the sparks themselves. However, the nature of the spark with the magnetic field differs substantially from the case when there was no magnetic field. The sparks without the field usually did not cause macroscopic changes on the surface of the electrodes. Thus, for example, in one experiment after 10^4 sparkings no substantial spark damage was detected. If a magnetic field was applied then,

Table 50. Electrical strength of vacuum insulation at a frequency of 13-14 MHz [224, 225].

(1) Материал электродов	(2) Зазор, мм	Напряжение, при котором наблюдается 10 искр в 1 мин, кв (3)	Максимальное приложенное во время опыта напряжение, кв (4)
(5) Инконель (14% Cr, 78,5% Ni, 0,25% Mn, 0,2% Cu)	60,3	900	960
	86	960—1080	1170
	136	1140	1140
(6) Нержавеющая сталь (25% Cr, 20% Ni, 2% Mn)	60,3	760—880	930
	86	1150	1250
(7) Инкаллой (21% Cr, 34% Ni, 1,5 % Mn, 0,05% Cu)	86	1150	1320
(8) Бескислородная медь высокой проводимости	86	810—880	980
(9) Медь, раскисленная фосфором	86	840—870	950
	136	840—900	1020
(10) Электролитическая холоднотянутая медь	136	1070	1250
(11) К-монель (66% Ni, 30,3% Cu)	136	980	1050
(12) Никель	136	970	1000
(13) Тантал	136	870	1110
(14) Серебро	136	670	790

KEY: (1) Electrode material; (2) Gap, mm; (3) Voltage at which 10 sparks per minute are observed, kV; (4) Maximum voltage applied during the experiment, kV; (5) Inconel; (6) Stainless steel; (7) Incoloy; (8) Unreduced copper with high conductivity; (9) Copper reduced by phosphorus; (10) Electrolytic cold-drawn copper; (11) K-Monel; (12) Nickel; (13) Tantalum; (14) Silver.

beginning with a certain field value, the sparks led to strong destruction of the surface of electrodes with smaller curvature, i.e., where E was less. The magnitude of the magnetic field at which sparking becomes destructive grows with an increase in the gap. With a 35-mm gap it equals 2000 Oe, while with a 135-mm gap it is 4000 Oe. In one experiment in a magnetic field 2500 sparks concentrated on a surface of approximately 30 cm^2 "broached" right through a stainless steel plate 1.5 mm thick. One spark can tear off up to several milligrams of metal with energy of 30 J stored in the resonator. It was found that the intensity of destruction

was approximately proportional to the energy stored in the resonator. The metallic powders obtained as the result of electrode destruction are partially transferred to the opposite electrode; a significant portion of the powder drops to the bottom of the vacuum container.

Microscopic analysis showed that as a result of destructive sparks craters with a diameter up to 0.7 mm are formed on the electrode with the smaller curvature; cracks proceed from these craters into the depths of the electrode, penetrating to 0.2 mm from the crater surfaces. A zone of recrystallization spreads to the same depth from the crater surfaces; this indicates intensive local heating during spark discharge. The consequences of local heating are also visible on the opposite electrode: this involves sintering of a portion of the electrical powder transferred from the other electrode onto the main mass of the electrode.[1]

The significant irregularity of the electrode surfaces appearing during destructive sparking leads to substantial reduction of breakdown voltage. A similar reduction in breakdown voltage is observed if fine cracks are formed on the electrode surfaces (for example, as the result of mechanical treatment). If the magnetic field is removed after the reduction in breakdown voltage due to the appearance of destroying sparks, the previous value of

[1]On the basis of experience in adjusting the high-current ion accelerator MTA Mark I (see Chapter 1) the following semiempirical criterion was developed: if an ion of hydrogen starting from the anode can pass to the opposite electrode (cathode) in one half-period of the high-frequency voltage, the appearance of destructive sparks is possible [226]. The physical basis for this position reduces to the fact that destruction on the anode requires a very fine beam of electrons proceeding from the cathode. Such a thin beam can exist only when it is focused (compressed) over its entire length by positive ions leaving the anode. (Hence the requirement that at least the very lightest ions be able to proceed from the anode to the cathode.) In the presence of a magnetic field the focusing is accomplished more easily and the appearance of destructive sparks is more probable.

breakdown voltage is slowly restored after multiple sparkings.

The particular feature of hf resonator operation (the need to maintain a certain relationship of the various geometric dimensions) does not allow changing the distance between the electrodes in the process of the experiment, due to the strong detuning of the resonator. Therefore determination of the influence of the magnitude of the gap d on breakdown is difficult and researchers, as is evident from Tables 50 and 51, are limited to a very small number of measurements in order to form judgments on the nature of this relationship. Measurements of breakdown voltage in a magnetic field (the case of greatest interest to the researchers) for Inconel electrodes with three different gaps showed that one and the same sparking rate is observed (with an accuracy to a few percent) at voltages obeying the Cranberg formula: $U_{br} = \text{const} \cdot d^{0.5}$ (see page 158). Extension of this formula to all measurement results and calculation by this method of the value of the constant made it possible to compare electrode materials with respect to their influence on breakdown voltage. These data are given in Table 51.

As a result of this work, Chupp and coworkers [224, 225] came to the conclusion that the highest voltage is withstood by those metals which form the least metallic dust during an identical number of sparkings and are least damaged.

The following is a listing of the metals in the order of diminishing capacity to withstand destruction:

Good Metals	*Poor metals*
Inconel	Copper of all types
Incoloy	Tantalum
Stainless steel	Duralumin and aluminum
Nickel	Silver
Molybdenum	
Titanium	
K-monel	

Table 51. Strength of vacuum insulation during high-frequency voltage of 13 MHz in a 10 kOe longitudinal magnetic field [224, 225].

(1) Материал электродов	(2) Зазор, мм	(3) Напряжение, при котором наблюдается 100 искр в 1 мин, кв	(4) Значение константы в формуле Крэнберга, кв/мм^{0,5}	(5) Примечание
(6) Нержавеющая сталь	35	700	118±0,5	
(7) Инконель	35	635	109±8	
	60	940	120±8	
	86	1065	116±8	
К-монель (8)	137	1050	98	(9) Напряжение ограничивалось мощностью генератора
Никель (10)	135	995	86	
Молибден (11)	137	1200	103±4	
	54	750	102±8	
(12) Бескислородная медь	84	950	103±5	
(13) Электролитическая медь	135	1200	103±4	
	60	700	91±6	
(14) Медь, раскисленная фосфором	131	500	46±2	(15) После обработки поверхности наклепом
	129	900	79±5	
(16) Тантал	138	920	78±5	
(17) Серебро	137	775	67±4	
(18) Графит	24	310	64±10	(9) Напряжение ограничивалось мощностью генератора

KEY: (1) Electrode material; (2) Gap, mm; (3) Voltage at which 100 sparks per minute are observed, kV; (4) Value of the constant in the Cranberg formula, kV/mm$^{0.5}$; (5) Remarks; (6) Stainless steel; (7) Inconel; (8) K-monel; (9) Voltage was limited by generator capacity; (10) Nickel; (11) Molybdenum; (12) Unreduced copper; (13) Electrolytic copper; (14) Copper reduced with phosphorus; (15) After treatment of the surface by work hardening; (16) Tantalum; (17) Silver; (18) Graphite.

Among the types of copper of paramount value for high-frequency equipment, the best is oxygen-free high-conductivity copper with a work-hardened surface.

From the technological point of view there is considerable interest in the behavior of welded and soldered electrodes when the point of junction, worked together with the remaining surface,

is located in the "working section" of the electrode. Chupp and Heard established the fact that while welding has virtually no influence on breakdown voltage, any soldering reduces it. When the electrodes are made from copper soldering of a eutectic copper-silver alloy (72% Cu, 28% Ag) with arc heating of the soldering area in a medium of helium or in the flame of an oxygen-acetylene torch (the latter is somewhat poorer) leads to a comparatively small negative effect. Solders containing lead, gold, phosphorus, cadmium, and zinc (not to speak of soft solders) give very poor results.

Nikolayev [209] studied the behavior of vacuum insulation under periodic 750-μs pulses of 24-MHz hf voltage. Voltage up to 450 kV was supplied to copper electrodes — a rod 2.5-10 mm in d diameter with a hemispherical face opposite a flat disk 170 mm in diameter — placed in a metallic tank with plexiglass flanges. A vacuum of 10^{-5} mm Hg was created with a vapor-oil pump. The shunting capacitance (electrode capacitance) comprised 11 pF. Under these conditions an interruption of oscillations occurred upon achievement of a certain value of intensity on the surface of the rod electrode, while a glow appeared in the interelectrode gap. The critical value of intensity (E_{br} = 30-120 kV/mm) did not depend on the magnitude of the interelectrode gap; however, in the process of conditioning by discharges it varied by 1.5-2 times, with the best results being obtained from conditioning with the largest gap between the electrodes. The value of E_{br} depends to a very great degree on the quality of preliminary mechanical treatment of the electrode surfaces; for different specimens of electrodes of identical shape manufactured from a single piece of copper E_{br} even after prolonged conditioning by discharges could differ by 3 times. The obtained characteristics point to the thought that in the given experiment destruction of the electrical strength of the vacuum insulation and, perhaps, even simply interruption of oscillations were caused by the achievement of dark currents of some more or less definite magnitude. At the same

time the appearance of a glow in the gap may be tied to the appearance upon restoration of voltage of a discharge similar to a secondary electron discharge, with the dark current flowing earlier acting as the initiator. In favor of the existence of such a discharge is the fact that the voltage on the gap after the interruption of oscillations is not restored up to the end of the pulse. It is not difficult to see an analogy between the obtained characteristics and the results of the work done by Tashek (see Fig. 41), where the presence of a critical intensity on the cathode was also observed with a low power of a constant-voltage source. Clearly the coincidence is not a chance one and is explained by the low power of the conditioning discharges.

Comparison of the data obtained by Nikolayev [209] with the results of works by Chupp and coworkers given earlier [224, 225] shows that the absolute values of breakdown voltage are extremely close, although in the works by Chupp and coworkers the length of the hf pulses and the area of the electrodes were substantially greater, while the frequency was two times lower. However, it does not follow from this that breakdown voltage does not depend on frequency or on pulse length. On the basis of the most general considerations it is possible to consider that breakdown voltage should grow with an increase in frequency and with a reduction in the duration of the applied voltage. This is confirmed by comparing the data from Chupp and coworkers and the results obtained by Halpern et al. [208], given at the beginning of the chapter. Additionally one should note the results obtained by Polyakov et al. [219], who studied electrical strength in a gap of 40 mm between copper electrodes (disks 200 mm in diameter with rounded edges) at a frequency of 100 MHz and a 750-μs length of hf voltage pulses. During the rise in voltage the first sparkings began at 500-600 kV, while after 3 hours of conditioning a single spark was observed in 3000 supplied pulses of hf voltage with a level of 1 MV. This is substantially higher than the value of breakdown voltage obtained by Chupp and his coworkers.

These data virtually exhaust the information available in the literature on the breakdown of vacuum insulation under hf voltage. In this chapter repeated references have been made to particular features of the destruction of vacuum insulation under hf voltage as compared with destruction occurring with constant voltage. However, note must be taken of the multiplicity of similar features, especially if we exclude from the comparative examination microdischarges, secondary electron discharge, and apparently the case of very high frequencies, for which there are as yet virtually no experimental data. This similarity lies first of all in the presence of dark currents, for which the values and the nature of the dependence on voltage at high frequency are the same as with constant voltage, to judge from measurements of x-radiation. The dependence of electrical strength on conditioning by discharges also demonstrates many common features. The quantitative data on the influence of electrode material on breakdown voltage are very similar. In certain experiments carried out by Chupp and Heard at 14 MHz the electrodes were strongly heated owing to the passage of dark currents (for example, molybdenum electrodes were heated red-hot); however, neither the magnitude nor the temperature of the electrodes had any noticeable influence on breakdown voltage, which in general agrees with observations at constant voltage. Such broad similarity of external characteristics apparently reflects a similarity in the physical processes leading to destruction of vacuum insulation, although substantial differences exist and were pointed out frequently above.

CHAPTER 6

POSTBREAKDOWN STAGES OF VACUUM DISCHARGE. VACUUM ARC

1. SPARK DISCHARGE

Breakdown of a vacuum gap leads to a spark — a discharge with a current which varies extremely rapidly, rising to several kiloamperes with sharply dropping voltage. The energy stored earlier in the capacitance of the electrodes and the structural elements directly connected to them is liberated in the interelectrode gap and on the electrodes. In view of the brevity of the process the "support" of the discharge from elements of the electrical circuit (generator, capacitors) which are remote from the electrodes is usually insignificant. After discharge of the electrode capacitance through a vacuum gap the voltage on the gap drops to a tens of volts and discharge shifts to another stage if the supplying circuit can insure passage of a current amounting to a few kiloamperes through the vacuum gap. If the power of the supply sources is small the discharge is terminated or it becomes unstable and intermittent.

Passage of those magnitudes of currents which are observed in a vacuum spark requires that the interelectrode gap be filled with plasma. In actual fact, if there is unlimited power of the source of electrons and ions on the cathode and anode respectively and even if there is no plasma in the gap, due to limitation of

the space charge from the side the density of the current between flat electrodes in a vacuum comprises

$$j = 1{,}86(j_e + j_i), \tag{33}$$

where j_e and j_i are the densities of unipolar currents of electrons and ions, respectively, limited by natural space charges; the magnitudes of the currents are determined by the widely known "three halves" law. In other words, the mutual compensation of positive and negative space charges with a bipolar current in a vacuum increases the unipolar electron current (limited by the natural space charge) by less than two times. Therefore, for example, with a gap of 1 mm and a voltage of 50 kV the density of current in the vacuum cannot exceed 500 A/mm^2. At the same time, in a vacuum spark it is easy to obtain currents of several kiloamperes of even tens of kiloamperes with substantially lower voltage, a larger gap, and a current channel cross section of less than 10 mm^2 [227].

The interelectrode gap can be filled with plasma in two ways: the first is the formation and accumulation of plasma in the gap "on place" due to ionization of residual gases resulting from imperfect vacuum; the second is the propagation into the entire interelectrode gap of plasma formed close to one of the electrodes – e.g., as the result of intensive ionization of a dense cloud of gas or vapor liberated from the electrode.

With interelectrode distances of a few millimeters the voltage drop during breakdown proceeds in a time span of less than 10^{-7} s. Obviously this is the duration of filling of the interelectrode gap with plasma and transition to low-voltage discharge in vapors of the electrode materials. It is true that sometimes the initial stage of discharge arising after breakdown of a vacuum gap will be extended in time – for example, under the special conditions in pulse x-ray tubes with ignition; processes in the latter will be examined below.

Although the actual process of transition to low-voltage discharge after breakdown has been studied virtually not at all (to a significant degree because of experimental difficulties), a certain amount of information and some physical ideas on this process can be drawn from experimental data on the propagation of glow in the vacuum gap after breakdown and from data on the propagation of the plasma of a spark discharge beyond the limits of the interelectrode gap. Clearly this has much in common with the processes occurring in a vacuum discharge which is artificially excited by an auxiliary spark close to one of the electrodes. This form of discharge will be examined in the following section. Here we will pause to describe the glow during vacuum discharge of, so to speak, natural origin.

The onset of breakdown is noted visually as the appearance of a more or less clearly outlined luminous channel or cloud between the electrodes. Study of this glow showed that it consists of the line spectrum of electrode materials, where an outstanding feature of the spectrum of the vacuum spark is the presence of lines of multiply ionized atoms in the region of the deep ultraviolet. With a condensed spark the luminous cloud has substantial brightness and can propagate beyond the limits of the interelectrode gap at a rate greater than several kilometers per second.

To determine the rate of the spatial development of glow between electrodes during vacuum breakdown, Chiles [228] used photography with image scanning over a photoplate by means of a rapidly rotating mirror. With pulse voltage up to 120 kV and with rod electrodes 1 mm in diameter made from different materials, Chiles found that as a rule the glow begins at the anode and is propagated to the cathode at an approximately constant speed. Even before this glow reached the cathode, illumination arose on the latter also. The results of these measurements are given in Table 52.

Table 52. Rate of propagation of the luminous cloud from the anode and the interval between appearance of glow on the anode and the cathode.

(1) Материал электродов	(2) Зазор, мм	(3) Напряжение, кв	(4) Диапазон интервалов, $\times 10^{-8}$ сек	(5) Средний интервал, $\times 10^{-8}$ сек	(6) Скорость, км/сек
Bi	1,0	85	4,2—5,7	4,7	8,9
(7) Графит	1,05	55	—	—	2,5
Al	1,1	75	1,8—5,9	4,1	7,3
Cu	0,89	80	2,4—9,3	5,6	5,8
(8) Pd (необезгаженный)	0,95	—	5,1—7,5	5,3	6,5
(9) Pd (насыщенный H_2)	1,0	—	1,3—6,9	4,5	5
Sn	1,3	80	(—0,9)—2,2	0,34	5,4
(10) W (коммерческий)	0,81	95	1,3—4,3	2,4	5,4
(11) W (чистый необезгаженный)	0,6	120	2,1—3,2	2,5	5,2
(12) W (чистый обезгаженный)	0,55	120	2,3—4,1	2,8	5,0

KEY: (1) Electrode material; (2) Gap, mm; (3) Voltage, kV; (4) Range of intervals, $\times 10^{-8}$ s; (5) Average interval, $\times 10^{-8}$ s; (6) Speed, km/s; (7) Graphite; (8) Pd (not degassed); (9) Pd (saturated with H_2); (10) W (commercial); (11) W (pure, not degassed); (12) W (pure, degassed).

With a change in the gap within the limits 0.78-0.84 mm the values obtained for the rate of propagation of glow between electrodes of commercial tungsten fall within the limits of scatter during measurements with d = 0.81 mm. On some of the photographs Chiles observed a weaker glow propagating in the same direction but at a greater speed — reaching up to 30 km/s. The measurements were conducted in a glass vessel with Picein seals, except for the measurements with electrodes of pure tungsten and palladium; these were mounted in an all-glass vacuum system (sealed off after evacuation by a mercury pump with a trap cooled by dry ice).

The constant level of the propagation rate of the glow during displacement of the latter from the anode to the cathode apparently attests to the fact that the source of this glow is made up of unionized gases and vapors liberated from the anode. If the rate

of glow propagation is equated to the thermal velocity of vapors of the anode base material, the velocity shown in Table 52 corresponds to excessively high temperatures; 67 eV for bismuth and 20 eV for tungsten ($2 \cdot 10^5$ and $7 \cdot 10^5$°K, respectively). It is possible, however, that there is some sort of analogy between the propagation of vapors from the anode and the theoretically investigated one-dimensional leakage into the vacuum of a previously compressed gas [229]. In the latter case the rate of motion of the front exceeds the speed of sound (close to the average thermal velocity) in a resting gas by $2\left(\frac{c_p}{c_v} - 1\right)^{-1}$ = 3-5 times (c_v and c_p are the molar specific heats at constant volume and pressure, respectively). Then a substantially lower temperature corresponds to the same velocities of front motion than during motion at thermal velocity; 6 times less with a monatomic gas and 14 times less with a diatomic gas. However, even with this explanation the initial temperature remains quite high and, apparently, velocities which are just as high are obtained as a result of electrodynamic processes which are still not quite clear. In connection with the broad use of condensed discharges in plasma research, certain properties and characteristics of the electrodynamic processes in such discharges have been studied; however, examination of these processes lies outside the framework of this presentation.

Unfortunately we do not know the stage of postbreakdown discharge (in particular, the instantaneous value of voltage on the gap and the magnitude of current) at which the propagation of glow described above takes place. It is, however, clear that the liberation of gases and vapors from the anode and the more rapid propagation of the glowing cloud in the gap should be preceded by heating of the anode (apparently local heating) by an electronic current already flowing in the gap. It is clear that besides excitation, under the action of electron bombardment partial ionization of the vapors emerging from the anode takes place. The positive ions thus formed will intensively bombard the cathode

until the glowing cloud reaches the cathode. Apparently the appearance of glow on the cathode can be explained by precisely this bombardment of the cathode. At the same time ionization of vapors may be the reason for the filling of the interelectrode gap with plasma, which favors transition to low-voltage discharge in the vapors of the electrode metal.

Simonov et al. [230] used electrical probes and a mass spectrometer of the drift type to study the propagation of the plasma created by a vacuum spark. These measuring instruments were installed to one side of the electrode, outside the sphere of action of the electrical field of the latter; therefore they recorded a plasma of the already developing discharge — plasma propagating more or less isotropically on all sides from the electrodes. During discharge through a vacuum gap between rod electrodes with capacitance amounting to fractions of a microfarad and which are charged to 10 kV, the plasma front propagation rate v_{pl} depends on the maximum current in the discharge: with a current of 10 A the rate v_{pl} equals $1.5 \cdot 10^4$-$2 \cdot 10^4$ m/s, while at 4 kV it is $1.2 \cdot 10^5$ m/s. Electrons with energies up to 70-80 eV move in the front (at high discharge currents); ions of light elements follow directly behind them. The plasma contains ions of the electrode material (Fe^+, Ni^+, W^+), ions of adsorbed gases (H_2^+, O_2^+) and frequently ions of the wall materials (Si^+, Ba^+, Na^+), since in the given experiments the container was glass (when tungsten electrodes were heated to 200°C there were no H^+ ions in the plasma). The velocities of these ions are not identical: H^+ had the highest velocity, while the heaviest ions (W^+) had the lowest — $8.0\ 10^3$-$1.1\ 10^4$ m/s. However, the energy of the latter ions (expressed, for example, in electron volts) is greater than the energy of motion of the light ions. The velocity of the fastest ions (hydrogen) determines the velocity of propagation of the plasma front. Owing to the scatter in velocities of different ions, the plasma undergoes separation into components as

it moves: the leading portion is enriched with light ions, while the heavy ions lag behind and are concentrated in the tail portion of the plasma cloud.

When a vacuum discharge is triggered by disconnecting the electrodes and when the supply source voltage ranges up to 700 V, depending upon the electrode materials and the parameters of the electric circuit only ions from the material of one of the electrodes – the anode or the cathode – may exist in a plasma which passes beyond the limits of the discharge channel. At higher voltages the cathode material is always present.

2. DISCHARGE IN A VACUUM WITH ARTIFICIAL IGNITION

Discharge between electrodes in a vacuum can be caused by an auxiliary spark on one of the electrodes, even if the breakdown voltage for the given interelectrode distance in the absence of a triggering spark is significantly greater than the voltage applied. Usually the igniting spark is created by making a small opening in one of the electrodes and installing an additional triggering electrode in the opening. The voltage on this auxiliary electrode is supplied either from a separate power-supply source or through an additional resistance from the same source which feeds the main electrodes. The latter circuit can be realized only with a pulse power supply.

In practice vacuum discharge with ignition is used to obtain short and very intense flares of x-radiation. To ensure an intense discharge a high-voltage capacitor is connected in parallel to the electrodes without limiting resistors. Besides this, such a condensed discharge is used to obtain plasma pinches in certain forms of plasma sources. Discharge with ignition also finds application in high-speed switching of large pulse currents at high voltage.

It is logical to assume that the processes in discharges with ignition have much in common with processes during a natural breakdown of vacuum insulation, especially in the final stages of its development. This similarity is obviously greater with a low-power igniting spark, when secondary processes on the electrode are necessary to ensure discharge between the main electrodes. If the energy of the igniting spark is great the plasma which is formed in such an igniting discharge can be sufficient to "short out" the gap between the main electrodes and ensure obtaining the required gap conductivity. There is less similarity between such a discharge and the discharge after natural breakdown.

Table 53 presents the minimum required magnitudes of electrical current expended on the formation of the auxiliary spark on the cathode which is capable of igniting discharge in the main interelectrode gap. The measurements were made in a vacuum of $5 \cdot 10^{-6}$ mm Hg. The voltage (0.5/60 μs pulse) was supplied to the main electrodes 1 μs earlier than the rectangular pulse (front less than 10 ns) of voltage was supplied to the igniting electrode [231]. The gap between the main electrodes was 4-10 mm.

Table 53. Minimum energy of the igniting spark during ignition on the cathode.

(1) Материал электродов	(2) Основное напряжение, кв	(3) Напряжение поджига, в	(4) Минимальная энергия поджига, мкдж
(5) Алюминий	90	109	0,013
(5) Алюминий	120	113	0,013
(6) Свинец	120	132	0,036
(7) Медь	96	450	0,24
(8) Нержавеющая сталь	120	640	0,51
(9) Катод—нержавеющая сталь; анод—алюминий	120	700	0,61

KEY: (1) Electrode material; (2) Main voltage, kV; (3) Ignition voltage, kV; (4) Minimum ignition energy, μJ; (5) Aluminum; (6) Lead; (7) Copper; (8) Stainless steel; (9) Cathode, stainless steel; anode, aluminum.

With minimum ignition energy breakdown of the main gap occurred on the average one time per 1000 igniting pulses. The total quantity of particles forming in the igniting spark and capable of passing into the gap between the main electrodes was evaluated by means of probe measurements and gave a quantity of 10^7-10^8 (at minimum ignition energy).

From Table 53 it is clear that the magnitude of the ignition energy depends mainly on the cathode material; the influence of the anode material and of the magnitude of the main voltage in the gap is small, if it exists at all. If the igniting pulse is supplied at least 0.1 μs earlier than the main pulse, no breakdown occurs in the main gap even with an increase in ignition energy by three orders of magnitude.

The quantities given in Table 53 were obtained when the igniting electrode was installed in the center of a hemispherical cathode 50 mm in diameter, virtually flush with the surface, and when the domain of the igniting spark lay within the electrical field of the main electrodes. If the igniting electrode was sunk into the body of the cathode in order to eliminate the influence of the field of the main electrodes on the igniting spark and to remove the point on the cathode where the igniting discharge occurs from this field, the minimum ignition energy grew by four orders of magnitude. In this case a current of a few amperes might flow between the main electrodes in the course of a fraction of a microsecond; this only rarely led to ignition of the main discharge.

With ignition on the anode the minimum energy comprised a few millijoules, growing rapidly with an increase in the gap from 4 to 20 mm. Although the contaminants of the electrode surfaces which are unavoidable in a technical vacuum might influence the absolute values of ignition energy, from the given measurements we can clearly draw certain conclusions concerning the more

common properties of discharge with ignition. The given characteristics allow us to assume that the local density of the plasma formed by the igniting spark on the cathode and the intensity of the electrical field at this point are important for triggering a discharge. These conclusions are confirmed by the results of investigating the processes in pulse x-ray tubes with ignition (with an igniting discharger on the cathode). Thus, Boym and Reykhrudel' [232] determined the conditions under which the greatest possible quantity of electrons can pass through the main vacuum gap until transition to intensive discharge in gases and vapors liberated from the electrodes occurs.[1] It was found that the current of electrons preceding a transition to intensive discharge in vapors which is not excessively fast can be multiplied by installing several igniting gaps on the same cathode instead of the usual single igniting gap. By applying a cathode with 11 igniting gaps operating simultaneously, these investigators were able to bring the electron current up to 160 A with a transition time to intensive discharge of 0.3-0.4 μs. In another work by the same authors [233] the duration of the electron current prior to transition to intensive discharge grew significantly with limitation of the current flowing in the igniting gap. Although in this case the current in the main gap was somewhat reduced, owing to its great duration the integral current grew. Both of these facts confirm that the density of the igniting plasma at the cathode is important for ignition of discharge in vacuum. The same can be said of the role of the intensity of the main field in the region

[1]With such a discharge, due to collisions in the space the energy of electrons arriving at the anode is less than the energy of the corresponding voltage on the electrodes; in this connection the x-ray yield is strongly reduced with the same flow of electrons. Besides this, because of the unavoidable voltage drop on the resistance and inductance of the circuit at a large current the voltage on the electrodes is also reduced with the onset of intensive discharge. Therefore the condition for obtaining the maximum quantity of electrons passing prior to the onset of intensive discharge is equivalent to the condition for obtaining the maximum x-ray yield with unchanged electric-circuit parameters.

of ignition; while it has not been studied directly, in practical designs of pulse x-ray tubes with ignition there is a noticeable effort (apparently reflecting the experience of the tube designers) to reduce the intensity of the main field at the point of ignition by sinking the igniting gap into the body of the cathode or by fusing a concave cathode with the igniting gas placed in the center.

Simonov and Kutukov [234] used a drift mass spectrometer to study the plasma of a vacuum discharge extending out of the discharge gap at an angle of 90° to the surface of the electrode. The discharge was initiated by an igniting spark with an ignition energy of more than 0.1 J and a main pulse voltage of 100-250 kV; the composition of the plasma and the energy of its particles during ignition on the cathode or on the anode were studied. The anode and cathode were made of different materials. With ignition on the cathode ions of the anode material appeared in the plasma only if the current of the main discharge was substantial (1.5-2 kA, when both electrodes were made of stainless steel or nickel, and 0.5-0.8 kA with a lead anode). During ignition on the anode ions of the cathode material were always present, in addition to the ions of the anode material. Triggering of the main discharge with ignition on the anode was strongly impeded with heating of a tungsten cathode to 2000°C. The velocity of ions in the plasma propagating from the electrodes during discharge with ignition turned out to be the same for the plasma forming during natural breakdown of a vacuum gap (see Section 1, Chapter 4).

It is logical to assume, as did Simonov and Kutukov [234], Flynn [235], and M. Goldman and A. Goldman [236] that the development of the main discharge in systems with ignition is connected with the propagation in the main interelectrode gap of the plasma which forms in the igniting spark. In order to obtain quantitative relationships, Flynn assumed that a current whose magnitude is limited by the natural space charge, i.e., determined by the "three/two" law, is "pumped out" from the leading edge of a plasma propagating in the discharge gap.

the "three/two" law. As the plasma moves it fills the gap to an ever greater degree and, as it were, shorts out the portion of the interelectrode gap which it has passed; the entire voltage is applied to the remaining portion of the gap. According to the "three/two" law this leads to a strong growth in current in the gap, thanks to which the capacitance of the electrodes and the structural elements connected directly to them is discharged. In view of the short term of the process the "support" of the discharge from the high-voltage generator is usually less essential than that due to the discharge of the indicated capacity.

Thus, we will assume that the plasma from a local source on one of the electrodes is propagated in the gap in the form of a diverging flow with the rate of motion of the leading front of the plasma, v_{pl}, and the angle of the divergence of the plasma flow being constant in time. Then the current from the frontal surface of the plasma, "pulled out" by the electrical field between the plasma and the opposite of electrode, will equal for the plane case (according to the "three/two" law)

$$I = \frac{\varepsilon_0}{9\pi}\sqrt{\frac{2e}{m}}\frac{U^{3/2}}{(d - v_{пл}t)^2}s\left(\frac{v_{пл}t}{d}\right)^2, \qquad (34)$$

[пл = pl]

where besides the accepted designations, s equals the area of the frontal surface of the plasma when the latter reaches the opposite electrode. If, in agreement with the above, we ignore support from the high-voltage generator, then

$$I = -\frac{dU}{dt}C_{ш}, \qquad (35)$$

[ш = sh]

where C_{sh} is the capacity of the electrodes.

For greater clarity it is convenient to shift to relative quantities and to express the time t, voltage U, and current I in fractions, respectively, of the time T of plasma propagation to

the opposite electrode, the initial voltage U_0, and the current defined by the expression

$$I_1 = \frac{t_*}{9\pi}\sqrt{\frac{2e}{m}}\frac{U_0^{3/2}}{d^2}s$$

(in subsequent calculations all the relative values are noted by an asterisk – e.g., I_*, U_*, etc.). Besides this, it is useful to introduce the parameter $\eta = U_0 C_{sh}/TI_1$, characterizing the electrical charge accumulated in the electrode capacity C_{sh}. Like I_1, the quantity η depends on the direction from which the plasma is propagated – from the cathode (electron current) or from the anode (current of positive ions). For example, when d = 5 mm, $s = d^2$, C_{sh} = 60 pF, $v_{pl} = 5 \cdot 10^6$ cm/s, and U_0 = 60 kV the quanlity η = 1.5 with propagation of plasma from the cathode and $\eta > 60$ with propagation from the anode. Using these relative units, the following expressions can be obtained from equations (34) and (35):

$$I_* = \frac{t_*^2}{(1-t_*)^2}U_*^{3/2}; \qquad (36)$$

$$U_* = \left\{\frac{1}{2\eta}\left[t_*\frac{2-t_*}{1-t_*} + 2\ln(1-t_*)\right] + 1\right\}^{-2}, \qquad (37)$$

characterizing the change in current and voltage when $t_* = 0\text{-}1$. Figure 64 shows these curves, while Table 54 shows the maximum instantaneous values of current I_{*max} calculated on the basis of expressions (36) and (37) for various η and the values of voltage and time $U_* I_{max}$, $t_* I_{max}$ corresponding to the current maximum.

The given value of I_{*max} in Table 54 is also the maximum current of spark discharge. It is clear that when $\eta >> 1$ this current is virtually proportional to η^2 – i.e., to the square of the capacity of the electrodes, C_{sh}. However, it should be noted that the calculation does not consider the inductance of the discharge (strictly, that of the electrodes and the discharged channel).

Table 54. Maximum value of discharge current I_{*max} and the values of $U_{*I_{max}}$ and $t_{*I_{max}}$ when the interelectrode gap is filled with plasma.

η	$I_{*макс}$	$t_{*I_{макс}}$	$U_{*I_{макс}}$	$\frac{I_{*макс}\, t_{*I_{макс}}}{\eta}$
0,1	0,26	0,44	0,56	1,11
0,3	0,72	0,6	0,48	1,44
1	2,8	0,78	0,35	2,18
3	12,1	0,9	0,26	3,6
10	87	0,97	0,18	8,4
30	610	0,99	0,14	20
100	6000	0,997	0,12	60

[макс = max]

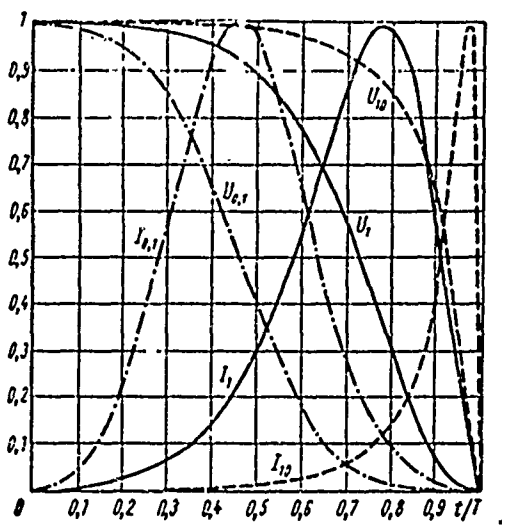

Fig. 64. Change in current and voltage in relative units when the interelectrode gap is filled with a moving plasma. (Subscripts at U and I – values of η).

Propagation of a plasma over the entire discharge gap up to the positive electrode requires that at any moment of time more charged particles arrive on the frontal surface of the plasma due to the thermal velocity v_T than are drawn off by the current to the opposite electrode. In particular, such a condition must be fulfilled with I_{*max}. This makes it possible to evaluate the total number of particles of one sign in the plasma – a necessary factor for propagation of the latter over the entire extent of the

discharge gap. Considering that n particles arrive on a unit surface at the boundary due to thermal motion 0.25 v_T and that under the assumed conditions the number of particles per unit volume, n, diminishes from the source of the plasma as the square of the distance, we can write the following relationship for the necessary total number of charged particles of the same sign in the propagating plasma:

$$N_{\text{мин}} = \left(4\frac{v_{\text{пл}}}{v_T}\frac{I_{*\text{макс}}\, t_{*I_{\text{макс}}}}{\eta} + 1\right)\frac{C_{\text{ш}}\, U_0}{e}. \qquad (38)$$

[мин = min; пл = pl; макс = max; ш = sh]

In this expression the second term on the right side takes into account the number of particles required for discharge of the charge accumulated on capacitance C_{sh}; values of $I_{*max}t_{*I_{max}}/\eta$ are given in Table 54.

When the plasma source is located on the anode then, other conditions being equal, η and (according to Table 54) $I_{*max}t_{*I_{max}}/\eta$ are larger than when the plasma source is located on the cathode. Besides this, for a plasma propagating from a local source in the form of a vacuum spark

$$v_{t.e} > v_{pl} > v_{t.i}, \qquad (39)$$

where $v_{t.e}$ and $v_{t.i}$ are the thermal velocities of electrons and ions, respectively [234]. Thus, the conditions for filling a discharge gap with plasma during motion of the plasma from the cathode to the anode are identical. In the second case (during propagation from the anode) the required quantity of plasma is significantly greater. This apparently can be explained to some degree by the differences described above in the phenomena observed during ignition on the cathode and ignition on the anode, when the plasma which is formed is comparable to the charge stored in the electrode capacitance with respect to the total charge of particles of the same sign.

The fact that a plasma which is generated on the cathode fills the discharge gap more easily and thus leads to arc discharge (like the substantially lower required energy of the igniting spark during ignition on the cathode as compared with the case of ignition on the anode) still is not proof that during natural breakdown of vacuum insulation the interelectrode gap is filled by plasma formed on the cathode. More than this, with minimum energy of the igniting spark (values given in Table 53), the quantity of plasma forming in the igniting spark is several orders less than that required to short-circuit the interelectrode gap. Therefore this shorting requires that a significantly greater quantity of plasma be formed as the result of subsequent processes on the electrodes. It is logical to assume that during natural breakdown of vacuum insulation the actual process which initiates vacuum breakdown is scarcely capable of creating a quantity of plasma on either electrode which is sufficient to short out the discharge gap. In other words, during natural breakdown the required quantity of plasma is also formed as the result of some sort of secondary processes. The fact that during breakdown the propagation of glow in the gap moves from the anode can be interpreted as evidence that the anode will be the site of formation of the plasma which then shorts out the discharge gap. Clearly, this is the result of bombardment of the anode by electrons.

If the plasma in the interelectrode gap is formed "on the spot," i.e., due to ionization of residual gas, the discharge does not develop in time in the same way as when the gap is filled with plasma propagating from a local source. In particular, the duration of the spark discharge should depend on the residual pressure, since the higher the pressure the more rapidly will the formation of plasma occur in the interelectrode gap and the faster will be the transition to arc.

The process of the formation of a plasma due to ionization of residual gas was examined analytically by Steenbek [237] and by

Fünfer [227] under the assumption that there is a sufficiently powerful source of electrons on the cathode – e.g., an igniting spark. Then the current between the electrodes is an electron current and it is limited by the natural space charge until the moment when a plasma is formed in the gap. Ionization of the residual gas leads to an accumulation of positive ions in the gap, while at the same time the electrons which are formed travel to the anode, due to their great mobility. As the accumulation of positive ions increases the space charge of the main electron current is compensated ever more completely; this leads to a growth in this current between the electrodes, until the average volume densities of the electron q_e and ion q_i charges are comparable in the first approximation.

With this outline of the development of discharge the rise in the density of the space charge of ions in time equals

$$q_и = n_0 \sigma_i \int_0^t j_э \, dt, \qquad (40)$$

[и = i]

where n_0 is the number of molecules of residual gas per unit volume and σ_i is the ionization cross section of its electrons, for which the current density equals j_e. Then we can write

$$j_э = q_э \sqrt{\frac{2eU}{m_э}}; \quad q_и \approx q_э; \quad j_э s = -C_ш \frac{dU}{dt}, \qquad (41)$$

[э = e; и = i; ш = sh]

where s is the area of the electrodes encompassed by the discharge current and C_{sh} is the capacity of the electrodes. From this the law of the change in discharge current will take the form

$$I = s j_э = n_0 \sigma_i q_Σ \sqrt{\frac{2e}{m_э}\left(U_0 - \frac{q_Σ}{C_ш}\right)}, \qquad (42)$$

[э = e; ш = sh]

where $q_Σ = s \int_0^t j_э \, dt$ is the charge passing the discharge gap. The

value of the current will be maximum:

$$I_{макс} = 0{,}54\sqrt{e/m}\,C_ш U_0^{3/2} n_0 \sigma_i$$

[макс = max; ш = sh]

where $q_\Sigma = 0.67U_0C_{sh}$ – i.e., three times less than initial U_0 at the instantaneous voltage.

With such an outline of its development, the duration of discharge depends on the value of the initial current I_0: with a very small initial current the accumulation of ions will proceed slowly. In practice the duration of discharge is determined from oscillograms and is usually equated to the intervals of time during which the current grows to the maximum from a quantity which is approximately 10 times less. Then by transforming expression (42) it is not difficult to obtain the duration of current rise or the duration of the spark stage of the discharge:

$$\tau_{0.1-1} \approx \frac{3}{n_0 \sigma_i}\sqrt{\frac{m}{2eU_0}}. \qquad (43)$$

In this case it is assumed that $I_0 < 0.1I_{max}$.

The fact that the discharge time is inversely proportional to the residual pressure and also the fact that $\tau_{0.1-1}$ is independent of the size of the gap, both of which ensue from relationship (43), serve as convenient criteria for checking the correctness of the initial assumption and in particular for clarifying the factor which is determining in a specific case – formation of the plasma "on the spot" or propagation of plasma into the gap from a local source on one of the electrodes. In the second case the time span of the spark stage does not depend on residual pressure and should increase with a growth in the interelectrode distance.

According to quite numerous measurements of the dependence of current rise time on pressure for discharges with an igniting spark,

a reduction in $\tau_{0.1-1}$ is observed only at a pressure exceeding a determined level (in mm Hg): according to Boim and Reykhrudel' [233], $8 \cdot 10^{-5}$; Fünfer [227], $3 \cdot 10^{-4}$; Reykhrudel' et al. [238], $2 \cdot 10^{-3}$. According to measurements made by Flynn [235], at 100 kV and with d = 3.5 mm the average duration of a spark discharge in the range $4 \cdot 10^{-6}$–$2 \cdot 10^{-3}$ mm Hg did not depend on pressure and comprised 3.5 μs.

This large scatter in the results obtained by different researchers is explained primarily by the difference in experimental conditions and in particular by the different degree of degassing of the electrodes [233] and in the composition of residual gases [238, 239]; different interelectrode distances also played a substantial part. According to measurements made by Reykhrudel' et al. [238], in that region of pressures where the formation of plasma due to ionization of residual gas is decisive the lifetime of the spark stage of discharge actually does not depend on the interelectrode gap as the latter varies in the range 50 to 150 mm.

The parameters of the igniting spark (its intensity) should also have a definite influence on the development of discharge. When ignition is more intense a hotter plasma is formed and there is a larger quantity of it. Therefore, with the other parameters remaining unchanged, rapid filling of the interelectrode gap by this plasma becomes more probable. In many cases the voltage to the igniting electrode is supplied from the same source as that to the main electrode, but it passes through an additional resistance. The magnitude of this resistance determines the current of the igniting discharge and, consequently, also its intensity. Therefore when the integrated resistance is small the basic discharge should develop more rapidly, especially in the region of low pressures where the role of ionization of residual gases is small. This has been confirmed experimentally [233].

3. THE ARC STAGE OF VACUUM DISCHARGE

Arc discharge and in particular an arc in vapors of electrode materials (to which an arc between electrodes in vacuum is reduced) has been the subject of a very substantial number of original works. The phenomenological description of arcs and processes on electrodes and also the outline of existing theoretical concepts are given in a number of large monographs (in particular in [240, 241]). This allows us here to limit ourselves to the phenomenological description of the common properties of arc processes arising after breakdown of vacuum insulation without going deeply into the physical essence of the phenomena. In this and the following sections of this chapter a certain emphasis has been laid on those problems which for one or another reason have not been clarified sufficiently in the indicated monographs or have not been considered at all.

The maximum magnitude of current during arc discharge usually is limited only by the parameters of the external electrical circuit; the minimum magnitude is limited by the physical processes which accompany the passage of current in the discharge gap and which are supported by high electrical conductivity of the latter. If the current which can be supplied by the external circuit is too small to maintain these processes the arc is terminated, i.e., goes out. Figure 65 shows a typical oscillogram of current after breakdown for such a case. Here the exponential drop in the current occurs due to the discharge of the filter capacity of the supplying high-voltage generator; when this current drops below a certain value the arc is cut off. Table 55 shows the values of currents at which arc quenching occurs. Each point shows the results of 10-15 measurements. The data in the table, like those in Fig. 65, were taken from the work by Denholm [46].

According to more detailed investigations [242-244], an arc in a vacuum possesses internal instability which creates the

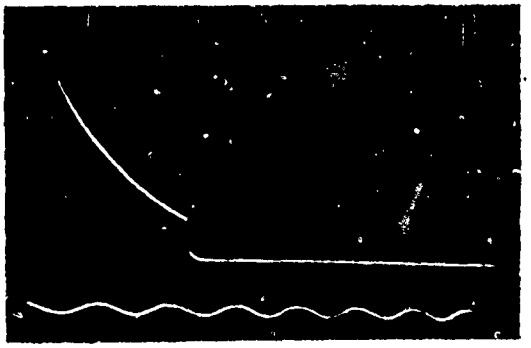

Fig. 65. Oscillogram of the current of a spark discharge between copper electrodes (d = = 1 mm; current amplitude 5 A; quenching current 0.95 A; U_{br} = = 58.2 kV; R_d = 11 kohm; scale gradation 0.2 MHz).

Table 55. Arc quenching currents (minimum currents of vacuum arc).

(1) Материал	(2) Зазор, мм	(3) Значение тока обрыва, а		
		максимальное (4)	минимальное (5)	(6) среднее
Сталь (7)	0,2	0,86	0,19	0,51
	0,3	1,3	0,14	0,52
	0,5	0,78	0,13	0,31
Медь (8)	0,5	2,0	0,33	0,74
	1,0	2,3	0,48	0,67
Алюминий (9)	0,5	0,58	0,14	0,29
	1,0	0,72	0,17	0,35

KEY: (1) Material; (2) Gap, mm; (3) Value of quenching current, A; (4) maximum; (5) minimum; (6) average; (7) Steel; (8) Copper; (9) Aluminum.

possibility of its arbitrary suppression in a broad range of current values. With the parameters of the external circuit remaining unchanged and with a steady-state current the duration of arc burning is subject to the probability law: during repeated measurements the number of arcs burning in the course of time t or longer is

$$N \sim \exp(-t/\tau_{av}),$$

where τ_{av} is the average duration of arc burning under the given conditions. The time τ_{av} depends mainly on the cathode material and on the magnitude of the current. Table 56 gives experimental data which characterize this relationship.

Table 56. Arc currents corresponding to certain average durations of arc burning.

(1) Катод		(2) Ток дуги при разных значениях $\tau_{ср}$, а				
(3) Материал	(4) Состояние	10^{-5} сек [243]	10^{-3} сек		0,1 сек	
			[243]	[244]	[243]	[244]
	(5)					
Hg	Жидкий	0,03	0,35	0,65	1,7	2
Ga	»	—	—	12	—	40
Sn	»	—	—	8	—	47
Cu	Твердый	2,5	4,6	16	31	—
Ag	(6)»	1,3	2	—	9	—
Sn	»	—	—	5,5	—	10
Al	»	2	3,3	15	30	—
Mo	»	4	12	—	—	—
W	»	4	8,5	—	—	—

KEY: (1) Cathode; (2) Current of arc at different values of τ_{av}, A; (3) Material; (4) State; (5) Liquid; (6) Solid.

Designation: сек = s = second.

The random nature of arc suppression leads to a situation in which at any moment of time some probability exists, different from zero, that a critical state at which the arc may be quenched will arise. The fact that such states do occur is confirmed by the presence of voltage flashes on the oscillograph which rise above the level of the normal voltage drop on the arc. These flashes, which have the nature of virtually continuous noise (individual pulses and pulses arranged in groups) represent nothing other than pulses of restoring voltage with more or less complete and sharp quenching of the arc and subsequent breakdown of the discharge gap in strongly eased conditions created by the preceding burning of the arc. The rate of voltage rise during quenching or reduction of the current depends on the parameters of the electrical circuit: the inductance and resistance in the circuit of the discharge current and the capacity which shunts the discharge gap. With a more rapid voltage rise the restoration of the arc is more probable. Therefore an increase in inductance and a reduction in the shunting capacity will increase the average duration of arc

burning. Clearly this is one of the reasons for the divergence between the results obtained by Kesayev [244] and those obtained by Kobine and Ferrall [243] (Table 56). In Kesayev's experiments the inductance did not exceed 100 μH, while Kobine and Ferrall show a value 1.5-3.5 times greater. At the same time in the first of these works the supply source voltage was smaller, which also favored suppression of the arc. According to the data from Kobine and Ferrall, the average duration of arc burning for copper electrodes with a current of 5 A was reduced by three times (from 0.3 ms) with an increase in the shunting capacity from 85 to 1000 pF.

The voltage at which the arc burns depends very little on the current which is flowing. Usually it is somewhat reduced with an increase in current. Table 57 gives values of the voltage drop on the arc obtained by Reece [245, 246] with different electrode material.

Table 57. Voltage drop on a vacuum arc with electrodes of different material.

(1) Материал	ΔU, в	(1) Материал	ΔU, в
Hg	8	Al	16
Bi	8,1	Ni	16,5
Sb	9	Нержавеющая сталь (2)	16,5
Pb	9,6	Ag	17
Cd	10	W	17,5
Zn	11	Графит (3)	20
Na	11	Cu	21
Sn	11,5	Сталь при комнатной температуре (4)	32
Mg	12	Сталь, нагретая выше точки Кюри (5)	17
Mo	15		

KEY: (1) Material; (2) Stainless steel; (3) Graphite; (4) Steel at room temperature; (5) Steel heated above the Curie point.

Designation: в = V.

4. RESTORATION OF ELECTRICAL STRENGTH OF VACUUM INSULATION AFTER SPARK AND ARC DISCHARGES

To determine the time required to restore electrical strength of vacuum insulation after breakdown, Maitland [247] applied two high-voltage pulses successively to the pair of electrodes under study. The first pulse, of constant amplitude, caused a breakdown; Maitland altered the amplitude of the breakdown in order to determine the voltage at which repeated breakdown would appear. The interval between pulses was regulated from 6 to 400 μs. The duration of the pulses themselves was 4 μs and the resistance of the discharge circuit was 20 kohm; during the first breakdown a charge of approximately 20 μC passed through the discharge gap. The electrodes were made from stainless steel and the gap between them was unchanged throughout the experiments at a value of 0.42 mm; the vacuum was $2 \cdot 10^{-5}$ mm Hg. Under these conditions the minimum voltage at which the probability of breakdown was close to unity comprised 38 kV. Figure 66 shows the results of the experiments – the average magnitudes of the voltage of the repeated breakdown and the scatter which was observed. The amplitude of the first pulse, 58 kV, corresponded to 50% overvoltage. From the given data it is clear that restoration of electrical strength is rapid (about 6 kV/μs) in the first few microseconds and continues for more than 400 μs at an ever-slowing rate; this is particularly noticeable during the more intensive first breakdown (at 58 kV). This time was substantially greater than the time of deionization in the volume and is even greater than the time required to cool the sites of local heating on the electrodes during the first breakdown.

Visual observations gave very interesting results. It was found that the channel for the repeated discharge arises, as a rule, at a certain distance from the channel of the first discharge; the distance between them may reach 10 mm. Clearly the processes

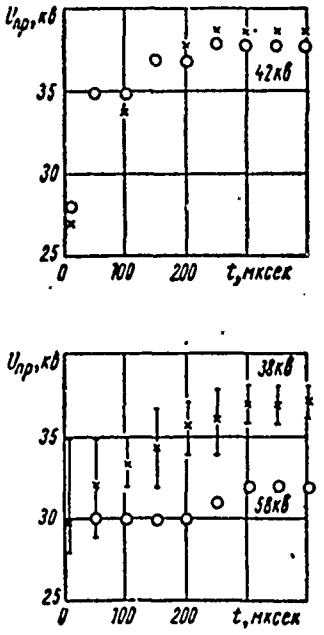

Fig. 66. Voltage of repeated breakdown as a function of the time interval between the first and second breakdowns for stainless steel electrodes (d = 0.42 mm). Figures on the graphs represent the amplitude of the first pulses.

Designations: кв = kV; мксек = = μs.

[пр = br]

during discharge after the first breakdown create favorable conditions for the subsequent breakdown at a certain distance from the channel of the first discharge.

The influence of the magnitude of the arc current of the preceding discharge on the repeated discharge voltage with application to vacuum switches was the object of a study by Khalifa [161]. Voltage with a frequency of 5 kHz was applied to the electrode at a given time interval after the pulse of discharge current in the form of a single semisinusoid of industrial frequency. Table 58 gives the values of 50% of the breakdown voltage for steel electrodes with a gap of 3.5 mm between them.

5. TRANSFER OF MATERIAL BETWEEN ELECTRODES AND DESTRUCTION OF ELECTRODES DURING SPARK AND ARC DISCHARGES

The changes in the electrode surfaces during vacuum discharges and even under prebreakdown currents are easily detected even with the unaided eye. More exact methods of observation make it

Table 58. Breakdown voltage with different time intervals after the passage of a current pulse through a 3.5 mm gap.

(1) Временной интервал, мксек	(2) Напряжение повторного пробоя после прохождения разных импульсов тока, ке			(1)' Временной интервал, мксек	(2) Напряжение повторного пробоя после прохождения разных импульсов тока, ке		
	44 а	85 а	170 а		44 а	85 а	170 а
2	6	5,2	4,5	54	32	28	22
12	13,5	12	8,5	75	35	35	27
35	24	22	18	95	—	—	29,5

KEY: (1) Time interval, μs; (2) Voltage of repeated breakdown after passage of different current pulses, kV.

Designation: а = A.

possible to reveal a number of interesting phenomena. During microscopic observation on the surface of an anode after comparatively low-power breakdowns, Maitland [177] detected the appearance of a great number of fine craters about 1 μm in diameter as the result of breakdowns. These craters were grouped in separate spots which were quite visible to the naked eye. Their diameters grew with an increase in the breakdown voltage (correspondingly, with an increase in the interelectrode gap), while the number of craters formed at each breakdown reached 5000-24,000 with a copper anode and 20,000-40,000 with a molybdenum anode. The shape of these craters also depended on the anode material. For example, on stainless steel they were formed, as a rule, around carbide inclusions which project in the form of very fine mounds in the center of the craters [51].

The intensity of anode destruction depends on the energy liberated on the electrodes during spark discharge. If the capacity which is connected directly to the electrodes is significant, brightly shining metallic particles of microscopic and even larger size will fly off from the anode [248]. The quantity of escaping particles grows with an increase in the nonuniformity of of the field and depends on the material of the electrode — for

example, there are more of them with graphite electrodes than with tungsten. The speed of the particles is 5-15 m/s. The particles are always positively charged, with the specific charge being 10^{-3}-10^{-1} C/kg [249]. However, even with a strongly limited post-breakdown discharge the removal of material from the anode and its transfer to the cathode occurs to a significant degree in the form of individual particles (see Fig. 81 in Chapter 8).

The changes on the cathode during postbreakdown discharge have a different form. At low spark energy this takes the form basically of a tarnish consisting of material transferred from the anode; the material is rather weakly bound to the basic mass of the cathode and when the cathode and anode are made of different materials the film of transferred materials is peeled off and flakes away [123]. With a discharge of greater power drops of molten metal appear on the cathode [164] (Fig. 67 in [164]).

Investigations using tagged atoms and spectroscopic methods [149-151] made it possible to establish that during a postbreakdown spark material is transferred not only from the anode to the cathode but also in the opposite direction – although in a substantially smaller quantity.

Tarasova and Razin [149] studied the transfer of electrode material from one to another during postbreakdown discharge with a capacity of 10^{-7}-10^{-8} F through a controlled resistor. Using the tagged-atom procedure, they found that with copper electrodes the quantity of material transferred from the anode to the cathode depends on the magnitude of the resistance connected into the circuit and is proportional to the charge which is passed; with R_d = 20 kohm approximately $2 \cdot 10^{-5}$ g/C is transferred; with R_d = = 5 kohm the quantity is 10 times greater, while at R_d equal to zero the transfer from the anode to the cathode reaches 0.1 g/C. Transfer of material in the opposite direction – i.e., from the cathode to the anode – does not depend on the magnitude of R_d and

comprises approximately 10^{-5} g/C. The voltage before breakdown in all these experiments comprised 50-100 kV. Judging from the data given, transfer from the cathode to the anode is simply proportional to the charge passing through the interelectrode gap, while transfer from the anode to the cathode not only depends on this charge but also grows with an increase in the amplitude of the discharge current. Although no oscillographing was done during these measurements, the parameters of the electrical circuit nonetheless provide a basis to assume that the obtained information on transfer of material relates to the spark stage of the discharge.

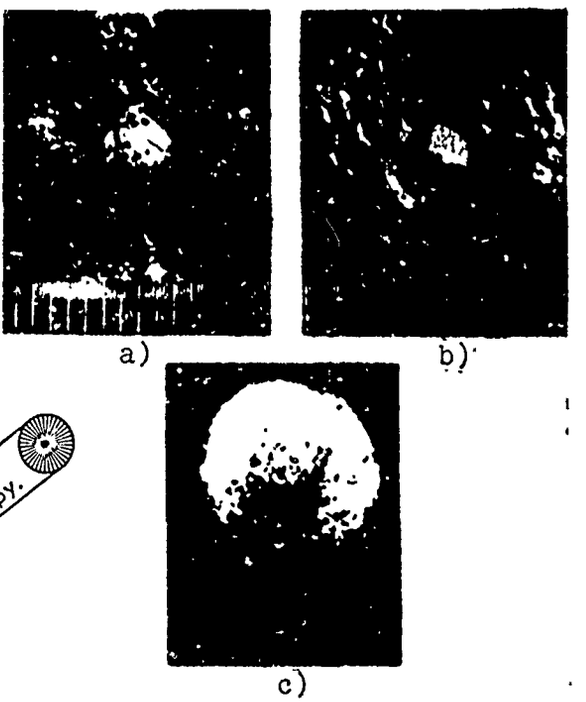

Fig. 67. Changes on the surface of electrodes after breakdown: a – segment of the surface of a steel anode prior to breakdown; b – the same, after breakdown; c – surface of a molybdenum cathode from the same experiment, after breakdown.

The destruction of electrodes and transfer of material during arc discharge differ from similar phenomena during a vacuum spark. With an arc the destruction on the cathode and the removal of

material from the cathode are substantially greater than on the anode. For example, during a discharge lasting 2 ms with the capacity of 1-5 μF through a vacuum gap of 0.25 mm between steel electrodes (per measurements by Kalifa [161]), the change in the weight of the cathode and anode are characterized by the quantities given in Table 59.

Table 59. Change in the weight of electrodes after discharge through a 0.25-mm vacuum gap with a large capacity in the course of 2 ms.

(1) Заряд емкости, $\times 10^{-3}$ к	(2) Изменение веса электрода, мкг/разряд		(1) Заряд емкости, $\times 10^{-3}$ к	(2) Изменение веса электрода, мкг/разряд	
	катода (3)	анода (4)		катода (3)	анода (4)
40	−2,6	+0,8	120	−8,5	+2,5
60	−4	+1,6	160	−12	+4
80	−5,5	+1,8			

KEY: (1) Capacity charge, $\times 10^{-3}$ C; (2) Change in weight of electrode, μg/discharge; (3) cathode; (4) anode.

The increase in anode weight occurs because of transfer of cathode material to it.

The data given in the table fit into the empirically selected formulas

$$\left.\begin{aligned}\Delta G_к &= -0{,}05\, q_\Sigma^{1{,}074};\\ \Delta G_а &= 0{,}029\, q_\Sigma^{0{,}94},\end{aligned}\right\} \qquad (44)$$

where q_Σ is the charge passing [through the gap] (in millicoulombs per discharge) and ΔG is the change in weight (in micrograms per discharge). It is interesting that measurements in air with the same electrodes and electric-circuit parameters gave

$$\left.\begin{aligned}\Delta G_к &= -2{,}48\cdot 10^{-6}\, q_\Sigma^{2{,}8};\\ \Delta G_а &= 1{,}15\cdot 10^{-6}\, q_\Sigma^{2{,}8}.\end{aligned}\right\} \qquad (45)$$

Thus, when $q_\Sigma > 0.35$ C the transfer of material from the cathode to the anode and the consequent destruction of the cathode

is less in vacuum than at atmospheric pressure; when $q_\Sigma < 0.35$ C the picture is reversed.

In connection with the development of electrodynamic plasma beams of the rail type, where the plasma is obtained through ionization of electrode material, Vargo and Taylor [250] studied the erosion of electrodes during discharge through a vacuum gap with a capacity of great magnitude (100-300 μF) charged to 10-20 kV. The quantity of electrode material deposited on the walls of the vacuum chamber was directly proportional to the electrical charge passing through the vacuum gap. This charge equaled that stored in the capacitor only with aperiodic discharge; with an oscillatory discharge the magnitude of the charge passing through the vacuum gap (the sum of absolute quantities of charge passing in either direction) grows and there is a corresponding growth in the erosion of the electrodes. Quantitative data are given in Table 60. The maximum value of the resistance in the discharge circuit was 3 ohm.

Table 60. Erosion of electrodes (reduction in weight) during strong-current discharge.

(1) Материал электродов	$\Delta G, \times 10^{-4}$ г/к		
	(2) максимальная	(3) минимальная	(4) средняя
Sn	12	5,3	8
Al	11	6	9,6
Ag	6	4,2	5
Cu	6,7	1,3	3
(5) Нержавеющая сталь	6	1,8	3
Ti	3,5	0,9	2,1
Mo	2,7	1,5	2
W	5,3	1,2	3,6

KEY: (1) Electrode material; (2) maximum; (3) minimum; (4) average; (5) Stainless steel.

Designation: г/к = g/C.

Although the authors did not detect a dependence of erosion on current magnitude (possibly because of the small range of variation of the parameters), it is evident nonetheless that erosion grows with an increase in current. At least such a conclusion suggests itself from comparison of the data in Tables 59 and 60.

CHAPTER 7

FORMS OF ELECTRICAL DISCHARGE IN GASES AT LOW PRESSURE IN THE REGION OF THE LEFT BRANCH OF THE PASCHEN CURVE

1. INTRODUCTION

The domain of vacuum breakdown for interelectrode gaps on the order of several centimeters corresponds to a residual gas pressure below 10^{-4}-10^{-5} mm Hg. At higher pressures gas discharge occurs.

In the presence of a magnetic field gas discharge can occur at lower pressure – i.e., in that region of pressures which is ordinarily considered to be the domain of vacuum insulation. It should be noted that atoms of adsorbed gas are usually present on the surface of electrodes in vacuum instruments and equipment. The quantity of adsorbed gas can be such that during its desorption under the action of any factor in the interelectrode gap a pressure is created at which different forms of gas discharge can occur. Causes of desorption of gas from the electrodes can include microdischarges, heating of the electrodes, etc. As was already noted in Chapter 3, during passage of a microdischarge from the electrodes approximately $2 \cdot 10^{16}$ atoms of gas are liberated, on the average; for example, in a volume of 10^3 cm^3 they create a pressure corresponding to conditions of the appearance of gas discharge. For a more complete understanding of the electrical processes occurring

in a vacuum it is necessary to consider the appearance of gas discharge at low pressure.

The discharge ignition voltage in a system of plane-parallel electrodes in a gas obeys the well-known Paschen law $U = f(pd)$, where p is the gas pressure and d is the distance between electrodes.

Figure 68 shows Paschen curves for several gases. As is evident from the figure, the curves have a minimum corresponding to the values pd ~ 0.1-5 (mm Hg)·cm. In the domain of higher values of pd a smooth growth is observed in discharge ignition voltage U_i (right branch of the Paschen curve). With values $pd < pd_{min}$ the ignition voltage grows sharply, reaching values of several tens and hundreds of kilovolts (left branch of the Paschen curve). This chapter is concerned with the forms of discharge which arise between the electrodes when $d \approx 1\text{-}10^2$ cm and the gas pressure is $10^{-2}\text{-}10^{-4}$ mm Hg – i.e., when $pd < pd_{min}$.

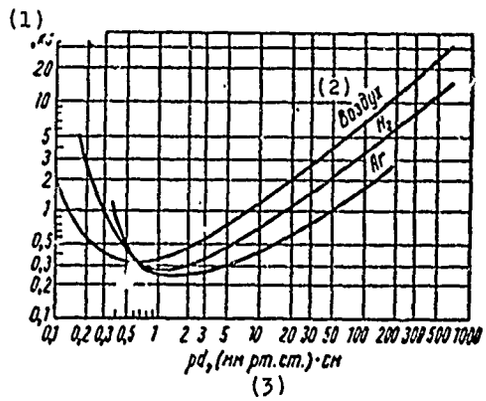

Fig. 68. Paschen curves.
KEY: (1) U_i, kV; (2) Air; (3) pd, (mm Hg)·cm.

Figure 69 shows characteristic curves of the dependence of ignition voltage U_i on pd in the region of the left branch of the Paschen curve for various gases. A large volume of information can be found in the book by Meek and Krags [253] and in the monograph by Loeb [254] concerning the dependence of U_i on pd for various gases, electrode materials, and other physical conditions. For the majority of gases (for example, such as air or mercury

vapor) the discharge ignition voltage coincides for different products of the factor pd in similar discharge gaps. However, it should be noted that ignition of discharge in uniform electrical fields does not obey the law of similarity in those cases when the intensity of the electrical field in the cathode region exceeds the quantity 10^6 V/cm and field-effect emission begins to play a role. These deviations occur either at extremely high gas pressures (on the order of tens of atmospheres), when voltage reaches hundreds of thousands of volts, or at very small gaps [255, 256].

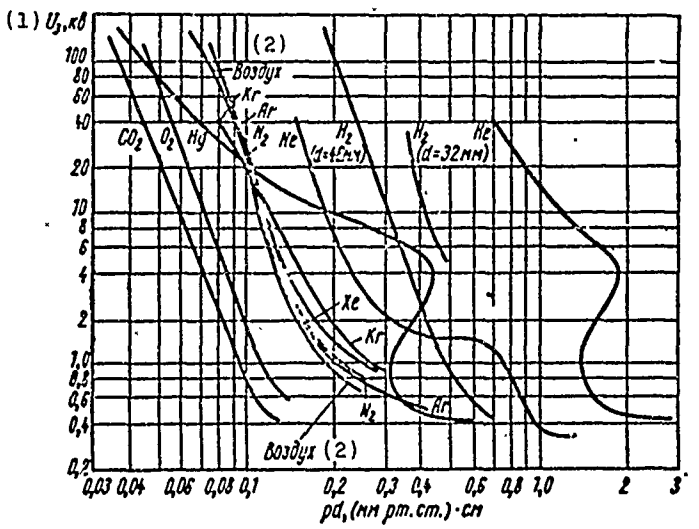

Fig. 69. Left branches of the Paschen curve in various gases. References: for N_2, O_2, CO_2, air, and H_2(d = = 46 mm), [252a]; for He, Ne, Ar, Kr, and Xe, [251]; for Hg [252]; for H_2(d = 32 mm), [257].

KEY: (1) U_i, kV; (2) Air.

Designation: мм рт. ст. = mm Hg.

A deviation from the law of similarity for ignition of a discharge in uniform electrical fields in hydrogen at $pd < pd_{min}$ was detected by Pokrovskaya-Soboleva and Klyarfel'd [257]. In this case the ignition potential can be presented as follows:

$$U_s = f(p_0 d^{0.58}), \quad (46)$$
$$[s = 1]$$

where p_0 is the pressure of the gas, reduced to 0°C. The authors offer only general considerations with respect to the reasons for the departure from the law of similarity.

2. VARIOUS FORMS OF DISCHARGE IN A UNIFORM ELECTRICAL FIELD AT LOW PRESSURE

The relationship between the discharge current and voltage and the transition from one form of discharge to another are described by the volt-ampere characteristics. The general characteristic of a gas discharge which is given on Fig. 70 (curve 1; ordinates magnified approximately ten times) was taken from the well-known survey work by Druyvesteyn and Penning [258]. We will examine the volt-ampere characteristics in the range $2 < pd < 20$ (mm Hg)·cm for a system of plane-parallel electrodes (the region of the minimum and right branch of the Paschen curve). The segments of curve 1 corresponding to different types of discharge are separated by broken lines. The first region of independent gas discharge – Townsend or dark discharge – is characterized by a weak influence of the space charge. With a growth in current the space charge of ions begins to play a significant role. The electrical field is concentrated in the cathode region – it approaches the region of transition to glow discharge. The voltage on the discharge drops, a positive column is formed, and normal glow discharge appears. In a glow discharge the electrical field is concentrated basically in the so-called cathode space; therefore the total voltage on the discharge is not great, comprising a few hundred volts. Electron emission from the cathode occurs under the action of ions and light quanta which bombard its surface. With an increase in current the emitting surface of the cathode is extended, while the voltage drop and current density on the cathode remain constant. When the entire cathode surface is encompassed

by the glow discharge, further growth in current can occur only through an increase in its density, which grows as a result of an increase in the cathode drop and contraction of the cathode space.

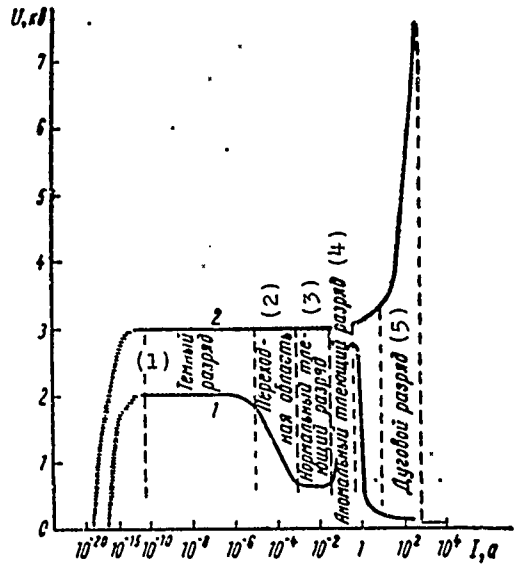

Fig. 70. Volt-ampere characteristics of discharge: 1 — when $pd > pd_{min}$; 2 — when $pd < pd_{min}$.

KEY: (1) Dark discharge; (2) Transition region; (3) Normal glow discharge; (4) Anomalous glow discharge; (5) Arc discharge.

Designations: кв = kV; а = A.

The voltage on a discharge is increased and the following type of discharge sets in: anomalous glow discharge. Finally, with an increase in the number and energy of the ions incident on the cathode and with a reduction in the width of the cathode space (currents on the order of several amperes through the discharge) a completely different mechanism of electron emission from the cathode sets in; cathode spots appear, the voltage on the discharge drops rapidly down to several tens of volts, and stable arc discharge is developed. For a glow discharge a reduction in pressure leads to a situation in which the density of the current is rapidly reduced and the domain of cathode drop is increased.

At very low values of $pd < pd_{min}$ (left branch of the Paschen curve) conditions occur in which the normal glow discharge is completely impossible, since the width of the cathode drop region is greater than the distance between the electrodes. The discharge

which arises in these conditions is characterized by very high burning voltage and therefore is called a high-voltage glow discharge. This form of discharge possesses properties of silent discharge, since it is characterized by weak development of space charges and by properties of the hindered [impeded] glow discharge; this is due to the fact that the increase in the interelectrode distance leads to a reduction of voltage on the discharge. The low density of the space charges of the high-voltage type of discharge is a consequence of the high velocities and great mean free paths of the particles moving in the strong electrical field.

As the current grows the space charge which appears concentrates the field at the cathode, reducing the domain of electron acceleration; also the volumetric ionization of the gas is reduced, since the ionization cross sections for electrons of these energies correspond to values lying to the right of the maximum on the curve showing the dependence of cross section on electron energy. As a result the voltage on the discharge is increased. Moreover, a state can arise in which the current through the discharge is even reduced with an increase in voltage [259].

With the considered values of pd the volt-ampere characteristic of the discharge takes on a completely different character. The domain of normal glow discharge is absent. The voltage on the discharge remains equal to the voltage of ignition until the space charge of the ions, causing a sharp rise in the characteristic (Fig. 70, curve 2), enters into action.

To investigate discharge in the left branch of the Paschen curve, Pokrovskaya-Soboleva and Klyarfel'd [257] used a glass tube containing two electrodes 80 mm in diameter. The field between the electrodes was quite uniform. The distance between the electrodes was varied from 4 to 32 mm. After the appearance of high-voltage discharge in the tube a diffusion glow was observed; its

brightness dropped from the anode to the cathode. The gas used to fill the tube was hydrogen.

As follows from the experiments, high-voltage discharge did not convert to arc during supply of direct current, although the discharge current reached 1 A. In the case when the discharge power supply was of the pulse type (pulse length 4 μs) transition to an arc was observed at a current of 1000 A only at pressures above 0.2 mm Hg. At lower hydrogen pressures there was no transition to arcing, although the total discharge current exceeded 1000 A ($j >> 20$ A/cm^2).

In a more recent work by Klyarfel'd and Guseva [260] it is shown that the rising segment of the volt-ampere characteristic of a high-voltage discharge is explained not only by the formation of a positive space charge between the electrodes and the redistribution of electrical field intensity connected with it, but also and mainly by the formation at the anode of a layer of plasma which is thickened with a further growth in current. Thickening of the plasma layer leads to contraction of the cathode potential drop space. Under the conditions obtaining in the left branch of the Paschen curve this leads to a reduction in volumetric ionization and to an increase in the potential difference required to maintain the discharge. The ion current from the plasma, which accomplishes ionization of gases and stripping of electrons from the cathode, leads to the appearance of new charged particles and consequently can bring about a reduction in voltage on the discharge. Evaluation of this factor showed that its significance is not highly essential. On a certain segment of the curve $U = f(I)$ lying between the horizontal region of the curve and the region of a steep rise a certain growth or reduction in the value of U with respect to the horizontal region is possible. The sign of the change in the level of U can differ for different gases. The reason for these rises or drops in the curve $U = f(I)$ is redistribution of the magnitude of electric field intensity preceding the appearance of plasma at the anode.

In order to clarify the role of various processes in a discharge at low pressure, McClure [261] carried out a series of experiments with pulse high-voltage discharge in deuterium at voltages of 40-80 kV and currents of 0.7-7 A. The voltage pulse length comprised more than 200 μs. Figu · 71 shows the volt-ampere characteristics of a high-voltage discharge referred to the segment of sharp rise in voltage. The data were obtained for a tube with a stainless steel cathode coated with titanium and saturated with deuterium; at pressures of 0.039-0.096 mm Hg the curves are approximated well by the following simple expression:

$$I = af(p)U^k. \qquad (47)$$

Here a and k are constants and f(p) is a function of pressure which can be presented in the form $f(p) = bp^m$, where b and m are constants. As follows from the experiments, a = 3, k = 2.9 and m = 2.6. The volt-ampere characteristics for a high-voltage discharge which were obtained in work [257] are described by an analogous equation.

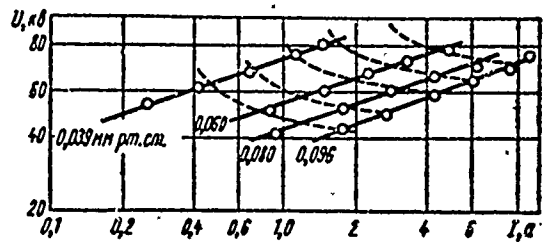

Fig. 71. Volt-ampere characteristics of a pulse high-voltage discharge.

Designations: кв = kV; мм рт. ст. = mm Hg; а = A.

Probe measurements made in such a discharge showed that the discharge which is formed is divided into a region of anode drop, a region filled with plasma, and a region of cathode drop. The density of the electrons of the plasma was, on the average, on the order of $2 \cdot 10^9$ cm^{-3}. The anode drop comprised approximately

9 V and was negative with respect to the plasma, while the potential along the plasma varied by no more than 10 V. A sharp scatter was observed in the region of high energies in the energy spectrum of electrons impinging on the anode; this was caused by electrons which passed the entire distance from the cathode to the anode without experiencing any significant loss of energy to collisions with atoms of the gas, while the continuous portion of the spectrum in the low-energy region was due to secondary electrons formed during ionization. In the energy spectrum of the ions impinging on the cathode D^+ and D_2^+ ions were observed; these had an average energy on the order of 20 kV, when the voltage on the discharge tube was 80 kV.

The formation of ions in the plasma is brought about mainly by secondary electrons knocked out from the glass walls of the tube under the action of high-energy electrons and positive ions. Electrons are knocked out from the cathode both by positive ions and by neutral atoms. These electrons pass through the entire region of the discharge, losing very little energy to collisions. The number of ions forming in the region of a cathode drop is comparable with the flow of ions from the plasma into the cathode region. Ions moving from the plasma into the domain of the cathode drop cause a complex cascade recharging process which results in the formation of 5 to 10 secondary neutral atoms and molecules whose average energy corresponds to approximately 1/5 of the magnitude of the cathode drop in potential. Fast heavy particles formed during the cascade process cause secondary processes during ionization of the gas.

As was shown above, anomalous glow discharge (like high-voltage discharge) possesses a positive volt-ampere characteristic. At low pressures and high current densities the difference in potentials on the electrodes of an anomalous glow discharge can reach tens of kilovolts [262], also as in the case of a high-voltage discharge. In an anomalous glow discharge virtually the

entire voltage drop is concentrated within the limits of the cathode drop space. A difference exists between these two forms; it consists in the fact that in a high-voltage discharge the plasma which forms at the anode is very thin and the density of the ion current proceeding from the plasma to the cathode is not great, while in an anomalous glow discharge the density of the ion current reaches greater values with significant distances between the electrodes. In work [260] it was shown that the role of the magnitude of density of the ion current entering the cathode space is not great either in high-voltage or anomalous glow discharges. Consequently, a high-voltage discharge with a plasma layer at the anode and an anomalous glow discharge are qualitatively identical.

3. DIFFERENCES IN THE TYPES OF DISCHARGE IN CERTAIN GAS-DISCHARGE GAPS IN A MAGNETIC FIELD

Charge e moving perpendicularly to magnetic field H with velocity component v is subject to the action of the force (ev/c)H at a right angle to v and H.

Under the simultaneous action of electrical and magnetic fields the total force equals

$$F = eE + \frac{ev}{c}H. \qquad (48)$$

Thus, the basic effect of the magnetic field is manifested in the fact that charged particles moving at an angle to it describe helical lines around the force lines of the magnetic field. In the majority of cases only the electron trajectories are altered. The trajectories of ions are changed comparatively little under the action of this force; the helical motion increases by far the path of the electron through the gas along the electrical field. The electron collides more frequently with molecules of the gas and has a greater probability of ionizing them. Thus the presence of

a magnetic field acts like an increase in gas pressure, but essentially only in directions perpendicular to the magnetic field.

Considering the curvature of the free path of an ion with molecular weight m and taking the chord between the extreme points as the effective free path, we can show that the apparent increase in pressure Δp will equal

$$\frac{\Delta p}{p} \approx 10^{-2} \frac{l^3}{mT} \left(\frac{H}{p}\right)^2, \tag{49}$$

where l is the mean free path of the electron in centimeters when p = 1 mm Hg, T is the absolute temperature of electrons; H is the magnetic field in oersteds. The numerical factor depends on the assumptions made in equation (49).

By placing several gas-discharge gaps with special electrode configurations in a magnetic field, it is possible to ignite a discharge at low pressure and with a voltage of a few kilovolts, while in the absence of a magnetic field discharge is ignited only at a voltage of several tens or hundreds of kilovolts ($pd < pd_{min}$) or does not arise at all (region of vacuum breakdown).

Investigation of gas discharge at low pressure, arising in electrical and magnetic fields, was begun originally in 1898, when Phillips [263] carried out the following experiment: in order to suppress a glow discharge excited in a glass vessel with two electrodes, he evacuated the volume to a lower pressure. After the discharge was extinguished, when pd was less than pd_{min}, Phillips switched on a magnetic field directed along the axis of the electrodes; in this case a glowing ring appeared between the electrodes and the glass wall (Fig. 72, left). In 1913 Strutt [264] explained the cause of the formation of such a glowing ring by the appearance of discharge due to ionization of the gas in the glass vessel by negative ions moving across the magnetic field: the glass walls of the vessel were positively charged by charged

particle due to the preceding discharge. In order to check this explanation, he placed a cylindrical electrode inside a vessel, putting it close to its inner surface and concentric to the electrodes. When the positive potential on the cylinder was suppressed and when a certain magnitude of magnetic field was switched on a discharge arose between the cylinder and the central electrodes, located under a ground potential (see Fig. 72, right). When Strutt connected the two central electrodes by a metallic cylinder, obtaining a system of two coaxial cylinders located in a longitudinal magnetic field, discharge was ignited with a positive potential on the outer cylinder. Further investigation of these two systems was carried out by Penning [265, 266].

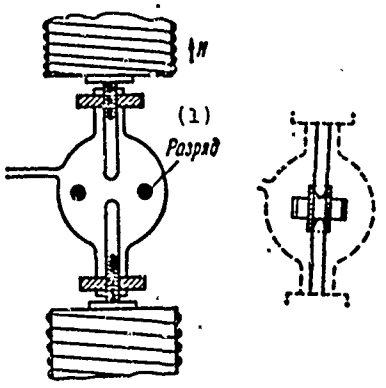

Fig. 72. Discharge tube used in the experiments by Phillips (left) and setup of Strutt's experiment (on the right).

KEY: (1) Discharge.

Investigation of the first system led to the creation of the ionization magnetic discharge manometer. Penning, using the Hall magnetron equation, analyzed the ignition of discharge in a system consisting of two coaxial cylinders in a longitudinal magnetic field with different polarities on the electrodes. He calculated the ranges of voltage and magnetic field within which electrons might pick up sufficient energy in the systems to accomplish ionization.

First we will examine the ignition of discharge in a tube with low pressure in a longitudinal magnetic field. The tube has an annular anode and flat cold cathodes arranged symmetrically on

both sides of it. The force lines of the magnetic field prevent electrons from traveling to the anode, creating for the electrons a region with a potential hole (trap) (Fig. 73). Entering the trap, electrons accomplish oscillations between the cathode and the anticathode, collecting, as it were, an average free path. In practice an electron can penetrate the region of the potential hole only as a result of multiple acts of ionization and scattering on molecules of the gas. In these conditions electrons carry out intensive ionization even at a pressure on the order of 10^{-5} mm Hg, when the length l of the free path is much greater than the distance between the electrodes. In the absence of the magnetic field U_i corresponds to values of pd for the left branch of Paschen curve and even for the region of vacuum breakdown.

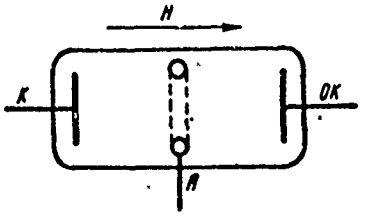

Fig. 73. Discharge tube in a longitudinal magnetic field: A – annular anode; K – cathode; OK – reflecting cathode.

From the solution of the equations of motion of an electron [267] in such a system up to the moment of triggering discharge it is possible to determine the quantity H_{cr} at which electrons will not reach the anode (collisions with gas molecules are not considered):

$$H_{кр} = \frac{2c\sqrt{\frac{2m}{e}(U_a - U_0)\frac{r_a^2 - r_0^2}{r_a^2} + \frac{m^2}{e^2}\dot{r}^2}}{r_a\left(1 - \frac{r_0^2}{r_a^2}\right)}, \qquad (50)$$

[кр = cr]

where U_a is the potential on the anode, U_0 is the potential on the discharge axis, r_a is the anode radius, r_0 is the distance from the axis, and r is the radial velocity.

For the case when $H > H_{cr}$, it follows from the equations of motion of electron that it describes a cycloid in a plane perpendicular to the axis, while simultaneously accomplishing harmonic oscillations along the axis. When $H < H_{cr}$ the trajectory represents an expanding spiral (Fig. 74). Electrons which are formed due to ionization in the discharge gap also participate in two motions. Calculation of the time span and path to arrival on the anode for an electron when $H < H_{cr}$ shows that at a pressure of 10^{-5} mm Hg the distance which it travels will be shorter than the length of the free path. For the ignition and onset of glow discharge at high vacuum a magnetic field $H > H_{cr}$ is necessary.

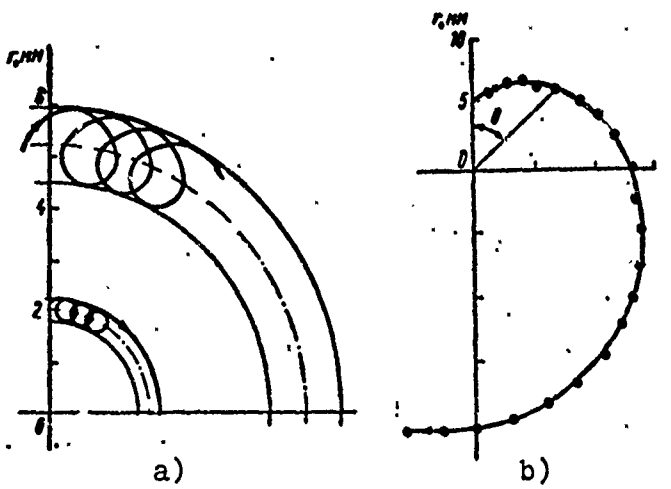

Fig. 74. Projection of the trajectory of an electron to the plane perpendicular to the direction of the magnetic field: a – when $H > H_{cr}$; b – when $H < H_{cr}$.

Owing to collisions with gas molecules, as the electrons approach the surface of the anode the amplitude of their oscillations in a plane perpendicular to the axis is increased; therefore the probability of ionization grows close to the surface of the anode. However, here the electrons travel to the anode more easily and they cannot play a basic role in the mechanism of maintaining the discharge.

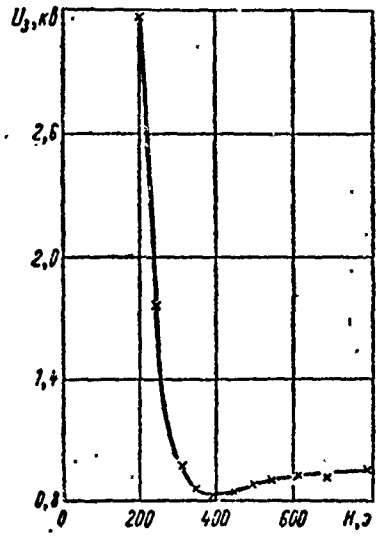

Fig. 75. Discharge ignition voltage as a function of magnetic field intensity.

KEY: (1) U_i, kV.

Designation: э = Oe.

Figure 75 shows the curve of the dependence of ignition potential on the magnitude of the magnetic field. An increase in the magnetic field hampers the escape of electrons to the anode and to the walls of the tube and increases ionization. As a result the ignition potential drops strongly. A further increase in magnetic field intensity leads to a reduction in ionization by a electrons rotating in the plane of the anode, owing to the significant shortening of the average length of the free path in the direction perpendicular to the magnetic field and to a reduction in the energy collected by these electrons during motion over the radius. The ignition potential in this case is somewhat increased. After ignition of the discharge the voltage on it drops and the current grows. The voltage drop on the discharge is the same as in a glow discharge and comprises several hundreds of volts. Investigation of the physical parameters of a discharge with oscillating electrons has been the subject of a number of works [268-271].

We will now consider a system of electrodes consisting of two coaxial cylinders at a pressure corresponding to the state of vacuum insulation (10^{-4}-10^{-9} mm Hg for an interelectrode distance on the order of a few centimeters).

In a longitudinal magnetic field, when the inner electrode (radius r_a) serves as the anode and the outer cylinder (radius r_c) is the cathode and the discharge ignition voltage in such a system occurs at a voltage equaling a few kilovolts, Townsend discharge occurs; it then converts to glow discharge. With a negative potential in the central electrode the appearance of discharge is hampered. Discharge in such a system was studied by Penning and then by Sommervill [272], Haffer [273], Redhead [274], and Blevin [275]. Electrode systems of this type in a longitudinal magnetic field were used as a manometer for measuring low pressure and also as a current rectifier.

The theory developed by Redhead concerning discharge ignition in a system of coaxial electrodes in a longitudinal magnetic field is examined for infinite cylinders. In this structure the electrical field is directed along the radius and its nonuniformities on the edges are ignored. In the considered case, when the electric field varies little along the radius, an electron which flies out from the surface of the cathode describes a cycloid. If an electron flying along a path corresponding to a single cycloid does not experience even a single collision it will once again impinge on the cathode.

In the case of elastic and inelastic collisions the electron will not return to the cathode, but will move along a cycloidal path. With every inelastic collision the radius of circumference of the hypocycloid will be reduced. On Fig. 76 the "x's" mark the points where inelastic collisions occur. If the maximum distance traveled by the electron in a radial direction during its motion along the cycloid (i.e., the height of the cycloid $h = 2E/(e/mH^2)$) is greater than the distance on which the electron collects energy equal to the ionization potential, ionization of the gas will occur. Elastic collisions of electrons do not reduce ionization, since almost all of them acquire the energy required for ionization during the travel following the scattering.

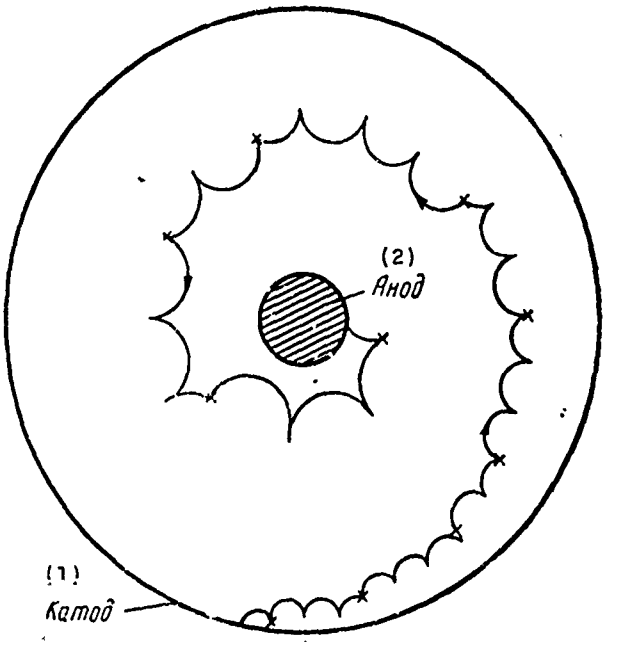

Fig. 76. Trajectory of an electron flying from the cathode (outer cylinder) to the anode (inner cylinder). The magnetic field is directed along the axis of the cylinders.

KEY: (1) Cathode; (2) Anode.

For the case $2h/l \ll 1$, where 2h is half the length of the cycloid, the first Townsend coefficient is determined from the expression

$$\alpha = \frac{3E}{g\left(\frac{4E^2}{e/mH^2} + U_i\right)}, \qquad (51)$$

where g is a correcting factor greater than unity, which explains the fact that when the energy of the electron exceeds eU_1 the probability of collision [leading to ionization*] does not equal unity.

*Translator's note. Ungrammatical Russian phrase meaning literally "by leading from it to ionization." Above translation of this phrase not verified.

Ignition of a self-sustaining discharge in the described system requires that the following condition be fulfilled:

$$\gamma^* \left\{ \exp \left[\int_{r_0}^{r_a} \alpha(r)\, dr \right] - 1 \right\} = 1, \qquad (52)$$

where γ^* is the effective third Townsend coefficient of all secondary processes, r_a is the radius of the anode, r_0 is the radius, beginning from which the electron accomplishes ionization. Secondary electrons arising during ionization of a gas by primary electrons acquire energy and enter into the process of avalanche formation.

Figures 77 and 78 give the theoretical and experimental characteristics $U_i = f(H)$. The broken lines separate the two regions of discharge ignition.

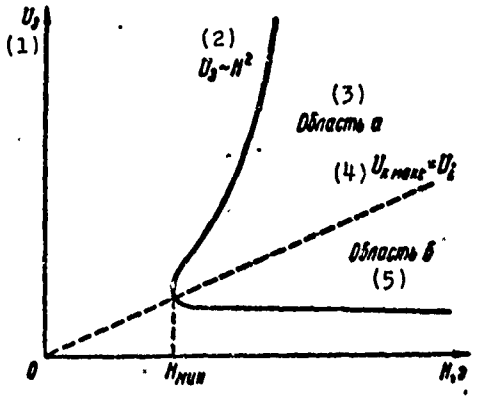

Fig. 77. Discharge ignition voltage U_i as a function of the magnitude of H (theoretical).
KEY: (1) U_i; (2) $U_i \sim H^2$; (3) Region a; (4) $U_{c\,max} = U_i$; (5) Region b; (6) H_{min}.
Designation: э = Oe.

In region a the discharge ignition voltage equals

$$U_i = \frac{\frac{3}{8}\frac{e}{m(Hr_к)^2}}{g \lg\left(1+\frac{1}{\gamma^*}\right)}, \qquad (53)$$

[э = i; к = c]

and consequently $U_i \sim H^2$.

In region b the discharge ignition voltage does not depend on an increase in H; this situation begins from a certain value of H_{min}:

$$H_{мин} = \frac{5}{3}\frac{g}{r_к}\sqrt{\frac{2U_i}{e/m}}\ln\left(1+\frac{1}{\gamma^2}\right).$$

[мин = min; к = c]

an then the ignition voltage is determined by the expression

$$U_э = \frac{5}{3}gU_i\lg\left(1+\frac{1}{\gamma^2}\right)\lg\left(\frac{r_к}{r_а}\right).$$

[э = i; к = c]

The deviation of the experimental curve from the relationship $U_i \sim H^2$ in region a is connected with inaccuracy of the theoretical calculations.

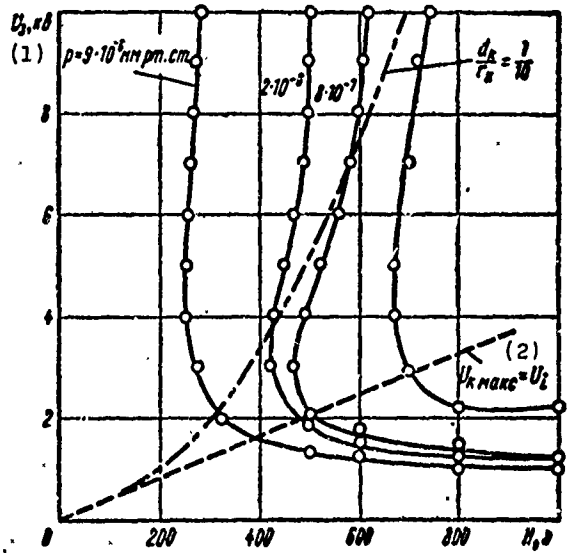

Fig. 78. Discharge ignition voltage U_i as a function of H for different pressure (r_a = 0.5 mm; r_c = 9.0 mm).

KEY: (1) U_i, kV; (2) $U_{c\ max} = U_i$.

Designations: мм рт. ст = mm Hg; к = c; э = Oe.

When the inner electrode becomes the cathode and the outer electrode becomes the anode, an electron leaving the cathode arrives in an electrical field of great intensity and rapidly acquires energy close to the cathode and is shifted along a weakly curving trajectory to the anode. Since $l >> d$ – the distance between the cathode and the anode – ignition of discharge does not occur, while with a negative potential of the outer electrode a

trap for electrons is formed; even in conditions of low pressure the electrons can accomplish ionization sufficient for the development of a discharge.

CHAPTER 8

PHYSICAL PROCESSES LEADING TO BREAKDOWN OF VACUUM INSULATION

Subscripts

$r_{ж}$ = radius of liquid surface

α_s = coefficient of surface tension

опт = optimum

макс = maximum

мин = minimum

$r_{осн}$ = radius of lower base of a conical projection

$T_{пл}$ = melting temperature

э.а = electron beam at anode

к.и = cathode/ion

к.э = cathode/electron

$r_{а.э}$ = electron-beam radius

э = electron, electronic

и = ion, ionic

$I_{зар} = I_{charge}$

$I_{нагр} = I_{heating}$

$I_{капель} = I_{drop}$

1. INTRODUCTION

The content of the preceding chapters shows a multitude of types and characteristics of breakdown of the electrical strength of vacuum insulation. It is explained by the fact that not one, but several physical processes can lead to breakdown of vacuum electrical insulation or can facilitate this event. In certain cases such processes can be pointed out quite positively; sometimes it is substantially more difficult to do so. For example, during secondary electron resonance high-frequency discharge a determining role is played by secondary electron emission. With constant or pulse voltage and a cathode in the form of a sharp point ohmic heating of the point-cathode by field-effect emission current will lead to breakdown. In both cases, although many essential aspects of the processes are as yet insufficiently clear, there is no doubt as to the basic physical scheme of the development of discharge. Unfortunantly this cannot be said about the appearance of discharge during application of high (constant, high-frequency, or pulse) voltage to electrodes with small curvature located in vacuum conditions which are not particularly clean. In this case (which is of the greatest practical value) the processes which lead to breakdown

have not been studied adequately. Probably this is the precise reason for the considerable number of conflicting hypotheses on the mechanism of vacuum breakdown under these conditions. Along with this, we cannot reject the principle of the possible existence of not one but a whole series of phenomena which can lead to breakdown of vacuum insulation; in such a case the existence of several hypotheses is not only possible but ven necessary. Different mechanisms of the breakdown in electrical strength might exist both under strongly differing conditions (magnitude and type of voltage, etc.), as is quite obvious in a number of cases, and also under virtually identical experimental conditions, when several different processes "compete" with one another and breakdown of vacuum insulation is due to that process which is most effective in a given specific case.

Existing hypotheses on the mechanism of vacuum breakdown can be divided into several groups in terms of those physical phenomena which are considered critical for the breakdown of electrical strength. These groups are as follows.

1. Breakdown is caused by secondary phenomena, mainly by evaporation and subsequent processes in vapors which accompany local heating on the cathode or anode caused by the passage of field-effect or prebreakdown current of a different nature. In this case the evaporation of material or desorption of gases and the subsequent phenomena arising after ionization in the volume of liberated vapors and gases are considered as the principal secondary processes accompanying heating.

2. The appearance of breakdown is due to the development of mutual secondary emission (electrons, negative and positive ions, and photons); this emission leads to a spontaneous growth in current and in the final stage to breakdown. In this case breakdown can also be connected with the prebreakdown currents,

but in contrast to the processes considered in the first group of hypotheses, in this case elementary processes of interaction of charged particles and quanta with the surface of the electrodes are determining.

3. Breakdown is caused by grains, by "dust," existing on the electrodes or by microparticles of material of the electrodes themselves. Such particles, weakly bound to the "mother" electrode, fly off from it and, after being electrically charged, are accelerated by the application of voltage to the electrodes. When such an accelerated and charged particle impacts on the opposite electrode a number of phenomena which lead to breakdown can occur. Another possibility of initiating breakdown by particles is the appearance of an igniting discharge between the electrode and an electrical charged particle flying toward it.

4. The mechanical action of electrostatic forces on the electrode is of decisive significance in the appearance of breakdown. Such an action can lead to a change in the surface relief and as a result, for example, to the appearance on the cathode of large projections with field-effect emission arising on their peaks. A more intensive effect of electrostatic forces is the destruction of the electrode surface, with pieces or drops being stripped away from it (drops occurring when a liquid phase is present on the surface).

5. Partial breakdown of dielectric films and inclusions which are almost always present on the surface of the electrodes is, as it were, an igniting spark and leads to breakdown of the entire interelectrode gap. Besides this, dielectric films or inclusions on the cathode may favor the formation of emission centers, which in turn can lead to breakdown with the development of the processes considered in the first group of hypotheses.

The appearance and development of hypotheses on the mechanism of vacuum breakdown proceeded in parallel with the experimental study of breakdown and were intended to explain the results of these investigations, primarily the dependence of breakdown voltage on the interelectrode gap. Thus the constant nature (criticality) of the breakdown intensity on the cathode - the absence of any dependence on the applied voltage or on electrode configuration - which is observed in certain cases is easily explained by the hypotheses in which field-effect emission is the factor which initiates breakdown (since this emission strongly depends on the intensity on the cathode). It is not difficult to explain the critical value of intensity by the destruction of the electrode by electrical forces, especially with low-strength material such as graphite or liquid metals. On the other hand, the reduction in breakdown intensity with a growth in applied voltage above 20-50 kV (total-voltage effect) which was detected even in the earlier stages of research on vacuum electrical insulation between flat electrodes cannot be explained simply by the processes which accompany field-effect emission. In order to "rescue" such an explanation it is necessary to assume that with a growth in applied voltage there will occur under the action, for example, of bombardment of the cathode by ions a growth in the irregularity of the cathode surface, so that despite the reduction in average intensity the local intensity at the points of emission of field-effect electrons will change very little. The anomalously large projections observed comparatively recently on the surface of a carefully treated cathode lend a certain degree of plausibility to such an assumption.

The effect of the total voltage and the influence of the intensity on both electrodes on the appearance of breakdown can be explained only by the fact that processes which lead to breakdown develop on both electrodes and that in these processes the passage of charged particles from one electrode to the other

play a noticeable role even in the very earliest stages of breakdown. Therefore the initiation of breakdown by the impact of a microparticle or by mutual secondary emission, where the applied voltage determines the energy of the particles, can from this point of view simply explain both the reduction in the breakdown intensity with an increase in voltage and the dependence of breakdown appearance on the intensity at both electrodes. Thus, the very closest connection exists between the basic characteristics of vacuum insulation of practical importance and the physical processes occurring on the electrodes and in the vacuum gap. The great variety of conditions under which vacuum electrical insulation is used and must operate - conditions which can differ substantially from cases which have been studied to a greater or lesser degree - make it necessary to carry out more detailed examination of the various physical processes which can lead to breakdown of the electrical strength of vacuum insulation.

As was shown in Chapter 6, breakdown with transition to low-voltage discharge is possible only when the interelectrode gap is filled with plasma. In a vacuum the "material" for the formation of a plasma must be "supplied" by the electrode. Therefore evaluation of the possibility of initiating breakdown by one or another physical process must include also determination of the capability of the given process during its development to lead to filling the interelectrode gap with plasma and to the formation on the cathode of an effective electron source. However, in certain cases the appearance of comparatively small currents, measured in milliamperes and even less, represents an impermissible disruption of vacuum insulation. Such currents do not require that the interelectrode gap be filled with plasma and the above-indicated requirements (formation of plasma) are "not imposed" on the physical processes which give rise to these currents. Therefore, for example, different forms of emission of charged particles such as field-effect emission, thermionic

emmision, mutual secondary emission, the Molter [spelling not verified - Translator] effect, and others may, in principle, explain the appearance of conductivity in a vacuum such that with low-power voltage sources (electrostatic generators supplying accelerating tubes, etc.) serious disruption of vacuum insulation can occur. However, without secondary processes connected with electrode heating (even though local), rapid desorption of gas, or evaporation of material, these processes cannot lead to vacuum breakdown with the possibility of transition to low-voltage discharge. Therefore it is particularly important here to examine those processes which can lead to filling of the inter-electrode gap with plasma and to the formation of an electron source on the cathode. These two conditions are to a significant degree identical, since filling of the interelectrode gap with plasma is impossible without intensive evaporation on one electrode or the other, while the primary source of energy for such evaporation should be an electron current; on the other hand, filling of the electrode gap with plasma concentrates the electrical field close to the cathode (brings about intensive bombardment by ions), which inevitably leads to the formation of a sufficiently effective electron source on the cathode.

An examination of the physical processes which can have a negative influence on the quality of vacuum insulation (which can bring it to breakdown) is the basic consideration of the following sections. The sequence of consideration is determined not by the "specific weight" of these processes in the disruption of vacuum insulation, but rather by convenience in exposition. Thus, the effect of electrical forces on electrons clearly does not play a significant role in initiating vacuum breakdown in many cases; however, it is convenient to examine this phenomenon among the first, since it may play a role in the development of breakdown which is initiated by other physical processes. For example,

field-effect emission from a projection on the cathode can lead to melting of the projection peak. But the subsequent behavior of this projection - whether it is rapidly drawn out (which leads to a growth in field-effect emission) or, vice versa, is rapidly smoothed and melted (which causes a drop in current) - this depends on the balance of mechanical forces, i.e., on the relationship between electrostatic forces and the forces of surface tension.

Of the five groups of hypotheses enumerated above, two will not be considered below in detail; however, the reasons for this are different. The first one - the hypothesis of initiation of breakdown by mutual secondary emission - was developed in its time by Trump and Van de Graaf [100, 276] to explain the effect of total voltage. According to their hypothesis, the condition for appearance of breakdown had the form (using the designations taken by these authors)

$$AD + CD \geq 1, \qquad (54)$$

where A and C are coefficients of the escape from the anode of ions and photons, respectively, during electron bombardment; B is the coefficient of electron emission under the action of cathode bombardment by positive ions, and D is the average number of electrons escaping from the cathode as the result of the photoeffect per photon emitted by the anode. However, subsequent measurements of these coefficients, in particular those carried out by the same investigators (see [100, 277-279]), showed the impossibility of observing condition (54). Therefore this hypothesis now presents, for the most part, only historical interest and will not be considered in detail here.

Unfortunately there is virtually no consideration of another group of hypotheses presented by a number of investigators [234, 280-283] concerning initiation of vacuum breakdown by various

processes in dielectric films and in inclusions on the surface. Although this group of hypotheses deserves serious examination, the almost total absence of appropriate experimental data at present prevents the analysis of the possibility of such initiation of breakdown. Certain general consideration speaking in favor of the cited hypotheses are given in Section 5.

2. THE ACTION OF ELECTROSTATIC FORCES

At the high values of electric field intensity which are characteristic for vacuum insulation, electrostatic forces achieve significant magnitudes; this can have a negative influence on the quality of this insulation. The effect of electrostatic forces can be manifested in two ways. First of all, as was already considered in Section 2 of Chapter 2, by changing the rate and even the direction of surface diffusion, electrostatic forces favor the growth of projections on the surface. As a result of this the coefficient μ can increase and the average breakdown intensity can be correspondingly reduced. Secondly, at individual points on the surface of the electrodes the electrostatic forces can reach the limit of the mechanical strength of the material, which leads to destruction of the surface, breakaway of particles of material from it, etc. Thus, the limit of mechanical strength of the electrode material is reached by electrostatic forces at an intensity of 2 MV/mm for graphite, 10 MV/mm for steel and nickel, and 20-30 MV/mm for tungsten [284]. These values are quite high, especially for the hard metals; however, they are not so high as to exclude the possibility of destruction of the material, since possible mechanical defects in the electrode material and also an increase in intensity on surface irregularities with $\mu > 1$ will substantially reduce the "destructive" intensity. Besides this, the figures given above relate to materials at room temperature; an increase in the temperature (due to local heating by dark currents, etc.), not to mention the appearance of melted segments on the electrodes, can reduce the "destructive" intensity even more significantly.

The appearance of breakdown due to destruction of the electrodes by electrostatic forces is most probable in two cases: first, when the electrode configuration of the cathode is flat and that of the anode is a sharp peak (destruction of the anode) and, secondly, when electrodes of any configuration are manufactured from materials with low mechanical strength. For example, it is known (see Section 6 of Chapter 4) that with a point anode and a flat cathode the breakdown voltage is 3-3.5 times higher than when the polarity of the electrodes is reversed. In the latter case the conditions for appearance of breakdown have been studied quite thoroughly and it has been established that breakdown will occur due to the passage of substantial currents of field-effect emission; the local intensity in this case should reach values of 3-8 MV/mm. Therefore we can assume that with a point anode the local intensity will exceed 10 MV/mm and, consequently, the electrostatic forces will be close to the limit of mechanical strength for even the strongest metals.

Clearly, however, due to various defects on the surface breakaway of individual microscopic particles from the electrodes is observed even in comparatively weak fields. Thus, Hawley and Walley [49] observed with a microscope growth and breakaway of individual projections 1.5 μm in diameter on a flat copper anode under constant voltage and with an interelectrode gap of 0.3 mm. The intensity at which projections will appear and break away depends on the initial treatment of the electrodes: for mechanical treatment $E \approx 40$ kV/mm, while with electropolishing $E \approx 60$ kV/mm. Such a breakaway is frequently accompanied by a breakdown; these investigators explain this as the initiation of breakdown by the impact of a microparticle (this process is examined in Section 4).

Investigating the effect of electrode material on breakdown, Rozanova and Granovskiy [164] found that the breakdown intensity grows smoothly with transition from low-strength electrode materials to stronger materials - it grows successively from graphite to aluminum, copper, nickel, molybdenum, and tungsten - although no quantitative correspondence has as yet been detected. It was noted in Chapter 4 that breakdown voltage is increased when the electrode surfaces are work-hardened.

The transfer of material from one electrode to the other in the form of multiatomic aggregates (microparticles) and traces of breakdowns on the electrodes in the form of craters with sharp edges all speak in favor of participation of electrostatic forces in the processes leading to breakdown or in processes which accompany breakdown. Electrostatic forces take on especially great significance when segments of melted metal appear on the electrodes or even when one electrode is in the form of liquid metal.

Tonks [285] examined the destruction of a liquid-metal surface under the action of electrostatic forces; his approximate calculations were then given, to a certain degree, a stricter foundation by Frenkel [286]. During derivation of the relationships Tonks examined the balance of the forces of surface tension, electrostatic forces, and gravity, and during examination of the dynamics of the processes he took the forces of inertia into account. The condition for instability of the surface of a liquid metal, if this surface is horizontal and if the electrical forces are acting upward, has the form

$$\varepsilon_0 E^2 > 4\pi \frac{\alpha_s}{r_ж} + \pi\delta g r_ж, \qquad (55)$$

where $r_ж$ - is the radius of the liquid surface; g is the acceleration of gravity; δ is the density of the substance; and α_s is the coefficient of surface tension. The minimum value of field

intensity leading to breakdown corresponds to the value $r_{ж} = r_{опт}$, at which the terms in the right side of inequality (55) are mutually equal. For mercury, for example, the minimum "destructive" intensity comprises 5.3 kV/mm and $r_{опт}$ equals 3.7 mm.

If inequality (55) is fulfilled a protuberance begins to grow on the surface. On the apex of this protuberance the electric field intensity is elevated; at the same time the electrostatic forces at this point are increased and the segment close to the apex of the protuberance begins to be stretched more strongly than the peripheral portions. Therefore while the initial protuberance has the form of an approximately spherical segment (up to a hemisphere), it subsequently takes on the form of a more pointed conical projection. The maximum possible height of the projection equals

$$h_{макс} = \frac{10{,}8\pi\sigma_s}{\varepsilon_0 E^2}. \qquad (56)$$

In this case the radius of the apex tends toward an infinitely small quantity. It is clear that before the projection reaches such a form breakaway of the projection peak can occur; however, the conditions of such breakaway are not considered in works [285, 286].

The total time for gorwth of the projection to the maximum possible height equals

$$\tau = 45\frac{\sigma_s\delta^{0,5}}{\varepsilon_0^{1,5}E^3}\left(3{,}25\lg\frac{\sigma_s}{\varepsilon_0 E^2 h_0}+2{,}7\right), \qquad (57)$$

where h_0 is the height of the initial irregularity on the electrode surface. The growth of the projection in time occurs with increasing rapidity, so that the major time is expended on the initial stages of the process. In addition, the first term on the right side of equality (57) goes to infinity when the surface of the melted electrode is absolutely smooth (h = 0), while

89% of the second term comprises time of growth of the projection up to the moment when the projection becomes hemispherical with a radius three times less than h_{max} [see expression (56)]. The formula given above is valid when $h_0 < \alpha_s \varepsilon_0 E^2$; thus, for example, for nickel (α_s = 1.6 N/m) when E = 100 kV/mm it gives $h_0 < 1.5$ μm.

Warmolz [168], investigating breakdown between electrodes of liquid mercury or gallium (see Fig. 46), found that the experimental data on delay of breakdown are in agreement with the time for destruction of the surface (time of projection growth) according to formula (57) if it is assumed that h_0 = 1-10 Å. The agreement is observed only for E < 20-30 kV/mm. At larger values of E the delay in the breakdown is less than the calculated value. For clarity the value of τ at h_0 = 10 Å as calculated by equation (57) is plotted on Fig. 46.

As was indicated in Section 3, field-effect emission from an individual projection on the cathode can lead to melting of the apex of this projection; in its turn this should lead to a change in the shape of the projection and consequently to a change in the emission of electrons and the processes accompanying it. Owing to the small size of the emitting peak gravity has no influence on the balance of forces acting on the projection peak and the condition for growth of the projection, analogous to the condition for instability of the surface (55), has the form

$$\frac{\varepsilon_0 E^2 \mu^2}{8\pi} = \varepsilon_0 \frac{E\mu}{8\pi} \frac{h}{2r} E > \frac{2\alpha_s}{r}, \qquad (58)$$

where $2\alpha_s/r$ is the force of surface tension; for convenience in subsequent analysis a μ is replaced by h/2r [see Section 2 of Chapter 2 and expression (11)]. Since melting of the projection requires a substantial field-effect emission current, the local intensity lies within completely defined limits. According to Table 3, when j is equal to 10^8-10^{12} A/m^2, the quantity

$\mu E = (4-8)\cdot 10^8 \Phi^{1.5}$ V/m. Substitution of this value of μE into expression (58) gives the following condition for growth of a projection under the action of electrostatic forces:

$$Eh > (360-720)\frac{\pi\alpha_s}{\Phi^{1.5}}. \qquad (59)$$

For example, for nickel α_s = 1.62 N/m, Φ = 4.5 eV, and Eh > > 190-380 V (the smaller value of Eh corresponds to melting of the projection peak with larger current densities).

If the inequality is not fulfilled melting of the projection leads to smoothing of its apex and, evidently, to liquidation of the projection. Thus, the subsequent path of the process after melting of the projection depends on its initial dimensions. If the height of the projection was small melting should lead to its elimination as an electron emitter - i.e., to improvement of vacuum insulation. On the other hand, melting of a projection with h which is greater than a few microns will lead to its increase and, although the time to complete destruction of the projection is extremely small, the strong surge in current which should accompany growth of the projection will apparently lead to breakdown. As yet there are no experimental data which directly confirm the above, but the experiments described above with an electrode configuration of a point cathode and a flat anode when melting of the point (projection of great height) leads to breakdown and also the jumpwise decrease in dark current observed due to liquidation of individual emission points[1] can clearly serve as arguments in favor of such a conclusion.

[1]Observations by Brodie [124] indicate that in certain cases the disappearance of the emission center and the reduction in dark current precede a small current surge; this can be explained as the result of heating of the projection before its final destruction.

The material outlined in this section shows that electrostatic forces can "enter into play" and can determine the further course of the process in a certain intermediate stage of the appearance of breakdown, when a melted segment, however small, appears on one of the electrodes. Several cases of melting on the electrode are examined in the following section, which presents numerical evaluations of the conditions for appearance of breakdown with consideration of the action of electrostatic forces.

3. PROCESSES WHICH ACCOMPANY FIELD-EFFECT EMISSION

Figure 79 gives a listing of the various secondary processes which accompany field-effect emission from a projection on the cathode and gives a tentative indication of the interconnection between them. The arrows indicate the sequence of development of the process (cause → effect). If two processes mutually intensify one another two arrows pointing in opposite directions are marked on the connecting line. From the given scheme the great variety and close interconnection of secondary processes is evident. Besides the elementary processes such as the emission of X-ray quanta, electrons, and ions from the anode, there is also a large group of processes whose manifestation is caused by electrode heating: here heating of the cathode is due to joule heat from the current flowing over it and the anode is heated by bombardment by electrons leaving the cathode and accelerated in the interelectrode gap. When the density of the electron current is high local heating on the cathode or anode is observed, even at comparatively small values of total current. Therefore field-effect emission can be an effective initiator of the secondary processes connected with electrode heating.

Heating of the emitting projection on the cathode by joule heat can cause a number of phenomena. One of these is a change in the shape of the projection due to diffusion, recrystallization, and also creep under the action of electrostatic forces. These processes, which are very weak in ordinary conditions, are sharply intensified and accelerated with approach to the melting temperature. As was indicated above, depending upon the balance of mechanical forces melting of a projection can lead both to its sharpening and therefore intensification of the current, etc., and also to its smoothing (melting of the projection peak) - i.e., to its destruction as an electron emitter. Another consequence of heating is the liberation absorbed gases and then vapors of the cathode material into the gap. Ionization of liberated gases and vapors intensifies the electric field close to the cathode; this in turn facilitates a further growth in current and the development of secondary processes (liberation of gases and vapors, etc.).

The enumerated processes are developed only on the cathode and in direct proximity to it. We can also note a number of processes connected with local heating on the anode when it is bombarded by electrons. The appearance of a melted spot on the anode can lead to breakaway of drops of material under the action of electrostatic forces. The liberation of sorbed gas, evaporation of material, and the subsequent ionization of vapors, like the similar phenomena on the cathode, in the end will intensify the field at the cathode and consequently will strengthen the field-effect emission current. Besides this, ions which are formed close to the anode acquire a great deal of energy and by bombarding the cathode heat the latter; they also cause cathode sputtering, which together with activation of surface processes on the cathode leads to a change in the relief and properties of the latter. In addition, the appearance of positive ions in the gap can lead to focusing of the electron beam - to its contraction. This increases the heating and evaporation on the anode.

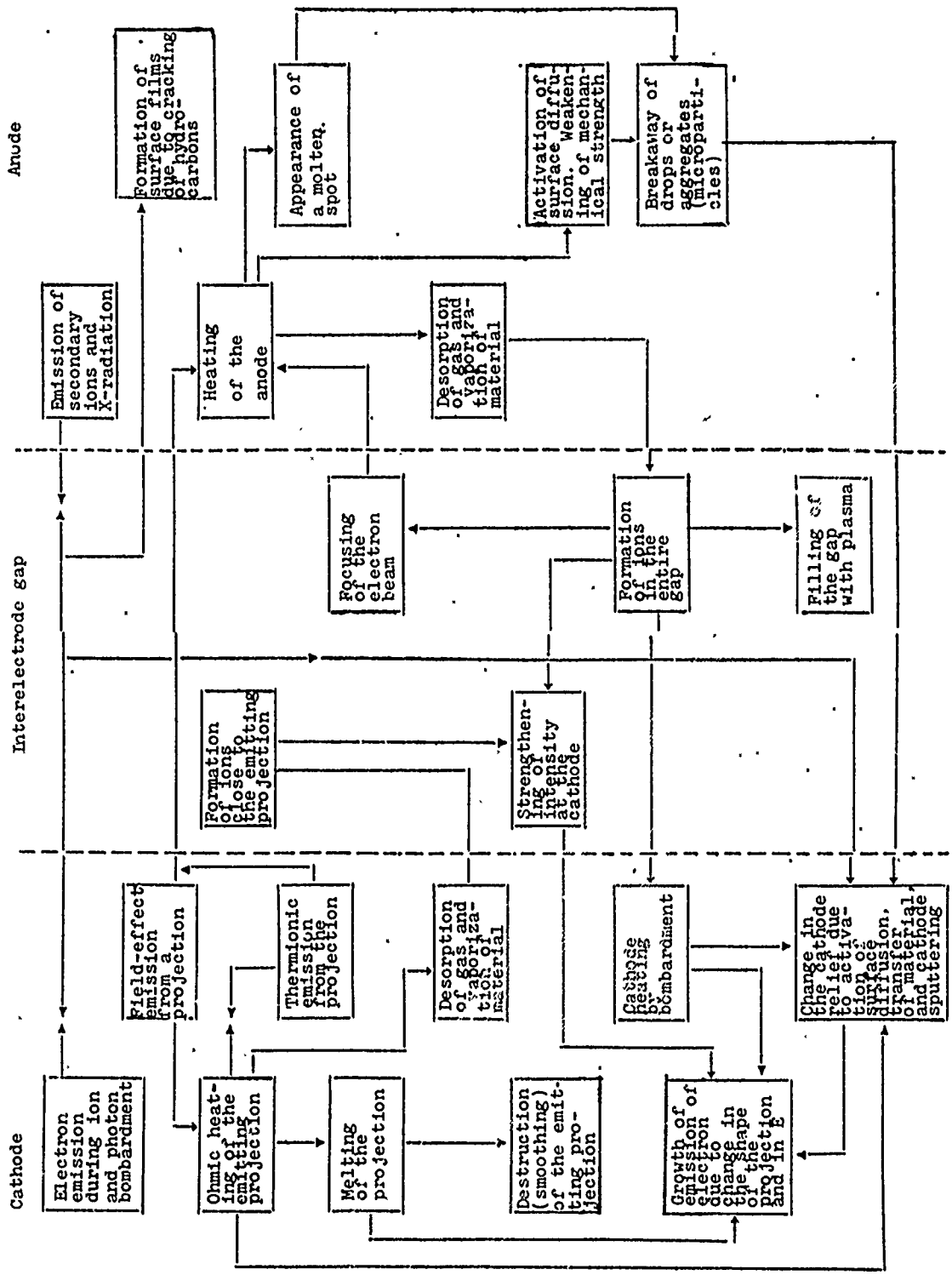
Anode
Interelectrode gap
Cathode
Formation of surface films due to cracking of hydrocarbons
Appearance of a molten spot
Activation of surface diffusion. Weakening of mechanical strength
Breakaway of drops or aggregates (microparticles)
Emission of secondary ions and X-radiation
Heating of the anode
Desorption of gas and vaporization of material
Focusing of the electron beam
Formation of ions in the entire gap
Filling of the gap with plasma
Formation of ions emitting projection
Strengthening of intensity at the cathode
Field-effect emission from a projection
Thermionic emission from the projection
Desorption of gas and vaporization of material
Cathode heating by bombardment
Change in the cathode relief due to activation of surface diffusion, transfer of material and cathode sputtering
Electron emission during ion and photon bombardment
Ohmic heating of the emitting projection
Melting of the projection
Destruction (smoothing) of the emitting projection
Growth of emission due to change in the shape of the projection and in E

Fig. 79.

The described processes can occur simultaneously but at different intensities, depending upon the specific conditions. For example with cathode-point and plane-anode electrodes the beam of electrons proceeding from the cathode is strongly expanded and the heating on the anode is insignificant. Therefore under these conditions only the processes connected with heating of the emitting point by joule heat can lead to breakdown, although the total quantity of energy emitted on the anode is greater than that liberated in the emitting point on the cathode. On the other hand, with flat electrodes the processes on the anode are more intensive and disruption of vacuum insulation can be caused by precisely these processes.

The initiation of vacuum breakdown by an electron current is the basis for a number of hypotheses on the mechanism of this phenomenon. One of the first was the Semenov hypothesis (see [287]), where the appearance of noticeable conductivity between electrodes in a vacuum is explained by electron ionization of the gases and vapors liberated from the anode and the subsequent escape of electrons from the cathode is explained as secondary emission (or thermionic emission) during bombardment of the cathode by the accelerated ions. Later similar presentations were developed by Arnal [142] and by Blewett and Turner [144] with application to the appearance of microdischarges and electron load in accelerating tubes. Presentations on the mechanisms of breakdown which are similar to the Semenov hypothesis were also developed by Glazanov [2]. Boyle et al. [179] created a theory of the breakdown of very small interelectrode gaps, with the major role, in their opinion, being played by the formation of a positive space charge due to ionization of vapors liberated from the anode and the intensification of the field-effect current connected with this, as described above. Processes connected with electron bombardment of the anode are used by Maitland [177] to explain the appearance of breakdown, although the precise physical processes which lead to breakdown are not specified in his works.

The appearance of breakdown due to melting of the emitting cathode point was studied by Dyke and coworkers and by a number of Soviet investigators: Yelinson, Sokolskaya, Furse, and others. For the most part the results of these studies were outlined in Chapter 4, since this is one of the few cases when the mechanism of the appearance of breakdown has been solidly established and in which very good agreement of experimental and calculated data is observed. In the same chapter the processes connected with heating on the cathode (as also other processes which destroy vacuum insulation) are examined with application to electrodes which are flat or which have a small curvature.

Heating of the emitting projection. We will assume that a projection on the surface of a solid electrode represents a body of revolution with axis X and that the joule heat which is liberated in the volume of the projection is drawn off only by thermal conductivity through the base of the projection. With values of electrical resistivity ρ and the coefficient of thermal conductivity λ which do not depend on temperature, solution of the heat-balance equation leads to the following expression for the steady-state temperature of the projection peak, representing an excess above the electrode temperature (with passage of a current which is unchanged in time):

$$T_{h\infty} = \frac{I^2 \rho}{2\pi^2 \lambda r^3} F, \qquad (60)$$

where r is the radius of the peak of the emitting projection; F is a numerical coefficient whose value depends very strongly on the configuration of the projection (in particular, this is clear from expression (61) given below, which also gives an idea of the magnitude of F).

In the work by Dyke and coworkers, as in a number of subsequent works by other authors (see Section 6 of Chapter 4), the emitting projection was approximated by a truncated cone. In this case

$$F = \left(\frac{h}{r_{\text{осн}}}\right)^2, \tag{61}$$

where $r_{\text{осн}}$ is the radius of the lower base of the conical projection, while h is the height of the projection. The distribution of temperature over the height of the projection is nonuniform and depends on the projection's shape. For example, for a projection in the shape of a truncated cone 80% of the total temperature drop (T_{max} - 0.2 T_{max}) falls on the portion of the height of the projection (counting from the peak):

$$\Delta h_{0,8} = h\frac{9r}{9r + r_{\text{осн}}}. \tag{62}$$

Thus, when $r_{\text{осн}} \gg r$ the major temperature drop is concentrated at the peak of the projection, while with $r_{\text{осн}} \approx r$, on the other hand, the temperature gradient at the base of the projection is large. The quantity $\Delta h_{0.8}$ determines in the first approximation the time for establishing the temperature of the projection peak, when heating is accomplished by a pulse current of constant amplitude. If the change in the peak temperature in time is expressed approximately in the form

$$T_h(t) = T_{h\infty}\left[1 - \exp\left(-\frac{t}{\tau}\right)\right],$$

then

$$\tau = \frac{\delta c}{2\lambda}(\Delta h_{0,8})^2, \tag{63}$$

where δ is the density and c is the heat capacity of the projection material.

For a quantitative evaluation of joule heating of a single emitting projection on a flat cathode we will use the expression for the field-effect emission current in the form (18). The maximum value of the current and, consequently, the most intensive heating will occur under the condition of equality of the exponent of this formula to zero. Under this condition the substitution of expression (18) into formula (60) and the replacement of h/r by 2μ (see Section 2 of Chapter 2) allow us to write an expression which determines the possibility of melting of the emitting projection by joule heat, in the form

$$\frac{\mu E^2 h}{\Phi} > 5{,}7 \cdot 10^6 \sqrt{\frac{T_{пл} \lambda}{\rho F}}, \qquad (64)$$

where $T_{пл}$ is the melting temperature (more exactly, the amount by which melting temperature exceeds room temperature).

As an example we will examine an ellipsoidal projection with μ = 50 - i.e., a fairly thin projection which will be heated, as is evident from inequality (64), more intensively than projections with smaller values of μ or which are more strongly expanded toward the base than the ellipsoidal projection. For the projection indicated above F = 15. The results of numerical solution of inequality (64) are given in Table 61.

Table 61. Values of E^2h/Φ which determine the minimum height h at which melting of an ellipsoidal projection with μ = 50 due to joule heating becomes possible.

Cathode material	ρ, $\times 10^{-6}$ ohm·m	λ, J/(m·deg·s)	E^2h/Φ, $\times 10^{10}$ V^2/(m·eV)
Molybdenum	0.814	66.8	1.4
Nickel	0.6	62	1.1
Aluminum	0.14	151	2.4

Equating the exponents in expression (18) to zero - the condition under which inequality (64) was obtained - assumes a certain relationship between local intensity on the emission surface and the work function Φ. For example, when $\mu E = 5 \cdot 10^9$ V/m (which for the data in Table 61 corresponds to $E = 10^8$ V/m) the figures indicated in this table will be valid if $\Phi \leq 2.56$ eV. This is substantially below the values of Φ for highly finished molybdenum and nickel surfaces.

The role of positive ions forming due to ionization of anode vapors. If the anode is subjected to bombardment by an electron beam with current I and with the radius $r_{э.а}$ close to the anode, the density of the vapors of anode material close to the anode itself, n_a, can be determined from the equation of the heat balance on the anode:

$$IEd = (T_a - 300)\pi\lambda r_{э.а} + 0{,}25 v_т n_a \pi r_a'^2 r, \qquad (65)$$

where the first term in the right side accounts for heat removal into the body of the anode due to thermal conductivity λ, while the second term considers the consumption of heat on evaporation ($v_т$ is the thermal velocity of the vapors, r is the heat of evaporation for one atom, r_a' is the radius of the spot on the anode where the basic portion of the vapors is formed). In turn temperature T_a (in the center of the spot) and the vapor density n_a are connected through the well-known Clapeyron-Clausius equation.

The ratio between r_a' and $r_{э.а}$ depends on many parameters: the fraction of heat consumed on evaporation and the total heat balance, the distribution of current density over the electron beam cross section, etc. If the heat consumed on evaporation is substantially greater than the escape of heat into the body of the anode, $r_a' \approx r_{э.а}$. When heat removal is dominant, with a

uniform current density in the electron beam cross section the temperature on the boundary of a circle with radius $r_{э.a}$ comprises a total of 67% of the temperature in the center of the spot. If in the latter case we assume that due to the strong dependence of evaporation on temperature evaporation is limited to a region in which the temperature is no less than 0.9 T_a, then $r'_a = 0.57\ r_{э.a}$.

As was stated above, one consequence of ionization of liberated vapors is an increase in the intensity at the cathode and a corresponding increase in field-effect current. The latter causes more intensive evaporation on the anode, an increase in the positive space charge, etc.; this can lead to a spontaneous growth in current and, apparently, to breakdown of electrical vacuum insulation.

If $\Delta E_{к.и}$ represents the increase in local intensity at the point of field-effect emission on the cathode caused by the formation of a positive space charge, $\Delta E_{к.э}$ is the reduction in the same intensity due to the space charge of the primary field-effect beam ($\Delta E_{к.и}$ and $\Delta E_{к.э}$ are rather complex functions of field-effect current I), then the condition for a spontaneous growth in current has the form

$$\frac{d}{dI}(\Delta E_{к.и} - \Delta E_{к.э}) > \left[\frac{dI}{d(\mu E)}\right]^{-1}, \qquad (66)$$

where the right side contains a derivative which is defined by the theoretical equation of field-effect emission - for example, in the form of expression (18).

If the energy liberated by electrons on the anode proceeds mainly to the formation of vapors, $\Delta E_{к.и} \sim I^2$, since $n_a \sim I$, while the number of ions formed is proportional to $n_a I$. Applying the formula for the current of field-effect emission in the form

$$I = \text{const}_1 \cdot \exp\left(-\frac{\text{const}_2}{\mu E}\right)$$

and considering that $\Delta E_{к.э} \ll \Delta E_{к.и} \ll \mu E$, we can write the following expression for the current of field-effect emission from the cathode when the intensity on the cathode equals $\mu E + \Delta E_{к.и}$:

$$I = I_0 \exp \frac{\text{const}_3 \cdot \Delta E_{к.и}}{(E\mu)^2}, \qquad (67)$$

where I_0 is the current in the absence of any influence of a positive space charge - i.e., when $\Delta E_{к.и} = 0$.

Together with the condition $\Delta E_{к.и} \sim I^2$, expression (67) makes it possible to rewrite the condition for spontaneous growth in current due to a rising influence of the space charge of positive ions:

$$I \geqslant I_0 e^{0.5} = 1{,}65\, I_0. \qquad (68)$$

This expression can be interpreted as follows: if the effect of the the space charge formed due to ionization of anode material vapors results in a growth of 65% in the initial field-effect current from the anode, a spontaneous growth in current will occur subsequently. The condition for initiating vacuum breakdown due to the growth in the positive space charge as a result of ionization of anode vapors was obtained by Boyle et al. [179].

Work [133] considers the case of flat electrodes, when the field-effect current is emitted by a single projection on the cathode; to determine the values of the coefficient μ, current I, and radius $r_{а.э}$ of the electron beam expressions (11), (18), and (19), derived above, are used. It is also assumed that the density of the anode material vapors diminishes in the direction toward the cathode as the square of the distance, while the positive ions being formed as a result of their ionization will then move to the cathode as a uniformly accelerated and parallel flow. With such assumptions the condition for a spontaneous growth in current (66) takes the form

$$\frac{\sigma_{i\,\text{макс}}\,h^{0,5}}{d}\,n_a\sqrt{\frac{m_u}{2eE}}\left(1+\frac{I}{n_a}\,\frac{dn_a}{dI}\right)\gamma-$$

$$-36h^{-1,5}\sqrt{\frac{m_a}{2eE}}>\frac{\varepsilon_0 E}{I\,(4{,}6\lg Eh-14{,}1-2{,}3\lg I)}. \qquad (69)$$

In this expression $\sigma_{i\ \text{макс}}$ is the maximum value of ionization cross section by electrons of the anode vapors (it is assumed in the calculation that the ionization cross section is constant up to electron energies of 300 eV and then undergoes a drop which is inversely proportional to the energy of the electrons); γ is a numerical coefficient which depends on the height of the omitting projection. When $2hE > 300$ V, $\gamma = 1$; when $2hE < 300$ V, $\gamma = 1 + \ln(300/2hE)$.

In this work an expression was also obtained which determines the heating of the emitting projection on the cathode due to its bombardment by the same positive ions of the anode material. Under the assumptions described above the increase in the temperature of the projection peak is determined by the relationship

$$\Delta T_{hu}=\frac{54I\sigma_{i\,\text{макс}}}{\lambda}\,n_a\left(\frac{h}{d}\right)^{0,5}. \qquad (70)$$

In contrast to the heating of the emitting projection by joule heat, its heating by ions does not depend on the shape (profile) of the projection if the projection is not narrowed toward the base. This holds true because with a protuberance which expands toward the base the ions not only impinge on the peak of the projection, but also its lateral surface; this bombardment is more intense, the more strongly the projection expands. This completely compensates the reduction in thermal resistance due to the increase in the cross section of the projection.

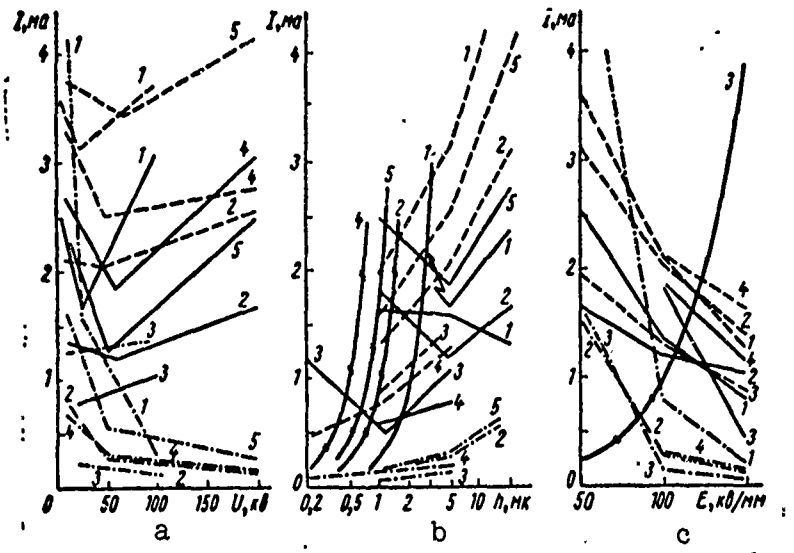

(1) График	a					b					c			
(2) Кривая	1	2	3	4	5	1	2	3	4	5	1	2	3	4
(3) Материал	Ni	Ni	Ni	Al	Mo	Ni	Ni	Ni	Ni	Al	Ni	Ni	Ni	Al
$E, \times 10^8$ в/м	0,5	1	2	1	1	0,5	1	2	2	1	Переменная (4)			
h, мк	5	5	5	5	5	Переменная (4)					5	5	1	5
d, мм	Переменный (4)					0,5	0,5	0,5	0,1	0,5	0,1	0,5	0,5	0,5

Fig. 80. The currents $I_{эар}$ (solid lines), $I_{нагр}$ (broken lines), $I_{капель}$ (dot-dash lines) and maximum possible current of a projection according to expression (18) (double lines) as functions of voltage U, projection height h, and average intensity E.

KEY: (1) Graph; (2) Curve; (3) Material; (4) Variable.

[ма = mA; кв = kV; мк = μm; кв/мм = kV/mm; мм = mm; в/м = V/m]

Figure 80 shows values of field-effect emission currents calculated from the relationships given above for a projection on a flat cathode; these currents may be caused by one or another process:

1) current $I_{эар}$, which according to expression (69) leads to a further spontaneous growth in current due to the influence of the positive space charge;

2) current $I_{нагр}$, which according to (70) causes heating up to melting of the emitting projection due to its bombardment by ions of anode material;

3) current $I_{капель}$, which creates conditions on the anode for breakaway of drops [this condition consists in the appearance on the anode of a melted spot with a radius which satisfies inequality (55)];

4) the maximum possible current of field-effect emission from the projection, according to expression (18).

Table 62 gives the magnitudes of the coefficient μ which are required for passage of the currents indicated above with nickel electrodes. Of the two currents $I_{зар}$ and $I_{нагр}$ values of μ are given only for $I_{зар}$, for which the required μ is as a rule always less. The height of the projection h was taken as one of the parameters of these calculations; besides the determination of currents capable of causing breakdown, this permits comparison of the "effectiveness" of projections of different height as initiators of breakdown of vacuum electrical insulation.

Table 62. Required values of coefficients μ corresponding to initiating currents $I_{зар}$ and $I_{капель}$ for nickel electrodes.

(1) h, мк	d, мм	(2) μ, соответствующий $I_{зар}$ при E, равном (кв/мм)			μ, соответствующий $I_{капель}$ при E, равном (кв/мм) (3)		
		50	100	200	50	100	200
5	0,1	184	66	26	200	62	24
5	0,5	170	65	27	169	55	22
5	2,0	190	72	—	133	51	—
1	0,5	200	200	35	200	78	28

KEY: (1) h, μm; (2) μ corresponding to $I_{зар}$ with E equal to (kV/mm); (3) μ corresponding to $I_{капель}$ with E equal to (kV/mm).

When the above data are evaluated, the rather significant magnitudes of the current stand out immediately; certainly these should be considered as critical, taking into account the special closeness of the conducted calculations. The values of the coefficient of field increase μ are also great, although information given in Chapters 2 and 3 shows that such values of μ are not unrealistic.

Of the considered processes connected with heating or evaporation on the anode it follows that breakaway of drops from the anode requires the smallest current of electrons if $E > 5 \cdot 10^7$ V/m. Following this in effectiveness is the formation of a positive space charge, although for light metals with small values of h and large d melting of the emitting projection due to ion heating is more probable.

From Fig. 80 and Table 62 it is evident that projections of small height are of lesser effectiveness as initiators of breakdown. Actually, with small h the required density of the electron current is greater[1] and consequently the required value of μ is higher, while when $h < 1$ μm the projection cannot emit the field-effect current required for initiation even with very large μ. Besides this, according to expression (59) the melting of a projection with small h will lead to the melting - i.e., the smoothing - of its peak. Therefore if the melting is not accompanied by intensive gas liberation it means the destruction of the field-effect emitter and a corresponding improvement in the vacuum insulation.

---

[1] $I \sim h^2$ corresponds to a constant level of current density and of the value of μ; as is evident from Fig. 80b, this differs from the obtained relationship.

There is interest in comparing the effectiveness of the enumerated processes with joule heating of the emitting projection by the passage of a field-effect current. For example, this can be done by comparing the data in Table 61 and those in Fig. 80b. It follows from such a comparison that with flat electrodes the processes connected with heating and evaporation on the anode are more effective than heating of the emitting projection by joule heat if, of course, the emitting projection has good thermal contact with the main mass of the cathode. If the work function Φ equals not 4 eV, as assumed for Table 62, but equals, for example, 2 eV, the required values of the coefficient μ will be 3.5-4.2 times less. However, even under this condition the required values of μ with E = 50 kV/mm are quite high.

Still another conclusion can be drawn from the data in Fig. 80 and Table 62 - this is the absence of a reduction in breakdown intensity with a growth in the applied voltage if breakdown is initiated by field-effect emission from individual projections on the surface of a flat cathode. Nevertheless, one possibility exists for a reduction in breakdown intensity: if the growth of projections on the cathode is influenced by the applied voltage in such a way that the projections become larger or sharper at high voltage, this can lead to a certain reduction in breakdown intensity with an increase in the applied voltage. However, such an assumption appears to be somewhat artificial.

As was stated above and as is clearly evident from Fig. 80, $I_{капель}$ has the smallest value among the currents if $E \geq 100$ kV/mm. It is possible that breakaway of drops from the anode is the reason for the predominant transfer of anode material to the cathode which is observed with dark current and in the initial stages of breakdown. However, it is not clear whether such drops can initiate breakdown and under what conditions this might be possible. In order to analyze such a possibility it is necessary first of all to determine the size of the drops and their kinetic energy at arrival on the cathode.

The above analysis of the role of field-effect emission from a projection on the cathode assumes a constant level of the work function on the cathode and, even more essential, complete degassing of both electrodes. We know of no evaluations, even semiquantitative, or of any experimental data on the role of desorption of gas. We can propose theoretically that desorption of gas from the emitting projection may have the most significant effect on the considered processes. Ionization of this gas close to the emitter and the appearance at this point of a positive space charge can significantly facilitate transition to spontaneous growth of the field-effect current and to breakdown of the vacuum gap. During the breakdown described in Chapter 4, with a cathode in the form of a sharp point, arguments of a number of investigators are given which favor participation of desorbed gas from the emitting point in the development of breakdown. It is obvious that this effect can occur also during field-effect emission from a cathode projection with flat electrodes. The influence of gases adsorbed by the anode on the formation of a positive space charge and on the bombardment of the cathode by ions is clearly less essential. This conclusion can be drawn on the basis of an evaluation which shows that a large number of molecular layers must be evaporated from the anode spot in order for ions to be formed by ionization of the liberated vapors in a quantity sufficient for initiation of breakdown by the considered processes. However, the presence of a large quantity of dissolved gases or of individual, even microscopic bubbles filled with gas in the surface layer of the anode can substantially facilitate the appearance of breakdown due to the formation of a significant number of positive ions in the interelectrode gap.

At present it does not appear possible to compare the calculated values of currents given on Fig. 80 with the results of experiments. Data available in the literature on the currents which directly precede breakdown between flat electrodes represent

the summary values of currents from the entire surface of the electrodes (and not from one projection) and, which is more important, were obtained by rather inertial methods which do not allow determination of currents within 10^{-7}-10^{-8} s prior to the appearance of breakdown - i.e., in a time interval corresponding to the time of development of the processes. Therefore the experimentally established fact that breakdown between flat electrodes can arise at very different points is not particularly helpful at this time. A number of observations show (see Chapter 3) that currents from individual projections begin to undergo separate short-term jumps when the average value of current in time from the point is greater than 10^{-5} A.[1] As a result of such a jump conditions can apparently be created for the appearance of breakdown even when the average current from the projection is comparatively small. On the other hand, currents amounting to a few milliamperes which do not convert to breakdown are sometimes observed from individual areas of emission [123, 164].

4. AN INDIVIDUAL PARTICLE OF MATERIAL AS AN INITIATOR OF BREAKDOWN

A metallic sphere of radius r lying on the surface of a smooth flat electrode picks up a charge [289] equal to

$$q = \varepsilon_0 \frac{\pi^2}{6} E r^2, \qquad (71)$$

[1] In work [288] a numerical calculation was carried out of the joule heating of an emitting projection in the form of a thin, relatively high cylinder on a flat cathode. This calculation showed that owing to the growth in electrical resistance of the material with temperature during a gradual rise of current a smooth growth in the temperature of the peak of the projection proceeds only up to a certain critical value; a further, even small increase in current leads to an uneven jump in temperature, so that the projection should melt. The critical value of temperature for tungsten comprises only a few hundred degrees (with the electrode body at room temperature). When the height of the tungsten projection is 1 μm and when $\mu = 100$ the current of the "skip" equals approximately 0.3 mA.

if r is significantly less than the interelectrode distance. Being pulled off from one of the electrodes under the action of electrostatic forces, the sphere attempts to travel to the opposite electrode. In passing through the potential difference U between the electrodes the sphere acquires a kinetic energy

$$W_k = qU = \varepsilon_0 \frac{\pi^3}{6} E r^3 U. \tag{72}$$

Even when the speed of motion of the sphere before impact is 1-10 m/s (depending on the material) the impact is inelastic and is accompanied by the conversion of kinetic energy into thermal energy [290]. When the speed of travel is greater than the speed of sound in the electrode material the collision time is so small that the liberated energy cannot travel outside the limits of the zone of deformation arising during impact. In this case the energy per unit mass is so great that evaporation of the material occurs in the deformation zone. The more the particle velocity exceeds the speed of sound in the material the more completely is the energy of motion of the particle consumed on evaporation of material. The temperature of the obtained vapors is not great and when the speed of travel of the particle is great prior to impact a large quantity of material is evaporated - i.e., energy is consumed mainly on the formation of vapors and not on heating them. The material outlined here represents elements of the theory of collision of bodies with cosmic velocities [291, 292] and clearly can be applied to our case. We will add that the dimensions of the zone of deformation during impact are commensurate with the size of the impacting particle if the speed of collision is close to the speed of sound, while equality of these velocities is quantitatively close to the condition that the kinetic energy of particle motion is equal to the heat required for evaporation (volatilization) of all of its material.

Until the sphere (particle) touches the opposite electrode it retains the charge acquired earlier and, consequently, possesses the electrostatic (potential) energy

$$W_p = \frac{q^2}{2C}, \tag{73}$$

where C is the capacitance of the sphere relative to the electrodes. With approach to the electrode C grows and W_p drops; however, as the calculation for the field of two spheres shows, even when the gap between the sphere and the electrode equals 0.15 r,

$$W_p = W_{p0.15} = \frac{q^2}{4\varepsilon_0 r} \approx 0{,}7\,\varepsilon_0 E^2 r^3, \tag{74}$$

i.e., comprises 50% of the potential energy of the sphere when it is located far from the electrodes. The intensity of the field between the sphere and the electrode at this distance exceeds E in the gap by almost 11 times (with flat, absolutely smooth electrodes). The greater the radius of the sphere the larger the amount of stored potential energy, the lower the speed of travel, and the greater the time during which the sphere is located at a distance from the electrode which is comparable with the radius of the sphere. Therefore with large r it is more probable that during the flight of the sphere toward the electrode an electrical charge will arise between them; besides this, with large r the power of the discharge will be great.

These phenomena, accompanying the flight of a conducting particle from one electrode to the other - heating and evaporation at the point of collision and an electrical charge between the flying particle and the electrode - can influence the electrical strength of vacuum insulation. Clearly the simplest case is that of the appearance of discharge between the electrode and the approaching particle. Such a discharge can act, as it were, as an igniting spark similar to that considered in Section 2 of

Chapter 6. If on the basis of the experimental data given in Table 53 we take for the evaluation the value of the minimum required ignition energy as 0.1 μJ, the potential energy equal to it [double the value according to expression (74)] will be possessed by a spherical particle 1 or 0.1 mm in diameter with a field intensity of 22 or 70 kV/mm, respectively.

According to the measurements made by Rozanova [152], metallic powder with particles 5-40 μm in size reduced the breakdown voltage to 7-9 kV with an interelectrode gap of 0.4 mm. Considering that the intensity at the point of particle breakaway may be higher than the average (22 kV/mm in the given case) because of surface irregularities, it can be considered that these figures do not contradict the evaluation given above for the possibility of initiation of vacuum breakdown by an electrical discharge between the electrode and an approaching particle. In the work by Rozanova the delay in the appearance of breakdown after application of voltage was approximately twice as great for particles initially located on the cathode than for particles on the anode - i.e., it was found that particles which initiate breakdown always fly from the anode (with supply of voltage particles begin to "skip" between the electrodes in both directions). This also agrees with the results given above from measurement of ignition energy, according to which an igniting spark on the cathode is significantly more effective than one on the anode.

Olendzskaya [153] studied the influence of steel and mercury spheres 0.5-9 mm in diameter on breakdown voltage. In the presence of the spheres the breakdown intensity was reduced to 5 kV/mm and was virtually independent of the applied voltage in the range 15-70 kV. In this same work the electrical discharge between the electrode and the approaching sphere was successfully fixed by means of high-speed cinematography. Higher effectiveness

of breakdown initiation during approach of steel spheres to the cathode than during approach to the anode was also observed. All of this is in good agreement with the assumption that breakdown in the given case is initiated by a discharge between the sphere and the electrode. However, the fact that the breakdown intensity was independent of the diameter of the sphere (0.5-9 mm) contradicts this assumption as it was outlined here and requires additional clarification. For example, it is possible that relationships (71) and (74) given above are invalid due to the commensurate size of the gap and the diameter of the sphere. In general, vacuum breakdown caused by a discharge between a particle and the electrode is clearly similar in its nature to drop flash-back in mercury rectifiers.

A completely undetermined factor is the possibility of initiation of breakdown due to thermal effects arising during impact of a microparticle - i.e., when the particle is small in size but its traveling speed and "specific" (per unit mass) energy are substantial. In 1952 Cranberg [178] put forth a hypothesis according to which breakdown occurs if the energy liberated per unit surface during collision reaches a critical magnitude. Since the area of the collision is proportional to r^2, according to (72) such a breakdown criterion has the form

$$UE = \text{const.} \tag{75}$$

For a uniform field between the electrodes the above expression is converted into the following:

$$U = \text{const} \cdot d^{0.5}, \tag{76}$$

which is usually called the Cranberg breakdown criterion.

Comparison with experimental data shows that the latter are arranged more or less satisfactorily around a line corresponding to expression (76) when the value of the constant is 100 kV/mm$^{0.5}$. Approximately the same result can be obtained from the data in Fig. 49, although (as more detailed analysis shows - see Table 34) the experimentally obtained value of the exponent at d is closer to 0.7. In works [293, 294] an effort was made to obtain theoretically the value of the constant in (76).

The simplicity of the physical foundation of the Cranberg formula and of the formula itself has brought the latter into wide acceptance at present; this is understandable if we consider that this was the first formula with some degree of physical foundation put forward to explain the reduction in breakdown intensity with a growth in voltage - an effect which was previously difficult to establish.

Further development of the hypothesis on initiation of breakdown by impact of a microparticle was undertaken in work [163], where it was assumed that breakdown appears if a gas discharge is triggered in the cloud of vapor formed as the result of collision. From the condition that evaporation takes place when the kinetic energy of the microparticle equals the heat of vaporization of the total material of the microparticle, it is possible to obtain the maximum radius for a spherical particle which can be evaporated under the given conditions in the gap during collision with the electrode (since the energy is proportional to r^2 and the heat of evaporation to r^3, such a calculation gives the maximum possible $r_{макс}$). On the other hand, ignition of a gas discharge in the cloud of vapor which is formed requires that the quantity of vapor be no less than a certain completely defined value - i.e., discharge can appear only with evaporation of a particle whose radius is no less than a certain value $r_{мин}$. By equating $r_{макс}$ and $r_{мин}$ it is possible

to write a general expression defining the condition when breakaway of a particle from one electrode and its collision with the opposite electrode will cause evaporation (in the presence of particles of various sizes on both electrodes) and when a gas discharge can arise in the cloud of vapors which is formed. If the ignition of a gas discharge in such a small cloud is defined by the Paschen curve, the condition indicated above will have the form

$$\mu_1 E_1 E_2^{2/3} U = 4{,}4 \cdot 10^{11} (pd)_{\text{мин}}^{1/3} U_{\text{э. мин}}^{2/3} \delta^{2/3} Q A^{-2/3}, \qquad (77)$$

where $\mu_1 E_1$ is the local intensity at the site from which the microparticle is stripped away; E_2 is the intensity at the collision point or, more exactly, at the point of ignition of the gas discharge; $U_{\text{э. мин}}$ and $(pd)_{\text{мин}}$ are the minimum ignition voltage on the Paschen curve and the value of pd corresponding to it in (mm Hg)·cm; δ, Q and A are the density of the electrode materials, the heat of vaporization (J/mole), and the atomic weight of the material of the microparticle (electrode material), respectively.

Specifically, for iron electrodes with $U_{\text{э. мин}} = 300$ V and $(pd)_{\text{мин}} = 0.5$ (mm Hg)·cm, which corresponds to the data for air, expression (77) is transformed into the following[1]:

$$\mu_1 E_1 E_2^{2/3} U = 1{,}67 \cdot 10^{20} \delta^{8/3} \cdot M^{-5/3}. \qquad (78)$$

[в = V]

When the gas cloud expands the pressure in it drops rapidly and discharge is quickly damped out if there is no additional arrival of gas into the discharge gap. Ions or electrons arising

[1] In work [163] the influence of electrostatic reflection was not taken into account during calculation of the charge; as a result the numerical coefficient in the right side of expressions (76) and (78) was understated by 2.2 times.

during such a microdischarge are not capable of heating the closest electrode; however, as they are accelerated in the interelectrode gap they will act incomparably more strongly on the opposite electrode, heating it, and causing secondary emission, and in the case of cathode bombardment thermionic emission can arise. Therefore a microdischarge occurring on the anode has greater "chances" of being "maintained" by the vapors and developing further, proceeding to encompass the entire interelectrode gap. Tentative calculations show that ionization of a few thousandths of the total quantity of atoms in a microparticle which is evaporated close to the anode is sufficient to heat the cathode up to the appearance of thermionic emission and thus to cause intensive evaporation on the anode due to its bombardment by thermoelectrons from the cathode. From this point of view expressions (77) and (78) represent criteria for appearance of breakdown if $E_1 = E_к$ and $E_2 = E_a$, i.e., the criterion of breakdown has the form

$$UE_к E_a^{2/3} = \text{const}, \qquad (79)$$

and for a uniform field,

$$U = \text{const} \cdot d^{0.625} \qquad (80)$$

The measurements carried out in this work of the breakdown voltage for sphere/sphere and sphere/plane iron electrodes (see Table 40) during repeated breakdowns showed good coincidence of the experimental data with the expression obtained above in the form of the dependence of U_{br} on $E_к$ and E_a. A quantitative agreement is obtained if the value $\mu = 12.8$ is substituted into expression (78). The diameter of microparticles which initiate breakdown as obtained from the calculations equals tenths of a micron - i.e., it is several orders smaller than the diameter of particles which can initiate breakdown due to the appearance of discharge between the electrode and the approaching particle.

From expression (77) it follows that the breakdown voltage is a function of electrode material. This dependence is in good agreement with the results of measurements made by Rozanova and Granovskiy [164]. With respect to tungsten (other conditions being equal) the breakdown voltage for molybdenum, iron, nickel, copper, and aluminum, according to the measurements, will comprise 0.88, 0.82, 0.82, 0.78, and 0.65 kV, respectively, while according to expression (77) this series should have the form 0.9, 0.79, 0.79, 0.76, 0.6 kV.

The fact that a microdischarge which arises on the anode has a greater chance of maturing into a discharge between the electrodes does not fit in with the fact that an igniting spark on the cathode is substantially more effective and will cause breakdown with a lower spark energy than in the case of a spark on the anode (see Section 2 of Chapter 6). Certainly, during artificial ignition the spark always appears in a certain depression in the electrode in which the igniting electrode is installed. This differs substantially from the conditions for a gas discharge in a cloud of evaporated material where, in particular, the conditions for the extraction and field acceleration of charged particles (especially ions) are strongly facilitated (as compared with those for an igniting spark). Therefore a direct comparison of the effectiveness of discharge in vapors between the electrodes and discharge in an igniting spark arising in a depression on the electrode is hardly justified. At the same time the very low energy required during ignition on the cathode permits us to assume that the initiation of breakdown can occur due to the formation in direct proximity to the cathode of a very small quantity of plasma with high local density. Tentative measurements carried out in work [231] showed that such a plasma should contain a total of 10^7-10^8 charged particles. This quantity amounts to less than 1% of the total number of particles which can be vaporized during collision of a microparticle with the electrode. Therefore the

probability of breakdown initiation in a vacuum by particles stripped away from the anode and impacting on the cathode cannot be excluded.

The possibility for initiation of breakdown by microparticles depends, of course, on the presence of such particles and the conditions under which they are stripped away from the electrodes. The first question which arises is that of the origin of such microparticles. Particles which represent the result of destruction of the surface during preliminary mechanical treatment or "dust" deposited on the electrodes during assembly can "favor" breakdown only in the initial period of operation with high voltage of the electrodes; as conditioning by breakdown proceeds this source of particles is exhausted. It is extremely probable that the well-known effect of conditioning (an increase in breakdown voltage during successive breakdowns) is explained to a significant degree by the destruction of microscopic particles initially present on the electrode surfaces. For example, it has been noted that electrodes which become more dusty in the assembly period not only require more prolonged conditioning but also have a lower value of breakdown voltage at the end of the conditioning period (see, for example, Table 31).

However, during conditioning by breakdowns there is not only destruction of the previously existing particles but also the formation of new particles which subsequently can become initiators of breakdown. Figure 81 shows photomicrographs of traces of transfer of anode material to the cathode during breakdown. This involved photographing not the actual surface of the cathode, but rather the coating on an object glass which was installed behind a fine metallic grid which represented the cathode in these experiments. It is evident that the particles transferred from the metallic anode have a predominantly spherical shape except for the case when the anode was made of graphite.

The size of the particles ranges from comparatively large down to fractions of a micron (the latter is determined by the limit of resolution of an optical microscope; obviously, there were other particles of even smaller size). On photographs made with iron and nickel anodes the formation of "lunar craters" - traces of splitting-off of material of particles during impact on the surface - is noticeable in certain cases. It is obvious that in this case the material was in the liquid state. This and the spherical shape of the majority of particles indicate that particles on the anode are formed from the liquid phase - i.e., the process of stripping away drops from the anode which was considered in Section 3 is apparently accomplished. The possibility that additional heating of the particles occurred during their collision with the surface is not excluded.

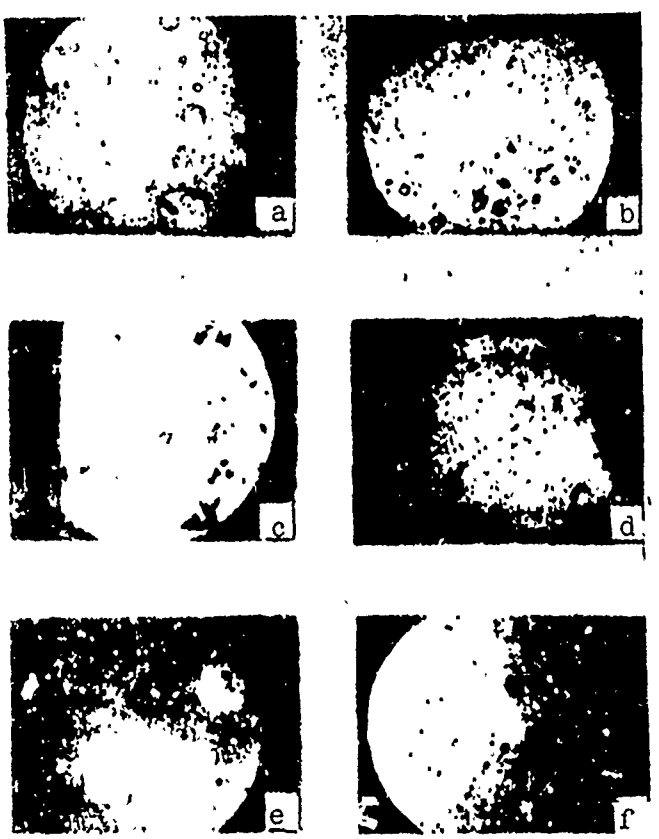

Fig. 81. Photomicrographs of a film on glass placed behind a grid cathode (×1350) after breakdowns: a - steel anode; b - nickel anode; c - graphite anode; d, e, f - copper anode; a, b, c, d - photographed in reflected light; e, f - photographed by transillumination (f is a picture of the same segment as on photo d).

With a graphite anode the transferred particles have a shape which differs sharply from spherical. It is natural to connect this with the fact that owing to its high vapor tension graphite does not have a liquid phase in vacuum.

The described experiments were carried out in a vacuum of $2 \cdot 10^{-6}$ to $3 \cdot 10^{-6}$ mm Hg created by oil pumps. In these conditions on both the object glass and ordinary electrodes a semitransparent film grew gradually, owing to cracking of adsorbed hydrocarbons under the action of dark currents. This film made it possible to observe certain additional details under the microscope in transmitted light. The photographs display white spots - points where, probably, the hydrocarbon film of the deposit was, in the literal sense of the word, evaporated during impact of a micro-particle - like the impacting particle itself. Since each photograph is the result of a 30-minute exposure, a portion of such "white spots" formed in the first minutes was once again covered over by a thinner film. The latter confirms that spots are formed during exposure of the electrodes under high voltage and are not a defect in the glass or damage which occurred during subsequent manipulations. Therefore the "white spots" can be interpreted with a substantial degree of probability as proof of strong heating occurring during collision with the electrode of particles of microscopic size stripped off from the opposite electrode.

In order to cross the interelectrode gap a particle must expend a certain amount of time; this can limit or completely exclude the probability of breakdown initiation by particles during a brief application of voltage. Since one of the conditions for appearance of breakdown is evaporation during collision, at the moment of impact a particle must have a velocity of several kilometers per second. A breakdown-appearance delay time of several microseconds corresponds to this velocity if $d \sim 1$ cm.

Under pulse voltage with a pulse length which is less than that given in the evaluation just completed, an increase in breakdown voltage should occur. In this case breakdown may be caused by particles of smaller dimensions which acquire a velocity greater than the minimum required for evaporation and which will lead to evaporation of the material in a quantity which is greater than that contained in the microparticle itself. Evaluation shows that in this case the pulse factor can be inversely proportional to the fourth route of the high-voltage pulse length. A somewhat different relationship for the pulse factor was obtained in work [295].

If breakdown is initiated by an electrical discharge between the electrode and an approaching particle, the required particle diameter is several orders greater than in the case of initiation by collision. In this case the flight time is large, approaching 1 ms with a particle diameter on the order of 0.1 mm. Therefore such a method of breakdown initiation can apparently be regarded as excluded in the case of pulses of high voltage of microsecond length. As regards high-frequency voltage, a situation occurs here which is to a certain degree the opposite of that found with constant or pulsed unipolar voltage. We will recall that the travel time of a charged particle from one electrode to the opposite can exceed by many times the duration of a single voltage period, while the energy acquired by the particle is determined by the potential difference, [whose] maximum is crossed by the particle in one half-period of hf voltage. Therefore with a frequency measured in tens of megahertz and with centimeter gaps between the electrodes we can consider the possibility of breakdown initiation by microparticle impact to be excluded. At the same time the initiation of breakdown by a discharge between the electrode and an approaching particle is completely possible if the duration of the applied voltage (and not the duration of one half-period)

is sufficient for the particle to fly from one electrode to the other. More than this, since with a certain phase with respect to the hf voltage in flight of a particle the latter can return after a half-period to the same electrode, the case of development of the total process of breakdown initiation on a single electrode alone becomes possible in principle. In this connection it is pertinent to cite the conclusion from studies of high-frequency vacuum breakdown carried out by Chupp [224, 225]. According to these studies, those electrode materials which give up the least metallic dust deposited both on the electrodes and on the bottom of the resonator during breakdown provide greater breakdown strength.

5. SEMIEMPIRICAL CRITERIA OF VACUUM BREAKDOWN

Practical problems in the application of vacuum electrical insulation frequently require quantitative analytical expressions of the dependence of breakdown voltage on the interelectrode gap, electrode geometry, and other parameters. Therefore numerous efforts have been made to obtain a formula which, on the one hand, would truly reflect the experimental relationships, and on the other hand would correspond in form to the physical concepts on the processes leading to vacuum breakdown. One such formula - among criteria for the appearance of vacuum breakdown - is the Cranberg formula examined above. However, the impact of micro-particles - the "physical basis" of the indicated formula - obviously cannot explain the appearance of breakdown in many specific cases: with a cathode in the form of a point, during application of hf voltage, during discharge in accelerator tubes, etc. From the utilitarian point of view this is a drawback of the Cranberg formula. A "universal" criterion defining the possibility of appearance of vacuum breakdown was developed by Kilpatrick [296, 297]. In his opinion this criterion is applicable

to the entire range of voltages, both constant and high-frequency, which are at present allowed and it determines the lower boundary - the minimum possible breakdown voltage. This criterion has the form

$$W_и E^2 \exp(-1{,}7 \cdot 10^7/E) = 1{,}8 \cdot 10^{18} \ \text{eV} \cdot \text{V}^2/\text{m}^2, \qquad (81)$$

where $W_и$ is the energy (in electronvolts) which a light ion (hydrogen ion) can acquire in the electrical field of the electrodes. Under constant voltage $W_и = eU$, and with hf voltage $W_и < eU$ (see Table 49).

The physical foundation for formula (81) is as follows: breakdown is caused by field-effect emission currents which are intensified by secondary cascade processes in which the major role is played by ions accelerated in the electrical field of the electrodes. Therefore the criterion of breakdown is presented as the product of a simplified expression for field-effect emission current and the energy which can be acquired by ions in the electrical field of the electrodes.

The numerical coefficients in expression (81) were selected empirically in order to obtain agreement with experimental data on breakdown. In this case the magnitude of the coefficient of the exponent of the exponential curve is such that when E > 20 kV/mm the exponential changes insignificantly, and with constant voltage and flat electrodes expression (81) takes on the form

$$U = \text{const} \cdot d^{2/3}. \qquad (82)$$

The line corresponding to expression (81) is plotted on Fig. 49, from which the close approximation of the Kilpatrick criterion with constant and pulse voltage is evident (we will recall that it should determine the minimum possible breakdown

voltage). There is no such close agreement with results of studies of vacuum electrical insulation under nf voltage. In a great number of works (for example, in [219]) it is noted that after good conditioning the vacuum gap will support without breakdown a voltage which substantially exceeds the voltage value from expression (81). In other words, the "universality" of the Kilpatrick criterion and its practical applicability are extremely limited.

We will pause briefly on the physical "basis" of the considered criterion. The numerical coefficient in the exponent of the exponential curve is 1-2 orders less than the analogous coefficient in relationship (13), which determines the magnitude of dark currents in the vacuum gap. In both formulas (13) and (81) the exponential term shows that the basic component of these currents is field-effect emission. In this case the indicated difference in the numerical values of the coefficients can be explained only by the fact that the electron current which gives rise to breakdown - so to speak, the most effective beam of electrons - comprises an insignificant portion of the total electron dark current, i.e., it is emitted by an insignificant portion of the total emitting surface - evidently the apex of a single sharp and very thin protuberance. From comparison of the path of the change in the exponential term in expression (81) with the same term in the theoretical formula of field-effect emission it follows that at the point of emission the coefficient μ and the work function Φ (in electron volts) have the relationship

$$\mu \approx (30 - 40)\Phi^2. \qquad (83)$$

If there are protuberances on the surface for which this condition is fulfilled, when E > 15-20 kV/mm the field-effect current from the projection is close to the maximum possible value (the exponential curve is close to unity), which makes melting of the projection due to the liberation of joule heat (according to expression (64) and Table 61) probable.

The presence in the Kilpatrick criterion of ion energy $W_и$ reflects the essential role played by ions proceeding from the anode in the initiation of breakdown. In the case when breakdown arises due to heating of the emitting projection by joule heat, $W_и$ can reflect the dependence of the size of projections on the energy of ions bombarding the cathode during dark currents and discharges. If breakdown occurs due to the action of an electron current on the anode, the Kilpatrick criterion can, on the basis of formulas (18) and (19), be interpreted as the condition when the energy liberated by the electron beam per unit surface on the anode achieves a critical value [in this case the dependence of U_{br} on frequency during high-frequency voltage would be different than indicated from expression (81)]. Thus the Kilpatrick criterion can be given a physical foundation if breakdown is caused by field-effect emission of very thin and sharp projections on the cathode. However, the assumptions outlined above have, in general, a speculative nature and new experimental data would be required before they were accepted or rejected.

Processes on the anode arising because of bombardment of the latter by an electron current in the form of a thin beam were used by Maitland [177] as the "physical basis" to obtain a relationship which defines the conditions for the appearance of breakdown. The conclusion is based on the assumption that breakdown occurs when the energy liberated per unit surface of the anode, W_a, due to incidence of a field-effect beam on the latter reaches a critical magnitude. To determine W_a it is necessary to know how the electron beam expands during travel of electrons from the cathode to the anode. Maitland used the Watson formula [298] (see also [299]), according to which under certain conditions the radius $r_{э.а}$ of a beam of electrons accelerated by the potential difference U after passage of gap d is defined by the relationship

$$r_{э.а} \sim d/U^{0.75}.$$

Since $W_a \sim UI/r_{s.a}^2$,

$$W_a \sim \frac{U^{2.5}}{d^2}, \tag{84}$$

and the constant value of the quantity W_a corresponds to the condition

$$\frac{U}{d^{0.8}} = \text{const}, \tag{85}$$

which was taken by Maitland as the criterion for the appearance of breakdown.

From a survey of experimental data in Chapter 4, in particular those from Table 34, it is clear that such a relationship between U and d is close to the most probable relationship obtained in the experiments.

The appearance on the anode of a multitude of microscopic craters favors the explanation of breakdown through the action of thin electron beams on the anode. Such craters are sometimes formed during the passage of dark currents, but they appear in considerably larger quantities in the initial stages of breakdown. For example, Maitland [177] observed the appearance of many thousand microscopic craters on the anode after breakdown on pulse voltage. The duration of the applied voltage comprised 4.5 μs; a 20-kohm resistor was installed in the discharge circuit, i.e., the postbreakdown spark was strongly limited in duration and power and therefore could not cause substantial melting of the electrode surfaces. The 1-1.5 μm radius of the craters agreed satisfactorily with the results of calculations carried out by Maitland according to the scheme described above. Maitland considered that such craters are formed directly before breakdown and are the result of the action of a multitude of "elementary" electron beams on the anode, with the totality of the beams comprising the usual prebreakdown dark current.

However, the Maitland method - a method of analytical determination of the specific energy liberated on the anode by the electron beam - can hardly be accepted as correct, since it is based on the Watson formula [298] (see also [299]), which describes the expansion of an initially parallel beam of already accelerated electrons during their motion in drift space, i.e., in space where E = 0. The reason for expansion of such a beam is the action of the intrinsic space charge. It is clear that the conditions under which the cited formula is valid differ substantially from those which obtain in the real case of the motion of constantly accelerated electrons from the cathode to the anode. In Section 2 of Chapter 3 data were presented which indicate that if the electrons are emitted by a projection on the cathode the expansion of such a beam with a current up to 8-10 mA is determined by the tangential components of the electrical field of the electrodes, with these components appearing due to distortion of the field close to the projection. If the electrons are emitted by a flat segment of the cathode, where the work function Φ is strongly reduced, in the initial portion of travel the expansion of the beam may actually be determined by the action of the inherent space charge, but after acceleration up to a few kilovolts the subsequent trajectory of motion of the electrons represents a parabola and, consequently, (just as during emission of electrons from a projection) the radius of the beam $r_э$ depends only on the ratio U/d - i.e., it is determined by field intensity and does not depend separately on the voltage and magnitude of the gap. Thus, the shape of the electron beam in the gap differs substantially from that accepted by Maitland. The expression for the maximum possible density released on the anode by the electron beam is significantly closer to the relationship obtained by Maitland. This equation can be obtained from expression (20) (by multiplying it by U):

$$W_a = 1{,}09 \cdot 10^{-3} I^{0.1} U^{2{,}325}/d^2. \qquad (86)$$

The expression thus found resembles condition (84) and depends very little on I. However, if this is the current of field-effect emission, its strong dependence on E does not permit us to ignore the dependence of W_a on $I^{0.1}$. Actually, with field-effect emission current densities greater than 10^4 A/m^2 a twofold change in E leads to a change in the current by 3-4 orders, and, consequently, $I^{0.1}$ is approximately proportional to E. In this case in an expression analogous to (85) the value -0.9 will stand in the exponent of the exponential curve at d instead of -0.8.

The possibility is not excluded that an electron beam initiating breakdown can have a nature similar to the Molter effect - i.e., caused by electron emission through a dielectric film whose outer surface is positively charged. There is a certain confirmation of this assumption in the results of studies by Maitland of the conditions for appearance of repeated breakdowns. In Section 4 of Chapter 6 it was stated that repeated breakdown is favored in the course of approximately 0.5 ms after suppression of the preceding discharge, where the "weak point" (where breakdown if favored) is located to one side of the channel of the preceding breakdown. Such properties can be explained by the fact that the currents flowing during the first discharge charge the dielectric films which exist during this discharge and are not destroyed by it; this intensifies electron emission through these films, while the charge on their surface is retained. Clearly, the charge is not retained for a very extended period, which explains the "recovery" of the vacuum gap to usual insulation strength after 0.5 μs. One can assume that similar but less intensive sites of electron emission usually appear during dark currents flowing when high voltage is applied to the electrodes. The dependence of electron emission through dielectric films on the intensity in the gap should be substantially weaker than that of the usual field-effect emission. If these currents can initiate breakdown through their bombardment of the anode, the

condition of criticality of specific energy on the anode (86) as a condition for the appearance of breakdown can have the form of the Maitland criterion (85).

The material outlined in this chapter shows the great diversity of of phenomena which can lead to the appearance of breakdown. Naturally, in such a situation no single criterion of breakdown appearance with a physical foundation can exist under the entire variety of conditions in which vacuum electrical insulation "operates," although from the practical point of view such a generalized formula would be extremely desirable. Finally, it is possible and necessary to select empirical relationships reflecting real laws for fairly narrow ranges of conditions. However, it appears illogical to create a "universal" criterion, since such a criterion inevitably simplifies the complex picture of the processes influencing the quality of vacuum insulation, reducing the entire variety of these phenomena to some single cause.

Another conclusion which suggests itself from the entire content of this chapter lies in the fact that the conditions under which vacuum electric insulation ordinarily "operates" are very far from the most favorable. Whether microdischarges cause breakdown, whether destruction of electrodes by electrostatic forces plays decisive role, or whether field-effect emission is the initiator of breakdown - in all these cases quantitative evaluations show that the presently achievable level of vacuum electrical insulation is determined either by the presence on the surface of impregnations and particles of various sizes which are weakly bound to the main mass of the electrode or by the presence of anomalously large and sharp projections, dielectric films, or contaminants which substantially reduce the work function or which cause the appearance of various types of emission of charged particles, etc. In other words, on the basis of the

analysis given above there is every reason to arrive at the extremely optimistic conclusion that there is a real possibility of substantially increasing the quality of vacuum electrical insulation.

BIBLIOGRAPHY

1. Тарасова Л. В. «Успехи физ. наук», 63, 321 (1956).
2. Глазков В. Н. «Электричество», № 3, 40 (1958).
3. Hawley R. Vacuum, 10, 310 (1960).
4. Каретников Д. В. и др. Линейные ускорители ионов. М., Госатомиздат, 1962, гл. 7.
5. Вальтер А. К. и др. Электростатические ускорители заряженных частиц. М., Госатомиздат, 1963, § 5 гл. 2.
6. Левитов В. И., Ляпин А. Г. Электростатические генераторы с жестким ротором. М., Госэнергоиздат, 1963.
7. Преобразование тепла и химической энергии в электроэнергию в ракетных системах. Пер. с англ. Под ред. Кириллина В. А. и Шейндлина А. Е. М., Изд-во иностр. лит., 1963.
8. Uhlin I. B. et al. Trans. 9-th. Nat. Vac. Sympos. Am. Vac. Soc., Los Angeles, 1962. N. Y., 1962, p. 371.
9. Каретников Д. В. и др. Линейные ускорители ионов. М., Госатомиздат, 1962, стр. 198.
10. Управляемые разрядники для коммутации больших импульсных токов в высоковольтных установках. Сб. рефератов. М., Госатомиздат, 1962.
11. Bracewell G. M. et al. Nucl. Power, 4, 115 (1959).
12. Hagerman D. C., Williams A. H. Rev. Scient. Instrum., 30, 182 (1959).
13. Бриш А. А. и др. «Приборы и техника эксперимента», № 5, 53 (1958).
14. Цукерман В. А., Манакова М. А. «Ж. техн. физ.», 27, 391 (1957).
15. Reece M. P. J. IEE, 5, 275 (1959).
16. Александров Д. Д. и др. «Ж. техн. физ.», 28, 896 (1958).
17. Добрецов Л. Н. Электронная и ионная эмиссия. М. —Л., Гостехиздат, 1952.
18. Development of Field emission flash x-Ray tubes and devices. UCRL-13025, California, USA, 1960.
19. Елинсон М. И., Васильев Г. Ф. Автоэлектронная эмиссия. М., Физматгиз, 1958.
20. Good R. H., Müller E. W. In: «Handbuch der Physik». Bd. 21. Berlin, 1956, S. 176.
21. Dolan W. W. Phys. Rev., 91, 510 (1953).
22. Dolan W. W., Dyke W. P. Phys. Rev., 95, 327 (1954).
23. Васильев Г. Ф. «Радиотехника и электроника», 5, 1857 (1960).
24. Компанеец А. С. В кн. «Некоторые вопросы катодной электроники». Ташкент, Изд-во САГУ, 1959, стр. 117.
25. Гофман И. И. «Физика твердого тела», 4, 2005 (1962).
26. Murphy E. L., Good R. H. Phys. Rev., 102, 1464 (1956).
27. Good R. H. J. Appl. Phys., 28, 1405 (1957).
28. Guth E., Mullin C. J. Phys. Rev., 61, 340 (1942).
29. Dyke W. P., Dolan W. W. Adv. Electronics and Electron Phys., 8, 90 (1956).
30. Dyke W. P. et al. Phys. Rev., 99, 1192 (1955).
31. Шуппе Г. Н. Электронная эмиссия металлических кристаллов. Ташкент, Изд-во САГУ, 1959.
32. Tuczek H. Z. Angew. Phys., 9, 388 (1957).
33. Херинг К., Никольс М. Термоэлектронная эмиссия. Перев. с англ. М., Изд-во иностр. лит., 1950.
34. Charbounnier F. M., Martin E. K., J. Appl. Phys., 33, 1897 (1962).

35. Robertson A. J. B. et al. Brit. J. Appl. Phys., 14, 278 (1963).
36. Young R. D., Müller E. W. J. Appl. Phys., 33, 91 (1962).
37. Kerner K. Z. Angew. Phys., 8, 1 (1956).
38. Llewellyne-Jones F., Owen W. D. Proc. Phys. Soc., 83, part 2, No. 532, 283 (1964).
39. Lewis T. J. Proc. Phys. Soc., Sec. B, 68, No. 428B, 504 (1955).
40. Drechsler M., Z. Phys., 167, 558 (1962).
41. Little R. P., Whitney W. F. J. Appl. Phys., 34, 2430 (1963).
42. Ландау Л. Д. Электродинамика сплошных сред. М., Физматгиз, 1959.
43. Lewis T. J. J. Appl. Phys., 46, 1405 (1955).
44. Bennette C. J. et al. J. AIAA, 3, 284 (1965).
45. Litte R. P., Smith S. T. Transaction on Electron Devices, ED-12, 77 (1965).
46. Denholm A. S. Canad. J. Phys., 36, 476 (1958).
47. Рашковский С. Ф. «Радиотехника и электроника», 3, 371 (1958).
48. Жаке П. Электролитическое и химическое полирование. Перев. с англ. М., Металлургиздат, 1959.
49. Hawley R., Walley C. A. Nature, 190, 252 (1961).
50. Hawley R. Vacuum, 11, 32 (1961).
51. Maitland A. J. Appl. Phys., 33, 248 (1962).
52. Гегузин Я. Е., Овчаренко Н. Н. «Изв. АН СССР. Отд. техн. наук», № 1, 108 (1956).
53. Sewell D. B. et al. J. Phys. Chem., 67, 2008 (1963).
54. Лозинский Я. Г. Высокотемпературная металлография. М., Машгиз, 1956.
55. Бекер Д. А. В кн. «Катализ. Электронные явления». Перев. с англ. Под ред. Баландина А. А., Бонч-Бруевича В. Л. и Рогинского С. З. М., Изд-во иностр. лит., 1958, стр. 215.
56. Benjamin M., Jenkins R. O. Proc. Roy. Soc., A176, 262 (1940).
57. Gomer R. J. Chem. Phys., 21, 293 (1953).
58. Boling J. Z., Dolan W. W. J. Appl. Phys., 29, 556 (1958).
59. Barbor J. P. et al. Phys. Rev., 117, 1452 (1960).
60. Сокольская И. Л. «Ж. техн. физ.», 26, 1177 (1956).
61. Сокольская И. Л. и др. «Физика твердого тела», 6, 1439 (1964).
62. Meelewski A. et al. Acta phys. polon., 21, 189 (1962); 22, 525 (1962).
63. Gomer R., Smith C. S. Structure and Properties of Solid Surfaces. Chicago, University of Chicago Press, 1953.
64. Müller E. W. Z. Phys., 126, 642 (1949).
65. Сокольская И. Л. «Изв. АН СССР. Сер. физ.», 20, 1151 (1956).
66. Bettler P. C., Charbounier P. R. Phys. Rev., 119, 85 (1960).
67. Тарасова Л. В. и др. «Радиотехника и электроника», 5, 666 (1960).
68. Sudan R. N., Gonzallez-Perez F. J. Appl. Phys., 35, 2269 (1964).
69. Надгорный Э. М. и др. «Успехи физ. наук», 67, 625 (1959).
70. Arnold C. M., Koonce S. E. J. Appl. Phys., 27, 964 (1956)
71. Melmed A. J., Gomer R. J. Chem. Phys., 30, 586 (1959).
72. Melmed A. J., Gomer R. J. Chem. Phys., 34, 1802 (1961).
73. Трепнел Б. Хемосорбция. М., Изд-во иностр. лит., 1958.
74. Химия твердого состояния. Перев. с англ. Под ред. В. Гарнера. М., Изд-во иностр. лит., 1961.
75. Eberhagen A. Fortschritte der Physik, 8, 245 (1960).
76. Очистка деталей электронных приборов. Перев. с англ. Под ред. Луфт Б. Д. и Шустиной А. Л. М. — Л., «Энергия», 1964.
77. Blears J. J. Scient Instrum., Suppl. No. 1, Vacuum Phys., 36 (1951).
78. Спивак Г. В. и др. «Изв. АН СССР», 28, 1382 (1964).
79. Ennos A. E. Brit. J. Appl. Phys., 4, 101 (1953); 5, 27 (1954).

80. Holland Z. et al. Rev. Scient. Instrum., 34, 377 (1963).
81. Donalson E. E., Robinovitz M. J. Appl. Phys., 34, 319 (1963).
82. Donalson E. E. Vacuum, 12, 11 (1962).
83. Фоменко В. С. Эмиссионные свойства элементов и химических соединений. Справочник. Киев, изд-во «Наукова думка», 1964.
84. Царев Б. М. Контактная разность потенциалов. М., Гостехиздат, 1955.
85. Калвер Р., Томпкинс Ф. В кн. «Катализ. Вопросы избирательности и стереоспецифичности катализаторов». Перев. с англ. Под ред. Баландина А. А. и Рубинштейна А. М. М., Изд-во иностр. лит., 1963, стр. 79.
86. Бонч-Бруевич В. Л. «Успехи физ. наук», 40, 369 (1950).
87. Broeder J. J. et al. Z. Electrochem., 60, 838 (1956).
88. Weissler G. L., Wilson T. N. J. Appl. Phys., 24, 472 (1953)
89. Чистяков П. Н. «Ж. техн. физ.», 33, 1395 (1963).
90. Maddison R. C. et al. Nuovo cimento, Suppl., 1, 742 (1963).
91. Зандберг Э. Я., Ионов Н. И. «Успехи физ. наук», 67, 581 (1959).
92. Агишев Е. И., Беляков Ю. Н. «Ж. техн. физ.», 29, 1481 (1959).
93. Зандберг Э. Я., Ионов Н. И. «Докл. АН СССР», 141, 139 (1961).
94. Бакулина И. Н. и др. «Ж. техн. физ.», 35, 562 (1965).
95. Агишев Е. И., Беляков Ю. И. «Ж. техн. физ.», 30, 223 (1960).
96. Брюнинг Г. Физика и применение вторичной электронной эмиссии. Перев. с англ. М., «Советское радио», 1958.
97. Бронштейн И. М., Фрайман Б. С. «Физика твердого тела», 3, 2859 (1961).
98. McKay K. G. Adv. in Electronics, 1, 66 (1948).
99. Бронштейн И. М., Денисов С. С. «Физика твердого тела», 6, 1921 (1964).
100. Trump J. G., van de Graaff R. J. J. Appl. Phys., 18, 327 (1947).
101. Trump J. G., van de Graaff R. J. Phys. Rev., 75, 44 (1949).
102. Еремеев М. А., Петров Н. И. «Проблемы современной физики», № 9, 133 (1956).
103. Парилис Э. С. «Радиотехника и электроника», 7, 1979 (1962).
104. Парилис Э. С., Кишиневский Л. М. «Физика твердого тела», 3, 1219 (1961).
105. Webster et al. J. Appl. Phys., 23, 264 (1952).
106. Bourne H. C. et al. J. Appl. Phys., 26, 596 (1955).
107. Aarset B. et al. J. Appl. Phys., 25, 1365 (1954).
108. Hill A. G. et al. Phys. Rev., 55, 463 (1939).
109. Waters P. M. Phys. Rev., 111, 1053 (1958).
110. Фогель Я. М. и др. «Ж. техн. физ.», 30, 64 (1960).
111. Тельковский В. Г. «Изв. АН СССР. Сер. физ.», 20, 1179 (1956); «Докл. АН СССР», 108, 444 (1956).
112. Large L. N. Proc. Phys. Soc., 81, 1101 (1963).
113. Mansfield W. K. Brit. J. Appl. Phys., 11, 454 (1960).
114. Фогель Я. М. и др. «Ж. техн. физ.», 30, 824 (1960).
115. Фогель Я. М. и др. «Радиотехника и электроника», 8, 684 (1963).
116. Арифов У. А. Взаимодействие атомных частиц с поверхностью металла. Ташкент, Изд-во АН УзССР, 1961, гл. 5.
117. Фогель Я. М. и др. «Ж. техн. физ.», 30, 64 (1960).
118. Митропан И. М., Гуменюк В. С. «Ж. эксперим. и теор. физ.», 32, 214 (1957).
119. Anderson H. W. Rev. Scient. Instrum., 6, 309 (1935); Electr. Engng., 26, 1315 (1935).
120. Пивовар Л. Н. и др. «Ж. техн. физ.», 27, 997 (1957).
121. Linder E. G., Christian S. M. J. Appl. Phys., 23, 1213 (1952).
122. Пивовар Л. И., Гордиенко В. И. «Ж. техн. физ.», 32, 1230 (1962).

123. Heard H. G., UCRL-1697 (1952); UCRL-2252 (1953), California, USA.
124. Brodie I. J. Appl. Phys., 35, 2324 (1964).
125. Wijker W. J. Appl. Sci. Res., B9, 1 (1961).
126. Hawley R. Nature, 196, 56 (1962).
127. Owen W. D., Beyon J. Vacuum, 15, 123 (1965).
128. Ионов Н. И. «Ж. техн. физ.», 30, 561 (1960).
129. Hawley R. Vacuum, 13, 367 (1963).
130. De Geeter D. L. J. Appl. Phys., 34, 919 (1963).
131. Morant M. J. Proc. Phys. Soc., B68, 513 (1955).
132. Llewellyn-Jones F. L., Micolas D. J. In: «Proc. 5-th Internat. Conf. Ions Phenomena Gas, Münich, 1961», Vol. 2. Amsterdam, 1962, p. 1179.
133. Сливков И. Н. «Ж. техн. физ.», 36, 342 (1966).
134. Calvert W. J. R. Proc. Phys., Soc., B69, 651 (1956).
135. Bertein F. Compt. Rend., 222, 64 (1946).
136. Clifford D. C., Fortesque R. L., Nature, 170, 503 (1952).
137. Arnal R. Compt. Rend., 237, 308 (1953).
138. Arnal R. Compt. Rend., 238, 2061 (1954).
139. Arnal R. Compt. Rend., 238, 2402 (1954).
140. Arnal R. Compt. Rend., 240, 610 (1955).
141. Arnal R. Compt. Rend., 242, 2308 (1956).
142. Arnal R. Annal. de Phys., 10, 310 (1955).
143. McKibben I. L., Boyer K. Bull. Amer. Phys. Soc., 26, 2 (1951); Phys. Rev., 82, 315 (1951).
144. Blewett J. P., Turner C. M. Phys. Rev., 81, 305 (1951).
145. Chick D. R., Miranda F. J. Bull. Amer. Phys. Soc., 25, 171 (1950); J. Scient. Instrum., 27, 337 (1950).
146. Mansfield W. K., Fortesque M. A. Brit. J. Appl. Phys., 8, 73 (1956).
147. Пивовар Л. И., Гордиенко В. И. «Ж. техн. физ.», 28, 2289 (1958).
148. Boersch H. et al. Z. angew. Phys., 13, 450 (1961).
149. Тарасова Л. В., Разин А. А. «Ж. техн. физ.», 29, 967 (1959).
150. Swabe S. Z. angew. Phys., 12, 244 (1960).
151. Browne P. F. Proc. Phys. Soc., B68, 564 (1955).
152. Розанова Н. Б. «Изв. АН СССР. Сер. физ.», 26, 1438 (1962).
153. Олендзская Н. Ф. «Радиотехника и электроника», 8, 479 (1963).
154. Heard H. G., Lauer E. L. UCRL-2051 (1952), California, USA.
155. Gross H. J. J. Appl. Phys., 8, 540 (1937).
156. Maitland A. In: «Proc. 5-th Internat. Conf. Ion Phenomen Gas, Münich, 1961», Vol. 1, Amsterdam, 1962, p. 718.
157. Боровик Е. С., Батраков Б. М. «Ж. техн. физ.», 28, 1971 (1958).
158. Тарасова Л. В., Калинин В. Г. «Ж. техн. физ.», 34, 666 (1964).
159. Рекомендуемые условия проведения опытов при изучении пробоя в высоком вакууме. «Радиотехника и электроника», 8, 2103 (1963).
160. Сливков И. Н. «Ж. техн. физ.», 28, 759 (1958).
161. Khalifa M. Canad. J. Phys., 34, 304 (1956).
162. Maitland A. J. Appl. Phys., 34, 996 (1963).
163. Сливков И. Н. «Ж. техн. физ.», 27, 2081 (1957).
164. Розанова Н. Б., Грановский В. Л. «Ж. техн. физ.», 26, 489 (1956).
165. Bennett W. P. Phys. Rev., 40, 416, 1013 (1933).
166. Безбатченко А. Л. и др. «Атомная энергия», 14, 446 (1963).
167. Кассиров Г. М., Ковальчук В. М. «Ж. техн. физ.» 34, 484 (1964).
168. Warmolz N. Philips Res. Rep., 2, 426 (1947).
169. Каляцкий И. И., Кассиров Г. М. «Ж. техн. физ.», 34, 348 (1964).
170. Каляцкий И. И., Кассиров Г. М. «Изв. вузов (физ.)», № 4, 78 (1963).

171. Seifert H. S. Phys. Rev., 62, 300 (1942).
172. Пивовар Л. И. и др. «Тр. физ. отд. Харьковского гос. унив.», 7, 171 (1958).
173. Denholm A. S. et al. Astronautics, No. 6, 46 (1962).
174. Gleichauf P. H. J. Appl. Phys., 22, 535 (1951).
175. Piersol R. J. Phys. Rev., 25, 112 (1925).
176. Hayden J. I. R. Trans. AIEE, 41, 852 (1922).
177. Maitland A. J. Appl. Phys., 32, 2399 (1961).
178. Cranberg L. J. Appl. Phys., 23, 518 (1952).
179. Boyle W. S. et al. J. Appl. Phys., 26, 720 (1955).
180. Mason R. C. Phys. Rev., 52, 126 (1937).
181. Sommeria J. Le Vide, 15, 52 (1960).
182. Maitland A. Brit. J. Appl. Phys., 13, 122 (1962).
183. Leader D. Proc. IEE, 100, 2A, 138 (1953).
184. Rabinowitz M., Donalson E. E. J. Appl. Phys., 36, 1314 (1965).
185. Rabinowitz M. Vacuum, 15, 59 (1965).
186. Сливков И. Н. «Ж. техн. физ.», 29. 1473 (1959).
187. Ahearn A. J. Phys. Rev., 50, 238 (1936).
188. Dyke W. P. et al. Phys. Rev., 89, 799 (1953).
189. Dyke W. P. et al. Phys. Rev., 91, 1043 (1953).
190. Dolan W. W. et al. Phys. Rev., 91, 1054 (1953).
191. Горьков В. А. и др. «Радиотехника и электроника», 7, 1501 (1962).
192. Фурсей Г. Н. «Радиотехника и электроника», 6, 298 (1961).
193. Сокольская И. Л., Фурсей Г. Н. «Радиотехника и электроника», 7, 1474, 1484 (1962).
194. Зубенко Ю. В. и др. «Ж. техн. физ.», 34, 911 (1964).
195. Фурсей Г. Н., Толкачева Н. Д. «Радиотехника и электроника», 8, 1210 (1963).
196. Dyke W. P. et al. J. Appl. Phys., 31, 792 (1960).
197. Елинсон М. И. «Радиотехника и электроника», 3, 438 (1958).
198. Елинсон М. И. и др. «Радиотехника и электроника», 5, 1318 (1960).
199. Hashimoto K. J. Phys. Soc. Japan, 2, 71 (1947).
200. Розанова Н. Б. В кн. «Тезисы докладов на конференции по пробою диэлектриков и полупроводников. 1963 г.» Томск, Изд-во Томского гос. унив., 1963, стр. 13.
201. Gleichauf P. H. J. Appl. Phys., 22, 766 (1951).
202. Kofoid M. J. Trans. AIEE, part III, 79, 991 (1960); Electrical Eng., 80, 182 (1961).
203. Britton R. B. et al. Rev. Scient Instrum., 34, 185 (1963).
204. Boersch H. et al. Z. angew. Phys., 15, 518 (1963).
205. Holse T. Trans. 9-th Nat. Vac. Symp. Am. Vac. Soc. Los Angeles, 1962. N. Y., 1962, p. 376.
206. Jedinak L. J. Appl. Phys., 35, 1727 (1964).
207. Trump J. G. In: «La Physique des Forces Electrostatiques et Leur Application». Ed du centre Nat. Res. Sci., Paris, 1961.
208. Halpern J. et al. Phys. Rev., 69, 688(A) (1946).
209. Николаев Ю. Н. «Ж. техн. физ.», 33, 479 (1963).
210. Gill E. W., Von Engel A. Proc. Roy Soc., A192, 446 (1948).
211. Hatch A., Williams H. B. Phys. Rev., 112, 681 (1958).
212. Сканави Г. И. Физика диэлектриков (область сильных полей). М., Физматгиз, 1958.
213. Браун С. Элементарные процессы в плазме газового разряда. М., Госатомиздат, 1961.
214. Френсис Г. Ионизационные явления в газах. М., Атомиздат, 1964.
215. Зайдин Д. Г., Кушин А. В. «Тр. РТИ АН СССР», 2160—36, М., 1960.
216. Hatch A. J., Williams H. B. J. Appl. Phys., 25, 417 (1954).
217. Загер Б. А., Тишин В. Г. «Ж. техн. физ.», 34, 297 (1964).
218. Callebaut D. K. Physica, 29, 784 (1963).
219. Поляков Б. И. и др. «Тр. РТИ АН СССР», 1, 93 (1959).
220. Aitken D. K. Proc. I. E. E., B105, Suppl., 1, 824 (1958).
221. Зайдин Д. Г. «Тр. РТИ АН СССР», 6, 253 (1964).
222. Загер Б. А. и др. «Приборы и техника эксперимента», № 2, 20 (1963).

232. Бойм А. Б., Рейхрудель Э. М. «Радиотехника и электроника», 8, 815 (1963).
233. Бойм А. Б., Рейхрудель Э. М. «Ж. техн. физ.», 31, 1127 (1961).
234. Симонов В. А., Кутуков Г. П. «Радиотехника и электроника», 4, 1311 (1959).
235. Flynn R. T. G. Proc. Phys. Soc., B69, 748 (1956).
236. Goldman M., Goldman A. Compt. rend., 253, 2654 (1961).
237. Steenbek M. Naturwiss., 26, 476 (1938).
238. Рейхрудель Э. М. и др. «Ж. техн. физ.», 24, 1179 (1954).
239. Кустова А. В., Рейхрудель Э. М. «Ж. техн. физ.», 24, 2183 (1954).
240. Финкельбург В., Меккер Г. Электрические дуги и термическая плазма. М., Изд-во иностр. лит., 1961.
241. Кесаев И. Г. Катодные процессы ртутной дуги и вопросы ее устойчивости. Труды ВЭИ. Вып. 67, М., Госэнергоиздат, 1961.
242. Copeland P., Sparing W. H. J. Appl. Phys., 16, 302 (1945).
243. Cobine I. D., Ferrall G. A. J. Appl. Phys., 31, 2296 (1960).
244. Кесаев И. Г. «Ж. техн. физ.», 33, 603, 616 (1963).
245. Reece M. P. Nature, 177, 1089 (1956).
246. Reece M. P. Nature, 181, 475 (1958).
247. Maitland A. Brit. J. Appl. Phys., 13, 41 (1962).
248. Shaaffs H. Phys. Verhandl., 3, 176 (1952).
249. Розанова Н. Б. и др. «Радиотехника и электроника», 4, 1267 (1959).
250. Vargo D. J., Taylor F. J. Appl. Phys., 33, 2911 (1962).
251. Дикиджи А. Н., Клярфельд Б. Н. «Ж. техн. физ.», 25, 1038 (1955).
252. Гусева Л. Г., Клярфельд Б. Н. «Ж. техн. физ.», 24, 1169 (1954).
252а. Гусева Л. Г. В кн. «Исследования в области электрического разряда в газах». Труды ВЭИ. М., Госэнергоиздат, 1958, стр. 7.
253. Мик Дж., Крэгс Дж. Электрический пробой в газах. М., Изд-во иностр. лит., 1960.
254. Loeb J. B. In «Handbuch der Physik». B21. Heidelberg, 1956, S. 445.
255. Boyle W., Kisliuk P. Phys. Rev., 97, 255 (1955).
256. Finkelman E. Arch. f. Elektrotechn., 31, 282 (1937).
257. Покровская-Соболева А. С., Клярфельд Б. Н. «Ж. эксперим. и теор. физ.», 32, 991 (1957).
258. Druyvesteyn M., Penning F. Rev. Mod. Phys., 12, 89 (1940).
259. Penning F. M. Phys. Zeit., 33, 816 (1932).
260. Клярфельд Б. Н., Гусева Л. Г. «Ж. техн. физ.», 35, 306 (1965).
261. McClure Cs. W. Phys. Rev., 4, 969 (1961).
262. Brewer A., Westhaver J. J. Appl. Phys., 8, 779 (1937).
263. Phillips G. E. S. Proc. Roy. Soc., A64, 172 (1898).
264. Strutt R. J. Proc. Roy. Soc., 89, 68 (1913).
265. Penning F. M. Physica, 3, 837 (1936).
266. Penning F. M. Physica, 4, 71 (1937).
267. Смирницкая Г. В., Рейхрудель Э. М. «Радиотехника и электроника», 10, 1303 (1957).
268. Backus J. J. Appl. Phys., 30, 1866 (1959).
269. Backus J. J. Appl. Phys., 31, 400 (1960)
270. Gou D., Foster J. S., Rev. Scient. Instrum., 27, 809 (1956).
271. Крейндель Ю. Е., Фахрутдинов Э. Н. «Ж. техн. физ.», 35, 312 (1965).
272. Sommervill J. M. Proc. Phys. Soc., B65, 620 (1952).
273. Haffer R. Acta Phys. Austriaca, 7, 52, 251 (1953); 8, 213 (1954).
274. Redhead R. A. Canad. J. Phys., 36, 225 (1958).
275. Blevin H. A. UKAEA, Research Group. Report 1961, CLM-R-10.

276. Trump J. G. Phys. Rev., 69, 692 (1946).
277. Filosofo I., Rostagni A. Phys. Rev., 75, 1269 (1949).
278. Bennett A. I. Appl. Phys., 28, 1251 (1957).
279. Bourne H. C. et al. J. Appl. Phys., 26, 596 (1955).
280. Llewellyn-Jones F., Morgan C. F. Proc. Roy. Soc., A218, 88 (1953).
281. Wroe H., Anderson R. H. Nature, 183, 1544 (1959).
282. Eckertowa L., Seskosl. casop. fys., A10, 412 (1960).
283. Balas V. Seskosl. casop. fys., A13, 441 (1963).
284. Розанова Н. Б., Грановский В. Л. «Изв. АН СССР. Сер. физ.», 20, 1162 (1956).
285. Tonks L. Phys. Rev., 48, 562 (1935).
286. Frenkel J. Phys. Z. Sowietunion, 8, 765 (1935).
287. Брагин С. М. и др. Теория и практика пробоя диэлектриков. Л., Госиздат, 1929.
288. Vibrans G. E. J. Appl. Phys., 35, 2855 (1964).
289. Лебедев И. Н., Скальская И. П. «Ж. техн. физ.», 32, 375 (1962).
290. Кильчевский Н. А. Теория соударения твердых тел. Л. — М., Гостехиздат, 1949.
291. Станюкович К. П. «Метеоритика», № 7, 39 (1950).
292. Станюкович К. П. Элементы теории удара твердых тел с большими (космическими) скоростями. В сб. «Искусственные спутники Земли». Вып. 4, М., Изд-во АН СССР, 1960.
293. Mayer W. E. Z. angew. Phys., 13, 51 (1961).
294. Boulloud A. Le Vide, 17, 240 (1962).
295. Ferall G. A. J. Appl. Phys., 33, 96 (1962).
296. Kilpatrick D. W. UCRL-2371, California, USA, 1953.
297. Kilpatrick D. W. Rev. Scient. Instrum., 28, 824 (1957).
298. Watson E. E. Phyl. Mag., 3, 849 (1927).
299. Зинченко Н. С. Курс лекций по электронной оптике. Харьков, Изд-во Харьковского университета, 1958.
300. Попов Н. А. Вакуумные выключатели. М., «Энергия», 1965.